UNIVERSITY OF LATVIA

Faculty of Biology

CRISTINA BAJO SANTOS

Plasma and urinary extracellular vesicles RNA content as potential biomarkers for detection, risk stratification and monitoring of prostate cancer

DOCTORAL THESIS

Submitted for the Degree of Doctor of Biology

Molecular Biology

Supervisor: Prof. Aija Linē, PhD

Rīga, 2023

The doctoral thesis was performed at Latvian Biomedical Research and Study Centre, Cancer Biomarkers group together with Faculty of Biology, Department of Molecular Biology, University of Latvia from 2014 to 2023.

The research was supported by ERDF grant No. 1.1.1.1/18/A/084; EEA/Norway grant NFI/R/2014/045, Latvian State Scholarship (2014-2016); ESF 8.2.2 Scholarship 2020-2023) and L'Oreal *UNESCO "For Women In Science"* Young Talents Program – Baltic with the support of the Latvian National Commission for UNESCO and the Latvian Academy of Sciences (2023).

Form of the thesis: dissertation, subfield – molecular biology.

Supervisor: Prof. Aija Linē, PhD

Reviewers:

1) Dr. biol. Artūrs Ābols, PhD. Latvian Biomedical Research and Study Centre

2) Prof. Una Riekstiņa, PhD. Faculty of Medicine, University of Latvia

3) Prof. Alireza Fazeli, PhD. Estonian University of Life Sciences, University of Tartu and University of Sheffield.

The thesis will be defended at the public session of the Doctoral Committee of Biology, University of Latvia at (EET), on December 11th 2023 at 13:00 p.m. at Latvian Biomedical Research and Study Centre, Ratsupites Str. k-1.

The thesis is available at the Library of the University of Latvia, Kalpaka blvd. 4.

This thesis is accepted for the commencement of the degree of Doctor of Biology on November 9th 2023 by the Doctoral Committee of Biology, University of Latvia.

Chairman of the Doctoral Committee _____/ *Dr. biol. Guntis Brumelis*

Secretary _____/ *Dr. biol. Daina Eze*

ABSTRACT

Prostate cancer (PC) poses a significant global burden among male malignancies, and the inherent heterogeneity of the disease presents ongoing challenges in achieving accurate detection and stratification. Hence, there exists an unmet need for non-invasive biomarkers capable of precisely identifying and classifying PC. Extracellular vesicles (EVs) derived from biofluids, such as plasma or urine, hold promise as valuable reservoirs of PC-specific biomarkers. EVs encapsulate a diverse range of molecules, including RNA, reflecting the molecular characteristics of their originating cells, including cancer cells and the prostate microbiota.

The aim of this study was to gain biologically and clinically meaningful insights into the RNA cargo of EVs from PC patients. Hence, the main objective was to analyze the RNA composition within plasma and urinary EVs obtained from PC patients before and after radical prostatectomy (RP) and compare it with the transcriptome of matched tumour and normal prostate tissues to identify potential RNA biomarkers derived from cancer cells and the prostate microbiota.

RNA sequencing analysis identified 69 different human RNAs that were overexpressed in tumour tissues, present in EVs before RP and decrease after surgery, with the majority of them being fragmented mRNAs. Validation using RT-ddPCR in an independent cohort of PC patients confirmed miRNA-375-3p, piR-28004, and AMD1 as prostate/PC-derived biomarkers in urinary EVs. Subsequently, the diagnostic potential of selected biomarkers was assessed using RT-ddPCR in PC and benign prostate hyperplasia (BPH) patients. Among the identified markers, NKX3.1(AUC = 0.81; $p<0.0001$) and GLO1 (AUC = 0.68; $p<0.05$) showed significant discrimination between PC and BPH in plasma EVs. Furthermore, a biomarker model consisting of seven candidates (miR-375-3p, piR-28004, GLO1, NKX3.1, RMB47, MAZ and AMD1) demonstrated superior discrimination between PC and BPH samples than PSA test in this sample set (Model AUC = 0.904, $p<0.001$; LOOCV AUC = 0.8029; $p = 0.001$ vs. PSA AUC = 0.431; $p = 0.51$). In terms of prognosis, urinary EV levels of NKX3.1 correlated with CAPRA scores ($r = 0.36$, $p< 0.05$). Additionally, MAZ levels in plasma EVs correlated with ISUP grade ($r = 0.415$; $p<0.05$).

Analysis of non-human RNA reads from PC and normal prostate tissues revealed the presence of 365 microbial species that were next used for constructing the prostate tissue metagenome. Mapping of non-human EV RNA reads against this metagenome showed that nearly all of these species were represented in EV RNA. Differential abundance analysis revealed 26 species that were represented by higher number of reads in plasma EVs from healthy males and 2 *Pseudomonas* species that were overrepresented in PC patients as compared to the controls. Moreover, *Pseudomonas spp*. RNA decreased after RP suggesting that their abundance is associated with the presence of PC.

Furthermore, a novel genome-agnostic analysis approach confirmed the overrepresentation of *Pseudomonas* RNA in PC EVs and identified several other microorganisms whose RNA abundance is altered in EVs of PC patients.

This thesis presents the identification of EV-based biomarkers derived from PC, which have the potential to be utilized as a liquid biopsy for the diagnosis and prognosis of PC. Implementing these biomarkers could significantly improve PC management and enhance the overall well-being of PC patients, although further validation in a larger cohort is necessary.

KOPSAVILKUMS

Prostatas vēzis (PV) ir globāla veselības problēma. Lai gan ir panākti būtiski uzlabojumi PV diagnostikā un ārstēšanā, slimības bioloģiskā un klīniskā neviendabība rada grūtības to savlaicīgi un precīzi diagnosticēt un izvēlēties katram pacientam piemērotāko ārstēšanu. Tādēļ pastāv nepieciešamība atrast jaunus neinvazīvus biomarķierus, kas dotu iespēju precīzi noteikt vēža klātbūtni un prognozēt slimības gaitu. Ekstracelulārās vezikulas (EVs), ko ārpus šūnu vidē producē lielākā daļa cilvēka šūnu, kā arī mikroorganismi, satur dažādas molekulas, to skaitā dažādu veidu RNS, kas atspoguļo to izcelsmes šūnu molekulāro saturu, ir perspektīvs PV biomarķieru avots šķidrajām biopsijām.

Šī pētījuma mērķis bija iegūt padziļinātu izpratni par EV RNS saturu un iespējām to izmantot PV diagnostikā un prognostikā. Pētījuma galvenie uzdevumi bija veikt EV RNS sekvenēšanas analīzi PV pacientu plazmas un urīna paraugos, kas ņemti pirms un pēc radikālas prostatektomijas (RP) un salīdzināt EV RNS saturu ar PV un normālu prostatas audu transkriptomu, tādējādi identificējot RNS biomarķierus, kas veidojušies no PV šūnām vai prostatas mikrobiotas.

RNS sekvencēšanas analīzē tika identificēti 69 RNS biomarķieru kandidāti, kas bija paaugstināti ekspresēti audzēju audos, salīdzinoši augstā līmenī sastopami pirms-operācijas EVs un samazinājās pēc RP. Lielākā daļa no šīm molekulām bija mRNS fragmenti. Izvēlēto biomarķieru kandidātu testēšana neatkarīgā PV paraugu kopā, izmantojot RT-ddPCR, apstiprināja, ka miRNA-375-3p, piR-28004 un AMD1 galvenais avots urīna vezikulās ir PV un/vai prostata. Tālāk izvēlētie marķieri tika salīdzināti PV un labdabīgas prostatas hiperplāzijas (LPH) pacientu plazmas un urīna EVs. Divi biomarķieri - NKX3.1 (AUC = 0.81; $p<0.001$) un GLO1 (AUC = 0.68; $p<0.05$) – individuāli uzrādīja būtisku diagnostisko vērtību, testējot plazmas EVs. Biomarķieru modelis, ko veidoja 7 plazmas biomarķieri (miR-375-3p, piR-28004, GLO1, NKX3.1, RMB47, MAZ un AMD1) uzrādīja ievērojami labāku spēju atšķirt PV no LPH kā PSA tests šajā paraugu kopā (modeļa AUC = 0.904, $p<0.001$; LOOCV AUC = 0.803; $p = 0.001$ *vs* PSA AUC = 0.431; $p = 0.51$). Trīs biomarķieri uzrādīja arī prognostisku vērtību: NKX3.1 līmenis urīna EVs korelēja ar CAPRA indeksu ($r = 0.36$, $p< 0.05$). Savukārt MAZ līmenis plazmas EVs korelēja ar ISUP indeksu ($r= 0.415$; $p<0.05$).

Analizējot eksogēnos RNS lasījumus, kas nekartējās pret cilvēka genomu, PV un normālos prostatas audos tika identificēta 365 dažādu mikroorganismu RNS klātbūtne. No šo mikroorganismu genomu sekvencēm, tika uzkonstruēts prostatas mikrobiotas metagenoms. Eksogēno EV RNS lasījumu kartēšana pret šo metagenomu parādīja, ka gandrīz visi audos sastopamie mikroorganismi ir pārstāvēti EV RNS saturā. Diferenciālā daudzuma analīze parādīja, ka 26 sugu RNS veselu vīriešu plazmas vezikulās bija sastopama augstākā līmenī kā PV pacientiem, bet divu *Pseidomonu* sugu RNS PV pacientiem bija vairāk kā kontrolēm. Turklāt vairāku *Pseidomonu* sugu RNS daudzums būtiski samazinājās pēc operācijas, kas liecina par tās saistību ar PV klātbūtni. Jauna alternatīva genoma-agnostiska datu analīzes metode apstiprināja *Pseidomonu* RNS līmeņa atšķirības, kā arī uzrādīja vairākas citas sugas, kuru RNS līmenis plazmas EVs PV pacientiem ir atšķirīgs.

Kopumā ņemot, šajā darbā tika identificēti vairāki jauni cilvēka un mikrobiālas izcelsmes PV biomarķieri, kas potenciāli varētu tikt izmantoti PV šķidro biopsiju testos diagnostikai un prognostikai. Šo biomarķieru ieviešana klīniskajā praksē varētu uzlabot PV pacientu ārstēšanu un dzīves kvalitāti, taču ir nepieciešama atrasto biomarķieru validācija lielākā pacientu kohortā.

Table of Contents

ABBREVIATIONS

adj. adjusted
ADT Androgen Deprivation Therapy
AGO2 Argonaute RISC catalytic component 2
AKT1 AKT serine/threonine kinase 1
ALIX programmed cell death 6 interacting protein
AMD1 AdenosylMethionine Decarboxylase 1
AR Androgen Receptor
ARE Androgen Response Element
ARMMs Arresting-domain-containing 1 Microvesicles
ATM ATM serine/threonine kinase
AUC Area Under the Curve
BCA BicinChoninic Acid
BCR BioChemical Recurrence
BRCA2 BRCA2 DNA repair associated gene
BPH Benign Prostate Hyperplasia
ºC Centigrade
Cag A Cytotoxin associated gene A
CAPRA Cancer of the Prostate Risk Assessment
CD Cluster of Differentiation
cDNA complementary DNA
CI Confidence Interval
CNV Copy Number Variation
dcSAm. decarboxylated S-adenosylmethionine
DDR DNA Damage Response
DEGS Differential Gene Expression
DHEA DeHydroEpiAndrosterone
DHT DiHydroTestosterone
DNA DeoxyriboNucleic Acid
DRE Digital Rectal Examination
EMT - Epithelial to mesenchymal transition
ETS Erythroblast Transformation Specific
ERG ETS-transcription factor
ERSPC. European Randomized Study of Screening for PC
ETV1 ETS Variant Transcription factor 1
ESCRT Endosomal Sorting Complexes Required for Transport
EV Extracellular Vesicle
exRNA extracellular RNA
EDTA EthyleneDyamine Tetraacetic Acid
F3 coagulation Factor III tissue factor
FC Fold Change
FDA U.S. Food and Drug Administration
FMT Fecal Microbiota Transplant
FOXA1 Forkhead box A1
GG Gleason Grade
GLO1 Glyoxalase 1
GS Gleason Score
HD Healthy Donor
HDI Human Development Index
HF High Fat
HG High Gleason
HOXB13 Homeobox B13
IGF-1 Insulin-like Growth Factor 1
IGFBP3 Insulin like Growth Factor Binding Protein 3
ILVs IntraLuminal Vesicles
ISUP International Socierty of Urological Pathology
kb kilobases
kDa kilo Dalton
LG Low Gleason
LNCaP Lymoh Node Carcinoma of the Prostate
lncRNA long-non-coding RNA
log2FC. Logarithmic 2 Fold Change
LOOCV Leave-One-Out Cross Validation
LPCAT1 LysoPhosphatidylCholine AcylTransferase 1
MAZ MYC Associated Zinc finger protein
mCRPC metastatic Castration Resistant Prostate Cancer
MDM mucin – degrading- microbes
mg milligrams
MISEV Minimal Information for Studies of Extracellular Vesicles
mtRNA mitochondrial RNA
MRI Magnetic Resonance Imaging
mRNA messenger RNA
min minutes
miscRNA miscellaneous RNA
miRNA mature micro RNA
ml milliliter
MVBs Multi Vesicular Bodies
MVP Major Vault Protein

MYC MYC proto-oncogene, bHLH transcription factor
ncRNA non-coding RNA
ng nano grams
NKX3-1 NK3-homeobox 1
Nm nano meter
nM nano Molar
N_L Normal prostate tissue long RNA
Ns Normal prostate tissue small RNA
nt nucleotides
NVEPs Non-Vesicular Extracellular Particles
p p-value
p53 Tumour protein 53
PAGE PolyAcrylamide Gel
PatoChip pan-Pathogen microarray metagenomics analysis
PBS Phosphate Buffer Saline
PC Prostate Cancer
PCR Polymerase Chain Reaction
PEG Polyethylene Glycol
PIA Proliferative Inflammatory Atrophy
PI3K Phospho-Inositol 3 Kinase
PI3KCA PhosphatidylInositol-4,5-biphosphate 3-Kinase Alpha
PI3KCB PhosphatidylInositol-4,5-biphosphate 3-Kinase Beta
PIN Prostatic Intraepithelial Neoplasia
piRNA piwi-interacting RNAs
PIWI P element-induced wimpy testis
PM Prostate Metagenome
PostOp Post Operation
PostOpP Post Operation Plasma
PostOpU Post Operation Urine
PreOP Pre Operation
PreOpP Pre Operation Plasma
PreOpU Pre Operation Urine
Pre-miRNA precursor-micro RNA
PSA Prostate Specific Antigen
P-Score Prostatype© risk score
PTEN Phosphatase and Tensin Homolog
r ratio
RAD51 RAD51 recombinase
RB1 RB transcriptional corepressor 1
RBM47 RNA Binding Motif protein 47
RBPs RNA-Binding Proteins
RIPA Radio-ImmunoPrecipitation Assay
RNA RiboNucleic Acid
RNAseq RNA sequencing
ROC Receiver Operation Characteristics curve
RP Radical Prostatectomy
rRNA ribosomal RNA
RT-ddPCR Reverse Transcriptase digital droplet Polymerase Chain Reaction
SAM S-adenosylmethionine
SCFA Short-Chain -Fatty-Acid
SDS Sodium DodecylSulfate
SEC Size Exclusion Chromatography
sec seconds
snRNA small nuclear RNA
snoRNA small nucleolar RNA
SPDEF SAM pointed domain containing ETS transcription factor
spp. species
SPOP Speckle type BTB/POZ Protein
TEs Transposable Elements
T_L Tumour tissue Long RNA
TMPRSS2 Trans-Membrane Serine Protease 2
TNM Tumour, Nodes and Metastasis systerm
TRAMP Transgenic Adenocarcinoma of the Mouse Prostate
Ts Tumour tissue small RNA
tRF transfer RNA fragment
tRNA transfer RNA
TSPAN4 Tetraspanin 4
TSG101 Tumour Susceptibility 101
UC UltraCentrifugation
µl microliter
VGLL3 VestiGial Like family member 3
vs. versus
vtRNA vault RNA
WNT Wnt fami

INTRODUCTION

Extracellular vesicles (EVs) are membrane-confined particles released by virtually all cell types into the extracellular space and can be isolated from various biofluids, such as plasma or urine. EVs have been proposed as key players in cell communication processes, including those associated with cancer. Among their cargo, EVs contain proteins, lipids, DNA fragments, and various RNA species that represent the cell of origin. Likewise, EVs released by microbes can carry unique microbial signatures, such as microbial DNA or RNA or other pathogen-associated molecules specific to a particular microbe.

Prostate cancer (PC) is the most prevalent male cancer in Western countries and despite the current advances in the medical field, there is still a need to find biomarkers for its detection in a non-invasive manner. By analysing the signatures in EVs isolated from the biofluids of PC patients, it may be possible to identify and classify different stages of PC and predict patient outcomes. Furthermore, understanding the PC-released molecular signatures could potentially lead to the development of targeted therapies or microbiome-modulating strategies to improve patient outcomes.

Importance of this study: The current primary diagnostic tool for PC, the serum Prostate specific antigen (PSA) test, lacks specificity and leads to overdiagnosis and overtreatment. In this study we explore the use of PC-derived EVs as novel biomarkers to advance the development of liquid biopsies for improved diagnosis, prognosis, and monitoring of PC, ultimately aiming to enhance the welfare of PC patients.

The **aim** of my research is to characterize the small RNA content in plasma and urinary EVs from PC patients and compare it with matched tumour and normal prostate tissues to identify PC-associated RNA biomarkers that can potentially be exploited for the detection, prognosis and surveillance of PC.

The **main tasks** of my research are:

1. To isolate EVs from plasma and urine of a longitudinal cohort of PC patients and controls.
2. To construct EV RNA sequencing libraries.
3. To construct whole transcriptome and small RNA sequencing libraries from PC and normal prostate tissues.
4. To analyze RNA sequencing data and identify RNA biomarkers that are present in the pre-operation EVs, decrease after the surgery and are overexpressed in PC tissues as compared to normal tissues.
5. To validate selected biomarkers by droplet digital PCR in an independent sample set.
6. To annotate microbial RNAs found in plasma and urinary EVs and assess their potential clinical use.

1. LITERATURE REVIEW

1.1 Hallmarks of Cancer

With almost 10 million deaths in 2020, cancer, also known as a malignant neoplasm, is the leading cause of death worldwide [1]. Cancer is a multifaceted and complex disease characterized by the uncontrolled growth and proliferation of abnormal cells. It arises from the disruption of normal cellular processes such as cell division, differentiation, and programmed cell death (apoptosis). This aberrant behavior results in the formation of a mass of cells called a tumour, which can invade nearby tissues and spread to distant sites in the body through a process called metastasis [2, 3]. In order to conceptualize the new functional capabilities acquired by cells moving away from normalcy to neoplastic growth states, an initial set of six hallmarks was proposed by Hanahan & Weinberg in 2000 [4], which were later extended to eight core hallmarks and two enabling characteristics after a decade [5]. Recently, few more were added and currently, cancer is characterized by the 14 characteristics that are shown in Figure 1[6].

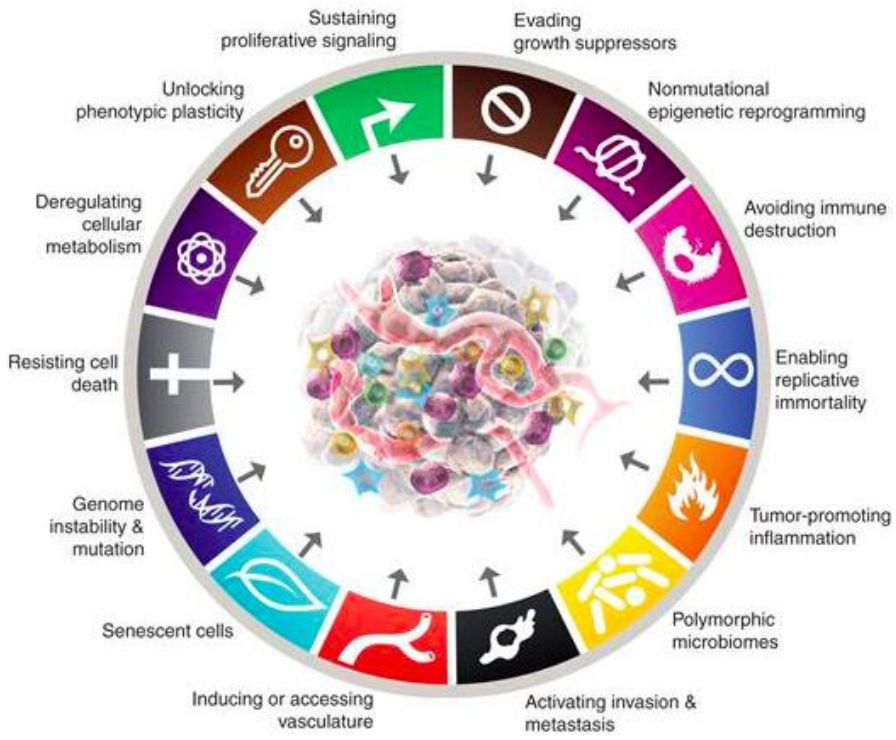

Figure 1. Current hallmarks of cancer [6].

1.2 Prostate Cancer

1.2.1 Anatomy and histology of the prostate

The prostate gland is a walnut-size exocrine gland that constitutes a component of the male reproductive system. Anatomically, it resides in close proximity to the bladder, with a circumferential arrangement around the urethra, which serves as the conduit for both urine and semen elimination [7, 8]. The fundamental purpose of the prostate gland resides in the production and secretion of prostate fluid, a critical constituent of semen. Prostate

fluid fulfills pivotal roles in nourishing and safeguarding spermatozoa, thereby fostering their motility and viability. During the ejaculatory process, coordinated contractions of the prostate's muscular components facilitate the propulsion of semen into the urethra, culminating in its subsequent release from the body [9]. Beyond its integral involvement in reproductive function, the prostate gland exerts an influence on urinary dynamics and its strategic anatomical positioning can impact the flow of urine. By encircling the urethra, the prostate gland can exert mechanical pressure, which, if the gland undergoes enlargement or pathological changes, may precipitate urinary symptoms [9].

Although five different anatomical zones can be identified in the prostate: peripheral, fibromuscular, transitional, periurethral and central (Figure 2a); the peripheral, the transitional and the central are the most studied [10, 11]. In normal prostate, the peripheral zone comprises the distal outside area of the prostate gland and it is the primary site of the majority of prostate cancer occurrences. In healthy individuals, it constitutes more than 70% of the glandular tissue [8]. The transition zone is located adjacent to the prostatic urethra (Figure 2a) and is usually barely apparent in younger males, accounting for approximately 5% of total prostate volume [10]. However, in the majority of older men, the transition zone enlarges significantly due to benign prostatic hyperplasia (BPH), a common benign proliferation in the transition zone [10]. Although tumours might develop in the transition zone, scientific evidence indicates that these tumours have higher likelihood of being confined within the prostate [12], presenting a more favorable prognosis [13, 14] despite displaying higher PSA levels and a bigger size when compared to those that develop in the peripheral zone [15]. The central zone, which resembles a cone-shaped structure, is the largest at the base of the prostate and narrows toward the verumontanum, which surrounds the ejaculatory ducts. It is not known to be the initial site of any disease process; but can be involved in advance cancer cases [10].

The mature prostate gland consists of numerous small glandular acini that have specialized epithelial cells (Figure 2b). These epithelial cells can be classified into two primary types: luminal cells and basal cells [7]. Luminal cells are columnar in shape and form the inner layer of the acini. They secrete PSA [10], a serine protease frequently elevated in men with prostate cancer, and a key enzyme involved in the liquefaction of semen, which growth is highly androgen-dependent [16]. Basal cells, on the other hand, are cuboidal in shape and are positioned adjacent to the basement membrane (Figure 2b). They provide structural support to the glandular epithelium and may also serve as progenitor cells for luminal cells [17]. Surrounding the acini and separating them is the fibromuscular stroma, which contains collagen and smooth muscle fibers (Figure 2b). These stromal components provide structural integrity and support for the prostate gland. Interlacing bands of smooth muscle can be observed within the stroma, facilitating the contraction and expulsion of prostatic fluid during ejaculation [18, 19]. Additionally, scattered within the stroma are neuroendocrine cells (Figure 2b), which are involved in the regulation of prostate function. These cells can produce and secrete various bioactive substances, such as serotonin and calcitonin, which may influence glandular activity and contribute to the overall physiology of the prostate [20]. Blood vessels, lymphatic vessels, and nerves traverse through the stroma, supplying nutrients, facilitating drainage, and conveying sensory and autonomic signals to the prostate gland [7]. Understanding the histological features of the prostate, including its glandular units, stromal elements, and cellular components, provides insights into its normal function and enables the

identification and characterization of pathological changes associated with conditions such as BPH and PC.

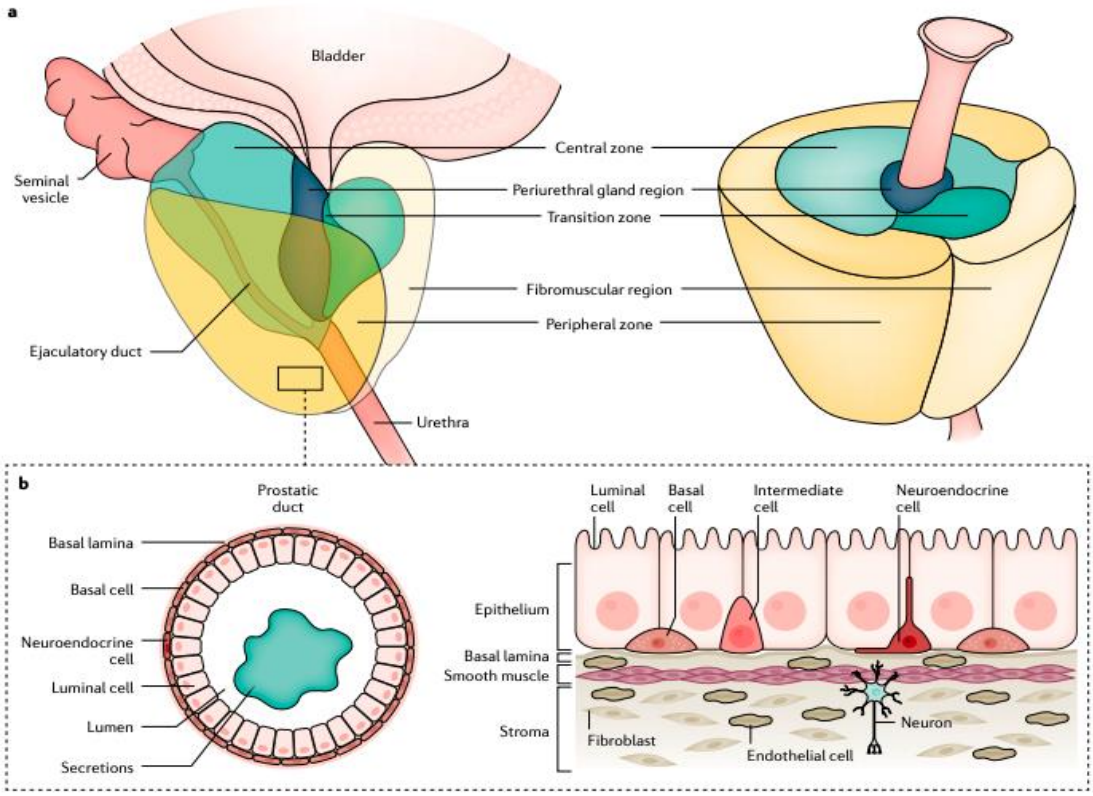

Figure 2. Prostate anatomy and histology. (a) The prostate gland can be anatomically categorized in five different regions: the fibromuscular, the peripheral, the transitional, the periurethral and the central. Majority of tumours develop in the peripheral zone. (b) Histologically, each region of the prostate consists of ducts and acini, embedded within the stroma. The stroma is composed primarily of smooth muscle cells, along with fibroblasts. The ducts and acini are comprised of a single columnar epithelium layer (luminal cells), surrounded by a layer of basal epithelial cells. Basal cells produce the basement membrane, which acts as a layer of extracellular matrix connected to stromal cells. Additionally, neuroendocrine cells are present within the duct. Picture taken from Rebello et al. [27]

1.2.2 Epidemiology and etiology

According to global cancer statistics, PC is the second most frequently diagnosed cancer in men and the fifth main cause of cancer-related fatalities worldwide [1]. The incidence of PC varies across regions, with developed countries reporting higher rates than developing countries [1]. In Latvia, PC is the most commonly diagnosed cancer among men [21]. The age-standardized incidence rate of PC in Latvia in 2020 was estimated to be 110.6 per 100,000 people [21]. Furthermore, prostate cancer is also a leading cause of cancer-related deaths among Latvian men. In 2020, the age-standardized mortality rate for PC in Latvia was reported to be 29.7 per 100,000 people[1]. It is worth mentioning that a positive link has been discovered between the human development index (HDI) and PC prevalence worldwide, with developed nations reporting a greater frequency of PC than underdeveloped countries [22].

This can be attributed to several factors related to socioeconomic development and healthcare access, such as better healthcare infrastructure and awareness programs or more advanced diagnostic technologies. In fact, long-term follow-up data studies have demonstrated that repeated screening has led to an increased PC detection rate and

subsequently resulted in reduced mortality [23, 24]. However, it has also caused an increase of overdiagnosis [25].

Although the concrete etiology of PC remains elusive, PC development has been linked to various risk factors. Innate risk factors include age, family history, special conditions (as Lynch syndrome) and ethnicity [26]. The incidence of PC rises steeply with age, being more than 85% of newly identify cases diagnosed after 60 years of age [1]. This association suggests that age-related changes in the prostate gland or cumulative exposure to other risk factors over time may contribute to the increased susceptibility to PC in older individuals.

Almost 10% of patients diagnosed with PC have a family history of cancer; and males who possess immediate family members diagnosed with prostate cancer are at a doubled risk of acquiring this disease [27]. Different germ-line mutations have been identified ligated to an increased risk of development of PC [9], being mutations in the BRCA2 DNA repair associated (BRCA2) and Homeobox B13 (HOXB13) genes the ones that confer the highest risk to PC malignancies [28, 29]. Additionally, certain ethnicities, such as African Americans, have a higher incidence and mortality rate compared to other populations [1, 30]. They are also more likely to develop the disease at an earlier age and present more aggressive forms [30]. Asian and Hispanic populations have lower PC rates than Caucasian men, while the rates in Caribbean and African populations are higher [1]. Modifiable risk factors that might be associated with advanced PC include obesity and metabolic syndrome, smoking and alcohol consumption, sedentarism and a predominantly Western diet [26, 31].

1.2.3 PC development

Acinar adenocarcinoma is the most prevalent type of PC, constituting over 90% of all PC cases [9]. Typically, it arises from the glandular epithelial cells situated in the peripheral zone of the prostate. In this region, potentially cancerous cells remain circumscribed by basal membrane leading to prostatic intraepithelial neoplasia (PIN), which is widely regarded as the antecedent stage of PC [32]. Afterwards, the transformed epithelium will undergo phenotypic changes that will assist in the transformation from latent adenocarcinoma (*in situ*) to clinical adenocarcinoma (after invasion of nearby tissues). This stage is androgen-dependent, and it is characterized by the total absence of basal cells [33]. Androgen-independent adenocarcinoma, also known as metastatic castration resistant prostate cancer (mCRPC), denotes the progression of adenocarcinoma that no longer relies on androgens for its growth, reaching metastatic stage [33]. While adenocarcinoma is the predominant type, there are also other several rare subtypes arising from the non-epithelial cells that are harbored in the prostatic tissue or related ducts. All the rare subtypes present an aggressive phenotype and are linked with poor prognosis [33].

1.2.4 Diagnostic and prognosis

Early-stage prostate cancer is typically asymptomatic and is frequently detected after the disease has already progressed to clinical stage. Nevertheless, >70% of diagnosed cancers are detected still at the organ-confined phase, with a 5-year overall survival of >99% [34]. Commonly employed diagnostic techniques for the detection of prostate cancer encompass: PSA blood test, digital rectal examination (DRE) and magnetic resonance imaging (MRI) [35]. DRE involves manually assessing the prostate gland's size, texture, and firmness through physical palpation. Overall, this examination has a positive

predictive value ranging from 5% to 30% in detecting prostate cancer among men with PSA levels lower than two ng/ml [35] and it is the main accepted method to determine the cT stage [36, 37]. Serum PSA levels have been identified as a more sensitive method of PC detection [35]. In normal conditions, PSA is secreted by luminal cells to the prostatic lumen, where the pre-PSA gets cleaved and activated. Rarely does active PSA reach the bloodstream and if so, it gets quickly inactivated [38]. However, in pathological conditions, such as PC or BPH, PSA precursors leaked to the bloodstream due to the loss of gland architecture, resulting in increased levels of pro-active PSA in the bloodstream [38]. A PSA level below four nanograms per milliliter is typically regarded as falling within the normal range. However, if patient's PSA level exceeds this threshold, it is commonly recommended that they undergo a biopsy procedure to confirm the presence of PC [35]. Serum PSA levels have been widely utilized as the primary screening method for PC detection in recent decades [39]. Despite the test's considerable sensitivity, PSA testing is associated with several limitations. In fact, it cannot distinguish between different grades of PC and lacks specificity due to factors such as age, race, and non-malignant conditions like BPH or prostatitis, which can lead to elevated PSA levels in the bloodstream [23, 40]. One of the primary concerns associated with PSA testing is the potential for overdiagnosis and overtreatment. Elevated PSA levels often trigger further diagnostic procedures, such as prostate biopsies, to confirm the presence of PC [23, 41]. However, these invasive procedures carry risks and can yield false-negatives results, and in certain cases, the biopsy itself can lead to adverse health outcomes [42, 43]. Moreover, treatment decisions based on PSA test can contribute to morbidity. If PC is detected, treatment options such as surgery, radiation therapy, or androgen deprivation therapy may be pursued. However, these interventions can result in side effects, including urinary incontinence, erectile dysfunction, bowel problems, and hormonal imbalances, significantly impacting the overall well-being and quality of life of affected individuals [44]. Furthermore, conflicting results have emerged from recent reviews and meta-analyses examining the effectiveness of PSA testing in reducing mortality rates. While some studies did not observe a significant decrease in mortality [39], others reported a reduction of approximately 20% [40].Therefore it is essential to evaluate whether the benefits of widespread PSA testing outweigh its negative impact, taking into considerations the potential risks, limitations and individual circumstances.

PC is commonly classified into stages based in the extent of the disease. The most widely used staging system is the Tumour, Nodes and Metastasis system (TNM) [36]. The Tumour Stage (T) describes the size and extent of the primary tumour within the prostate gland. It is further divided into 4 categories and subcategories depending on tumour's size and whether it has spread beyond the prostate [36, 45]. The Node stage (N) indicates whether the cancer has infiltrated lymph nodes (N1) or not (N0). The metastasis stage (M) refers to the presence (M1) or absence (M0) of distant metastasis [45]. PC cells predominately metastasize bones, lungs or liver [11]. Using the TNM classification, an overall stage is assigned, ranging from early-stage localized cancer (Stage I or II) to advances or metastatic disease (Stage III or IV) [36]. This staging helps guide treatment decisions and provides valuable information about the prognosis or the disease.

To assess the severity of PC and determine the extent of morphological changes, the Gleason Score (GS) is employed. GS is a histological grading system specifically developed to evaluate the prognosis of PC affected individuals [46].

The GS is determined by adding the grades of the most predominant patterns, resulting in low (≤6), intermediate (7) or high (8-10) [46, 47]. Within the current evaluation system, GS 3 and GS4 pose challenges in histologic evaluation, and the criteria for assessing them lack robustness and reproducibility [47]. Originally, five Gleason Grades (GG), ranging from one to five, each associated with different characteristics based on tissue and cell differentiation levels were proposed (Fig.3). GG 3 (3+3) is characterized by the presence of glands with highly variable sizes and shapes, maintaining their glandular architecture. GG 4 (4+4) is characterized by cribriform, poorly formed, and fused glands; while Gleason 5 (5+5) corresponds to the absence of glandular structures, with sheets, cords, single cells, solid nest and necrotic areas taking their place [47, 48].

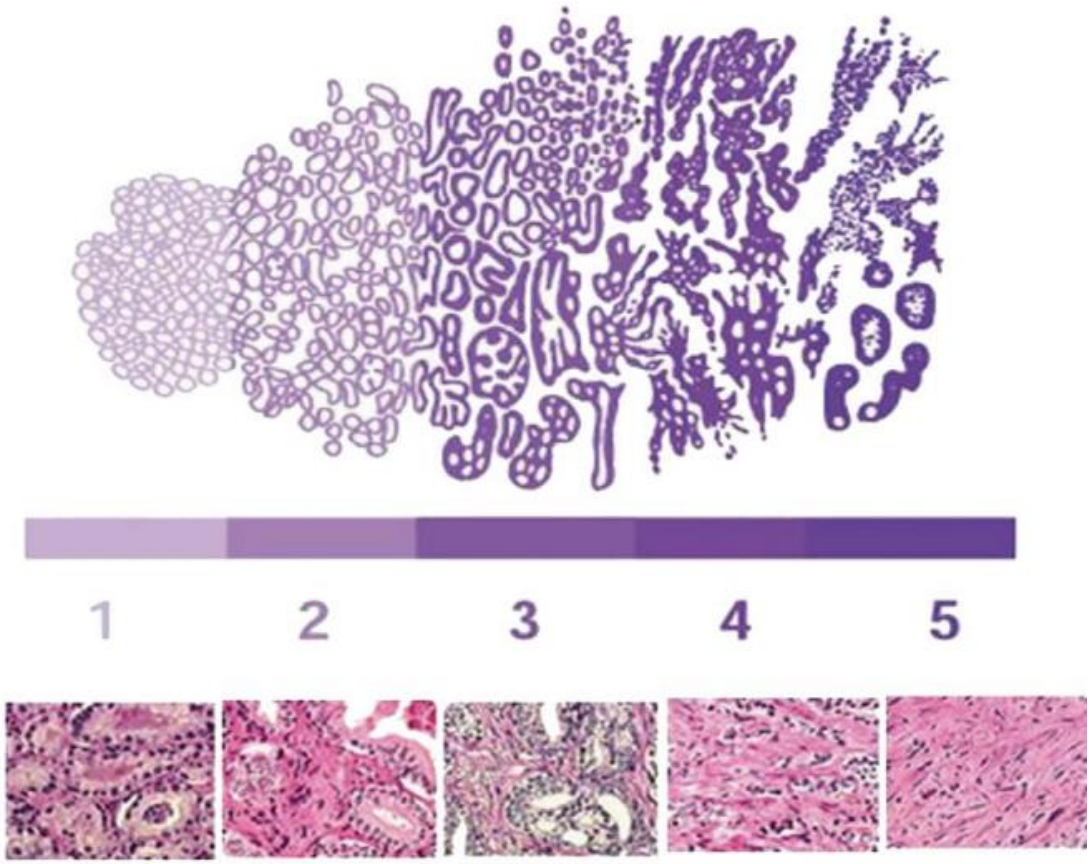

Figure 3. Schematic representation of the Gleason grading system, with numerical values assigned to each grade. The upper section showcases the original Gleason illustrations for each grade, while the lower section features the corresponding micrographs stained appropriately for each grade. Picture taken [48].

Currently, the recommended grading system for PC is the modified GS introduced by International Society of Urological Pathology (ISUP) [37]. The determination of the biopsy GS in this particular system is based on the individual consideration of the GS of the most extensive pattern and the highest pattern, without taking into account their respective extents. However, in radical prostatectomy (RP) specimens, a pattern representing less than 5% of the cancer volume is not included in the GS [37]. The introduction of the PC grade groups by ISUP aimed to standardize the grading of prostate cancer with other types of carcinomas and address the inconsistency of assigning a GS of 6 to the least aggressive PC. The objective of this approach is to accentuate the clinical distinctions between GS 7a (3+4) and GS 7b (4+3), thereby designing a more exhaustive comprehension of the disease, and highlighting the potential risk of biochemical recurrence (BCR) (Table 1) [37, 49].

Table 1. Comparison of risk assessment tools for PC diagnostics [37, 50, 51]

	ISUP grade		D'Amico	CAPRA
Factors	Gleason Score	ISUP GG grade	T-stage, serum PSA level (ng/ml) and ISUP grade	Age, serum PSA level (ng/ml), GS biopsy, T-stage, % of biopsy cored involved with cancer
Low risk	2-6	1	cT1-cT2A, PSA<10ng/ml, and ISUP grade 1	0-2
Intermediate risk	7a (3+4)	2	cT2b or PSA >10-20ng/ml or ISUP grade 2 or 3	3-5
	7b (4+3)	3		
High risk	8 (4+4 or 3+5 or 5+3)	4	(>cT2b or PSA >20ng/ml or ISUP grade >3	6-10
	9-10	5		

The risk classification developed by D'Amico et al. is the most widely utilized and serves as a useful initial assessment tool. It includes T-stage and serum PSA levels at the moment of diagnosis in addition to ISUP grade (Table 1) [35, 50]. It is important to note that both classification systems have certain limitations, since they only approach risk of BCR and they do not account for multiple risk factors, such as patient age or comorbidities. Kattan Normograms on the other hand utilize mathematical models that incorporate multiple variables such as PSA, GS, clinical stage, age and other relevant clinical factors [52]. Their main advantage is their ability to provide personalized risk assessment by considering multiple factors simultaneously, but they can just at best, provide a prediction index [52]. In an endeavor to overcome the limitations associated with previous approaches, the Cancer of the Prostate Risk Assessment (CAPRA) score was created [51]. The CAPRA score is a simplified numerical scoring system ranging from 0 to 10 (Table 1). It offers a comparable level of accuracy to more complex normograms while maintaining the ease of calculations similar to the D'Amico classification. In addition, the CAPRA score provides valuable prognostic information across different treatment modalities and can predict risk of metastasis and overall mortality for an individual patient [53, 54]. Recently, a new molecular-based risk assessment test has been developed. The Prostatype® risk score (P-Score) is an algorythmic-based risk assessment tool that calculates a risk score combining the previous mentioned clinical factors with the insulin like growth factor binding protein 3 (IGFBP3), the coagulation factor III, tissue factor (F3) and the vestigial like family member 3 (VGLL3) gene expressions in patient's biopsies [55]. Compared to previous tests, Prostatype® risk score offers a more personalized and precise assessment of PC risk, and it has been shown to improve risk stratification and prediction of outcomes [56, 57]. The addition of molecular information into the risk assessment classification could help guide treatment decisions, potentially avoiding overtreatment in low-risk cases and ensuring appropriate interventions in high-risk cases.

1.2.5 PC management

PC management involved a comprehensive approach that considered various factors such as cancer state, tumour characteristics, patient preferences and overall health status [11]. The management strategies aim to control the disease, minimize symptoms, and improve

the patient's quality of life. The management options for PC include active surveillance, local treatments, systematic therapies, and supportive care measures [35].
Active surveillance is suitable for men with low-risk, non-aggressive PC. It consists of regular monitoring through PSA tests, DRE, and sometimes repeat biopsies. Active surveillance allows for close observation of tumour's behavior, and if signs of progression are detected, active treatment options are considered [35].

Local treatments target the cancerous cells within the prostate gland and nearby tissues. RP, the total removal of the prostate gland, is the most commonly used technique. But other therapies, such as internal or external radiation, brachytherapy, or focal therapies, such as cryotherapy or high-intensity focused ultrasound, may be used as well [35]. Once the adenocarcinoma has spread beyond the prostate or if, during the diagnosis, it is classified as high-risk, systematic therapies will be chosen [58]. Initially, hormonal therapies might be selected. Androgen deprivation therapy (ADT) aims to lower levels of male hormones that promote PC. This can be achieved through medication or by testicle removal [58]. If hormonal therapies do not bear results or if the PC has evolved to mCRPC state, chemotherapy or targeted therapies might be employed [58].

1.2.6 PC genetical background

PC is a multifocal heterogeneous disease at genetic level and is significantly linked to the accrual of somatic mutations in the genome of prostate epithelial cells through a patient's lifespan [33]. Aberrations primarily manifest in oncogenes or tumour suppressor genes, inducing alterations in gene transcription and/or translation and thereby causing disturbances in cellular homeostasis [59]. Since most PC cancer-associated genetic changes are copy number variations (CNV) or gene structural rearrangements, PC has been classified as a C-class tumour with a limited mutational burden [60, 61].

The pathogenesis of localized prostate cancer is frequently associated with modifications that involve the fusion of promoter regions regulated by androgen receptor (AR) with regions that encode members of the erythroblast transformation specific (ETS) family of transcription factors [59, 62]. The presence of these fusions has been observed in approximately 50% of biopsy specimens of prostate cancer in Caucasian males [63], while their incidence is comparatively lower in males of Black and Asian ethnicities [64]. The analysis of localized prostate tumours with varying degrees of risk through whole-genome sequencing has demonstrated infrequent genetic alterations in tumours that are negative for Trans-membrane serine protease 2 (TMPRSS2) - ETS transcription factor (ERG). These alterations include loss-of-function mutations in speckle type BTB/POZ protein (SPOP), fusion of TMPRSS2 with ETS variant transcription factor 1(ETV1), and gain-of-function mutations in forkhead box A1 (FOXA1) [59, 65, 66]. Establishing specific gene alterations that differentiate aggressive from indolent prostate cancer has been a challenging task in patients with localized disease [11]. The presence of various genetic markers, such as copy number alterations, gene methylation, and intricate mutational events like kataegis, chromothripsis, and chromoplexy, may provide a stronger indication of the severity of a disease [67].

The prevalent mutations observed in mCRPC entail amplification of gain-of-function mutations in AR, or amplification of regulators of AR transcription (such as FOXA1), along with inactivating mutations or deletions of genes that repress AR pro-tumourigenic signal [68]. The AR oncogene has been extensively researched and is a primary therapeutic target in the context of prostate cancer [69]. The luminal epithelium of the

prostate in its normal state undergoes a process wherein androgens, particularly dihydrotestosterone (DHT), facilitate the translocation of the AR from the cytoplasm to the nucleus. The AR then binds to target genes that possess an androgen response element (ARE), thereby triggering a transcriptional response. The AR primarily operates as a transcription factor that governs the transcription of genes responsible for preserving cellular equilibrium and genes that encode proteases that play a crucial role in the regular functioning of the prostate. In the pathological condition, AR primarily induces a transcriptional program that is related to growth, thereby facilitating the development of tumours [69]. The transition from confined adenocarcinoma to its clinical state and later on to mCRPC is hypothesized to entail the aberrant modulation of pivotal genes that govern cellular growth**.** The prevalence of homozygous deletions in chromosome 10q, which encompasses phosphatase and tensin homolog (PTEN), and loss-of-function mutations is notably higher in mCRPC, with over 40% of tumours exhibiting these genetic alterations [59, 68]. Alterations in phospho-inositol 3 kinase (PI3K) pathway are frequently observed, whereby gain-of-function mutations in the pathway intermediates phosphatidylinositol-4,5-biphosphate 3-kinase catalytic subunit alpha (PIK3CA) and -beta (PIK3CB) are present in 6% of advanced tumours, and in AKT serine/threonine kinase 1(AKT1) in 2% of such tumours. The activation of the Wnt family (WNT) signaling pathway does not exhibit a prominent characteristic in localized disease. However, modifications in the pathway intermediates are present in 18% of mCRPC tumours [68]. The prevalence of advanced disease in patients is attributed to the frequent occurrence of chromosome 8 instability, which encompasses CNVs of genes located on 8q, housing the MYC proto-oncogene, bHLH transcription factor (MYC), and loss of 8p, which harbors the NK3-homeobox 1 (NKX3-1) gene. This phenomenon is observed in approximately 20-30% of cases with advance disease [68]. MYC is believed to have a broader involvement in the development of prostate cancer, given its nearly ubiquitous expression throughout all stages of tumour progression, even in the absence of copy number alterations. Additionally, MYC can be upregulated through direct transcriptional targeting by numerous other genes, thereby promoting proliferation and resistance to therapy [70, 71]. The genes responsible for regulating cell cycle arrest, namely tumour protein p53 (p53) and RB transcriptional corepressor 1(RB1), exhibit frequent alterations in mCRPC. The aforementioned genes exhibit a higher prevalence in metastatic disease, with a frequency of occurrence of 50% and 21% in mCRPC, respectively [59, 68, 72]. The loss of RB1 is significantly correlated with unfavorable outcomes [73]. Somatic aberrations in DNA damage response (DDR) genes are markedly widespread in mCRPC, wherein BRCA2 and ATM serine/yhreonine kinase (ATM) are recognized as pivotal genes implicated in homologous recombination repair that are frequently modified in progressive stages of the disease [28, 68]. The investigation of genetic instability is currently a thriving field of study, and there is evidence to suggest that therapeutic agents that selectively target the underlying mechanisms have the potential to postpone mortality specifically related to cancer [74].

1.2.7 PC microbiome

According to estimates, the human body harbors over 38 trillion microorganisms that coexist with our cells [75]. The microbiota of the human body, comprising bacteria, eukaryotes, and viruses, primarily inhabits the aerodigestive tract, although they may also colonize other regions such as the urinary tract [76]. The microbiome refers to the dynamic interaction between particular microorganisms and a pathological condition, wherein the mutually beneficial association between the two entities swifts to one of parasitic nature. [77].

In recent years, there has been a surge in research interest regarding the potential correlation between cancer and the distinct microbiome of various cancer subtypes, such as PC [77-79]. Studies assessing the relationship between inflammation and prostate carcinogenesis have reported the presence of a significant number of chronic inflammatory cells upon histopathological examination of PC tissue, particularly in the peripheral zone [78]. Proliferative inflammatory atrophy (PIA) refers to the presence of inflammatory lesions in glandular tissue that contain basal and secretory cells. The aforementioned lesions are predominantly observed in the peripheral zone of the prostate gland. As this area has been identified as the primary site of origin for the majority of PC cases, consequently, a hypothesis has emerged suggesting that these lesions act as precursors to the development of PC cells [80]. Moreover, it has been hypothesized that bacteria may be responsible for inducing neoplasia through chronic, low-grade inflammation [77, 80, 81]. In particular, microorganisms belonging to the *Enterobacteriaceae* family, as well as sexually transmitted pathogens such as *Chlamydia trachomatis*, possess the ability to infect the prostate gland, thereby causing the onset of bacterial prostatitis [82, 83]. Studies exploring the possible correlation between prostatitis and the onset of prostate cancer have produced inconclusive results [81]. Nevertheless, there is no conclusive evidence linking any specific infectious microorganism to the development of prostate cancer [78]. This may be because the majority of epidemiological investigations concerning the association between infections and prostate cancer risk have concentrated on singular or a limited number of infectious agents, usually recognized pathogens; while it is plausible that various types of microorganisms could induce the prostatic inflammation state linked to prostate cancer [81].

Research has demonstrated that the microbiome can impact the progression of cancer and the efficacy of treatments through two mechanisms: direct influence on tumours involving the microbiome in the urinary tract and prostatic tissue; or indirect involvement through interaction of the gut microbiome leading to immune modulation, metabolic alterations, and epithelial impairment [78]. Although thus far, establishing the existence of a typical microbiome in the prostate has been challenging, partly due to the obstacles encountered in obtaining prostate samples from healthy donors [78]. Early studies were able to identify microbial DNA from BPH and PC tissues but were not able to retrieve positive evidence from healthy donors [84, 85]. Thus, led to the hypothesis that the prostate gland lacks a widespread microbial population, and instead, microbial genetic material is probable to exist in specific regions and zones linked with acute or chronic inflammation. Even more, it is conceivable that certain identified bacterial DNA might be derived from *insitu* macrophages [81]. More recently, various studies employing 16rRNA sequencing have been published showing different findings [86, 87]. Yow et al. studied tumour and benign tissue obtained from 10 PC donors. They found 95% presence of different members of the *Enterobacteriaceae* family being *Escherichia coli* the most abundant species. *Pseudomonas* species were also identified in the benign sample [86]. Cavaretta et al. used the same technique to assess different microbial presence in tumour, peri-tumour and non-tumour areas. *Cutibacterium acnes* was the dominant specie found across all the prostate, while *Staphylococcus sp.* was predominantly found in tumour or peri-tumoural areas, and *Streptococcus sp.* was more abundant in benign tissue [87]. The study conducted by Feng et al. involved the examination of frozen tissue samples obtained from 65 Chinese patients, who had undergone RP. The findings of the study revealed over 40 different bacteria with *Acinetobacter*, *Pseudomonas*, *Escherichia* and *Cutibacterium* being the most abundant [88]. Interestingly, they observed the presence of *Pseudomonas*

spp. in PC, alongside increased expression of small RNAs, in a specific group of patients showing limited metastatic activity. This finding implies a potential inverse relationship between the occurrence of *Pseudomonas spp.* and TNM[88]. The study conducted by Banerjee et al. involved the assessment of 50 formalin-fixed tissue samples from PC RP donors and 15 BPH using a pan-pathogen microarray metagenomics analysis (PathoChip) [89]. Although no significant differences were found between groups, the most commonly observed phyla were *Firmicutes, Proteobacteria, Bacteroides* and *Actinobacteria* [89]. Interestingly, they detected *Helicobacter pylori* in over 90% of PC specimens [89]. This provides additional confirmation of the integration of the *H. pylori* - cytotoxin associated gene A (Cag A) gene into the DNA of the prostatic tumour [90]. Furthermore, the authors observed the existence of various oncogenic viruses, including cytomegalovirus, human papillomavirus 16, and papillomavirus 18, whereby these three pathogens constitute 41% of the total viruses detected [89]. A similar study assessing the presence of sexually transmitted infection agents and their association with PC was carried out by Miyake et al., [91]. The study involved the examination of 33 patients with BPH and 45 PC patient, where the sole association observed was between *Mycoplasma genitalium and* an elevated GS as well and thus, to PC development [91].

According to recent data, there appears to be a strong correlation between the presence of certain microbes and biomarkers associated with prostate cancer [92]. These markers include increased AR expression with *Escherichia coli*; elevated PSA levels with *Campylobacter concisus* and *Streptococcus pneumoniae*; higher GS with *Nevskia ramosa*; overexpression of stem-cell related genes with *Staphylococcus aureus* and *Paraburkholderia phymatum*; and dysregulation of immune-associated genes with *Gardnerella vaginalis*, *Nitrobacter hamburgensis*, and *Staphylococcus aureus* [92]. The study revealed that *Gardnerella vaginalis* exhibited a significant correlation with downregulation of immune-associated genes, along with the highest number of deletions [92]. Hence, it is plausible that bacteria may facilitate the advancement of prostate tumours by actively inhibiting the expression of immune cells, rather than instigating inflammation.

The investigation of the urinary microbiome in relation to PC is currently underway, albeit with restricted data availability. The notion that urine is sterile is widely held, however, studies have reported otherwise [81, 93]. The etiology of microbiota present in urine is yet to be fully understood, including their potential origin within the urinary tract or from other sources [94]. Shrestha et al. conducted a study wherein they employed 16S rRNA gene amplicon sequencing to assess urine samples. A total of 135 male individuals were subjected to sample collection prior to prostate biopsy [95]. The findings of the study revealed the existence of varied bacterial populations in the urine and suggested the possible involvement of pro-inflammatory bacteria in a particular group of patients with prostate cancer. The bacteria identified in this subset of patients included *Actinobaculum schaalii, Anaerococcus lactolyticus, Anaerococcus obesiensis, Streptococcus anginosus, Propionimicrobium lymphophilum, and Varibaculum cambriense*. However, the study found no significant distinction between the benign and malignant specimens [95]. Alanee et al. conducted a research study wherein they analyzed the gut microbiota and urinary microbiota of 30 patients who underwent transrectal prostate biopsy [96]. The study's authors arrived at a robust conclusion that individuals with prostate cancer exhibited a notable predominance of *Bacteroides* and *Streptococcus*, while displaying a reduced prevalence of *Acinetobacter*, *Lactobacilli,* and *Faecalibacterium* in comparison to those with benign prostatic hyperplasia [96].

Several studies have demonstrated a possible link between the gut microbiome and PC development [97]. In pathological conditions, gut chronic inflammation processes generates dysbiosis, allowing gut microbial metabolites and in some cases microbiome to leak into the bloodstream and reach distant organs [98]. Prior studies have indicated that individuals with PC exhibit a greater prevalence of *Bacteroides massiliensis* in their intestinal microbiota compared to those with non-malignant prostatic disorders or healthy individuals. Conversely, *Faecalibacterium prausnitzii* is found to be present in a lower relative abundance in these patients [99]. Thus, correlates with a study conducted by Liss et al., where they utilized 16S rRNA sequencing to identify rectal swabs and revealed that *Streptococcus* and *Bacteroides* species were more prevalent in males with PC than in the control group [100]. Interestingly, few studies have demonstrated the relevance of the "gut-prosate-axis"[101-103]. Matsuhita et al. investigation of the gut microbiome of a cohort of 152 Japanese males who underwent prostate biopsy, demonstrated a noteworthy elevation in the abundance of Short-Chain-Fatty-Acid(SCFA) -producing bacteria in individuals diagnosed with high Gleason score PC [101]. Moreover, they elucidate using a PC PTEN-knockout mice model, that PC progression induced by high-fat (HF) diet can be impeded through the use of antibiotics. It seems antibiotics exert a significant impact on the gut microbiota, leading to a reduction of insulin-like growth factor 1 (IGF-1) reduction in both tumour tissue and blood [101]. Using mouse models as well, Liu et al. transplanted fecal microbiota (FMT) obtained from mCRPC male donors to transgenic adenocarcinoma of the mouse prostate (TRAMP) resulted in the induction of high levels of gut *Ruminococcus*. This, in turn, led to an increase in PC growth, which is likely attributed to the upregulation of lysophosphatidylcholine acyltransferase 1 (LPCT1). In the study it was demonstrated that CRPC FMT-treated mice exhibited increased levels of LPCT1, RAD51 recombinase (RAD51), and DNA-dependent protein kinase catalytic subunits in their prostate region [104]. Similarly, in Pernigoni et al., study the *Ruminococcus* genus was observed to be the prevailing microbes in the gut microbiota of patients with mCRPC who exhibited unfavorable outcomes. Conversely, the existence of *Prevotella stercorea* was associated with a favorable prognosis [102]. Furthermore, the authors demonstrated that the administration of antibiotics to mice resulted in a reduction of gut microbiota and a decline in the levels of circulating dehydroepiandrosterone (DHEA) and testosterone [102]. Noteworthy, Terrisse et al. have presented potential novel pathways of communication between the gut microbiota and the immune system in preclinical mouse models and in humans with mCRPC undergoing ADT. The study conducted by the authors demonstrated that PC and ADT have divergent effects on the immune system's functionality. Additionally, the authors posited that thymus-dependent T cells play a role in regulating the progression of PC, as evidenced by the partial reduction in tumour growth control and accelerated progression from hormone-sensitive prostate cancer to mCRPC following the depletion of CD4+ and CD8+ T cells during therapy [103]. All these studies proved the existence of a "gut-prostate axis" connection with PC development and most likely diet and geographical restricted.

Although all these studies seem promising, caution should be taken since few of microbiome species previously mentioned such as, *Streptococcus* and *Staphylococcus spp*. are frequently present on the human skin and are frequently implicated in laboratory analysis contaminations [105, 106]. Therefore, proper controls should be used to discard the potential microbial species present in the reagents while carrying nucleic acid testing. Based on this and the diverse microorganisms phyla identified in the studies aforementioned, it is suggested that the normal, healthy prostate might not have a

commensal microbiome [78]. In addition, prostatic fluid is thought to be highly antimicrobial and possess high levels of zinc and antimicrobial immune proteins [30, 107, 108]. Therefore, it is probable that microorganisms are only found in prostate during pathological state. Nevertheless, further studies are needed to elucidate the corresponding mechanisms underneath.

1.3 Extracellular vesicles

1.3.1 Classification and biogenesis

EVs are bi-lipid membrane spherical structures released by prokaryotic and eukaryotic cells to the extracellular environment in healthy and pathological conditions [109, 110]. They play essential roles in intercellular communication, carrying a diverse cargo such as, proteins, lipids and nucleic acids, partly resembling the cell of origin [111]. EVs have been categorized according to their source and biogenesis. Based on that, three main groups: apoptotic bodies, ectosomes and exosomes; have been differentiated [112, 113]. Apoptotic bodies are large vesicles, typically ranging from 50 to 2000 nm, produced through cell fragmentation undergoing apoptosis [114, 115]. They contain various intracellular components, including fragmented DNA and organelles from the dying cell and can be identified by specific markers such as Annexin V and the presence of histones [115]. Apoptotic EVs are believed to play a role in immune regulation and inflammation in the tumour microenvironment [116]. Ectosomes, are primarily generated through direct outward budding of the plasma membrane, and its shedding is believed to take place in the majority of healthy cells [113]. There are multiple variations of ectosomes, such as "the classical" microvesicles with a size range of 150-1000 nm; microvesicles with a diameter of less than 200nm; arrestin-domain-containing 1 microvesicles (ARMMs), synaptic ectosomes and small ectosomes (30-150nm, enriched in CD9 CD63 and CD81 tetraspanins) [112]. Moreover, large oncosomes represent a distinct subset of large microvesicles released by tumour cells due to the overexpression or intrinsic activation of oncoproteins [117, 118]. On the other hand, exosomes are small vesicles with a diameter typically ranging from 30 to 150nm. They originate from the endosomal pathway, where inward budding of the multivesicular bodies (MVBs) results in the formation of intraluminal vesicles (ILVs) contained within the MVBs. Upon fusion of MVBs with the plasma membrane, exosomes are released into the extracellular space [112, 113]. In addition to the biogenesis process of extracellular vesicles (EVs), distinguishing features such as size or protein markers are frequently employed to differentiate among the three categories. Nonetheless, the employment of EV protein markers is constrained by the absence of consensus within the scientific community, resulting in their non-population-specific nature [119]. As such, The Minimal Information for Studies of Extracellular Vesicles (MISEV) has adopted a practical approach to address the diversity of EVs by categorizing EVs into two groups based solely on their size: large EVs (>200nm) and small EVs (<200nm). This categorization is employed in situations where the origin or biogenesis of EVs cannot be definitively determined or proven [119]. It is widely recognized that small EVs are characterized by the presence of specific markers, including tetraspanins (CD9, CD63, CD81), endosomal sorting complexes required for transport (ESCRT) proteins and ESCRT-associated proteins such as tumour susceptibility 101 (TSG101) or ALIX [119]. This classification system allows for a more standardized and practical approach in studying and characterizing EVs, focusing on their size and marker composition.

In addition to the traditional EV types aforementioned, recently, new EV types and non-vesicular extracellular nucleoid-associated proteins (NVEPs) have been described [112].

Migrasomes, are 500-3000nm vesicles released by the retraction fibers of migrating cells. Migrasomes display a distinctive morphology resembling a teardrop shape, and their genesis is linked to the presence of expansive macrodomains containing elevated levels of tetraspanin 4 (TSPAN4) and cholesterol [120, 121]. They are believed to play a role in cell migration and tissue regeneration processes and may function as mitochondria removers [122]. Similarly, exophers are large vesicles containing damaged mitochondria and protein aggregates. They have been found to be secreted in response to neurotoxic and metabolic stress by *Caenorhabditis elegans* neurons and murine cardiomyocytes; and hypothesized to be autophagy related EVs, although the exopheres biogenesis is yet unknown [123, 124].

While the majority of studies have focused their attention in EVs, it has been acknowledged that cells secrete also NVEPs that can facilitate the release of proteins, RNA, and DNA from cells. In contrast to EVs, the majority of NVEPs are amembranous, although lipoproteins do exhibit an outer lipid shell [112]. Exomeres are smaller in diameter than exosomes, ranging from 35 to 50nm; and they are enriched in metabolic enzymes [125, 126]. Supermeres are smaller than exomeres (22-32nm), and they have been reported to exhibit selective enrichment of proteins and RNA [127]. Notably, supermeres are found to contain a higher proportion of extracellular RNA (exRNA) compared to smallEVs and exomeres [128]. It is more, in the recent study performed by Zhang et al. indicated that supermeres derived from cancer cells promote increased lactate secretion, facilitate transfer of cetuximab resistance and lead to a decrease in hepatic lipids and glycogen levels *in vivo*. Thus, demonstrating the active role than supermeres play in cell communication [125, 127]. However, the origin and biogenesis mechanisms of exomeres and supermeres are still largely unknown.
Another type of NVEPs that shares a similar size range with smallEVs is vaults. Vaults are ribonucleoprotein complexes present in the cytoplasm of eukaryotic cells, composed of the major vault protein (MVP) and small non-coding vault RNA (vtRNA) [129, 130]. These structures have been observed in amphisomes, which are intermediate endosomes-autophagosomes, and it is hypothesized that vaults may be released from them [131]. Vaults exhibit a distinctive cylindrical shape and have been implicated in various cellular processes, including intracellular transport, signaling, and drug resistance [130].

1.3.2 Isolation techniques

Several techniques have been developed for EV isolation from biological specimens [132]. Ultracentrifugation (UC) is a widely employed technique that facilitates the attainment of elevated yield and purification of EVs via a series of centrifugation steps that are predicated on their size and density [133]. The technique of density gradient centrifugation, frequently employed in conjunction with ultracentrifugation, confers an additional level of refinement by segregating EVs on the basis of their floating density [134]. On the other hand, size exclusion chromatography (SEC) is a beneficial approach for the isolation of EVs with a high degree of purity. This technique operates on the principle of segregating EVs based on their size through the utilization of porous columns, thereby leading to minimal contamination [135, 136]. The utilization of precipitation techniques, such as polyethylene glycol (PEG) or other polymer-based precipitation, is a feasible and effective approach for the isolation of EVs on a large scale. This method is capable of producing high yields, although it may result in relatively lower purity levels [132]. The employment of immunocapture-based techniques involves the use of antibodies that are specific to EV surface markers. This enables the selective isolation and purification of EVs with a high degree of specificity and purity [132, 134].

Microfluidic technologies, including lab-on-a-chip devices and microfluidic chips, present benefits in scalability, swift isolation, and high throughput, rendering them appropriate for the isolation of EVs on a large scale [132, 137]. In general, the selection of a suitable EV isolation technique is contingent upon the particular demands of the research or practical implementation, taking into account variables such as output, homogeneity, and capacity for expansion [132, 135].

1.3.3 EV corona

The EV field is undergoing a significant transformation, as evidenced by recent independent studies have identified the spontaneous formation of a protein corona surrounding EVs [138, 139]. This phenomenon occurs when molecules in the extracellular environment associate with the outer surface of EVs after they are released by the producing cell [138]. The dynamic process of EV corona formation is influenced by a multitude of factors, such as the composition of the biological fluid, the specific characteristics of EVs, and the presence of particular binding patterns [138]. The biomolecules attach to the EV surface through various mechanisms such as electrostatic, hydrophobic, or specific receptor-ligand interactions. The aforementioned procedure has the potential to yield distinct protein and lipid constituents within the EVs, thereby inducing alterations in their biological characteristics and functions [140].

The EV corona is composed of various biomolecules such as proteins, lipids, nucleic acids, and other entities that exhibit surface binding affinity towards EVs [140]. The mechanism underlying the association of RNA with EVs has not been fully elucidated, despite reports indicating that RNA is capable of binding to the surface of EVs [139]. RNA-binding proteins are not commonly found in protein coronas [138]. Nevertheless, it is plausible that lipoproteins associated with EVs could facilitate the binding of RNA molecules to the exterior of these vesicles [141]. The biocorona of EVs has an impact on the biological processes mediated by EVs in both healthy and diseased states. The comprehension of the composition, dynamics, stability, and structure of the EV biocorona is valuable not only for the translation of EVs into diagnostic and therapeutic applications but also for the development of biomimetic nanomaterials intended for drug delivery [139].

1.3.4 EV RNA cargo

EVs contain a heterogeneous assortment of RNA sequences that encompass a variety of biotypes [142]. The complex arrangement of RNA molecules in EVs, along with their heterogeneity, and uncertain concentration of RNA molecules per EV [143], pose difficulties to accurately characterize the RNA content of discrete EV subtypes [142]. Preliminary investigations discovered the presence of messenger RNAs (mRNAs), mature microRNA (miRNA) sequences, and non-coding RNAs (ncRNAs) sequences inside EVs ranging in size from 200 nucleotides (nt) to over 5 kilobases (kb) [144, 145]. Further investigations have demonstrated that the majority of RNA were ncRNA biotypes, such as: miRNAs, piwi-interacting RNAs (piRNAs), long-non-coding RNAs (lncRNAs), transfer RNAs (tRNAs), small nuclear RNAs (snRNAs), small nucleolar RNAs (snoRNAs), ribosomal RNAs (rRNAs), mitochondrial RNAs (mtRNAs), Y-RNAs and vtRNAs [146-149]. miRNAs are a class of small ncRNAs that typically consist of approximately 22 nucleotides in length on average. The majority of miRNAs undergo transcription from DNA sequences, resulting in the formation of primary miRNAs (pri-miRNAs). These pri-miRNAs are then subjected to processing, leading to the formation of precursor miRNAs (pre-miRNAs) and mature miRNAs [150]. Typically, microRNAs (miRNAs) are involved in regulatory interactions with target mRNAs, leading to the

repression of translation or cleavage and degradation of the targeted mRNAs [151].Additionally, miRNAs can also bind to specific DNA promoter regions, resulting in the stimulation of transcription [152]. Evidence shows that miRNA expression in human cancer is disrupted through gene amplification, abnormal transcription, epigenetic changes, and biogenesis defects. These miRNAs can act as oncogenes or tumour suppressors [153, 154]. piRNAs are a class of short single-stranded ncRNA RNAs that range from 24 to 32 nucleotides in length. These molecules are known to bind to P element-induced wimpy testis (PIWI) proteins, which are a subclass of the Argonaute family. piRNAs are responsible for regulating the expression of transposable elements (TEs), which helps to maintain the integrity of the genome [155]. The diverse action modes exhibited by piRNAs endow them with the capacity to function as pivotal regulators of cellular processes. piRNAs exhibit dissimilarities in both expression and genomic derivation between normal and tumour cells [156], indicating their potential involvement in cancer-specific functions. Moreover, recent studies have shown that piRNAs can influence the expression of oncogenes and tumour suppressors, thereby playing a role in the development and progression of cancer [157, 158]. tRNAs are small ncRNAs, which are folded into a clover secondary structure ranging from 70 to 90nt; and comprising 4-10% of all cellular RNAs [187]. As a fundamental component of the translation process, tRNA molecules transport amino acids to the ribosome and facilitate the conversion of the nucleotide sequence into the corresponding polypeptide chain through the interaction of codons (mRNA) and anticodons (tRNA)[159]. New evidence suggests that tRNAs and their derivatives such as, tRNA fragments (tRFs) [160], 31-40nt in length produced by the cleavage of the anticodon loop of mature tRNAs [161], play a crucial role not only in the translation process, but also in signaling pathways that respond to stress conditions, which could be detected in urine or blood from cancer patients and which could be used as prognostic markers [162-164]. snRNAs are RNA molecules with 100-200 nt, essential for RNA processing and gene expression regulation in eukaryotic cells. Their main function is to regulate the pre-mRNA splicing through spliceosome-mediating processes [165]. snRNAs have been associated to cancer proliferation and resistance to anti-androgen treatment through mediation of splicing events [166]. snoRNAs are a type of non-coding RNA that typically ranges in size from 60 to 300 nucleotides. They are known to play a role in the chemical modification of ribosomal RNA, serving as a directive for the post-transcriptional alteration of ribosomal RNA. [167]. However, a novel function in the regulation of additional cellular pathways and cancer development has surfaced in recent times, especially since snoRNAs have been reported to be able to induce post-transcriptional gene silencing similar to miRNAs [168, 169]. Y RNAs (69-150nt), consisting of four types in humans, are involved in various cellular mechanisms, including DNA replication, RNA processing, and stress responses [170]. In cancer, they have been shown to affect proliferation, apoptosis and to promote metastasis [171]. In PC, aberrant Y RNA expression was linked to increase invasive capacity and overexpression with poor prognosis [172, 173]. Vaults RNAs (88-140nt), found on chromosome 5q31, are a component of vault particles but they are present in free form as well [174]. The precise roles and action mechanisms of vtRNAs remain unknown, but studies hypothesized their involvement in various cellular processes, including gene expression control, signaling and transportation [174, 175]. In cancer, they have been reported to play a role in cell proliferation, apoptosis and drug resistance[130, 176]. mtRNAs (10-1000nt) are molecules synthesized from the mitochondrial genome, crucial for regulating mitochondrial gene expression, maintaining mitochondrial function, and modulating cellular metabolism [177]. In cancer, abnormal mtRNA expression is associated with tumour progression and metastasis [178, 179]. The length

of rRNAs varies based on the organism and the particular type of rRNA. The major rRNAs in humans exhibit the following lengths: 28S rRNA (approx 4,700nt); 18S rRNA (approx. 1900 nt) and the 5.8S rRNA (approx. 160 nt) [180]. rRNAs are integral constituents of ribosomes, which are the intracellular apparatuses accountable for the biosynthesis of proteins. Aberrations in rRNA processing and expression have been detected in various types of cancer and may play a role in neoplastic [181, 182]. lncRNAs (200 nt or more) are transcripts that plat a crucial role in transcriptional and post-transcriptional regulation [183]. They interact with DNA, RNA, and proteins, affecting gene transcription and mRNA splicing [183-185]. lncRNAs also act as oncogenes or tumour suppressors through various signaling pathways, influencing oncogenesis and tumourigenesis [186]. EVs have shown to carry also functional mRNAs in their cargo, in full length or fragmented [142]. mRNAs are products of transcription of protein-coding genes, which can subsequently undergo translation to synthesize proteins in later phases of genome expression[188]. They varied in size, but most full-length mRNAs present in EVs are smaller than 1kb [189]. mRNAs contained within exosomes have been shown to regulate protein expression and facilitate cellular proliferation in normal and pathological conditions [190]. In addition, mRNA therapy is emerging for various cancer types [191].

The question of whether the content of EVs represents the entirety of the cellular content or is selectively sorted remains a topic of debate. The process of extracellular biogenesis involves the cellular vesiculation machinery, which facilitates the packaging of various RNA species into distinct subclasses of EVs. This process significantly increases the exRNA pool [192]. The majority of RNA molecules undergo transportation from the nucleus to designated cellular sites through interaction with RNA-binding proteins (RBPs). These RBPs have the ability to aggregate into larger ribonucleoprotein particles that migrate along the cytoskeleton [193]. Insufficient data exists pertaining to the dispersion of RBPs across various EVs and their function in the encapsulation of RNA within said vesicle [142]. Nevertheless, various mechanisms have been suggested with respect to the loading of RNA into EVs, including secondary configurations or specific RNA motifs [194], associations with RBPs, such as Argonaute RISC catalytic component 2 (AGO2) [195], programmed cell death 6 interacting protein (ALIX) [196] and MVPs [130]; or RNA or RBP modifications such as ubiquitylation, sumoylation, phosphorilation and uridylation [197-200], which impact RNA splicing, stability and translation and miRNA biogenesis [201]. Noteworthy, studies proved that the quantity of RNA enclosed within EVs is influenced by the physiological condition of the EV-generating cell [148, 149], thus suggesting the cell might decide upon packing full length RNAs or just fragments.

In summary, EV cargo comprises different types of small RNAs at least partially resembling the cell of origin [202]. Thus, and the fact that EVs can be isolated in a non-invasive manner from different body fluids, such as urine or plasma; highlights their potential to serve as liquid biopsies.

1.4 EVs as a source of biomarkers for PC

British Journal of Cancer www.nature.com/bjc

REVIEW ARTICLE OPEN Check for updates

Molecular Diagnostics

Extracellular vesicles as a source of prostate cancer biomarkers in liquid biopsies: a decade of research

Manuel Ramirez-Garrastacho[1,12], Cristina Bajo-Santos[2,12], Aija Line[2], Elena S. Martens-Uzunova[3], Jesus Martinez de la Fuente[4,5,11], Maria Moros[4,5,11], Carolina Soekmadji[6,7,11], Kristin Austlid Tasken[8,9,11] and Alicia Llorente[1,10]✉

Prostate cancer is a global cancer burden and considerable effort has been made through the years to identify biomarkers for the disease. Approximately a decade ago, the potential of analysing extracellular vesicles in liquid biopsies started to be envisaged. This was the beginning of a new exciting area of research investigating the rich molecular treasure found in extracellular vesicles to identify biomarkers for a variety of diseases. Vesicles released from prostate cancer cells and cells of the tumour microenvironment carry molecular information about the disease that can be analysed in several biological fluids. Numerous studies document the interest of researchers in this field of research. However, methodological issues such as the isolation of vesicles have been challenging. Remarkably, novel technologies, including those based on nanotechnology, show promise for the further development and clinical use of extracellular vesicles as liquid biomarkers. Development of biomarkers is a long and complicated process, and there are still not many biomarkers based on extracellular vesicles in clinical use. However, the knowledge acquired during the last decade constitutes a solid basis for the future development of liquid biopsy tests for prostate cancer. These are urgently needed to bring prostate cancer treatment to the next level in precision medicine.

British Journal of Cancer (2022) 126:331–350; https://doi.org/10.1038/s41416-021-01610-8

BACKGROUND

Prostate cancer

In 2020, almost 20 million people were diagnosed with cancer and 10 million were estimated to die of cancer worldwide [1]. Prostate cancer (PCa) was the most frequent cancer type among men in 112 countries and the second leading cause of cancer deaths. It is expected that improving the diagnosis and treatment of PCa patients will increase men's life expectancy.

Prostate cancer is classified as localised, locally advanced or metastatic disease. Localised PCa is further subdivided into risk groups based on prostate-specific antigen (PSA) level, International Society of Urological Pathology (ISUP) grade/Gleason score (GS) and clinical TNM stage [2, 3]. In general, low-risk patients are offered active surveillance (AS) and intermediate-risk patients are treated by radical prostatectomy (RP) or curative radiotherapy (RT). High-risk patients are treated with RP with extended lymph-node dissection or RT in combination with long-term androgen-deprivation therapy. Locally advanced patients are offered extended lymph-node dissection and RP or RT as part of multimodal therapy. Metastatic disease is at present incurable, and these patients are offered systemic treatment, eventually in combination with surgery or RT.

The incidence of PCa increased dramatically when PSA testing for early detection and screening of PCa was introduced into the market in the 1990s [4, 5]. Overdiagnosis and subsequent overtreatment became a problem, and the search for biomarkers that could discriminate indolent localised PCa that can be followed by AS from aggressive localised PCa that needs radical treatment was intensified. Thirty years later, a handful of molecular biomarkers are finally slowly approaching the clinic, such as the prostate cancer antigen 3 (PCA3) RNA test or the SelectMDx test based on RNA detection of DLX1 and HOXC6, both using urine collected after prostate massage [4, 6–8]. These tests can improve detection of clinically significant PCa and change clinical decisions for patients within each risk group. They are, however, still not routinely recommended in the clinical guidelines as more data are needed to prove their cost–benefit. At the same time, the treatment landscape of metastatic PCa is rapidly changing [9]. As new expensive drugs are entering the clinic, there is an intense search

[1]Department of Molecular Cell Biology, Institute for Cancer Research, Oslo University Hospital, Oslo, Norway. [2]Latvian Biomedical Research and Study Centre, Riga, Latvia. [3]Erasmus MC Cancer Institute, University Medical Center Rotterdam, Department of Urology, Laboratory of Experimental Urology, Erasmus MC, Rotterdam, The Netherlands. [4]Instituto de Nanociencia y Materiales de Aragón (INMA), CSIC-Universidad de Zaragoza, Zaragoza, Spain. [5]Biomedical Research Networking Center in Bioengineering, Biomaterials and Nanomedicine (CIBER-BBN), Madrid, Spain. [6]Department of Cell and Molecular Biology, QIMR Berghofer Medical Research Institute, Brisbane, QLD, Australia. [7]School of Biomedical Sciences, Faculty of Medicine, University of Queensland, Brisbane, QLD, Australia. [8]Department of Tumor Biology, Institute for Cancer Research, Oslo University Hospital, Oslo, Norway. [9]Institute of Clinical Medicine, University of Oslo, Oslo, Norway. [10]Department for Mechanical, Electronics and Chemical Engineering, Oslo Metropolitan University, Oslo, Norway. [11]These authors contributed equally: Jesus Martinez de la Fuente, Maria Moros, Carolina Soekmadji, Kristin Austlid Tasken. [12]These authors contributed equally: Manuel Ramirez-Garrastacho, Cristina Bajo-Santos. ✉email: Alicia.Martinez.Llorente@rr-research.no

Received: 16 June 2021 Revised: 19 October 2021 Accepted: 21 October 2021
Published online: 22 November 2021

Published on Behalf of CRUK

for predictive biomarkers that aim to identify responsive patients and thereby reduce unnecessary side effects.

PCa is a multifocal and heterogeneous malignancy. To bring precision medicine in PCa treatment to the next level, we need to identify biomarkers reflecting the phenotype of multiple tumour foci, which is determined by the cancer-cell genotype and shaped by the tumour microenvironment and systemic factors. The use of liquid biopsies constitutes an attractive approach in this respect because the intratumoural heterogeneity within and between the tumour foci can potentially be mirrored by molecular analyses of body fluids. Body fluids are easily accessible, enabling screening of men at risk of developing PCa as well as real-time monitoring of disease progression and treatment responses. In fact, molecular biomarkers in liquid biopsies have a long history in PCa. This is exemplified by the use of prostatic acid phosphatase (PAP) for the diagnosis of PCa since 1938 [10] and later PSA, which was FDA-approved to monitor PCa relapse in 1986 [5].

Liquid biopsies

Liquid biopsies have emerged as a promising alternative to tissue biopsies for the detection, prognosis and prediction of response to therapy, AS and post-operative monitoring of PCa. The term 'liquid biopsies' refers to the analysis of tumour cells and molecules providing information about the disease in samples of body fluids like blood or urine [11]. Such samples can be obtained in a minimally invasive or non-invasive way; therefore, liquid biopsies are particularly suitable for monitoring patients and tracking tumour evolution. Commonly studied cancer-derived analytes in liquid biopsies are circulating tumour cells (CTCs) and circulating tumour DNA (ctDNA) [12, 13]. CTCs are disseminated cancer cells that may exist in the circulation as single cells or clusters of 2–50 cells consisting of only CTCs or CTCs associated with stromal or immune cells [14]. The methods for CTC analyses range from enumeration of CTCs, which can be exploited for prognosis and early detection of relapse, to genomic, transcriptomic and proteomic profiling of CTCs and establishing ex vivo cultures or xenografts that may be of use for guiding the choice of drug treatment [15]. However, the main challenges in CTC clinical use are their very low counts in peripheral blood and their phenotypic heterogeneity [16, 17]. In localised PCa, CTCs are detectable only in a minority of patients [18, 19]. However, CTCs are detectable in 33–75% of patients with metastatic castration-resistant prostate cancer (mCRPC) and have a high prognostic and predictive significance [20–23].

Cell-free DNA (cfDNA) fragments are released into the circulation from a variety of cell types. Tumour cell-free DNA (ctDNA) represents a fraction of cfDNA that is released from apoptotic or necrotic tumour cells. ctDNA can be distinguished from normal tissue-derived cfDNA by the presence of genetic or epigenetic alterations such as somatic point mutations, rearrangements, copy number variations and tumour-specific methylation markers [17]. The half-life of ctDNA varies from around 16 min to 2.5 h, allowing real-time monitoring of tumour burden [24, 25]. Hence, ctDNA analyses could be applied for monitoring treatment responses and disease progression, and tracking intratumoural heterogeneity and evolution [26]. However, the fraction of ctDNA in the cfDNA may vary from 0.01 to 90%, and ultrasensitive methods such as digital-droplet PCR, BEAMing or tagged amplicon sequencing are required for the detection of rare tumour-derived variants in the background of wild-type cfDNA [27]. Another challenge in the clinical application of ctDNA assays is that a fraction of the genetic alterations in the cfDNA may arise from age-related clonal expansion of mutated hematopoietic cells [28].

Extracellular vesicles

EVs represent an alternative source of cancer-derived molecules in liquid biopsies [16, 17, 29, 30]. 'EV' is a generic term for all types of lipid bilayer-delimited particles that are naturally released from cells and cannot replicate [31]. According to the biogenesis pathway, the main subtypes of EVs are exosomes, microvesicles (also called ectosomes, shedding vesicles or microparticles) and apoptotic bodies [32–35]. Exosomes correspond to the released intraluminal vesicles found in the lumen of multivesicular bodies and range in size from 30 to 150 nm. Microvesicles are formed by budding and blebbing from the plasma membrane and the majority have a size range from 100 to 1000 nm [36]. Finally, apoptotic bodies are formed by blebbing of the plasma membrane or formation of membrane protrusions such as microtubule spikes, apoptopodia and beaded apoptopodia in apoptotic cells. The majority of apoptotic bodies range in size from 1 to 5 µm in diameter, though the formation of smaller vesicles during the progression of apoptosis has also been reported [37]. In PCa, large EVs (1–10 µm), usually referred to as large oncosomes, have been found to be released by shedding of membrane blebs from highly migratory cancer cells, but their biogenesis is not fully understood [38, 39]. Although the mean size of various EV subtypes is different, their size range overlaps and the current EV-isolation methods do not allow accurate separation of the EV subtypes. Therefore, the International Society for Extracellular Vesicles recommends using operational terms for EV subtypes referring to their physical or biochemical characteristics instead of the terms 'exosome' or 'microvesicle', unless their biogenesis pathway is clearly established [31].

EVs are secreted by virtually all cell types in the body and are able to reach various body fluids, including blood, urine, semen, milk, saliva, etc. [32, 40, 41]. There is not much known about the specific mechanism of EV release into body fluids, and vesicles formed by different mechanisms and cell types are expected to coexist in biofluids. Thus, vesicles that are found in biofluids would be more appropriately referred to as EVs. This is the term that will be used in this review, even if other terms may have been used in the original articles.

Although initially considered to be a waste-disposal mechanism [42], it is now clear that both EVs generated by living or apoptotic cells can be taken up by recipient cells and are important mediators of intercellular communication [37, 43]. A growing body of evidence suggests that cancer-derived EVs promote cancer progression by acting in a paracrine and systemic manner: they transfer aggressive phenotypic features and drug resistance to other cells, mediate the cross-talk with stromal cells and bone marrow, modulate the antitumour immune response and promote the formation of pre-metastatic niches [30, 44, 45].

EVs carry a variety of proteins, lipids, carbohydrates (attached to proteins and lipids), coding and non-coding RNAs, DNA fragments, metabolites and even entire organelles, such as in apoptotic bodies and possibly other EV types [32, 46–51]. Their molecular cargo partially reflects the intracellular status and physiological state of their parental cells. EVs isolated from cancer patients' body fluids have been shown to contain cancer-derived molecules such as truncated EGFRvIII [52], overexpressed MET [53], cancer-specific miRNAs and protein signatures and mutated DNA or mRNA fragments [23, 54–56]. These findings have raised the idea that the analysis of EV molecular cargo could inform about the presence and behaviour of cancer and, therefore, could be of use for diagnosis, monitoring of response to therapy, early detection of relapse and tracking tumour evolution. In fact, emerging evidence shows that DNA molecules in blood-derived EVs show superiority over ctDNA as a cancer biomarker [57, 58]. The study of EVs is a very active area of research at the moment, and several resources have been made available in the last few years to facilitate research in this exciting field (Table 1) [59].

EV-based biomarkers for PCa have been a very active research area in the last decade [60–69], and the first works already appeared in 2009 [70, 71]. In this review, we discuss the preanalytical and methodological considerations in developing EV-based assays for the diagnosis and management of PCa, and summarise patient studies investigating EV-based biomarkers for diagnosis, prognosis and monitoring of PCa (Fig. 1).

Table 1. Some resources for EV research.

Type	Name	Purpose/Description	Web address
EV molecular databases	Exocarta/Vesiclepedia	Compendium of molecular data (protein, RNA and lipid) of EVs from multiple sources.	http://www.exocarta.org/ http://www.microvesicles.org/
	EVpedia	Integrated database of high-throughput molecular data (protein, RNA and lipid) for analyses of prokaryotic and eukaryotic EVs.	http://www.evpedia.info
	exoRBase	Repository of EVs long RNAs (mRNA, lncRNA, and circRNA) derived from RNA-seq data analyses in different human body fluids.	http://www.exoRBase.org
	exRNA Atlas	Data repository of the Extracellular RNA Communication Consortium including small RNA sequencing and qPCR-derived exRNA profiles from human and mouse biofluids.	https://www.exrna-atlas.org/
Courses	Basics of Extracellular Vesicles	This MOOC course provides basic knowledge about EVs.	https://www.coursera.org/learn/extracellular-vesicles
	Extracellular Vesicles in Health and Disease	This MOOC course provides current understanding about EVs and their role in health and diseases.	https://www.coursera.org/learn/extracellular-vesicles-health-disease
	Extracellular Vesicles: From Biology to Biomedical Applications	Practical course organised by EMBO covering different EV purification and characterisation techniques and strategies to understand the role of EVs in biomedical applications.	https://www.embl.org/about/info/course-and-conference-office/events/exo22-01/
Reporting	EV-TRACK platform	Platform for recording experimental parameters of EV-related studies.	https://www.evtrack.org/
	MIFlowCyt-EV	Framework for standardised reporting of EV flow cytometry experiments.	https://www.tandfonline.com/doi/full/10.1080/20013078.2020.1713526
Guidelines/ Position papers	MISEV2018	Provide guidance in standardisation of protocols and reporting in the EV field.	https://www.pubmed.ncbi.nlm.nih.gov/30637094/
	Urinary EVs	A position paper by the Urine Task Force of the International Society for Extracellular Vesicles.	https://www.onlinelibrary.wiley.com/doi/10.1002/jev2.12093
	Blood EVs	Considerations towards a roadmap for collection, handling and storage of blood EVs.	https://www.tandfonline.com/doi/full/10.1080/20013078.2019.1647027
	EV RNA	Obstacles and opportunities in the functional analysis of extracellular vesicle RNA – an ISEV position paper.	https://www.tandfonline.com/doi/full/10.1080/20013078.2017.1286095
	EVs in therapy	Applying EV-based therapeutics in clinical trials – an ISEV position paper.	https://www.tandfonline.com/doi/full/10.3402/jev.v4.30087
Societies /Task Forces/ Working groups	ISEV	Global society of EV researchers.	https://www.isev.org/
	National societies	Societies of national EV researchers.	https://www.isev.org/national-societies
	ISEV task forces	The Rigor & Standardization Subcommittee includes several task forces for advancing specific EV areas of research such as urine EVs, blood EVs and reference materials.	https://www.isev.org/rigor-standardization
	EV Flow Cytometry Working Group	This groups aims to establish guidelines for best practices for flow cytometry analysis of EVs.	http://www.evflowcytometry.org
Conferences/Seminars	ISEV Annual Meeting	This seminar brings together EV interested scientists from around the world.	https://www.isev.org/isev-annual-meeting
	WebEVTalk	These online weekly seminars aim to support networking and to push EV science forward.	https://www.youtube.com/user/MsOlinolin/featured
	EV Club	These online weekly seminars are a venue for discussing research and published articles.	https://www.isev.org/ev-club

Table 1 continued

Type	Name	Purpose/Description	Web address
	Exosomes, Microvesicles and Other Extracellular Vesicles	Keystone symposia are a series of seminars organised for the advancement of biomedical and life sciences.	https://www.keystonesymposia.org/KS/Online/Events/2022B3/Exosomes-Microvesicles-and-Extracellular-Vesicles.aspx?EventKey=2022B3
	Extracellular vesicles	Gordon Research Conferences are a series of seminars bringing a global network of scientists together to discuss frontier research.	https://www.grc.org/extracellular-vesicles-conference/2022/
SpecializedJournals	Journal of extracellular vesicles	Publication of EV research.	https://www.onlinelibrary.wiley.com/journal/20013078
	The European journal of extracellular vesicles	Publication of EV research.	http://www.libpubmedia.co.uk/ejev/
	Extracellular Vesicles and Circulating Nucleic Acids	Publication of EV research.	https://www.evcna.com/
	Journal of extracellular biology	Publication of EV research. (Launching Late 2021)	https://www.isev.memberclicks.net/journal-of-extracellular-biology

circRNA circular RNA, *exRNA* extracellular RNA, *lncRNA* long non-coding RNA, *MISEV* minimal information for studies of extracellular vesicles, *ISEV* International Society for Extracellular Vesicles, *MOOC* massive open online course.

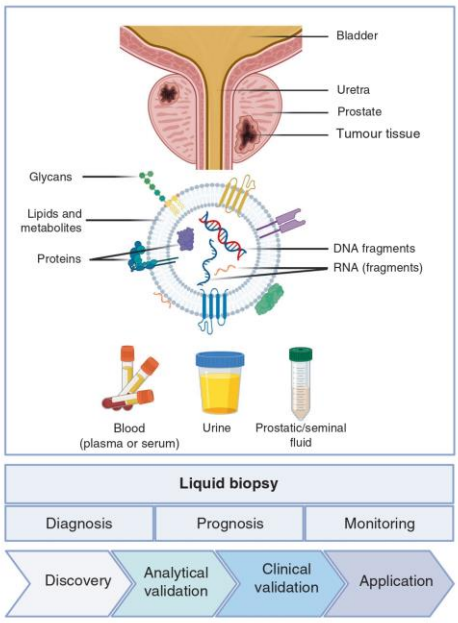

Fig. 1 Extracellular vesicles as liquid biopsies for prostate cancer. Figure designed by Elena S. Martens-Uzunova using BioRender.

EVS AS LIQUID BIOMARKERS FOR PROSTATE CANCER: METHODOLOGICAL CONSIDERATIONS

Relevant biofluids for the identification of EV-based biomarkers for prostate cancer

Several biofluids are expected to contain prostate-derived EVs [72]. The prostate is an excretory gland of the male genitourinary system located below the bladder, surrounding the proximal urethra, composed of stroma and an epithelium component [73]. The prostatic acinar epithelial cells secrete prostatic fluid, which constitutes approximately one-fifth to one-third of the semen volume and plays an essential role in male fertility [73]. Remarkably, an EV population, called prostasomes, was identified ~40 years ago in prostatic and seminal fluid [74–77]. The highest concentration of prostate-derived EVs can be expected to be found in prostatic fluid and seminal plasma. However, direct collection of prostatic fluid can be relatively invasive and the use of semen for diagnostic purposes of aging PCa patients does not appear as the best option [78]. It should also be mentioned that in addition to the prostate, EVs in seminal fluid may have other origins, such as the epididymis [79]. Importantly, gentle prostate massage can induce the secretion of prostatic fluid into the urethra, which is then mixed with urine during urination. Since prostate massage is often done in connection with a digital rectal examination (DRE), this urine is often called DRE urine. Prostatic fluid is also drained during urination in normal conditions, and possible mechanisms have been proposed [80]. Further, it has been demonstrated that the fraction of prostate-derived EV in urine is significantly enriched after DRE due to the increased amount of prostatic fluid released in the urine [71, 81, 82]. Thus, it could be beneficial to collect urine for EV analysis after DRE to enhance sensitivity. On the other hand, collection of non-DRE urine is more amenable. In any case, urine is seen as a highly suitable and desirable biofluid for liquid biopsy that can be utilised for the clinical management of PCa. Several factors contribute to this, including the minimally invasive character of urine collection, the possibility to collect relatively large volumes and the limited number of organs, i.e., the kidneys, ureters, bladder, seminal vesicles and the prostate (although several recent reports also suggest that EVs from the bloodstream can be found in urine) from which the majority of urinary EVs originate [83]. At the same time, urine is a highly dynamic biofluid and its composition and concentration depend on biorhythm, fitness and diet. This causes a large inter- and intrapersonal variability, which complicates the study of urinary EVs and the discovery and validation of urinary biomarkers in general. Other exogenic factors, such as the presence of microorganism-derived EVs from bacteria and yeast present in urine, as well as viruses with size similar to that of EVs, can additionally contribute to the complexity of the urinary EV population and complicate EV analysis in urine, for example EV quantification [84–90]. The extent by which different organs from the urogenital tract contribute to the urinary EV repertoire is yet to be established, but it has been shown that several prostate-related proteins and their mRNAs, such as PAP, PSA, prostate-specific

membrane antigen (PSMA), prostate stem cell antigen (PSCA), protein–glutamine gamma-glutamyltransferase 4 (TGM4) or transmembrane protease serine 2 (TMPRSS2), are found in urinary EVs [72, 91–93].

Blood-derived EVs have also been extensively investigated in biomarker studies. Blood is a rich source of EVs, but also contains structures that can possibly co-isolate with EVs and mask or disturb EV analyses such as cells, cell-free DNA and lipoproteins. Hence, the isolation and characterisation of blood-derived EVs with high purity is not straightforward. Blood EVs are mainly derived from platelets, red blood cells and leucocytes, as indicated by specific markers of these cell types, CD41, CD235a and CD45, respectively [94]. Blood may be especially relevant for patients with metastatic PCa, considering the distal location of the advanced metastasis of PCa (often bone metastasis) and that many patients with metastatic PCa may have undergone RP. It is not clear how prostate-derived EVs reach the blood circulation. PSA, which is normally secreted from prostate epithelial cells into prostatic fluid, can reach the blood circulation and shows increased serum levels in PCa and other prostatic diseases. This is probably due to morphological and functional changes of prostate and endothelial cells, resulting in increased permeability and leakage of the tumour vasculature, which facilitates the entrance of PSA into blood [95]. EVs are larger in size than PSA, but they may reach the blood system by a similar mechanism. Finally, a recent analysis of the literature of EVs and PCa, including articles with 50 or more patients from 2010 to 2017 (13 articles), showed that almost 30% of the analyses were performed with blood, while in the rest, urine was the selected biofluid [68].

Preanalytical considerations in EV-biomarker research

Determining inclusion patient criteria for identification of EV-based PCa biomarkers depends on the main purpose of such biomarkers, whether early diagnosis, AS, prognosis or cancer recurrence. Correct sample-size determination is vital if robust conclusions are going to be drawn from EV-biomarker studies. In any case, patient information should be carefully reported, including at a minimum gender, age and clinical-relevant information. In some studies, it may also be important to include additional information such as diet, ethnicity, body mass index, medication, food and fluid intake. In addition, it is fully recognised today that after collection of the biofluid of choice, preanalytical variables should be carefully controlled to avoid degradation before being used for EV-biomarker analysis. Preanalytical variables such as collection method, volume of sample, preservatives, processing and storage temperature can influence the results [83, 96–99], and it is, therefore, essential to report these conditions in detail. To facilitate this, a possibility is to use the Standard PREanalytical Code (SPREC), a seven-element code corresponding to the most critical preanalytical variables of biospecimens [100, 101].

Optimal parameters for the study of EVs in urine and blood (plasma is usually preferred to serum [98]), the two more relevant biofluids for PCa, are being investigated by the respective task forces of the International Society for Extracellular Vesicles (ISEV) [83, 97]. For blood, the fasting status of the donors and the choice of anticoagulant during collection are especially important, and the degree of haemolysis and levels of residual platelets in platelet-free plasma should be measured before using the samples for EV analysis [98, 99]. Concerning the latter, platelets need special attention when studying blood EVs because they can be easily activated under blood collection, handling and storage, and release EVs that may confound the results [99, 102–105]. Two subsequent centrifugations at $2500 \times g$ for 15 min have often been used to deplete platelets from plasma samples, but a protocol using a single-step centrifugation has recently been proposed [98, 102, 106]. Moreover, blood samples contain lipoproteins of similar sizes to EVs [35, 107]. When working with blood EVs, separation of lipoproteins is necessary as they are found to be more abundant (100-fold than EVs) in plasma and may confound EV analysis. Combination of methodologies such as ultracentrifugation followed by density gradient or size-exclusion chromatography can improve the purity of EV samples [108].

Urine is a biofluid in close anatomical proximity with the prostate through the prostatic urethra, and it has been the biofluid of choice in several recent studies of EV-based PCa biomarkers (Tables 2 and 3). In these studies, both urine and DRE urine have been used. As mentioned above, DRE urine is a rational choice if high amounts of EV molecules of prostatic origin are needed or if the analyte under investigation has a relatively low abundance [60]. The physiological characteristics of urine and its dynamic character as an excretory biofluid require specific preanalytical steps to assure consistent analysis and experimental results. Timely urine pre-clearing (within hours after collection) by mild centrifugation to remove shed cells is important to prevent cell lysis, which could contaminate the EV fraction with cell debris. If the precleared urine is not to be processed immediately for EV analysis, which is often the case in biobanking and in large clinical studies, it is warranted to store the precleared fraction in aliquots at temperatures below −70 °C [83]. Removal of uromodulin (also known as Tamm–Horsfall protein), a high-abundance protein in urine, has also been the focus of several studies because it forms polymer networks that can trap EVs and skew downstream analysis [109–111]. Urine composition is highly variable (pH, osmolality and concentration) and influenced by certain medications and diet, therefore, an assessment of urine-sample characteristics using dipsticks (e.g., proteins, glucose, ketones, haemoglobin, nitrite, leucocytes and pH) can provide an easy and inexpensive quality-control measure to identify deviating samples. In addition, microbial presence (endogenous, pathological or caused by contamination during sample collection) should also be taken into consideration as it can influence not only EV quantitation, but also the normalisation of experimental data.

Conventional and novel methodological approaches for the analysis of EVs in liquid biopsies

In early days, the most common method to isolate EVs was differential centrifugation, and the smaller EV population was enriched by ultracentrifugation (often at $100{,}000 \times g$) for 1–2 h [112]. Today, a plethora of methods based on different physical and molecular EV characteristics are available, including filtration, precipitation, hydrostatic dialysis, ultrafiltration, size-exclusion chromatography, immunocapture and acoustic trapping [113–119]. Moreover, a combination of different isolation methods can also be an option in some cases. Considering the diverse methodology available for EV separation, it is important to be aware of the advantages and disadvantages of the different methods, which have been presented in numerous publications [59, 114, 115, 117–120]. For example, when working with biofluids, it can be an advantage to use immunocapture with a cancer-related or a tissue-specific molecule because biofluids contain several EV populations that can mask the signal of the EV population of interest.

As shown in Tables 2 and 3, several EV-isolation methods have been used to separate EVs from biofluids to identify PCa biomarkers. A challenge in EV isolation is that different isolation methods may lead to different results, probably because the methods separate to different degrees the different types of EVs and other molecular structures present in the sample [121–124]. Moreover, it is not always practical to use some of these methods in a clinical setting for different reasons, such as low throughput, requirement of a large amount of sample or expensive and difficult-to-use instrumentation. Indeed, several easy-to-use isolation kits have been commercialised. Although these methods could be very useful in a clinical setting, a main drawback is that the isolation principle, the kit components and how they affect

Table 2. Prostate Cancer Extracellular Vesicles as Diagnostic Biomarkers.

Biomarker	Biofluid	EV isolation	Target detection	Number of patients	Comparison	Performance	Ref.
				mRNAs			
PCA3 ERG SPDEF	Urine	Urine clinical sample concentration kit (Exosome diagnostics)	RT-qPCR	195 men at initial biopsy	GS ≤ 6 vs. GS ≥ 7	RNAs + SOC AUC 0.8	[157]
				Men undergoing biopsy: Training set: 255 Testing set: 519		Training set: mRNAs + SOC AUC 0.77 Testing set: RNAs + SOC AUC 0.73	[155]
				519 men at initial biopsy		RNAs + SOC AUC 0.71	[159]
PCA3 ERG SPDEF GATA2	Urine	Ultracentrifugation	RT-qPCR	Men undergoing initial biopsy: Training set: 52 Testing set: 165	PCa vs. healthy	RNAs + SOC AUC: Training set: 0.88 Testing set: 0.72	[161]
					GS ≤ 6 vs. GS ≥ 7	RNAs + SOC AUC: Training set: 0.9 Testing set: 0.75	
PCA3 PRAC	Urine	Ultracentrifugation	RT-qPCR	89 men undergoing biopsy	PCa vs. healthy	AUC 0.723	[127]
					GS ≤ 6 vs. GS ≥ 7	AUC 0.736	
PCA3 PCGEM1	Urine	Exosome RNA isolation kit (Norgen)	RT-qPCR	271 men undergoing RP	GS ≤ 6 vs. GS ≥ 7	RNAs + SOC AUC 0.875	[162]
BIRC5 ERG PCA3 TMPRSS2:ERG TMPRSS2	Urine	100 K MWCO filtration concentrator (Millipore)	RT-qPCR	47 PCa 19 healthy men	PCa vs. healthy	BIRC5 AUC 0.674 ERG AUC 0.785 PCA3 AUC 0.681 TMPRSS2:ERG AUC 0.744 TMPRSS2 AUC 0.637	[155]
CDH3	Urine	Ultracentrifugation	Illumina gene expression microarray, RT-qPCR	Discovery cohort: 6 PCa, 4 healthy men Validation cohort: 9 PCa, 7 BPH	PCa vs. BPH	Percentage of samples where CDH3 was detected: BPH 77.78%, PCa 28.57%	[163]
		Norgen exosomal RNA purification kit		Validation cohort: 18 PCa, 7 BPH		CDH3 level significantly decreased in PCa (p 0.01)	
AGR2 splice variants	Urine	Ultracentrifugation	RT-qPCR	24 PCa 15 BPH	PCa vs. BPH	AGR2 SV-H AUC 0.96 AGR2 SV-G ACU 0.94 AGR2 WT AUC 0.91	[164]
				miRNAs			
miR-21 miR-574 miR-375	Serum	Total exosome isolation kit (Invitrogen)	RT-qPCR	10 healthy men 6 PCa post-RP 8 mPCa	PCa vs. post-RP vs. healthy men	PCa vs. healthy men: miR-21 increased 2-fold miR-574 increased 4-fold miR-375 increased 8-fold Post-RP patients showed intermediate values	[167]
miR-21 miR-200c let-7a	Plasma	SEC	RT-qPCR	50 PCa 22 BPH	PCa vs. BPH	miR-21 AUC 0.67 miR-200c AUC 0.68	[168]
					GS ≤ 6 vs. GS ≥ 8	let-7a AUC 0.68	
miR-574 miR-141 miR-21	Urine	Lectin induced agglutination	RT-qPCR	35 PCa 35 healthy men	PCa vs. healthy	miR-574 AUC 0.85 miR-141 AUC 0.86 miR-21 AUC 0.65	[169]
miR-21 miR-375 let-7c	Urine	Ultracentrifugation	RT-qPCR	60 PCa 10 healthy men	PCa vs. healthy	miR-21 AUC 0.713 miR-375 AUC 0.799 let-7c AUC 0.679	[170]
miR-21 miR-200c	Urine	miRCURY exosome isolation kit (Exiqon)	RT-qPCR	30 non-mPCa 30 mPCa 20 BPH	Non-mPCa vs. mPCa vs. BPH	miR-21 increased in non-mPCa ($p = 0.001$) and mPCa ($p = 0.018$) vs. BPH miR-200c decreased in non-mPCa (p	[128]

Table 2 continued

Biomarker	Biofluid	EV isolation	Target detection	Number of patients	Comparison	Performance	Ref.
						= 0.001) and mPCa ($p = 0.018$) vs. BPH	
					mPCa vs. non-mPCa	miR-21 decreased in mPCa ($p = 0.037$)	
miR-375 miR-451a miR-486-3p miR-485-5p	Urine	Exoquick-TC (Systems biosciences)	NGS RT-qPCR	Discovery cohort: 6 PCa 3 healthy men Validation cohort: 47 PCa 29 BPH 25 healthy men	PCa vs. healthy	miR-375 AUC 0.788 miR-451a AUC 0.757 miR-486-3p AUC 0.704 miR-486-5p AUC 0.796	[139]
					PCa vs. BPH	miR-375 + miR-451a AUC 0.726	
					Localised vs. mPCa	miR-375 AUC 0.726	
miR-21 miR-204 miR-375	Urine	Ultracentrifugation	NGS RT-qPCR	Discovery cohort: 9 PCa, 4 healthy men Validation cohort: 48 PCa, 26 healthy men	PCa vs. healthy	isomiRs AUC 0.821	[173]
miR-141	Serum	Exoquick (Systems biosciences)	RT-qPCR	31 non-mPCa 20 mPCa 40 healthy men	PCa vs. healthy	miR-141 significantly increased in PCa ($p < 0.0001$)	[174]
					Non-mPCa vs. mPCa	miR-141 AUC 0.869	
miR-141 miR-125	Plasma	ExoEasy maxi kit (Qiagen)	RT-qPCR	31 PCa 19 healthy men	PCa vs. healthy	miR-125/miR-141 AUC 0.793	[175]
miR-107 miR-574	Plasma	Filtration and concentration	Microarray RT-qPCR	Discovery cohort: 79 PCa, 28 healthy men Validation cohort: 55 PCa, 28 healthy men	PCa vs. healthy	Both miRNAs significantly increased in PCa ($p < 0.05$)	[179]
	Urine		RT-qPCR	135 men after DRE		miR-107 AUC 0.74 miR-574 AUC 0.66	
miR-145	Urine	Hydrostatic filtration dialysis, ultracentrifugation	RT-qPCR	60 PCa 37 BPH 24 healthy men	PCa vs. BPH	miR-145 + PSA AUC 0.86	[176]
miR-2909	Urine	miRCURY Exosome Isolation Kit (Exiqon)	RT-qPCR	90 PCa 10 BPH 60 bladder cancer 50 healthy men	GS ≤ 6 vs. GS 7 vs. GS ≥ 8	miR-2909 significantly increased in GS 7 compared to GS 6 and in GS 8 compared to GS 7 ($p < 0.001$)	[177]
miR-196a miR-501	Urine	Ultracentrifugation	NGS RT-qPCR	Discovery cohort: 20 PCa, 9 healthy men Validation cohort: 28 PCa, 19 healthy men	PCa vs. healthy	miR-196a AUC 0.73 miR-501 AUC 0.69	[180]
miR-30b miR-126	Urine	Ultracentrifugation	Microarray RT-qPCR	Discovery cohort: 10 PCa, 4 healthy men Validation cohort: 28 PCa, 25 healthy men	PCa vs. healthy	miR-30b AUC 0.663 miR-126 AUC 0.664	[181]
miR-23b miR-27a miR-27b miR-1 miR-10a miR-423	Urine	Acoustic trapping	NGS	147 PCa 60 healthy men	GS ≤ 8 vs. GS ≥ 9	miR-23b $p = 0.0033$ miR-27a $p = 0.0027$ miR-27b $p = 0.0136$ miR-1 $p = 0.0037$ miR-10a $p = 0.0239$ miR-423 $p = 0.0271$	[144]
miR-1246	Serum	Total exosome isolation reagent (Life technologies)	Nanostring nCounter microarray, RT-qPCR	Discovery cohort: 6 PCa, 3BPH, 3 healthy Validation cohort: 44 PCa, 4 BPH, 8 healthy	PCa vs. BPH	miR-1246 significantly increased in PCa ($p = 0.0041$)	[178]
					PCa vs. healthy	miR-1246 AUC 0.926	
miR-142-3p miR-142-5p miR-223	Semen	Ultracentrifugation	RT-qPCR	24 PCa 7 BPH 8 healthy men	PCa vs. BPH + healthy men	miR-142-3p AUC 0.739 miR-142-5p AUC 0.733 miR-233 AUC 0.722	[183]

Table 2 continued

Biomarker	Biofluid	EV isolation	Target detection	Number of patients	Comparison	Performance	Ref.
					PCa vs. BPH	miRNAs + PSA AUC 0.821	
miR-142 miR-196b miR-30c miR-34a miR-92a	Semen	Ultracentrifugation	RT-qPCR	9 PCa 5 BPH 12 healthy men	PCa vs. healthy men	miR-142, miR-196b, miR-30c and miR-34a significantly different ($p < 0.05$)	[184]
		miRCURY Exosome Cell/UrineCSF Kit (Qiagen)				No significant differences found	
		ExoGAG (NasasBiotech)				miR-142 and miR-92a significantly different ($p < 0.05$)	
				Proteins			
PSA	Plasma	Ultracentrifugation	ELISA	15 PCa 15 BPH 15 healthy men	PCa vs. BPH *vs.* healthy men	PSA expression was 4.5–5 times higher in PCA than in healthy men and BPH	[185]
				80 PCa, 80 BPH, 80 healthy men	PCa vs. BPH	PSA AUC 1	[186]
					PCa vs. healthy	PSA AUC 0.98	
TGM4 ADSV PSA PPAP CD63 SPHM GLPK5	Urine	Ultracentrifugation	SRM-proteomics	22 PCa low risk (GS 3 + 4 or lower) 31 PCa high risk (GS 4 + 3 or higher) 54 healthy men	PCa vs. healthy	TGM4 + ADSV AUC 0.65	[187]
					PCa low vs. PCa high risk	PPAP + PSA + CD63 + SPHM + GLPK5 AUC 0.7	
CD9, CD63, PSA	Urine	Ultracentrifugation	TR-FIA	67 PCa 76 healthy men	PCa vs. healthy	CD63/PSA AUC 0.68 CD9/PSA AUC 0.61	[81]
CD9	Plasma	Ultracentrifugation	TR-FIA	6 PCa 10 BPH	PCa vs. BPH	CD9 significantly increased in PCa ($p = 0.0291$)	[188]
Surface proteins	Plasma	CD13 capture	Proximity ligation assay, qPCR	Two cohorts: 20 PCa, 20 healthy men 13 PCa, 13 healthy men	PCa vs. healthy	PCa signal significantly higher in both cohorts ($p < 0.001$)	[190]
				20 GS ≤ 6 19 GS 7 20 GS 8–9	GS ≤ 6 vs. GS 7 vs. GS 8–9	GS 7 and GS 8–9 significantly higher signal than GS 6 ($p < 0.001$). No significant difference between GS 7 and GS 8–9.	
Survivin	Plasma	Ultracentrifugation	Western blot, ELISA	28 PCa 6 healthy men	PCa vs. healthy	Survivin significantly increased in PCa ($p < 0.05$)	[191]
	Serum	Exoquick (Systems Biosciences)		19 PCa, 20 BPH, 10 healthy men	PCa vs. BPH vs. healthy men	Survivin significantly increased in PCa compared to both BPH and healthy ($p < 0.001$)	
	Serum	Exoquick (Systems Biosciences)	ELISA	17 PCa (European American) 21 PCa (African American) 10 healthy men	PCa (European American) *vs.* PCa (African American) vs. healthy men	Survivin significantly higher in both PCa populations compared to healthy men ($p < 0.001$). Survivin significantly increased in African American patients ($p < 0.001$)	[192]
	Plasma			10 PCa (European American) 12 PCa (African American)	PCa (European American) vs. PCa (African American)	Survivin significantly increased in African American patients ($p < 0.001$)	
TMEM256 LAMTOR1	Urine	Ultracentrifugation	MS	16 PCa 15 healthy men	PCa vs. healthy	TMEM256 + LAMTOR1 AUC 0.94	[93]
FABP5	Urine	Ultracentrifugation	LC-MS/MS, SRM	Discovery cohort: 6 PCa GS 6, 9 PCa GS 8–9, 6 healthy men Validation cohort: 5 PCa GS 6, 13 PCA GS ≥ 7, 11 healthy men	PCa vs. healthy	FABP5 AUC 0.757	[193]
					GS ≤ 6 vs. GS ≥ 7	FABP5 AUC 0.856	

Table 2 continued

Biomarker	Biofluid	EV isolation	Target detection	Number of patients	Comparison	Performance	Ref.
PTEN	Plasma	Ultracentrifugation	Western blot	30 PCa 8 healthy men	PCa vs. healthy	PTEN detected only in EVs from PCa patients	[194]
Flot2 Park7	Urine	Ultracentrifugation	ELISA	26 PCa 16 healthy men	PCa vs. healthy	Flot2 AUC 0.65 Park7 AUC 0.71	[195]
EphrinA2	Serum	Ultracentrifugation	ELISA	50 PCa (19 GS 6–7, 31 GS 8–9; 18 T1-T2, 32 T3-T4) 21 BPH 20 healthy men	PCa vs. BPH vs. healthy	EphrinA2 AUC 0.766	[196]
					GS 6–7 vs. GS 8–9 T1-T2 vs. T3-T4	EphrinA2 level increased in GS 8–9 compared to GS 6–7 ($p = 0.02$) and in T3-T4 compared to T1-T2 ($p = 0.03$)	
Del-1	Serum	CD63 capture	ELISA	276 PCa 182 benign	PCa vs. BPH	Del-1 AUC 0.68	[197]
ITGA3 ITGB1	Urine	Ultracentrifugation	Western blot	5 non-mPCa 3 mPCa 5 BPH	mPCa vs. non-mPCa vs. BPH	Both proteins significantly increased in mPCa: ITGA3 ($p < 0.005$) ITGB1 ($p < 0.01$)	[198]
GGT1	Serum	Ultracentrifugation	Protein activity with Proteo-GREEN-gGlu	31 PCa 8 BPH	PCa vs. BPH	GGT1 activity increased in PCa EVs ($p < 0.05$), but not when measured directly in serum	[199]
STEAP1	Plasma		Nanoscale flow cytometry	121 PCa 55 healthy men	PCa vs. healthy	STEAP1 AUC 0.95	[200]
Other EV molecules or quantification methods							
LacCer(d18:1/16:0), PS 18:1/18:1, PS 18:0/18:2	Urine	Ultracentrifugation	MS	15 PCa 13 healthy men	PCa vs. healthy	Lipid combination AUC 0.989	[201]
Metabolites profile	Urine	Ultracentrifugation	UHPLC-MS	31 PCa 14 BPH	PCa vs. BPH	76 metabolites differentially expressed between PCa and BPH ($p < 0.05$)	[202]
lncRNA-p21	Urine	Urine exosome RNA isolation kit (Norgen)	RT-qPCR	30 PCa 49 BPH	PCa vs. BPH	lncRNA-p21 AUC 0.663	[204]
SAP30L-AS1, SChLAP1	Plasma	Total exosome isolation reagent (Invitrogen) followed by immunoaffinity	RT-qPCR	34 PCa 46 BPH 30 healthy men	PCA vs. BPH and healthy men	SAP30L-AS1 AUC 0.65 SChLAP1 AUC 0.87 Both RNAs AUC 0.92	[205]
sncRNA profile (miR Sentinel Test)	Urine	Urine exosome RNA isolation kit (Norgen)	Affimetrix geneChip miRNA 4.0 array	Discovery cohort: 146 PCa (90 grade 1, 34 grade 2, 9 grade 3, 7 grade 4, 6 grade 5) 89 healthy men Validation cohort: 868 PCa (437 grade 1, 162 grade 2, 131 grade 3, 66 grade 4, 72 grade 5) 568 healthy men	PCa vs. healthy	Sensitivity 94% and specificity 92%	[206]
					ISUP grade 1 vs. ISUP grade 2–5	Sensitivity 93% and specificity 90%	
					ISUP grade 1–2 vs. ISUP grade 3–5	Sensitivity 94% and specificity 96%	
Vesicle amount	Serum	Ultracentrifugation	Microfluidic raman biochip	10 PCa 8 healthy men	PCa vs. healthy	Number of vesicles significantly increased in PCa ($p < 0.0001$)	[208]

Only studies with over 10 individuals were included.

AUC area under the curve, *BPH* Benign prostate hyperplasia, *DRE* digital rectal exam, *EVs* extracellular vesicles, *GS* Gleason score, *LC* liquid chromatography, *mPCa* metastatic prostate cancer, *MS* mass-spectrometry, *MWCO* molecular weight cut off, *PCa* prostate cancer, *RP* radical prostatectomy, *SEC* size-exclusion chromatography, *SOC* standard of care, *SRM* selective reaction monitoring, *TR-FIA* time-resolved fluorescence immunoassay, *UHPLC* ultra high performance liquid chromatography, *vs.* versus.

Table 3. Prostate cancer extracellular vesicles as prognostic and monitoring biomarkers.

Biomarker	Biofluid	EV isolation	Target detection	Number of patients	Comparison	Performance	Ref.
				mRNAs			
AR-V7	Plasma	ExoRNeasy kit (Qiagen)	ddPCR	36 mCRPC before second-line hormonal treatment	AR-V7$^+$ vs. AR-V7$^-$	PFT 3 vs. 20 months, OS not reached vs. 8 months	[221]
				9 CRPC, 7 HSPC 5 healthy men	PCa vs. healthy	Similar level of AR-V7 expression in EVs	[222]
		Exoquick (System Biosciences)		35 CRPC	AR-V7$^+$ vs. AR-V7$^-$	PFT 16 vs. 28 months	[219]
AR-V7/AR-FL ratio	Urine	Exo-Hexa	ddPCR	22 HSPC, 14 CRPC 11 healthy men	CRPC vs. HSPC	AUC 0.87	[223]
	Plasma	ExoRNeasy kit (Qiagen)		73 CRPC	AR-V7$^+$ vs. AR-V7$^-$	PFS 4 vs. 20 months OS not reached vs. 9 months	[218]
CD44v8–10	Serum	ExoRNeasy kit (Qiagen)	ddPCR	50 docetaxel naive 10 docetaxel resistant 15 healthy men	Docetaxel resistant vs. docetaxel naive	46 vs. 12 copies/ml ($p = 0.032$)	[226]
					Docetaxel resistant vs. healthy men	46 vs. 17 copies/ml ($p = 0.032$)	
BRN4 BRN2	Serum	Total exosome isolation reagent (Life Technologies)	RT-qPCR	42 mCRPC 6 mCRPC with NED	mCRPC-NE vs. mCRPC	Higher levels of BRN4 and BRN2 in mCRPC-NE: EV-BRN4 AUC 1 EV- BRN2 AUC 0.944	[228]
				42 mCRPC 6 mCRPC with NED 23 CRPC	mCRPC with enz. vs. mCRPC wo enz.	EV-BRN4 FC ≈ 7 ($p < 0.0001$) EV-BRN2 FC ≈ 4 ($p < 0.0001$)	
CK-8	Plasma	ExoRNeasy kit (Qiagen)	RT-qPCR	62 mCRPC 10 healthy men	Positive vs. negative	OS 16.9 vs. 31.8 months ($p = 0.001$)	[210]
LASSO criteria (36 different mRNAs)	Urine	Microfiltration	Nanostring expression	Discovery cohort: 535 PCa Diagnostic cohort: 177 PCa Prognostic cohort: 87 PCa	D'Amico classification (normal vs. low vs. medium vs. high risk)	Model predicted the presence of clinically significant intermediate- or high-risk disease. AUC 0.77	[214]
						Able to detect BCR with HR 2.86 ($p < 0.001$)	
				miRNAs			
miR-375 miR-1290	Plasma	Exoquick (System Biosciences)	NGS RT-qPCR	Discovery cohort: 23 mCRPC Validation cohort: 100 mCRPC	High vs. low miR-375 and miR-1290 levels	OS 7.23 vs. 19.3 months miRNAs + PSA + ADT failure time predict OS with AUC 0.73	[209]
miR-141 miR-375	Serum	ExoMiR extraction kit (Bioo Scientific)	RT-qPCR	47 recurrent PCa, 72 non-recurrent PCa	Recurrent PCa vs. non-recurrent PCa	Increased levels in metastasis ($p < 0.0001$)	[179]
miR-151a miR-204 miR-222 miR-23b miR-331 PSA	Urine	miRCury exosome isolation kit (Qiagen)	RT-qPCR	Discovery cohort: 215 RP Validation cohorts: Cohort 2: 199 RP Cohort 3: 205 RP	Pre- vs. post- RT	Predictor of BCR Discovery: HR 3.12, ($p < 0.001$) Cohort 2 HR 2.24 ($p = 0.002$) Cohort 3: HR 2.15 ($p = 0.004$)	[215]
				Proteins and other molecules or EV quantification methods			
ACTN4	Serum	Ultracentrifugation	Proteomic analysis	36 PCa (8 untreated, 8 ADT, 20 CRPC different therapies)	CRPC vs. ADT	FC 1.4 ($p < 0.01$)	[227]
GSTP1 and RASSF1A methylation	Plasma	ExoRNeasy kit (Qiagen)	RT-qPCR	62 mCRPC 10 healthy men	Positive vs. negative	GSTP1 OS 8.6 vs. 21.4 months ($p = 0.015$) RASSF1A OS 8.0 vs. 22.6 months ($p = 0.007$)	[210]

Table 3 continued

Biomarker	Biofluid	EV isolation	Target detection	Number of patients	Comparison	Performance	Ref.
Vesicle amount	Serum	Total exosome isolation kit (Invitrogen)	RT-qPCR	11 PCa GS ≥ 7	Post- vs. pre-RT	FC 1.3 ($p < 0.52$)	[225]
	Plasma	Antibody-captured	Nanoscale FACS	265 PCa, 67 mCRPC, 156 BPH, 22 healthy men	mCRPC vs. PCa	Higher levels of $PSMA^+$ EVs in mCRPC	[211]
					GS ≤ 7 vs GS ≥ 8	Higher levels of $PSMA^+$ EVs in GS ≥ 8	
				25 mCRPC	Pre-RP vs. post-RP	Higher levels $PSMA^+$ EVs in pre-RP	
	Blood	Antibody-captured	ACCEPT software image analysis	190 CRPC	Low vs. high amount of EVs	OS 31.6 vs. 14.7 months HR 2.2 ($p = 0.001$)	[213]
	Blood	Antibody-captured	ACCEPT Software image analysis	Discovery: 84 mCRPC Validation: 45 mCRPC 93 Healthy men	Low vs. high amount of EVs	OS 23 vs. 8.1 months ($p < 0.001$) HR 3.8 ($p < 0.001$)	[212]

Only studies with more than 10 individuals were included in the table.
ADT androgen-deprivation therapy, *AR* androgen receptor, *AUC* area under the curve, *BCR* biochemical recurrence, *BPH* Benign prostate hyperplasia, *CI* confidence interval, *CRPC* Castration-resistant prostate cancer, *CTCs* circulating tumour cells, *ddPCR* digital-droplet PCR, *enz.* Enzatulamide, *EV* extracellular vesicles, *FL* full-length, *GS* Gleason score, *HR* Cox hazard ratio, *HSPC* hormone-sensitive prostate cancer, *mCRPC* metastatic castration-resistant prostate cancer, *NED* neuroendocrine differentiation, *OS* overall survival, *PCa* prostate cancer, *PFS* progression-free survival, *PSA* prostate-specific antigen, *RP* radical prostatectomy, *RT* radiation therapy, *v7* Variant 7, *vs.* versus, *wo* without.

other structures in the biofluid are often not clearly specified [123]. Careful consideration of the pros and cons of each method, the availability of starting material and the downstream analysis, is needed to determine the most suitable methodology for the isolation of EVs from biofluids. In fact, it should be considered if it is necessary to separate EVs from the biofluid because isolation protocols often lead to EV loss and can be biased towards an EV population. Direct and rapid analyses of EVs in biofluids would be an advantage for clinical implementation [83].

The molecular content of EVs shows a large diversity, but the search for novel PCa EV biomarkers has focused mainly on the analysis of proteins, mRNAs, lncRNAs and miRNAs in EVs isolated from urine or blood. Standard analytical methods to analyse the molecule of interest, such as immune-based methods for protein analysis and PCR for nucleic acid analysis, have often been used (Tables 2 and 3). In addition, several omics methods allowing simultaneous analysis of many molecules, i.e., mass spectrometry (MS) and next-generation sequencing, have also been very useful for identifying novel EV biomarkers for PCa [83]. Moreover, changes in EV numbers are also being investigated as a PCa biomarker. For EV-biomarker analysis, the normalisation method should be carefully chosen to obtain solid results. Several normalisation methods have been used when analysing EVs in liquid biopsies for prostate cancer, such as the levels of urinary PSA, the number of vesicles or the total vesicle-protein amount [81, 83]. There is not a universal normalisation method for the results of EV experiments, and the ideal normalisation method depends on the biofluid, sample handling and target molecule. Working with urine requires additional care because the concentration of EVs in this biofluid is affected by the overall urine concentration, which shows great inter- and intra-patient variability. A recent study has shown that the levels of creatinine, which is commonly used to normalise soluble urinary biomarkers, are highly correlated with the number of EVs [125]. The same study also reported that the addition of uromodulin affects the particle counts. It is also important to consider that the preparation and analysis of EVs is a potential source of variability. In order to account for this, trackable recombinant EVs have recently been developed [126, 127]. Spiking this or other reference materials in biofluids can be used to normalise for technical errors during sample preparation and analysis between samples. Finally, the normalisation of molecular data is also a challenge. For example, several strategies have been developed for the normalisation of RNA results [126]. The results of some studies have been normalised to the level of one or several reference transcripts [127–129]. An interesting alternative is the use of the geometric mean of all the studied RNA species [130]. Finally, adding a synthetic spike-in RNA during different stages of the RNA analysis can be a helpful tool to avoid bias caused by library preparations or PCR efficiencies [131].

Since the different areas of EV research have different demands in terms of EV isolation, some recent articles have focused on the isolation and analysis of EVs from biofluids using novel technologies such as microfluidic, nanotechnology and label-free approaches [132–134]. For example, microfluidic EV-isolation technologies have gradually emerged in the last few years, having the potential to overcome many of the drawbacks associated with conventional isolation techniques [135]. These techniques offer several benefits such as low sample volumes, low costs, high precision and automation. The advances in nanofabrication and the possibility to integrate nanomaterials to enhance the performance of the devices can provide unprecedented opportunities in the biosensing field [134, 136–138]. Further, the integration of isolation of EVs with their detection and analysis on the same platform can boost the next generation of point-of-care devices. Microfluidic EV-isolation techniques are generally based on EV-surface markers (immunoaffinity capture) or physical characteristics of EVs such as size, charge or density

[107, 117, 139, 140]. Immunoaffinity relies on the use of antibodies (or beads coated with antibodies) against EV-surface proteins. The most commonly used antibodies target tetraspanin proteins such as CD63 or CD9, which are generally enriched in EV membranes. Besides, EVs from different cell origin can be selectively recognised by using antibodies against molecules overexpressed in cancer cells [141]. On the other side, EVs can be isolated, depending on their physical properties. Nanoscale deterministic lateral-displacement pillar arrays are an efficient technology to sort and separate EVs, because EVs follow different trajectories in a pillar array depending on their size [142]. When integrating these arrays on a chip, a superior yield of EVs was isolated from serum and urine compared with conventional isolation techniques such as ultracentrifugation or density-gradient ultracentrifugation [143]. Ultrasonic waves can also be used to isolate and enrich EVs, enabling downstream small RNA sequencing from PCa clinical samples [144]. In addition, electrostatic interactions were used as separation principle in a nanowire-anchored microfluidic device that also allowed in situ extraction of RNA [140]. When applied to urine samples, the device showed higher efficiency of miRNA extraction and a much larger variety of miRNAs than ultracentrifugation. However, the positively charged surface nanowires have low selectivity in terms of EV analysis because they collect indiscriminately negatively charged structures in urine, including EVs and free negatively charged molecules such as miRNAs [140]. Another technology that has been described to separate EVs in a size-dependent and label-free manner is viscoelasticity-based microfluidics, showing a high level of recovery (>80%) and purity (>90%) of EVs [145]. Similarly, sheathless oscillatory viscoelastic microfluidics has been used to separate EVs, although further research is needed to bring these technologies into the clinics [146].

In addition to EV isolation, the possibility to integrate EV detection and analysis within the same platform is gaining considerable attention. Combining microfluidics with techniques, such as fluorescence, surface plasmon resonance, colorimetric or electrochemical detection, has opened the path towards clinical translation [147]. Pioneering examples of these platforms include the ExoChip device that can isolate EVs directly from blood using a microfluidic device functionalized with anti-CD63 antibodies and quantify them using a fluorescent dye and a plate reader [148]. Going a step further, the ExoSearch chip allows on-chip isolation and multiplexed detection of tumoural EV in 40 min [149]. The integration of these platforms with detection systems or smartphones as imaging read-out systems is emerging as an ideal approach for point-of-care diagnosis due to the excellent portability and cost-effectiveness of these devices [150–153]. Although much effort has been done for the development of portable and automatised devices for the isolation, detection and analysis of EVs, many of the reports are still at a proof-of-concept level [134].

EV-BASED BIOMARKERS FOR PROSTATE CANCER

A main aim of the studies of EV-based biomarkers for PCa is to improve detection of clinically significant PCa and aid clinical decision-making for patients within each risk group. Biomarkers can be divided into different categories based on their particular application [154]. In this review, we have classified the identified EV biomarkers into two main groups. In the group of diagnostic biomarkers, we have included the biomarkers used for the detection of PCa and/or the stratification of patients according to GS or ISUP grade (Table 2). The biomarkers that predict survival rates, cancer progression, probability of metastasis and development of treatment resistance or cancer recurrence have been included in the prognostic and monitoring group (Table 3). Only studies containing more than 10 individuals are included in the tables.

Prostate-cancer extracellular vesicles as diagnostic biomarkers

Studies of diagnostic biomarkers have compared PCa patients with healthy individuals, but also to patients afflicted with benign prostate hyperplasia (BPH), which is also usually related to an increased serum PSA level. Additionally, several publications have addressed the necessary distinction between low-risk PCa, which may not require aggressive treatment, and intermediate- and high-risk prostate tumours that require treatment. Usually GS or the equivalent ISUP grade, together with PSA and clinical stage, is used to classify the PCa risk [3].

In 2009, Nilsson et al. showed that the RNAs PCA3 and TMPRSS2:ERG were found in urinary EVs [71]. Interestingly, the presence or absence of TMPRSS2:ERG in urinary EVs mimics the results from prostate biopsies [155]. While one study claimed that the expression of PCA3 alone in urinary EVs is not a good predictor of PCa [156], others found that PCA3, ERG, BIRC5, TMPRRS2 and TMPRRS2:ERG can differentiate between healthy and PCa patients [155]. The analysis of a cohort of 195 men showed that the expression of PCA3 and ERG genes (including the fusion gene TMPRSS2:ERG) normalised to the level of SPDEF (SAM-pointed domain-containing Ets transcription factor) can be used to differentiate between GS ≤ 6 and GS ≥ 7 tumours [157]. This result was later confirmed in independent cohorts of 519 and 503 patients [158, 159]. These results are the basis of the EV-based ExoDx PCa test, which helps to decide about biopsy for men over the age of 50 and PSA 2–10 ng/ml [160]. In the first study from 2009, sequential centrifugation was used to isolate EVs from both DRE- and non-DRE urine [71]. Later studies have used non-DRE urine and ultrafiltration centrifugation to concentrate the vesicles and detect PCA3 and ERG [158, 159]. Additionally, a recent independent study including 217 men proposed that the addition of GATA2 to this model could improve the detection of high-risk PCa [161]. Further studies with urinary EVs have reported that the ratio between PCA3 and PCa-susceptibility candidate (PRAC) can differentiate both between healthy men and PCa patients and between GS ≤ 6 and GS ≥ 7 in a cohort of 89 individuals [127] and that PCA3, together with PCGEM1, can be used to distinguish between favourable and unfavourable intermediate tumours (GS 3 + 4 vs GS 4 + 3 or higher) in a racially diverse cohort of 271 patients [162]. Analysis of a microarray panel identified a decrease in CDH3-expression level in PCa patients compared with BPH in independent cohorts using different EV-isolation methods [163]. The different AGR2 splice variants can also distinguish between BPH and PCa [164].

Several miRNAs previously identified as PCa biomarkers have been detected in EVs. miR-21 is one of the most commonly identified [165, 166]. Li et al. compared the expression of miR-21, miR-574 and miR-375 in serum EVs of treated and untreated PCa patients as well as healthy men, and showed that the miRNAs levels were higher in untreated patients than in healthy donors, while patients after RP showed an intermediate level [167]. Later studies have confirmed the increase in miR-21 levels in PCa patients compared with healthy individuals or BPH patients in plasma [168] and urine [128, 169, 170]. Other prominent miRNAs previously detected in liquid biopsies for PCa and later identified in EVs are miR-375 and miR-141 [171, 172]. miR-375 was also found differentially expressed between PCa patients and healthy donors in urinary EVs in a cohort of 70 men [170], and was also selected in an independent discovery cohort [129]. Interestingly, one study could not find differences in miR-21 or miR-375 levels in urinary EVs, but detected a significant change in the expression of their corresponding isomiRs [173]. miR-141 has also been found to be deregulated in EVs in both urine [169, 174] and plasma [175]. A few other miRNAs previously related to PCa have also been validated in urinary EVs, such as miR-145 [176], miR-2909 [177] and miR-200c [128].

Several studies have been designed to identify novel EV miRNAs for PCa diagnosis. miR-1246 was found significantly altered in the

serum of PCa patients [178]. In addition, miR-574 and miR-107 have been identified in plasma samples as PCa biomarkers [179]. These miRNAs showed a similar behaviour in urinary EVs [169, 179]. Other miRNAs such as miR-196a and miR-501 [180], miR-451a and miR-486 [129] and miR-30b and miR-126 [181] were found to be altered in urinary EVs of PCa patients compared with healthy men. Recently, Ku et al. developed a new technique for urinary EV isolation, acoustic trapping, and detected several miRNAs deregulated in patients with high-risk PCa (grade 3 or lower versus grades 4 and 5) [144]. One of them was miR-23b, which had previously been found to be deregulated in plasma EVs of PCa patients compared with healthy donors [182]. In terms of other biofluids, Barcelo et al. showed that miRNAs found in EVs isolated from semen can also be used as biomarkers in a discovery cohort of 12 patients and in a validation cohort of 39 individuals. They reported that a model including PSA and 3 miRNAs (miR-142-3p, miR-142-5p and miR-223) could differentiate between PCa and BPH patients, while the combination of PSA, miR-342 and miR-374 was able to distinguish GS 6 from GS 7 [183]. The first model was later confirmed using 3 different EV-isolation protocols in an independent cohort of 26 donors [184].

Logozzi et al. studied the potential of PSA associated with plasma vesicles as a biomarker. In a cohort of 45 individuals, the EV–PSA level was higher in PCa patients than in BPH patients or healthy individuals [185]. A follow-up study, including 240 individuals, showed that EV-derived PSA outperforms the conventional PSA test [186]. An MS analysis of urinary EVs also included PSA in a panel of 5 proteins (CD63–GLPK5–SPHM–PSA–PAPP) able to distinguish between low- and high-grade patients [187]. Moreover, the tetraspanins CD63 and CD9 were analysed in DRE urine (100 µl of cell-free urine) using a time-resolved fluorescence immunoassay developed by Duijvesz et al. for capture/detection of PCa-derived EVs. Using this sensitive assay, the expression level of CD63 and CD9, normalised to urinary PSA, was higher in PCa patients than in healthy men [81]. Interestingly, it was also found that the levels of CD9 and CD63 were very low in urine from women, men after prostatectomy and non-DRE urine. Using the same assay, Soekmadji et al. reported that the CD9 level was higher in plasma of PCa patients than in benign patients [188]. Moreover, EV immunocapture with CD13/aminopeptidase N, a protein found in semen EVs [189], was used to develop a proximity-ligand assay using four antibodies attached to DNA strands as analytical method [190]. It was shown then that the signals measured directly in blood samples from PCa patients were higher compared with healthy men. This assay also distinguished patients with GS ≤ 6 from patients with higher GS.

Another protein that has been investigated as PCa biomarker is survivin, a member of the inhibitor of apoptosis family of proteins. The levels of this protein in plasma EVs measured by ELISA were reported to be higher in PCa patients than in BPH patients or healthy individuals [191], and this result was later confirmed in an independent cohort [192]. MS allows the identification of over 1000 proteins simultaneously and has been used for the discovery of novel EV-based PCa biomarkers. For example, MS analysis of urinary EVs from healthy men and PCa patients found several deregulated proteins, including TMEM256 and LAMTOR1 [93]. Another study showed that FABP5 distinguished between healthy individuals and patients with low-risk (GS 6) and intermediate–high-risk PCa tumours [193]. The EV levels of PTEN [194], flotillin 2 and PARK7 [195], ephrinA2 [196], Del-1 [197], the integrins ITGA3 and ITGB1 [198] and GGT1 activity [199] have also been reported to differentiate between PCa patients and healthy individuals and/or BPH patients. In addition, the prostate-enriched protein STEAP1 was found to be increased in plasma samples of PCa patients compared with healthy males [200].

While mRNAs, miRNAs and proteins are the most common molecules studied as PCa biomarkers, some reports highlight the potential of using other types of EV cargos. Skotland et al. found several lipid species in urinary EVs that were differentially expressed in PCa patients and healthy men [201]. Moreover, Clos-Garcia et al. identified 76 lipids and metabolites differentially expressed between PCa and BPH in urinary EVs [202]. Interestingly, urinary EVs seem to reflect several metabolic alterations reported in PCa, including phosphathidylcholines, acyl carnitines and citrate. Puhka et al. have also shown the potential of metabolomics analysis of urinary EVs in PCa [203]. For EV-derived nucleic acid cargo, three long non-coding RNAs have been proposed to differentiate between prostate tumours and BPH: lncRNA-p21 in urine [204] and SAP30L-AS1 and SChLAP1 in plasma [205]. The different miR Scientific's Sentinel tests use a profile of urinary EV small non-coding RNAs to differentiate between healthy and PCa patients or stratify according to the ISUP grade [206]. Other projects have explored the possibility of using light-scattering techniques for EV analysis. Krafft et al. showed that the Raman spectra of EVs from PCa patients and healthy individuals were different [207], and in another study, the amount of vesicles estimated by spectroscopy was higher in PCa patients than in healthy men [208].

Prostate-cancer extracellular vesicles as prognostic and monitoring biomarkers

Several studies have reported alterations in the expression levels of EV miRNAs isolated from CRPC patients and their prognostic power. For instance, an increase in miR-1290 and miR-375 levels has been associated with poor overall survival (OS) (7.23 months vs. 19.3 months) [209]. In serum EVs, the expression of miR-375 and miR-141 was able to distinguish recurrent from non-recurrent PCa [179].

Another study performing a direct comparison of DNA-methylation markers and gene expression between paired CTCs and plasma-derived EVs of mCRPC patients showed that CK-8 expression, together with RASSF1A and GSTP1 methylation, correlated with lower OS (16.9 months vs. 31.8 months, 8.0 months vs. 22.6 months and 8.6 months vs. 21.4 months, respectively) [210]. Moreover, when comparing PSMA-positive plasma EV levels in mCRPC patients, BPH patients and healthy men, PSMA-positive EVs were predominant in mCRPC [211]. This result correlates with recent findings by Nanou et al. where a higher amount of tumour-derived EVs were found in the plasma of CRPC patients compared with healthy men, and that an increase in EV numbers was associated with lower OS [212, 213]. Another approach used the RNA expression profiles from urinary EVs to predict cancer progression within 5 years in a cohort of AS patients [214]. RNA profiling also showed that the expression of five miRNAs in EV-enriched urine (miR-151a-5p, miR-204-5p, miR-222-3p, miR-23b-3p and miR-331-3p) and serum PSA levels predicted the time of recurrence after RP in 3 independent cohorts [215].

Several studies have identified biomarkers that could serve as drug-resistance predictors for PCa treatment [216, 217]. Androgen receptor (AR) variants, in particular, the AR-Variant 7 (AR-V7), are of special interest due to their crucial role in CRPC development [218–220]. In 2016, Del Re et al. reported that 36% patients of a CRPC cohort were positive for AR-V7 mRNA in plasma-derived EVs. AR-V7 EV expression correlated with lower mean progression-free survival (20 vs. 3 months) and OS (not reached vs. 8 months) [221]. In contrast, other studies reported that only a minor fraction of plasma-derived EVs from CRPC patients contained AR-V7 and suggested that CTCs might be a better predictor for AR-therapy failure [23, 222]. Higher levels of AR-V7 transcripts have also been shown in urinary EVs derived from CRPC patients compared with hormone-sensitive PCa patients [223].

Among other potential biomarkers, studies analysing EVs in serum of CRPC patients have shown that the tandems miR-654-3p and 379-5p and miR let-7a-5p and miR-21-5p might predict the efficiency of RT [224, 225]. In addition, CD44v8–10 mRNA copy numbers could predict resistance to docetaxel [226]. While comparing serum EV-protein content released by CPRC patients versus localised PCa patients receiving ADT treatment, proteomic analysis revealed that actinin-4 was highly expressed in the CPRC

Table 4. Challenges and possible solutions for the analysis of EVs in liquid biopsies for prostate cancer.

Limitations & challenges	Solutions & future directions
Translational	
Poor reproducibility due to incomplete description of patient cohorts and biofluid collection and storage protocols.	- Increase awareness of reporting importance. - Implement guidelines for minimal reporting information.
Low availability of biobanks designed specifically for the needs of EV research.	- Better understanding of how biofluid collection and storage parameters affect EV properties. - Establish biobanks that match the needs of EV research.
High variability of study outcome due to low cohort size and lack of cross-validation.	- Use larger cohorts. - Increase the number of multisite studies.
Biomarker studies do not always address a real clinical need in prostate cancer.	- Identify clinical questions where EVs analysis can be an advantage. - Improve dialog between EV scientists, urologists and oncologists.
Sub-optimal performance of the identified EV biomarkers.	- Use multiplexing of different types of EV molecules such as different RNA molecular types, or RNA and proteins. - Use multiplexing of EV molecules and non EV molecules in the biofluid. - Study if the candidate biomarker performs better in other biofluid or in a specific subpopulation of prostate-cancer patients. - Study EV molecules that have not received much attention so far and molecular modifications (e.g. lipids, glycans).
Methodological	
Poor reproducibility due to incomplete description of EV isolation methods.	- Increase awareness of reporting importance. - Implement guidelines for minimal reporting information. - Advocate transparent information sharing about the components of commercial kits for EV isolation.
Poor reproducibility due to the high variety of EV-isolation methods.	- Use reference materials to compare and normalise the results obtained by different methods. - Explore direct analysis of EVs without prior isolation.
Misinterpretation of results due to confounders in biofluids.	- Perform control experiments to confirm that the molecule of interest is associated with EVs. - Use spike-in and endogenous controls. - Register and monitor biofluid parameters (e.g. blood and uromodulin in urine, urine pH and protein concentration, haemolysis, platelets, lipoprotein content).
High heterogeneity of the EV population in biofluids (different release mechanisms, different cells of origin) and low relative abundance of prostate-derived EVs hamper the detection of prostate-cancer biomarkers.	- Gain insight into how different EV-isolation methods affect the yield of different EV populations. - Identify prostate and prostate-cancer-specific EV molecules. - Develop methods to isolate prostate-specific EV populations.
Low sensitivity of the analytical method.	- Develop more sensitive analytical tools for EV analysis. - Optimise yield of EV-isolation methods. - For urine, perform DRE to increase prostate-derived EV numbers.
Lack of optimal normalisation methods and endogenous normalisation controls.	- Design and execute systematic studies addressing normalisation methods and their optimal utilisation. - Develop reference materials.
Laboratory methodology is too complex for clinical implementation.	- Develop robust, fast and cheap methods for detection and quantification of EVs and EV biomarkers. - Improve communication between academia, hospitals and industry.

cohort [227]. An interesting study conducted by Bhagirath et al. has shown that enzalutamide treatment increases the release of BRN4 and BRN2 mRNA via serum EVs and that it may modulate the progression from CRPC to neurocrine PCa [228].

Finally, it is plausible that some of the previously identified PCa biomarkers in biofluids are indeed part of EVs, for example, caveolin-1, a membrane protein that plays a role in PCa cell survival [229, 230]. The levels of caveolin in serum have been reported to be higher in PCa patients than in healthy men and men with BPH [231]. In addition, the preoperative level of serum caveolin-1 can predict decreased time to cancer recurrence [232].

CHALLENGES AND POSSIBLE SOLUTIONS FOR THE USE OF EVS IN LIQUID BIOPSIES FOR PROSTATE CANCER

As presented in this review, EVs have actively been investigated in the last decade as potential biomarkers for PCa in liquid biopsies. However, the analysis of EVs in biofluids is not trivial, and several challenges have been found in the translation of EV-based biomarkers into the clinic [233–235]. Table 4 shows the main challenges and possible solutions for the analysis of EVs in liquid biopsies for PCa. For example, a main challenge has been the initial lack of methodological consensus and reporting in the EV field, now addressed by several initiatives such as MISEV and EV-track [31, 236]. Another hurdle that still needs to be overcome is the heterogeneity of EVs. All biofluids contain a complex mixture of EVs released by various mechanisms from various cell types. Cancer-derived EVs most likely constitute a small and variable fraction of EVs present in biofluids, therefore, cancer-derived molecules are highly diluted. Moreover, various subsets of EVs produced by the same cell type have been shown to differ in their protein and RNA composition [237–239]. Hence, a deeper understanding into the heterogeneity of EVs in terms of their biophysical properties, composition of surface molecules and molecular cargo, is needed to develop more specific and sensitive assays for detecting EV-based cancer biomarkers. Finally, when

EVs began to be considered as a potential source for biomarkers, there was in general an incomplete understanding in the EV community about the specific clinical needs and the long and thorough pipeline required for the successful development of clinical biomarkers [233, 240–242]. These initial studies constitute, however, a proof-of-principle that can be further developed in multidisciplinary teams in the coming years. Importantly, in the last few years, EV-biomarker studies have been more carefully planned and have included more patients. Therefore, it is to be expected that in a close future some of these biomarkers will move from the discovery phase to analytical validation, clinical validation and finally clinical application. Besides, it would be very interesting to investigate the function of novel EV biomarkers in the disease and their possible use as therapeutic target.

Today, it is considered that multiplex biomarker assays perform better than single cancer biomarkers, and many available cancer-diagnostic assays are based on the detection of several molecules [4, 6–8]. In this respect, EVs are particularly interesting because they contain hundreds of proteins, nucleic acids, lipids and metabolites. EV molecules belonging to the same molecular type can be analysed together, but different types of molecules such as proteins and RNAs can also be analysed in the same sample. This constitutes a promising approach, still in its early days [29]. Moreover, the molecular content of EVs could be analysed together with other liquid biomarkers to increase the robustness of cancer diagnostic tests.

CONCLUSION

The implementation of novel liquid biopsies in the clinic is necessary to bring PCa care to the next level in the field of precision medicine. Body fluids are easily accessible, enabling screening of men at risk of developing PCa and real-time monitoring of disease progression and treatment responses. Therefore, liquid biopsies are expected to become part of PCa care from diagnosis till the end of treatment, helping to improve the treatment-response rate and reduce unnecessary side effects. To reach these goals, we need to continue the search for biomarkers addressing real clinical needs, to increase the number of prospective studies to show clinical benefits of the putative markers already known and to analyse the costs of using biomarkers in the clinic from a societal perspective.

While the majority of the identified EV-based biomarkers have still not reached the clinic, many studies have shown their clinical potential, and the first test has been commercialised [159, 206]. In the coming years, we expect to obtain a better understanding of (cancer) EV biology and develop more precise and sensitive technology for their detection. Furthermore, the use of a multidisciplinary approach in the design of EV-biomarker studies, the design of clinically friendly EV analytical assays and a good understanding of the requirements for regulatory approval will help to accelerate the translation of EV-based biomarkers into clinical assays for PCa and other diseases.

DATA AVAILABILITY

Not applicable.

REFERENCES

1. Sung H, Ferlay J, Siegel RL, Laversanne M, Soerjomataram I, Jemal A, et al. Global cancer statistics 2020: GLOBOCAN estimates of incidence and mortality worldwide for 36 cancers in 185 countries. CA Cancer J Clin 2021;71:209–49.
2. Egevad L, Delahunt B, Srigley JR, Samaratunga H. International society of urological pathology (ISUP) grading of prostate cancer—An ISUP consensus on contemporary grading. APMIS 2016;124:433–5.
3. D'Amico AV, Whittington R, Malkowicz SB, Cote K, Loffredo M, Schultz D, et al. Biochemical outcome after radical prostatectomy or external beam radiation therapy for patients with clinically localized prostate carcinoma in the prostate specific antigen era. Cancer. 2002;95:281–6.
4. Prensner JR, Rubin MA, Wei JT, Chinnaiyan AM. Beyond PSA: the next generation of prostate cancer biomarkers. Sci Transl Med. 2012;4:127rv123.
5. De Angelis G, Rittenhouse HG, Mikolajczyk SD. Blair Shamel, L., Semjonow, A. Twenty years of PSA: from prostate antigen to tumor marker. Rev Urol. 2007;9:113–23.
6. Murphy L, Prencipe M, Gallagher WM, Watson RW. Commercialized biomarkers: new horizons in prostate cancer diagnostics. Expert Rev Mol Diagn. 2015;15:503.
7. Tonry C, Finn S, Armstrong J, Pennington SR. Clinical proteomics for prostate cancer: understanding prostate cancer pathology and protein biomarkers for improved disease management. Clin Proteom. 2020;17:41.
8. Sharma, P, Zargar-Shoshtari, K, Pow-Sang, JM. Biomarkers for prostate cancer: present challenges and future opportunities. Futur Sci OA. 2016;2:FSO72.
9. Silberstein JL, Pal SK, Lewis B, Sartor O. Current clinical challenges in prostate cancer. Transl Androl Urol. 2013;2:122–36.
10. Gutman AB, Gutman EB. An "acid" phosphatase occurring in the serum of patients with metastasizing carcinoma of the prostate gland. J Clin Invest. 1938;17:473–8.
11. Babayan A, Pantel K. Advances in liquid biopsy approaches for early detection and monitoring of cancer. Genome Med. 2018;10:21.
12. Pantel K, Alix-Panabieres C. Liquid biopsy and minimal residual disease—latest advances and implications for cure. Nat Rev Clin Oncol. 2019;16:409–24.
13. Siravegna G, Mussolin B, Venesio T, Marsoni S, Seoane J, Dive C, et al. How liquid biopsies can change clinical practice in oncology. Ann Oncol. 2019;30:1580–90.
14. Amintas, S, Bedel, A, Moreau-Gaudry, F, Boutin, J, Buscail, L, Merlio, JP et al. Circulating tumor cell clusters: united we stand divided we fall. Int J Mol Sci. 2020;21:2653.
15. Mout L, van Dessel LF, Kraan J, de Jong AC, Neves RPL, Erkens-Schulze S, et al. Generating human prostate cancer organoids from leukapheresis enriched circulating tumour cells. Eur J Cancer. 2021;150:179–89.
16. Alix-Panabieres C, Pantel K. Liquid biopsy: from discovery to clinical application. Cancer Disco. 2021;11:858–73.
17. De Rubis G, Rajeev Krishnan S, Bebawy M. Liquid biopsies in cancer diagnosis, monitoring, and prognosis. Trends Pharm Sci. 2019;40:172–86.
18. Zapatero A, Gomez-Caamano A, Cabeza Rodriguez MA, Muinelo-Romay L, Martin de Vidales C, Abalo A, et al. Detection and dynamics of circulating tumor cells in patients with high-risk prostate cancer treated with radiotherapy and hormones: a prospective phase II study. Radiat Oncol. 2020;15:137.
19. Meyer CP, Pantel K, Tennstedt P, Stroelin P, Schlomm T, Heinzer H, et al. Limited prognostic value of preoperative circulating tumor cells for early biochemical recurrence in patients with localized prostate cancer. Urol Oncol. 2016;34:235 e211–236.
20. Goldkorn A, Tangen C, Plets M, Morrison GJ, Cunha A, Xu T, et al. Baseline circulating tumor cell count as a prognostic marker of PSA response and disease progression in metastatic castrate-sensitive prostate cancer (SWOG S1216). Clin Cancer Res. 2021;27:1967–73.
21. Scher HI, Armstrong AJ, Schonhoft JD, Gill A, Zhao JL, Barnett E, et al. Development and validation of circulating tumour cell enumeration (Epic Sciences) as a prognostic biomarker in men with metastatic castration-resistant prostate cancer. Eur J Cancer. 2021;150:83–94.
22. Wang C, Zhang Z, Chong W, Luo R, Myers RE, Gu J, et al. Improved prognostic stratification using circulating tumor cell clusters in patients with metastatic castration-resistant prostate cancer. Cancers. 2021;13:268.
23. Strati A, Zavridou M, Bournakis E, Mastoraki S, Lianidou E. Expression pattern of androgen receptors, AR-V7 and AR-567es, in circulating tumor cells and paired plasma-derived extracellular vesicles in metastatic castration resistant prostate cancer. Analyst. 2019;144:6671–80.
24. Wan JCM, Massie C, Garcia-Corbacho J, Mouliere F, Brenton JD, Caldas C, et al. Liquid biopsies come of age: towards implementation of circulating tumour DNA. Nat Rev Cancer. 2017;17:223–38.
25. Saarenheimo J, Eigeliene N, Andersen H, Tiirola M, Jekunen A. The value of liquid biopsies for guiding therapy decisions in non-small cell lung cancer. Front Oncol. 2019;9:129.
26. Leja M, Line A. Early detection of gastric cancer beyond endoscopy—new methods. Best Pr Res Clin Gastroenterol. 2021;50–51:101731.
27. Diaz LA Jr, Bardelli A. Liquid biopsies: genotyping circulating tumor DNA. J Clin Oncol. 2014;32:579–86.
28. Xie M, Lu C, Wang J, McLellan MD, Johnson KJ, Wendl MC, et al. Age-related mutations associated with clonal hematopoietic expansion and malignancies. Nat Med. 2014;20:1472–8.
29. Yu W, Hurley J, Roberts D, Chakrabortty SK, Enderle D, Noerholm M, et al. Exosome-based liquid biopsies in cancer: opportunities and challenges. Ann Oncol. 2021;32:466–77.

30. Vasconcelos MH, Caires HR, Abols A, Xavier CPR, Line A. Extracellular vesicles as a novel source of biomarkers in liquid biopsies for monitoring cancer progression and drug resistance. Drug Resist Updat. 2019;47:100647.
31. Thery C, Witwer KW, Aikawa E, Alcaraz MJ, Anderson JD, Andriantsitohaina R, et al. Minimal information for studies of extracellular vesicles 2018 (MISEV2018): a position statement of the International Society for Extracellular Vesicles and update of the MISEV2014 guidelines. J Extracell Vesicles. 2018;7:1535750.
32. Yanez-Mo M, Siljander PR, Andreu Z, Zavec AB, Borras FE, Buzas EI, et al. Biological properties of extracellular vesicles and their physiological functions. J Extracell Vesicles. 2015;4:27066.
33. Hessvik NP, Llorente A. Current knowledge on exosome biogenesis and release. Cell Mol Life Sci. 2018;75:193–208.
34. van Niel G, D'Angelo G, Raposo G. Shedding light on the cell biology of extracellular vesicles. Nat Rev Mol Cell Biol. 2018;19:213–28.
35. Mathieu M, Martin-Jaular L, Lavieu G, Thery C. Specificities of secretion and uptake of exosomes and other extracellular vesicles for cell-to-cell communication. Nat Cell Biol. 2019;21:9–17.
36. Gurung S, Perocheau D, Touramanidou L, Baruteau J. The exosome journey: from biogenesis to uptake and intracellular signalling. Cell Commun Signal. 2021;19:47.
37. Caruso S, Poon IKH. Apoptotic cell-derived extracellular vesicles: more than just debris. Front Immunol. 2018;9:1486.
38. Vagner T, Spinelli C, Minciacchi VR, Balaj L, Zandian M, Conley A, et al. Large extracellular vesicles carry most of the tumour DNA circulating in prostate cancer patient plasma. J Extracell Vesicles. 2018;7:1505403.
39. Minciacchi VR, You S, Spinelli C, Morley S, Zandian M, Aspuria PJ, et al. Large oncosomes contain distinct protein cargo and represent a separate functional class of tumor-derived extracellular vesicles. Oncotarget. 2015;6:11327–41.
40. Murillo OD, Thistlethwaite W, Rozowsky J, Subramanian SL, Lucero R, Shah N, et al. exRNA atlas analysis reveals distinct extracellular RNA cargo types and their carriers present across human biofluids. Cell. 2019;177:463–77 e415.
41. Zonneveld MI, van Herwijnen MJC, Fernandez-Gutierrez MM, Giovanazzi A, de Groot AM, Kleinjan M, et al. Human milk extracellular vesicles target nodes in interconnected signalling pathways that enhance oral epithelial barrier function and dampen immune responses. J Extracell Vesicles. 2021;10:e12071.
42. Johnstone RM, Adam M, Hammond JR, Orr L, Turbide C. Vesicle formation during reticulocyte maturation. Association of plasma membrane activities with released vesicles (exosomes). J Biol Chem. 1987;262:9412–20.
43. Tkach M, Thery C. Communication by extracellular vesicles: where we are and where we need to go. Cell. 2016;164:1226–32.
44. Henrich SE, McMahon KM, Plebanek MP, Calvert AE, Feliciano TJ, Parrish S, et al. Prostate cancer extracellular vesicles mediate intercellular communication with bone marrow cells and promote metastasis in a cholesterol-dependent manner. J Extracell Vesicles. 2020;10:e12042.
45. Peinado H, Zhang H, Matei IR, Costa-Silva B, Hoshino A, Rodrigues G, et al. Pre-metastatic niches: organ-specific homes for metastases. Nat Rev Cancer. 2017;17:302–17.
46. Williams C, Royo F, Aizpurua-Olaizola O, Pazos R, Boons GJ, Reichardt NC, et al. Glycosylation of extracellular vesicles: current knowledge, tools and clinical perspectives. J Extracell Vesicles. 2018;7:1442985.
47. Colombo M, Raposo G, Thery C. Biogenesis, secretion, and intercellular interactions of exosomes and other extracellular vesicles. Annu Rev Cell Dev Biol. 2014;30:255–89.
48. O'Brien K, Breyne K, Ughetto S, Laurent LC, Breakefield XO. RNA delivery by extracellular vesicles in mammalian cells and its applications. Nat Rev Mol Cell Biol. 2020;21:585–606.
49. Peruzzotti-Jametti L, Bernstock JD, Willis CM, Manferrari G, Rogall R, Fernandez-Vizarra E, et al. Neural stem cells traffic functional mitochondria via extracellular vesicles. PLoS Biol. 2021;19:e3001166.
50. Skotland T, Sagini K, Sandvig K, Llorente A. An emerging focus on lipids in extracellular vesicles. Adv Drug Deliv Rev. 2020;159:308–21.
51. Kakarla R, Hur J, Kim YJ, Kim J, Chwae YJ. Apoptotic cell-derived exosomes: messages from dying cells. Exp Mol Med. 2020;52:1–6.
52. Al-Nedawi K, Meehan B, Micallef J, Lhotak V, May L, Guha A, et al. Intercellular transfer of the oncogenic receptor EGFRvIII by microvesicles derived from tumour cells. Nat Cell Biol. 2008;10:619–24.
53. Peinado H, Aleckovic M, Lavotshkin S, Matei I, Costa-Silva B, Moreno-Bueno G, et al. Melanoma exosomes educate bone marrow progenitor cells toward a pro-metastatic phenotype through MET. Nat Med. 2012;18:883–91.
54. Broggi MAS, Maillat L, Clement CC, Bordry N, Corthesy P, Auger A, et al. Tumor-associated factors are enriched in lymphatic exudate compared to plasma in metastatic melanoma patients. J Exp Med. 2019;216:1091–107.
55. Garcia-Silva S, Benito-Martin A, Sanchez-Redondo S, Hernandez-Barranco A, Ximenez-Embun P, Nogues L, et al. Use of extracellular vesicles from lymphatic drainage as surrogate markers of melanoma progression and BRAF (V600E) mutation. J Exp Med. 2019;216:1061–70.
56. Lazaro-Ibanez E, Sanz-Garcia A, Visakorpi T, Escobedo-Lucea C, Siljander P, Ayuso-Sacido A, et al. Different gDNA content in the subpopulations of prostate cancer extracellular vesicles: apoptotic bodies, microvesicles, and exosomes. Prostate. 2014;74:1379–90.
57. Mohrmann L, Huang HJ, Hong DS, Tsimberidou AM, Fu S, Piha-Paul SA, et al. Liquid biopsies using plasma exosomal nucleic acids and plasma cell-Free DNA compared with clinical outcomes of patients with advanced cancers. Clin Cancer Res. 2018;24:181–8.
58. Wan Y, Liu B, Lei H, Zhang B, Wang Y, Huang H, et al. Nanoscale extracellular vesicle-derived DNA is superior to circulating cell-free DNA for mutation detection in early-stage non-small-cell lung cancer. Ann Oncol. 2018;29:2379–83.
59. Sahoo S, Adamiak M, Mathiyalagan P, Kenneweg F, Kafert-Kasting S, Thum T. Therapeutic and diagnostic translation of extracellular vesicles in cardiovascular diseases: roadmap to the clinic. Circulation. 2021;143:1426–49.
60. Duijvesz D, Luider T, Bangma CH, Jenster G. Exosomes as biomarker treasure chests for prostate cancer. Eur Urol. 2011;59:823–31.
61. Minciacchi VR, Zijlstra A, Rubin MA, Di Vizio, D. Extracellular vesicles for liquid biopsy in prostate cancer: where are we and where are we headed? Prostate Cancer Prostatic Dis. 2017;20:251–8.
62. Urabe F, Kosaka N, Kimura T, Egawa S, Ochiya T. Extracellular vesicles: toward a clinical application in urological cancer treatment. Int J Urol. 2018;25:533–43.
63. Dhondt B, Van Deun J, Vermaerke S, de Marco A, Lumen N, De Wever O, et al. Urinary extracellular vesicle biomarkers in urological cancers: From discovery towards clinical implementation. Int J Biochem Cell Biol. 2018;99:236–56.
64. Rimmer MP, Gregory CD, Mitchell RT. Extracellular vesicles in urological malignancies. Biochim Biophys Acta Rev Cancer. 2021;1876:188570.
65. Linxweiler J, Junker K. Extracellular vesicles in urological malignancies: an update. Nat Rev Urol. 2020;17:11–27.
66. Gao Z, Pang B, Li J, Gao N, Fan T, Li Y. Emerging role of exosomes in liquid biopsy for monitoring prostate cancer invasion and metastasis. Front Cell Dev Biol. 2021;9:679527.
67. Hatano K, Fujita K. Extracellular vesicles in prostate cancer: a narrative review. Transl Androl Urol 2021;10:1890–907.
68. Campos-Fernandez E, Barcelos LS, de Souza AG, Goulart LR, Alonso-Goulart V. Research landscape of liquid biopsies in prostate cancer. Am J Cancer Res. 2019;9:1309–28.
69. Vlaeminck-Guillem V. Extracellular vesicles in prostate cancer carcinogenesis, diagnosis, and management. Front Oncol. 2018;8:222.
70. Mitchell PJ, Welton J, Staffurth J, Court J, Mason MD, Tabi Z, et al. Can urinary exosomes act as treatment response markers in prostate cancer? J Transl Med. 2009;7:4.
71. Nilsson J, Skog J, Nordstrand A, Baranov V, Mincheva-Nilsson L, Breakefield XO, et al. Prostate cancer-derived urine exosomes: a novel approach to biomarkers for prostate cancer. Br J Cancer. 2009;100:1603–7.
72. Drake RR, Kislinger T. The proteomics of prostate cancer exosomes. Expert Rev Proteom. 2014;11:167–77.
73. Verze P, Cai T, Lorenzetti S. The role of the prostate in male fertility, health and disease. Nat Rev Urol. 2016;13:379–86.
74. Brody I, Ronquist G, Gottfries A. Ultrastructural localization of the prostasome - an organelle in human seminal plasma. Ups J Med Sci. 1983;88:63–80.
75. Ronquist G, Brody I, Gottfries A, Stegmayr B. An Mg^{2+} and Ca^{2+}-stimulated adenosine triphosphatase in human prostatic fluid: part I. Andrology. 1978;10:261–72.
76. Ronquist G, Brody I. The prostasome: its secretion and function in man. Biochim Biophys Acta. 1985;822:203–18.
77. Ronquist G, Nilsson BO. The Janus-faced nature of prostasomes: their pluripotency favours the normal reproductive process and malignant prostate growth. Prostate Cancer Prostatic Dis. 2004;7:21–31.
78. Drake RR, Elschenbroich S, Lopez-Perez O, Kim Y, Ignatchenko V, Ignatchenko A, et al. In-depth proteomic analyses of direct expressed prostatic secretions. J Proteome Res. 2010;9:2109–16.
79. Baskaran S, Panner Selvam, MK, Agarwal, A. Exosomes of male reproduction. Adv Clin Chem. 2020;95:149–63.
80. Zaichick V. The prostatic urethra as a Venturi effect urine-jet pump to drain prostatic fluid. Med Hypotheses. 2014;83:65–68.
81. Duijvesz D, Versluis CY, van der Fels CA, Vredenbregt-van den Berg MS, Leivo J, Peltola MT, et al. Immuno-based detection of extracellular vesicles in urine as diagnostic marker for prostate cancer. Int J Cancer. 2015;137:2869–78.
82. Hendriks RJ, Dijkstra S, Jannink SA, Steffens MG, van Oort IM, Mulders PF, et al. Comparative analysis of prostate cancer specific biomarkers PCA3 and ERG in whole urine, urinary sediments and exosomes. Clin Chem Lab Med. 2016;54:483–92.
83. Erdbrugger U, Blijdorp CJ, Bijnsdorp IV, Borras FE, Burger D, Bussolati B, et al. Urinary extracellular vesicles: a position paper by the urine task force of the

International Society for Extracellular Vesicles. J Extracell Vesicles. 2021;10: e12093.
84. Hiemstra TF, Charles PD, Gracia T, Hester SS, Gatto L, Al-Lamki R, et al. Human urinary exosomes as innate immune effectors. J Am Soc Nephrol. 2014;25:2017–27.
85. Nolte-'t Hoen E, Cremer T, Gallo RC, Margolis LB. Extracellular vesicles and viruses: are they close relatives? Proc Natl Acad Sci Usa 2016;113:9155–61.
86. van Dongen HM, Masoumi N, Witwer KW, Pegtel DM. Extracellular vesicles exploit viral entry routes for cargo delivery. Microbiol Mol Biol Rev. 2016;80:369–86.
87. Goetsch, HE, Zhao, L, Gnegy, M, Imperiale, MJ, Love, NG, Wigginton, KR. Fate of the urinary tract virus BK human polyomavirus in source-separated urine. Appl Environ Microbiol. 2018;84:e02374-17.
88. Polo C, Perez JL, Mielnichuck A, Fedele CG, Niubo J, Tenorio A. Prevalence and patterns of polyomavirus urinary excretion in immunocompetent adults and children. Clin Microbiol Infect. 2004;10:640–4.
89. Lee Y, Park JY, Lee EH, Yang J, Jeong BR, Kim YK, et al. Rapid assessment of microbiota changes in individuals with autism spectrum disorder using bacteria-derived membrane vesicles in urine. Exp Neurobiol. 2017;26:307–17.
90. Yoo JY, Rho M, You YA, Kwon EJ, Kim MH, Kym S, et al. 16S rRNA gene-based metagenomic analysis reveals differences in bacteria-derived extracellular vesicles in the urine of pregnant and non-pregnant women. Exp Mol Med. 2016;48:e208.
91. Principe S, Jones EE, Kim Y, Sinha A, Nyalwidhe JO, Brooks J, et al. In-depth proteomic analyses of exosomes isolated from expressed prostatic secretions in urine. Proteomics. 2013;13:1667–71.
92. Wang Z, Hill S, Luther JM, Hachey DL, Schey KL. Proteomic analysis of urine exosomes by multidimensional protein identification technology (MudPIT). Proteomics. 2012;12:329–38.
93. Øverbye A, Skotland T, Koehler CJ, Thiede B, Seierstad T, Berge V, et al. Identification of prostate cancer biomarkers in urinary exosomes. Oncotarget. 2015;6:30357–76.
94. Tripisciano C, Weiss R, Karuthedom George S, Fischer MB, Weber V. Extracellular vesicles derived from platelets, red blood cells, and monocyte-like cells differ regarding their ability to induce factor XII-dependent thrombin generation. Front Cell Dev Biol. 2020;8:298.
95. Stenman UH, Leinonen J, Zhang WM, Finne P. Prostate-specific antigen. Semin Cancer Biol. 1999;9:83–93.
96. Clayton, A, Buschmann, D, Byrd, JB, Carter, DRF, Cheng, L, Compton, C et al. Summary of the ISEV workshop on extracellular vesicles as disease biomarkers, held in Birmingham, UK, during December 2017. J Extracell Vesicles. 2018;7:1473707.
97. Clayton A, Boilard E, Buzás EI, Cheng L, Falcón-Perez JM, Gardiner C, et al. Considerations towards a roadmap for collection, handling and storage of blood extracellular vesicles. J Extracell Vesicles. 2019;8:1647027.
98. Coumans FAW, Brisson AR, Buzas EI, Dignat-George F, Drees EEE, El-Andaloussi S, et al. Methodological Guidelines to Study Extracellular Vesicles. Circ Res. 2017;120:1632–48.
99. Witwer KW, Buzas EI, Bemis LT, Bora A, Lasser C, Lotvall J, et al. Standardization of sample collection, isolation and analysis methods in extracellular vesicle research. J Extracell Vesicles. 2013;2.
100. Lehmann S, Guadagni F, Moore H, Ashton G, Barnes M, Benson E, et al. Standard preanalytical coding for biospecimens: review and implementation of the Sample PREanalytical Code (SPREC). Biopreserv Biobank. 2012;10:366–74.
101. Betsou F, Bilbao R, Case J, Chuaqui R, Clements JA, De Souza Y, et al. Standard PREanalytical code version 3.0. Biopreserv Biobank. 2018;16:9–12.
102. Lacroix R, Judicone C, Poncelet P, Robert S, Arnaud L, Sampol J, et al. Impact of pre-analytical parameters on the measurement of circulating microparticles: towards standardization of protocol. J Thromb Haemost. 2012;10:437–46.
103. Mullier F, Bailly N, Chatelain C, Chatelain B, Dogne JM. Pre-analytical issues in the measurement of circulating microparticles: current recommendations and pending questions. J Thromb Haemost. 2013;11:693–6.
104. Gyorgy B, Paloczi K, Kovacs A, Barabas E, Beko G, Varnai K, et al. Improved circulating microparticle analysis in acid-citrate dextrose (ACD) anticoagulant tube. Thromb Res. 2014;133:285–92.
105. Tegegn TZ, De Paoli SH, Orecna M, Elhelu OK, Woodle SA, Tarandovskiy ID, et al. Characterization of procoagulant extracellular vesicles and platelet membrane disintegration in DMSO-cryopreserved platelets. J Extracell Vesicles. 2016;5:30422.
106. Rikkert LG, Coumans FAW, Hau CM, Terstappen L, Nieuwland R. Platelet removal by single-step centrifugation. Platelets 2021;32:440–3.
107. Liangsupree T, Multia E, Riekkola ML. Modern isolation and separation techniques for extracellular vesicles. J Chromatogr A. 2021;1636:461773.
108. Karimi N, Cvjetkovic A, Jang SC, Crescitelli R, Hosseinpour Feizi, M.A., Nieuwland, R. et al. Detailed analysis of the plasma extracellular vesicle proteome after separation from lipoproteins. Cell Mol Life Sci. 2018;75:2873–86.
109. Fernandez-Llama P, Khositseth S, Gonzales PA, Star RA, Pisitkun T, Knepper MA. Tamm-Horsfall protein and urinary exosome isolation. Kidney Int. 2010;77:736–42.
110. Musante, L, Saraswat, M, Duriez, E, Byrne, B, Ravida, A, Domon, B et al. Biochemical and physical characterisation of urinary nanovesicles following CHAPS treatment. PLoS ONE. 2012;7:e37279.
111. Xu X, Barreiro K, Musante L, Kretz O, Lin H, Zou H, et al. Management of Tamm-Horsfall protein for reliable urinary analytics. Proteom Clin Appl. 2019;13: e1900018.
112. Thery, C, Amigorena, S, Raposo, G, Clayton, A. Isolation and characterization of exosomes from cell culture supernatants and biological fluids. Curr Protoc Cell Biol. 2006;Chapter 3:Unit 3.22.
113. Gardiner C, Di Vizio D, Sahoo S, Thery C, Witwer KW, Wauben M, et al. Techniques used for the isolation and characterization of extracellular vesicles: results of a worldwide survey. J Extracell Vesicles. 2016;5:32945.
114. Konoshenko MY, Lekchnov EA, Vlassov AV, Laktionov PP. Isolation of extracellular vesicles: general methodologies and latest trends. BioMed Res Int. 2018;2018:8545347.
115. Li P, Kaslan M, Lee SH, Yao J, Gao Z. Progress in exosome isolation techniques. Theranostics. 2017;7:789–804.
116. Royo, F, Thery, C, Falcon-Perez, JM, Nieuwland, R, Witwer, KW. Methods for separation and characterization of extracellular vesicles: results of a worldwide survey performed by the ISEV Rigor and Standardization subcommittee. Cells. 2020;9:1955.
117. Gandham S, Su X, Wood J, Nocera AL, Alli SC, Milane L, et al. Technologies and standardization in research on extracellular vesicles. Trends Biotechnol. 2020;38:1066–98.
118. Choi JY, Kim S, Kwak HB, Park DH, Park JH, Ryu JS, et al. Extracellular vesicles as a source of urological biomarkers: lessons learned from advances and challenges in clinical applications to major diseases. Int Neurourol J. 2017;21:83–96.
119. Ayala-Mar S, Donoso-Quezada J, Gallo-Villanueva RC, Perez-Gonzalez VH, Gonzalez-Valdez J. Recent advances and challenges in the recovery and purification of cellular exosomes. Electrophoresis. 2019;40:3036–49.
120. Yamamoto T, Kosaka N, Ochiya T. Latest advances in extracellular vesicles: from bench to bedside. Sci Technol Adv Mater. 2019;20:746–57.
121. Van Deun J, Mestdagh P, Sormunen R, Cocquyt V, Vermaelen K, Vandesompele J, et al. The impact of disparate isolation methods for extracellular vesicles on downstream RNA profiling. J Extracell Vesicles. 2014;3.
122. Dhondt B, Geeurickx E, Tulkens J, Van Deun J, Vergauwen G, Lippens L, et al. Unravelling the proteomic landscape of extracellular vesicles in prostate cancer by density-based fractionation of urine. J Extracell Vesicles. 2020;9:1736935.
123. Royo F, Zuniga-Garcia P, Sanchez-Mosquera P, Egia A, Perez A, Loizaga A, et al. Different EV enrichment methods suitable for clinical settings yield different subpopulations of urinary extracellular vesicles from human samples. J Extracell Vesicles. 2016;5:29497.
124. Macias M, Rebmann V, Mateos B, Varo N, Perez-Gracia JL, Alegre E, et al. Comparison of six commercial serum exosome isolation methods suitable for clinical laboratories. Effect in cytokine analysis. Clin Chem Lab Med. 2019;57:1539–45.
125. Blijdorp CJ, Tutakhel OAZ, Hartjes TA, van den Bosch TPP, van Heugten MH, Rigalli JP, et al. Comparing Approaches to Normalize, Quantify, and Characterize Urinary Extracellular Vesicles. J Am Soc Nephrol. 2021;32:1210–26.
126. Mateescu B, Kowal EJ, van Balkom BW, Bartel S, Bhattacharyya SN, Buzas EI, et al. Obstacles and opportunities in the functional analysis of extracellular vesicle RNA—an ISEV position paper. J Extracell Vesicles. 2017;6:1286095.
127. Ye LF, He S, Wu X, Jiang S, Zhang RC, Yang ZS, et al. Detection of prostate cancer antigen 3 and prostate cancer susceptibility candidate in non-DRE urine improves diagnosis of prostate cancer in chinese population. Prostate Cancer. 2020;2020:3964615.
128. Danarto R, Astuti I, Umbas R, Haryana SM. Urine miR-21-5p and miR-200c-3p as potential non-invasive biomarkers in patients with prostate cancer. Turk J Urol. 2020;46:26–30.
129. Li Z, Li LX, Diao YJ, Wang J, Ye Y, Hao XK. Identification of urinary exosomal miRNAs for the non-invasive diagnosis of prostate cancer. Cancer Manag Res. 2021;13:25–35.
130. Vandesompele, J, De Preter, K, Pattyn, F, Poppe, B, Van Roy, N, De Paepe, A et al. Accurate normalization of real-time quantitative RT-PCR data by geometric averaging of multiple internal control genes. Genome Biol.2002;3, RESEARCH0034.
131. Srinivasan S, Duval MX, Kaimal V, Cuff C, Clarke SH. Assessment of methods for serum extracellular vesicle small RNA sequencing to support biomarker development. J Extracell Vesicles. 2019;8:1684425.
132. Liang Y, Lehrich BM, Zheng S, Lu M. Emerging methods in biomarker identification for extracellular vesicle-based liquid biopsy. J Extracell Vesicles. 2021;10: e12090.

133. Di Santo R, Romanò S, Mazzini A, Jovanovic S, Nocca G, Campi G, et al. Recent advances in the label-free characterization of exosomes for cancer liquid biopsy: from scattering and spectroscopy to nanoindentation and nanodevices. Nanomaterials 2021;11:1476.
134. Martin-Gracia B, Martin-Barreiro A, Cuestas-Ayllon C, Grazu V, Line A, Llorente A, et al. Nanoparticle-based biosensors for detection of extracellular vesicles in liquid biopsies. J Mater Chem B. 2020;8:6710–38.
135. Lin S, Yu Z, Chen D, Wang Z, Miao J, Li Q, et al. Progress in microfluidics-based exosome separation and detection technologies for diagnostic applications. Small. 2020;16:e1903916.
136. Zhang P, Zhou X, He M, Shang Y, Tetlow AL, Godwin AK, et al. Ultrasensitive detection of circulating exosomes with a 3D-nanopatterned microfluidic chip. Nat Biomed Eng. 2019;3:438–51.
137. Zhang P, He M, Zeng Y. Ultrasensitive microfluidic analysis of circulating exosomes using a nanostructured graphene oxide/polydopamine coating. Lab Chip. 2016;16:3033–42.
138. Yang B, Chen Y, Shi J. Exosome biochemistry and advanced nanotechnology for next-generation theranostic platforms. Adv Mater. 2019;31:e1802896.
139. Guo SC, Tao SC, Dawn H. Microfluidics-based on-a-chip systems for isolating and analysing extracellular vesicles. J Extracell Vesicles. 2018;7:1508271.
140. Yasui T, Yanagida T, Ito S, Konakade Y, Takeshita D, Naganawa T, et al. Unveiling massive numbers of cancer-related urinary-microRNA candidates via nanowires. Sci Adv. 2017;3:e1701133.
141. Tauro BJ, Greening DW, Mathias RA, Mathivanan S, Ji H, Simpson RJ. Two distinct populations of exosomes are released from LIM1863 colon carcinoma cell-derived organoids. Mol Cell Proteom. 2013;12:587–98.
142. Wunsch BH, Smith JT, Gifford SM, Wang C, Brink M, Bruce RL, et al. Nanoscale lateral displacement arrays for the separation of exosomes and colloids down to 20 nm. Nat Nanotechnol. 2016;11:936–40.
143. Smith JT, Wunsch BH, Dogra N, Ahsen ME, Lee K, Yadav KK, et al. Integrated nanoscale deterministic lateral displacement arrays for separation of extracellular vesicles from clinically-relevant volumes of biological samples. Lab Chip. 2018;18:3913–25.
144. Ku A, Fredsoe J, Sorensen KD, Borre M, Evander M, Laurell T, et al. High-throughput and automated acoustic trapping of extracellular vesicles to identify microRNAs with diagnostic potential for prostate cancer. Front Oncol. 2021;11:631021.
145. Liu C, Guo J, Tian F, Yang N, Yan F, Ding Y, et al. Field-free isolation of exosomes from extracellular vesicles by microfluidic viscoelastic flows. ACS Nano. 2017;11:6968–76.
146. Asghari M, Cao X, Mateescu B, van Leeuwen D, Aslan MK, Stavrakis S, et al. Oscillatory viscoelastic microfluidics for efficient focusing and separation of nanoscale species. ACS Nano. 2020;14:422–33.
147. Ziaei P, Berkman CE, Norton MG. Isolation and detection of tumor-derived extracellular vesicles. ACS Appl Nano Mater. 2018;1:2004–20.
148. Kanwar SS, Dunlay CJ, Simeone DM, Nagrath S. Microfluidic device (ExoChip) for on-chip isolation, quantification and characterization of circulating exosomes. Lab Chip. 2014;14:1891–1900.
149. Zhao Z, Yang Y, Zeng Y, He M. A microfluidic ExoSearch chip for multiplexed exosome detection towards blood-based ovarian cancer diagnosis. Lab Chip. 2016;16:489–96.
150. Jeong S, Park J, Pathania D, Castro CM, Weissleder R, Lee H. Integrated magneto-electrochemical sensor for exosome analysis. ACS Nano. 2016;10:1802–9.
151. Hernandez-Neuta I, Neumann F, Brightmeyer J, Ba Tis T, Madaboosi N, Wei Q, et al. Smartphone-based clinical diagnostics: towards democratization of evidence-based health care. J Intern Med. 2019;285:19–39.
152. Ko J, Hemphill MA, Gabrieli D, Wu L, Yelleswarapu V, Lawrence G, et al. Smartphone-enabled optofluidic exosome diagnostic for concussion recovery. Sci Rep. 2016;6:31215.
153. Liang LG, Kong MQ, Zhou S, Sheng YF, Wang P, Yu T, et al. An integrated double-filtration microfluidic device for isolation, enrichment and quantification of urinary extracellular vesicles for detection of bladder cancer. Sci Rep. 2017;7:46224.
154. Califf RM. Biomarker definitions and their applications. Exp Biol Med. 2018;243:213–21.
155. Motamedinia P, Scott AN, Bate KL, Sadeghi N, Salazar G, Shapiro E, et al. Urine exosomes for non-invasive assessment of gene expression and mutations of prostate cancer. PLoS ONE. 2016;11:e0154507.
156. Dijkstra S, Birker IL, Smit FP, Leyten GH, de Reijke TM, van Oort IM, et al. Prostate cancer biomarker profiles in urinary sediments and exosomes. J Urol. 2014;191:1132–8.
157. Donovan MJ, Noerholm M, Bentink S, Belzer S, Skog J, O'Neill V, et al. A molecular signature of PCA3 and ERG exosomal RNA from non-DRE urine is predictive of initial prostate biopsy result. Prostate Cancer Prostatic Dis. 2015;18:370–5.
158. McKiernan J, Donovan MJ, O'Neill V, Bentink S, Noerholm M, Belzer S, et al. A novel urine exosome gene expression assay to predict high-grade prostate cancer at initial biopsy. JAMA Oncol. 2016;2:882–9.
159. McKiernan J, Donovan MJ, Margolis E, Partin A, Carter B, Brown G, et al. A prospective adaptive utility trial to validate performance of a novel urine exosome gene expression assay to predict high-grade prostate cancer in patients with prostate-specific antigen 2–10 ng/ml at initial biopsy. Eur Urol. 2018;74:731–8.
160. Tutrone R, Donovan MJ, Torkler P, Tadigotla V, McLain T, Noerholm M, et al. Clinical utility of the exosome based ExoDx Prostate(IntelliScore) EPI test in men presenting for initial Biopsy with a PSA 2-10 ng/mL. Prostate Cancer Prostatic Dis. 2020;23:607–14.
161. Woo J, Santasusagna S, Banks J, Pastor-Lopez S, Yadav K, Carceles-Cordon M, et al. Urine extracellular vesicle GATA2 mRNA discriminates biopsy result in men with suspicion of prostate cancer. J Urol. 2020;204:691–700.
162. Kohaar I, Chen Y, Banerjee S, Borbiev T, Kuo HC, Ali A, et al. A urine exosome gene expression panel distinguishes between indolent and aggressive prostate cancers at biopsy. J Urol. 2021;205:420–5.
163. Royo F, Zuniga-Garcia P, Torrano V, Loizaga A, Sanchez-Mosquera P, Ugalde-Olano A, et al. Transcriptomic profiling of urine extracellular vesicles reveals alterations of CDH3 in prostate cancer. Oncotarget. 2016;7:6835–46.
164. Neeb A, Hefele S, Bormann S, Parson W, Adams F, Wolf P, et al. Splice variant transcripts of the anterior gradient 2 gene as a marker of prostate cancer. Oncotarget. 2014;5:8681–9.
165. Yaman Agaoglu F, Kovancilar M, Dizdar Y, Darendeliler E, Holdenrieder S, Dalay N, et al. Investigation of miR-21, miR-141, and miR-221 in blood circulation of patients with prostate cancer. Tumour Biol. 2011;32:583–8.
166. Zhang HL, Yang LF, Zhu Y, Yao XD, Zhang SL, Dai B, et al. Serum miRNA-21: elevated levels in patients with metastatic hormone-refractory prostate cancer and potential predictive factor for the efficacy of docetaxel-based chemotherapy. Prostate. 2011;71:326–31.
167. Li M, Rai AJ, DeCastro GJ, Zeringer E, Barta T, Magdaleno S, et al. An optimized procedure for exosome isolation and analysis using serum samples: Application to cancer biomarker discovery. Methods. 2015;87:26–30.
168. Endzelins E, Berger A, Melne V, Bajo-Santos C, Sobolevska K, Abols A, et al. Detection of circulating miRNAs: comparative analysis of extracellular vesicle-incorporated miRNAs and cell-free miRNAs in whole plasma of prostate cancer patients. BMC Cancer. 2017;17:730.
169. Samsonov R, Shtam T, Burdakov V, Glotov A, Tsyrlina E, Berstein L, et al. Lectin-induced agglutination method of urinary exosomes isolation followed by miRNA analysis: application for prostate cancer diagnostic. Prostate. 2016;76:68–79.
170. Foj L, Ferrer F, Serra M, Arevalo A, Gavagnach M, Gimenez N, et al. Exosomal and non-exosomal urinary miRNAs in prostate cancer detection and prognosis. Prostate. 2017;77:573–83.
171. Haldrup C, Kosaka N, Ochiya T, Borre M, Hoyer S, Orntoft TF, et al. Profiling of circulating microRNAs for prostate cancer biomarker discovery. Drug Deliv Transl Res. 2014;4:19–30.
172. Mitchell PS, Parkin RK, Kroh EM, Fritz BR, Wyman SK, Pogosova-Agadjanyan EL, et al. Circulating microRNAs as stable blood-based markers for cancer detection. Proc Natl Acad Sci USA. 2008;105:10513–8.
173. Koppers-Lalic D, Hackenberg M, de Menezes R, Misovic B, Wachalska M, Geldof A, et al. Noninvasive prostate cancer detection by measuring miRNA variants (isomiRs) in urine extracellular vesicles. Oncotarget. 2016;7:22566–78.
174. Li Z, Ma YY, Wang J, Zeng XF, Li R, Kang W, et al. Exosomal microRNA-141 is upregulated in the serum of prostate cancer patients. Onco Targets Ther. 2016;9:139–48.
175. Li W, Dong Y, Wang KJ, Deng Z, Zhang W, Shen HF. Plasma exosomal miR-125a-5p and miR-141-5p as non-invasive biomarkers for prostate cancer. Neoplasma. 2020;67:1314–8.
176. Xu Y, Qin S, An T, Tang Y, Huang Y, Zheng L. MiR-145 detection in urinary extracellular vesicles increase diagnostic efficiency of prostate cancer based on hydrostatic filtration dialysis method. Prostate. 2017;77:1167–75.
177. Wani S, Kaul D, Mavuduru RS, Kakkar N, Bhatia A. Urinary-exosomal miR-2909: a novel pathognomonic trait of prostate cancer severity. J Biotechnol. 2017;259:135–9.
178. Bhagirath D, Yang TL, Bucay N, Sekhon K, Majid S, Shahryari V, et al. microRNA-1246 Is an exosomal biomarker for aggressive prostate cancer. Cancer Res. 2018;78:1833–44.
179. Bryant RJ, Pawlowski T, Catto JW, Marsden G, Vessella RL, Rhees B, et al. Changes in circulating microRNA levels associated with prostate cancer. Br J Cancer. 2012;106:768–74.
180. Rodriguez M, Bajo-Santos C, Hessvik NP, Lorenz S, Fromm B, Berge V, et al. Identification of non-invasive miRNAs biomarkers for prostate cancer by deep sequencing analysis of urinary exosomes. Mol Cancer. 2017;16:156.

181. Matsuzaki K, Fujita K, Tomiyama E, Hatano K, Hayashi Y, Wang C, et al. MiR-30b-3p and miR-126-3p of urinary extracellular vesicles could be new biomarkers for prostate cancer. Transl Androl Urol 2021;10:1918–27.
182. Zhou C, Chen Y, He X, Zheng Z, Xue D. Functional implication of exosomal miR-217 and miR-23b-3p in the progression of prostate cancer. Onco Targets Ther. 2020;13:11595–606.
183. Barcelo M, Castells M, Bassas L, Vigues F, Larriba S. Semen miRNAs contained in exosomes as non-invasive biomarkers for prostate cancer diagnosis. Sci Rep. 2019;9:13772.
184. Mercadal M, Herrero C, Lopez-Rodrigo O, Castells M, de la Fuente A, Vigues F, et al. Impact of extracellular vesicle isolation methods on downstream mirna analysis in semen: a comparative study. Int J Mol Sci. 2020;21:5949.
185. Logozzi M, Angelini DF, Iessi E, Mizzoni D, Di Raimo R, Federici C, et al. Increased PSA expression on prostate cancer exosomes in in vitro condition and in cancer patients. Cancer Lett. 2017;403:318–29.
186. Logozzi M, Angelini DF, Giuliani A, Mizzoni D, Di Raimo R, Maggi M, et al. Increased plasmatic levels of PSA-expressing exosomes distinguish prostate cancer patients from benign prostatic hyperplasia: a prospective study. Cancers. 2019;11:1449.
187. Sequeiros T, Rigau M, Chiva C, Montes M, Garcia-Grau I, Garcia M, et al. Targeted proteomics in urinary extracellular vesicles identifies biomarkers for diagnosis and prognosis of prostate cancer. Oncotarget. 2017;8:4960–76.
188. Soekmadji C, Riches JD, Russell PJ, Ruelcke JE, McPherson S, Wang C, et al. Modulation of paracrine signaling by CD9 positive small extracellular vesicles mediates cellular growth of androgen deprived prostate cancer. Oncotarget. 2017;8:52237–55.
189. Carlsson L, Nilsson O, Larsson A, Stridsberg M, Sahlen G, Ronquist G. Characteristics of human prostasomes isolated from three different sources. Prostate. 2003;54:322–30.
190. Tavoosidana G, Ronquist G, Darmanis S, Yan J, Carlsson L, Wu D, et al. Multiple recognition assay reveals prostasomes as promising plasma biomarkers for prostate cancer. Proc Natl Acad Sci USA. 2011;108:8809–14.
191. Khan S, Jutzy JM, Valenzuela MM, Turay D, Aspe JR, Ashok A, et al. Plasma-derived exosomal survivin, a plausible biomarker for early detection of prostate cancer. PLoS ONE. 2012;7:e46737.
192. Khan S, Simpson J, Lynch JC, Turay D, Mirshahidi S, Gonda A, et al. Racial differences in the expression of inhibitors of apoptosis (IAP) proteins in extracellular vesicles (EV) from prostate cancer patients. PLoS ONE. 2017;12:e0183122.
193. Fujita K, Kume H, Matsuzaki K, Kawashima A, Ujike T, Nagahara A, et al. Proteomic analysis of urinary extracellular vesicles from high Gleason score prostate cancer. Sci Rep. 2017;7:42961.
194. Gabriel K, Ingram A, Austin R, Kapoor A, Tang D, Majeed F, et al. Regulation of the tumor suppressor PTEN through exosomes: a diagnostic potential for prostate cancer. PLoS ONE. 2013;8:e70047.
195. Wang L, Skotland T, Berge V, Sandvig K, Llorente A. Exosomal proteins as prostate cancer biomarkers in urine: From mass spectrometry discovery to immunoassay-based validation. Eur J Pharm Sci. 2017;98:80–85.
196. Li S, Zhao Y, Chen W, Yin L, Zhu J, Zhang H, et al. Exosomal ephrinA2 derived from serum as a potential biomarker for prostate cancer. J Cancer. 2018;9:2659–65.
197. Chung JW, Kim HT, Ha YS, Lee EH, Chun SY, Lee CH, et al. Identification of a novel non-invasive biological marker to overcome the shortcomings of PSA in diagnosis and risk stratification for prostate cancer: Initial prospective study of developmental endothelial locus-1 protein. PLoS ONE. 2021;16:e0250254.
198. Bijnsdorp IV, Geldof AA, Lavaei M, Piersma SR, van Moorselaar RJ, Jimenez CR. Exosomal ITGA3 interferes with non-cancerous prostate cell functions and is increased in urine exosomes of metastatic prostate cancer patients. J Extracell Vesicles. 2013;2.
199. Kawakami K, Fujita Y, Matsuda Y, Arai T, Horie K, Kameyama K, et al. Gamma-glutamyltransferase activity in exosomes as a potential marker for prostate cancer. BMC Cancer. 2017;17:316.
200. Khanna, K, Salmond, N, Lynn, KS, Leong, HS, Williams, KC. Clinical significance of STEAP1 extracellular vesicles in prostate cancer. Prostate Cancer Prostatic Dis. 2021;24:802–811.
201. Skotland T, Ekroos K, Kauhanen D, Simolin H, Seierstad T, Berge V, et al. Molecular lipid species in urinary exosomes as potential prostate cancer biomarkers. Eur J Cancer. 2017;70:122–32.
202. Clos-Garcia M, Loizaga-Iriarte A, Zuniga-Garcia P, Sanchez-Mosquera P, Rosa Cortazar A, Gonzalez E, et al. Metabolic alterations in urine extracellular vesicles are associated to prostate cancer pathogenesis and progression. J Extracell Vesicles. 2018;7:1470442.
203. Puhka M, Takatalo M, Nordberg M-E, Valkonen S, Nandania J, Aatonen M, et al. Metabolomic profiling of extracellular vesicles and alternative normalization methods reveal enriched metabolites and strategies to study prostate cancer-related changes. Theranostics. 2017;7:3824–41.
204. Isin M, Uysaler E, Ozgur E, Koseoglu H, Sanli O, Yucel OB, et al. Exosomal lncRNA-p21 levels may help to distinguish prostate cancer from benign disease. Front Genet. 2015;6:168.
205. Wang YH, Ji J, Wang BC, Chen H, Yang ZH, Wang K, et al. Tumor-derived exosomal long noncoding RNAs as promising diagnostic biomarkers for prostate cancer. Cell Physiol Biochem. 2018;46:532–45.
206. Wang WW, Sorokin I, Aleksic I, Fisher H, Kaufman RP Jr, Winer A, et al. Expression of small noncoding RNAs in urinary exosomes classifies prostate cancer into indolent and aggressive disease. J Urol. 2020;204:466–75.
207. Krafft C, Wilhelm K, Eremin A, Nestel S, von Bubnoff N, Schultze-Seemann W, et al. A specific spectral signature of serum and plasma-derived extracellular vesicles for cancer screening. Nanomedicine. 2017;13:835–41.
208. Wang Y, Li Q, Shi H, Tang K, Qiao L, Yu G, et al. Microfluidic Raman biochip detection of exosomes: a promising tool for prostate cancer diagnosis. Lab Chip. 2020;20:4632–7.
209. Huang X, Yuan T, Liang M, Du M, Xia S, Dittmar R, et al. Exosomal miR-1290 and miR-375 as prognostic markers in castration-resistant prostate cancer. Eur Urol. 2015;67:33–41.
210. Zavridou M, Strati A, Bournakis E, Smilkou S, Tserpeli V, Lianidou E. Prognostic significance of gene expression and DNA methylation markers in circulating tumor cells and paired plasma derived exosomes in metastatic castration resistant prostate cancer. Cancers. 2021;13:780.
211. Biggs, CN, Siddiqui, KM, Al-Zahrani, AA, Pardhan, S, Brett, SI, Guo QQ, et al. Prostate extracellular vesicles in patient plasma as a liquid biopsy platform for prostate cancer using nanoscale flow cytometry. Oncotarget. 2016;78839–49.
212. Nanou A, Coumans FAW, van Dalum G, Zeune LL, Dolling D, Onstenk W, et al. Circulating tumor cells, tumor-derived extracellular vesicles and plasma cytokeratins in castration-resistant prostate cancer patients. Oncotarget. 2018;9:19283–93.
213. Nanou A, Miller MC, Zeune LL, de Wit S, Punt CJA, Groen HJM, et al. Tumour-derived extracellular vesicles in blood of metastatic cancer patients associate with overall survival. Br J Cancer. 2020;122:801–11.
214. Connell SP, Yazbek-Hanna M, McCarthy F, Hurst R, Webb M, Curley H, et al. A four-group urine risk classifier for predicting outcomes in patients with prostate cancer. BJU Int. 2019;124:609–20.
215. Fredsøe J, Rasmussen AKI, Mouritzen P, Borre M, Ørntoft T, Sørensen KD. A five-microRNA model (pCaP) for predicting prostate cancer aggressiveness using cell-free urine. Int J Cancer. 2019;145:2558–67.
216. Tian S, Lei Z, Gong Z, Sun Z, Xu D, Piao M. Clinical implication of prognostic and predictive biomarkers for castration-resistant prostate cancer: a systematic review. Cancer Cell Int. 2020;20:409.
217. Rice MA, Stoyanova, T. Biomarkers for diagnosis and prognosis of prostate cancer. Prostatectomy. 2019;9.
218. Del Re M, Crucitta S, Sbrana A, Rofi E, Paolieri F, Gianfilippo G, et al. Androgen receptor (AR) splice variant 7 and full-length AR expression is associated with clinical outcome: a translational study in patients with castrate-resistant prostate cancer. BJU Int. 2019;124:693–700.
219. Joncas F-H, Lucien F, Rouleau M, Morin F, Leong HS, Pouliot F, et al. Plasma extracellular vesicles as phenotypic biomarkers in prostate cancer patients. Prostate. 2019;79:1767–76.
220. Fujita K, Nonomura N. Role of androgen receptor in prostate cancer: a review. World J Mens Health. 2019;37:288–95.
221. Del Re M, Biasco E, Crucitta S, Derosa L, Rofi E, Orlandini C, et al. The detection of androgen receptor splice variant 7 in plasma-derived exosomal RNA strongly predicts resistance to hormonal therapy in metastatic prostate cancer patients. Eur Urol. 2017;71:680–7.
222. Nimir M, Ma Y, Jeffreys SA, Opperman T, Young F, Khan T, et al. Detection of AR-V7 in liquid biopsies of castrate resistant prostate cancer patients: a comparison of AR-V7 analysis in circulating tumor cells, circulating tumor RNA and exosomes. Cells. 2019;8:688.
223. Woo H-K, Park J, Ku JY, Lee CH, Sunkara V, Ha HK, et al. Urine-based liquid biopsy: non-invasive and sensitive AR-V7 detection in urinary EVs from patients with prostate cancer. Lab Chip. 2019;19:87–97.
224. Yu Q, Li P, Weng M, Wu S, Zhang Y, Chen X, et al. Nano-vesicles are a potential tool to monitor therapeutic efficacy of carbon ion radiotherapy in prostate cancer. J Biomed Nanotechnol. 2018;14:168–78.
225. Malla B, Aebersold DM, Dal Pra A. Protocol for serum exosomal miRNAs analysis in prostate cancer patients treated with radiotherapy. J Transl Med. 2018;16:223.
226. Kato T, Mizutani K, Kawakami K, Fujita Y, Ehara H, Ito M. CD44v8-10 mRNA contained in serum exosomes as a diagnostic marker for docetaxel resistance in prostate cancer patients. Heliyon. 2020;6:e04138–e04138.
227. Ishizuya Y, Uemura M, Narumi R, Tomiyama E, Koh Y, Matsushita M, et al. The role of actinin-4 (ACTN4) in exosomes as a potential novel therapeutic target in castration-resistant prostate cancer. Biochem Biophys Res Commun. 2020;523:588–94.

228. Bhagirath D, Yang TL, Tabatabai ZL, Majid S, Dahiya R, Tanaka Y, et al. BRN4 is a novel driver of neuroendocrine differentiation in castration-resistant prostate cancer and is selectively released in extracellular vesicles with BRN2. Clin Cancer Res. 2019;25:6532.
229. Thompson TC, Timme TL, Li L, Goltsov A. Caveolin-1, a metastasis-related gene that promotes cell survival in prostate cancer. Apoptosis. 1999;4:233–7.
230. Thompson TC, Tahir SA, Li L, Watanabe M, Naruishi K, Yang G, et al. The role of caveolin-1 in prostate cancer: clinical implications. Prostate Cancer Prostatic Dis. 2010;13:6–11.
231. Tahir SA, Ren C, Timme TL, Gdor Y, Hoogeveen R, Morrisett JD, et al. Development of an immunoassay for serum caveolin-1: a novel biomarker for prostate cancer. Clin Cancer Res. 2003;9:3653–9.
232. Tahir SA, Frolov A, Hayes TG, Mims MP, Miles BJ, Lerner SP, et al. Preoperative serum caveolin-1 as a prognostic marker for recurrence in a radical prostatectomy cohort. Clin Cancer Res. 2006;12:4872–5.
233. Ayers L, Pink R, Carter DRF, Nieuwland R. Clinical requirements for extracellular vesicle assays. J Extracell Vesicles. 2019;8:1593755.
234. Moller, A, Lobb, RJ. The evolving translational potential of small extracellular vesicles in cancer. Nat Rev Cancer. 2020;20:697–709.
235. Yekula A, Muralidharan K, Kang KM, Wang L, Balaj L, Carter BS. From laboratory to clinic: translation of extracellular vesicle based cancer biomarkers. Methods 2020;177:58–66.
236. Consortium E-T, Van Deun J, Mestdagh P, Agostinis P, Akay O, Anand S, et al. EV-TRACK: transparent reporting and centralizing knowledge in extracellular vesicle research. Nat Methods. 2017;14:228–32.
237. Zhang H, Freitas D, Kim HS, Fabijanic K, Li Z, Chen H, et al. Identification of distinct nanoparticles and subsets of extracellular vesicles by asymmetric flow field-flow fractionation. Nat Cell Biol. 2018;20:332–43.
238. Lasser C, Shelke GV, Yeri A, Kim DK, Crescitelli R, Raimondo S, et al. Two distinct extracellular RNA signatures released by a single cell type identified by microarray and next-generation sequencing. RNA Biol. 2017;14:58–72.
239. Lunavat TR, Cheng L, Kim DK, Bhadury J, Jang SC, Lasser C, et al. Small RNA deep sequencing discriminates subsets of extracellular vesicles released by melanoma cells—evidence of unique microRNA cargos. RNA Biol. 2015;12:810–23.
240. Pavlou MP, Diamandis EP, Blasutig IM. The long journey of cancer biomarkers from the bench to the clinic. Clin Chem. 2013;59:147–57.
241. Pepe MS, Etzioni R, Feng Z, Potter JD, Thompson ML, Thornquist M, et al. Phases of biomarker development for early detection of cancer. J Natl Cancer Inst. 2001;93:1054–61.
242. Fuzery AK, Levin J, Chan MM, Chan DW. Translation of proteomic biomarkers into FDA approved cancer diagnostics: issues and challenges. Clin Proteom. 2013;10:13.

ACKNOWLEDGEMENTS
Not applicable

AUTHOR CONTRIBUTIONS
ALL and AL: conceptualisation, paper preparation and editing. CB, EM, JM, MM, MR, CS and KT: paper preparation and editing. MR, CB, ALL, EM and AL: table content and design. EM: figure design. All authors have read and agreed to the published version of the paper.

FUNDING INFORMATION
This work was supported by the TRANSCAN2-JTC2016 call (Project PROSCANEXO), The South-Eastern Norwegian Regional Health Authority, The Norwegian Cancer Society and The Research Council of Norway and the Latvian Council of Science grant No. lzp-2018/0269. CS was supported by the Office of the Assistant Secretary of Defense for Health Affairs through the US Department of Defense Congressionally Directed Medical Research Program Prostate Cancer Research Program Idea Development Award [Number: W81XWH-16-1-0736]. Opinions, interpretations, conclusions and recommendations are those of the author and are not necessarily endorsed by the DoD.

COMPETING INTERESTS
The authors declare no competing interests.

ETHICS APPROVAL AND CONSENT TO PARTICIPATE
Not applicable.

CONSENT TO PUBLISH
Not applicable.

ADDITIONAL INFORMATION
Correspondence and requests for materials should be addressed to Alicia Llorente.

Reprints and permission information is available at http://www.nature.com/reprints

Publisher's note Springer Nature remains neutral with regard to jurisdictional claims in published maps and institutional affiliations.

2. METHODOLOGY

2.1 Patients and sample processing

A total of 30 patients with newly diagnosed resectable PC and 20 BPH patients were enrolled in this study between October 2018 and January 2020 at Riga East University Hospital and Latvian Genome Center and were followed-up until September 2021. All patients had elevated levels of PSA (2.5-50 ng/ml) at the time of diagnosis. Patient exclusion criteria included: blood transfusion in the last six months, another oncological disease, urinary tract infection and use of long-term urinary catheter. Clinical characteristics of the study population are provided in Table S1 (Appendix). A total of 10 male healthy donors (HD) were enrolled in the study. Samples were provided by the Latvian Genome Database.

Sixty milliliters (ml) of the first morning urine were collected, centrifuged at 2000*g* for 15 minutes (min) at room temperature, aliquoted and stored at -80ºC. Blood samples from PC patients were collected in ethylenediamine tetra acetic (EDTA)-coated tubes and processed at room temperature within 2 hours. Plasma samples were centrifuged twice at 3000*g* for 10 min, aliquoted and stored at -80 centigrade (°C). PC samples were collected at two different time points: before RP (PreOp) and 3 months after the surgery (PostOp).

Tumour and normal prostate tissue samples were macroscopically dissected immediately after the surgery by an experienced uropathologist. One slice of the tissue specimens was subjected to histological evaluation in order to verify the presence or absence of tumour cells in the tissue specimens and to assess the GS in the given specimen, whereas the other part of the specimen was immediately placed into the RNALater solution (Thermo Fisher Scientific, USA) and stored at -20°C until processing.

The study was conducted according to the Declaration of Helsinki. The specimens were collected after the patients' informed written consent was obtained and anonymized. The study protocol was approved by the Latvian Central Medical Ethics Committee (decision No. 01-29.1/488).

2.2 Isolation and characterization of EVs

EVs were extracted from both plasma and urine sample using SEC. Urine samples (20 ml) were thawed at +37˚C in a water bath, followed by centrifugation at 10 000g for 15 min. at +4˚C in order to eliminate large vesicles and uromodulin. Afterwards, samples were concentrated up to 500 µl using 100 kDa centrifugal filters (Merck Millipore, USA). 1ml of plasma and 500 µl of urine were loaded into Sepharose CL2.B 10ml columns. The elution process yielded 12 consecutive fractions of 0.5ml each, in which particle concentration and size was subsequently measured using Zetasizer Nano ZS (Malvern, UK). Fractions containing particles larger than 40nm were combined and concentrated up to 100 microliters (µl) using 3 kilodaltons (kDa) centrifugal filters (Merck Millipore, USA). Afterwards, EV samples were treated with Proteinase K (1 milligrams (mg)/ml) (Thermo Fisher Scientific) for 1 hour at a 37°C, heat - inactivated for 10 min and incubated with RNAseA (100 nanograms (ng)/µl) (Thermo Fisher Scientific) for 15 min. at 37°C. EV sample purity, size distribution profile and concentration were assessed by transmission electron microscopy (TEM), Western Blot (WB) and nanoparticle tracking analysis (NTA).

2.3 TEM

The morphology and size of EVs was investigated through observation of samples by TEM. A volume of 10 µl of each sample was affixed onto a 300-mesh grid coated with carbon, followed by incubation with 1% (w/v) uranyl formate. The mesh was positioned beneath the JEM-1230 TEM (JEOL, Peabody, MA, USA), and a series of images were captured at various places. Images were taken by Dr. Juris Jansons.

2.4 WB

WB targeting specific small EV markers was performed to characterize EVs as follows. EVs were lysed in Radioimmunoprecipitation assay (RIPA) buffer containing 50 nanomolar (nM) Tris (pH 8.0), 150ml NaCl, 1% Triton X-100, 0.5% Na deoxycholate, and 0.1% sodium dodecyl sulfate (SDS). The protein concentration was determined using the Pierce™ Bicinchoninic acid (BCA) Protein Assay kit (Thermo Scientific). Lymph node carcinoma of the prostate (LNCaP) cells obtained from American type culture collection (ATCC) (Manassasas, VA, USA) were utilized as positive control. A proportional fraction (one fifth) of the EV proteins and 10 µg of cellular proteins were separated using 10% SDS-polyacrylamide gel (PAGE), transferred into a nitrocellulose membrane, and blocked with 10% (w/v) fat-free milk. Subsequently, membranes were exposed to primary antibodies targeting PDCD6IP/ALIX (Santa Cruz Biotechnology, # sc-166952, 1:1000 dilution), TSG101 (Abcam, #ab15011, 1:1000 dilution), CD63 (Santa Cruz Biotechnology, #sc-5275, 1:500 dilution) and Calnexin (Abcam, #ab22595, 1:2000 dilution). Following washes, the membranes were incubated with horseradish peroxidase-conjugated secondary antibodies, specifically goat anti-mouse m-IgGκ BP-horseradish peroxidase (HRP) (Santa Cruz Biotechnology, #sc-516102) and goat anti-rabbit IgG, F(ab')2-HRP: (Santa Cruz Biotechnology, #sc-3837) at a dilution of 1:2000. Immunoreactive bands were identified using Western Blotting Detection Reagent kit (GE HealthCare Lifesciences). A Nikon d610 dSLR body (Nikon) with Sigma 35mm f/1.4 DG HSM Art lens (Sigma) was used to collect the images.

2.5 NTA

NanoSight NS300 (Malvern Analytical, UK) with an incorporated scientific metal-oxide-semiconductor camera and a green (532 nm) laser, was used to quantify the amount of isolated EVs. Samples were diluted 1:1000 in 20nm filtered phosphate buffer saline (PBS) prior measurement. Every sample was measured 5 times for a duration of 60 seconds each time with the following settings: 25ºC, 0.944–0.948 cP, 1259 slider shutter, 366 slider gain, camera level 11 and screen gain 1. The data obtained was analyzed using NanoSight NTA software v3.4 Build 3.4.003, in the auto mode.

2.6 RNA isolation and library construction

Tissue homogenization was performed on 20mg of prostate tissue utilizing QIAzol Lysis Reagent (Qiagen, USA) and Lysing Matrix A tubes in a FastPrep-24 homogenizer (MP Biomedicals, USA). RNA was isolated using miRNeasy Micro Kit (Qiagen, USA) following the small RNA enrichment protocol and manufacturer's instructions. This method allowed for the acquisition of both the long and small RNA fractions from each sample. EV RNA was extracted using miRNeasy Micro Kit Qiagen, USA) following manufacturer's instructions with the addition of on-column DNAse treatment. The assessment of RNA quantity and quality was conducted using Agilent pico RNA kit and Agilent 2100 Bioanalyzer (Agilent Technologies, USA).

EV-RNA libraries were generated by utilizing 50% of the total extracted EV RNA, without implementing any size separation procedure. 10 ng of tissue small RNA fraction

were used to build tissue small RNA libraries. Libraries were built by employing the CleanTag® Small RNA Library Prep Kit (Trilink Biotechnologies, USA). Afterwards, libraries were cleaned and size-selected using Blue Pippin DNA Size Selection method, with the use of a 3% gel Blue Pippin Cassette (Sage Science, USA) with a set target length range of 130-250 bp. All libraries were built in duplicates. Libraries were seqeunced on an Illumina NextSeq500 instrument, utilizing the NextSeq 500/550 Mid Output Kit v2.5 (150 cycles) (Illumina, USA).

Duplicate transcriptome libraries were constructed using 100 ng of tissue long RNA fraction through the utilization of TruSeq Stranded mRNA library Prep (Illumina, USA) in accordance with the manufacturer's guidelines. The libraries were subjected to size selection using the Blue Pippin system, which the employment of 2% gel Blue Pippin Cassette (Sage Science, USA) with a size range of 200 - 600 bp. The quality and quantity of the libraries were evaluated using the Agilent DNA kit (Agilent technologies, USA). The libraries underwent pooling and sequencing procedures utilizing a NextSeq 500/550 High Output Kit v2.5 (300 cycles) (Illumina, USA).

2.7 Sequencing data analysis

RNA sequencing data analysis was performed by Dr. Pawel Zayakin. Briefly, the raw data, obtained in FASTQ format, underwent analysis through a custom R script pipeline using R version 4.1.2 [203]. The methodology for small RNA libraries involved several steps, including adapter trimming using Cutadapt [204], read mapping against the Ensembl human genome (GRCh38) using Bowtie2 [205], repositioning of multi-aligned reads using ShortStack [206], counting using the htseq-count package [207] with GRCh38 and miRbase [208], GtRNAdb [209], LNCipedia [210], lncRNAdb [211], piRBase [212], piRNABank [213], and piRNAdb [214] annotations. In the context of transcriptome libraries, the process of read mapping was carried out utilizing the STAR algorithm [215], with a focus on exclusively considering unique alignments for the purpose of quantification. The process of analyzing differentially expressed genes (DEGs) involved the normalization and subsequent analysis of reads using the DESeq2 package [216]. The Benjamini-Hochberg procedure was utilized for the purpose of multiple testing correction, and a significance level of ≤ 0.05 was deemed significant after adjusting the Adj. p-value. The RNA sequences datasets are available at ArrayExpress, accession number E-MTAB-11910 (https://www.ebi.ac.uk/biostudies/arrayexpress/studies/E-MTAB-11910).

2.8 RNA metagenome pipeline

In order to detect microbial reads, RNA reads that were not previously mapped to GRCh38, were subjected to analysis using Kraken 2 [217]. To ensure the exclusion of human read traces, the unmapped reads from transcriptome libraries, were first filtered using BMTagger [218]. Results were filtered Conifier with a set threshold of 50% RTL confidence score using Conifier (https://github.com/Ivarz/Conifer). Reads assigned to family or genus levels were remapped at species level proportionally to the hits. Species with a minimum of 10hits were selected and their genomes were downloaded from the following databases: RefSeq [219], Ensembl [220], GenBank [221], in order to build our prostate metagenome (PM).

Non-template libraries were sequenced to eliminate potential environmental contaminants. The reads that exhibited exact matches or contained sequences found in the non-template control libraries were subtracted from the EV RNA libraries. Remaining exogenous RNA reads from the EV RNA libraries were mapped against the PM using

Bowtie2 [205] with the following parameters: end to end, very sensitive, no 1mm upfront, score min L, -1.15, -0.24.

2.9 Genome-agnostics pipeline

Identical exogenous EV RNA reads were counted using ad-hoc R script pipeline [222] and differential expression analysis was performed using EdgeR [223]. To obtain consensus sequences of overlapping reads, a multiple sequence alignment for the top 1000 overexpressed (log2FC >1, top 1000 by adj.p-value) and downregulated (log2FC < -1, top 1000 by adj. p-value) reads was performed using the MSA package [224] and ClustalW [225]. The largest clusters were manually selected, and their corresponding consensus sequences were combined. Exogenous EV RNA reads were then aligned against these consensus sequences, and differential expression analysis using EdgeR [223] was conducted. Volcano plots were generated using Enhance Volcano package [226]. The differentially expressed consensus sequences were identified through BLAST [227] analysis.

2.10 Droplet digital PCR (RT-ddPCR)

Half of the total extracted extracellular vesicle RNA yield was used for reverse transcription using the miRCURY LNA RT kit (Qiagen, USA) in accordance with the manufacturer's instructions. In the experiment, a polymerase chain reaction (PCR) reaction of 20 µl was prepared, which included 1:2 diluted complementary DNA (cDNA), 10 µl of 2xEvaGreen Supermix (Bio-Rad, USA), and either 1µl of miRCURY LNA primer mix (Qiagen, USA) or 2 µl of QuantiNova LNA primer mix (Qiagen,USA) (Appendix Table S2). The mixture was then placed into a disposable droplet generator cartridge (Bio-Rad, USA). Subsequently, 70 µl of droplet generation oil intended for EvaGreen was introduced into the respective wells and transferred to a QX200 droplet generator (Bio-Rad, USA). Once droplets were generated, they were transferred to a RT-ddPCR clear semi-skirted 96-well plate (Bio-Rad, USA), covered with a Pierceable Foil Heat Seal (Bio-Rad, USA) and amplified in a T100 Thermal Cycler (Bio-Rad, USA) under the following conditions: 95ºC for 5 min; 40 cycles at 95ºC for 30 seconds (sec) followed by specific primer annealing temperature (Appendix Table S2), 4ºC for 5 min; 90ºC for 5 min. and indefinite hold at 4ºC. The experiment was conducted at a ramp rate of 2ºC per second. The plate was assessed utilizing a QX200 Droplet Reader (Bio-Rad, USA), and the outcomes were evaluated utilizing the QuantaSoft™ Software (Bio-Rad, USA). The determination of the optimal annealing temperature for each assay was achieved by subjecting it to a thermal gradient ranging from 50-60°C.

2.11 RNA biomarker model

The RNA biomarker model was developed in R Studio [203] with the glm package [228], using the Binary Logistics regression technique. The model was created using RT-ddPCR data from PC and BPH patients, demonstrating the simultaneous effects of multiple independent factors on the target variable. The equation for the model is the following:

$$P(Y) = \frac{e^{b_0+b_1x_1+b_2x_2+\ b_nx_n}}{1+\ e^{b_0+b_1x_1+b_2x_2+\ b_nx_n}}$$

P: probability of Y, e: natural logarithm base, b 0: interception at y-axis, b1: line gradient, $b\ n$: Xn regression factor and X1: variable [229]. The built-in Binary Logistics function model was examined and displayed on the output data using the ROCR software package [230]. The RNA biomarker analysis was performed by the bioinformatician Dr. Pawel Zayakin.

Validation of the RNA model was developed in R Studio [203] using Leave-One-Out Cross Validation (LOOCV) [231] procedure by the bioinformatician Pawel Zayakin. LOOCV is based on splitting the data set into two groups, a training set and a validation set. Validation set includes one observation, and the training set includes n-1. This process was repeated for all observations. The equation behind the procedure is the following:

$$CV_n = \frac{1}{n} \sum_{i=1}^{n} (y_i - \hat{y}_i)^2$$

2.12 Statistical analysis

The statistical analyses were conducted utilizing GraphPad Prism 9.5.1 software (GraphPad, USA). The Wilcoxon matched-paired signed rank test was utilized to evaluate the comparison between PreOp and PostOp data. Mann-Whitney test was performed to compare High Gleason versus Low Gleason and BPH versus PC. A statistical analysis utilizing the Kruskal-Wallis test, followed by multiple comparisons corrected by Dunn's test, was conducted in order to ascertain any disparities among RNA biotypes; CAPRA score; and ISUP grade. Spearman rank correlation test was performed to study the correlation between prognostic tests and selected biomarkers. A $p \leq 0.05$ was considered significant.

3. RESULTS

3.1. EV RNA PC biomarker discovery - validation workflow

In order to identify PC-derived RNA biomarkers, we performed RNA sequencing analysis of plasma and urine EV samples from PC patients collected before (PreOp) and three months after (PostOp) RP; and tumour and matched normal prostate tissue samples from 10 PC patients. Patients were classified based on their GS. Patient's characteristics ae shown in Table S1 (Appendix), and a workflow of the experiment is shown in Figure 4. Once potential biomarkers were identified, validation was carried out in an independent set of urine and plasma EVs from 20PC and 20 BPH patients by RT-ddPCR.

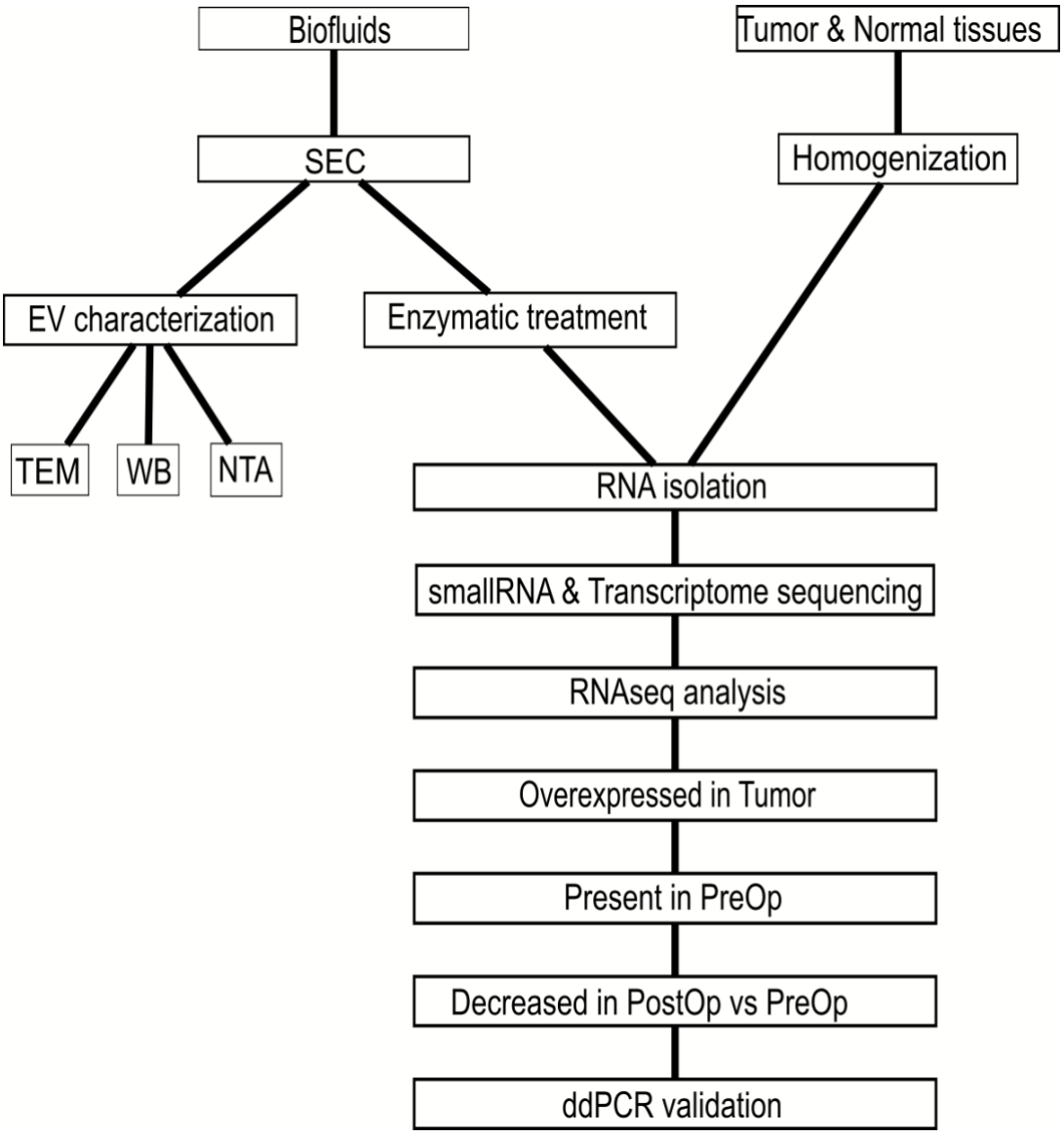

Figure 4. Workflow of the study. SEC: Size-exclusion chromatography; TEM: transmission electron microscopy; WB: Western Blot; NTA: Nanoparticle tracking analysis; PreOp: Pre-Operation, PostOp: Post-operation; ddPCR: Reverse transcription digital droplet PCR.

3.2 Characterization of EVs

In order to evaluate the purity and size distribution of EVs, the obtained EVs were characterized by TEM (Figs. 5 & 6) and WB analysis (Fig.7); while particle concentration was assessed by NTA (Figs. 8 & 9).

Urinary and plasma EVs were assessed by TEM in order to ascertain size and morphological characteristics. Our results show that most of the particles identified in urine samples ranged between 30 and 150 nanometers (nm) in size (Fig. 5); while plasma EVs (Fig. 6) exhibit a slightly broader range, from 30 to 250nm. In addition, smaller particles (less than 30 nm in diameter) were also observed in plasma samples (Fig.6). Both sample types exhibit the typical cup-shaped morphology expected of small EVs present in TEM. This cup-shaped morphology is an artifact that occurs during the sample fixation process [119].

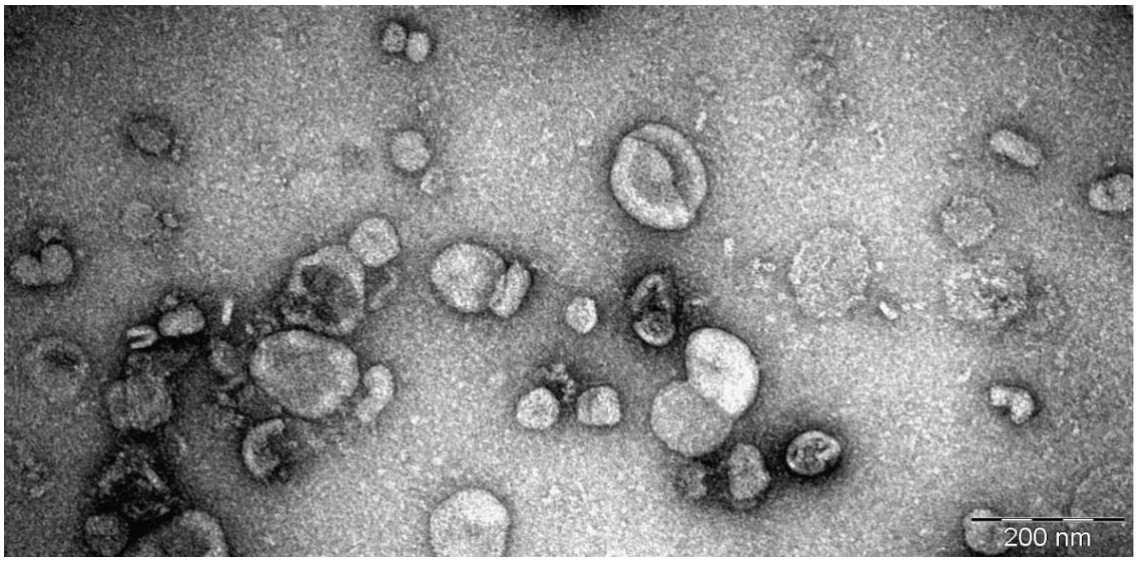

Figure 5. Representative TEM image of urinary EVs. Scale: 200nm

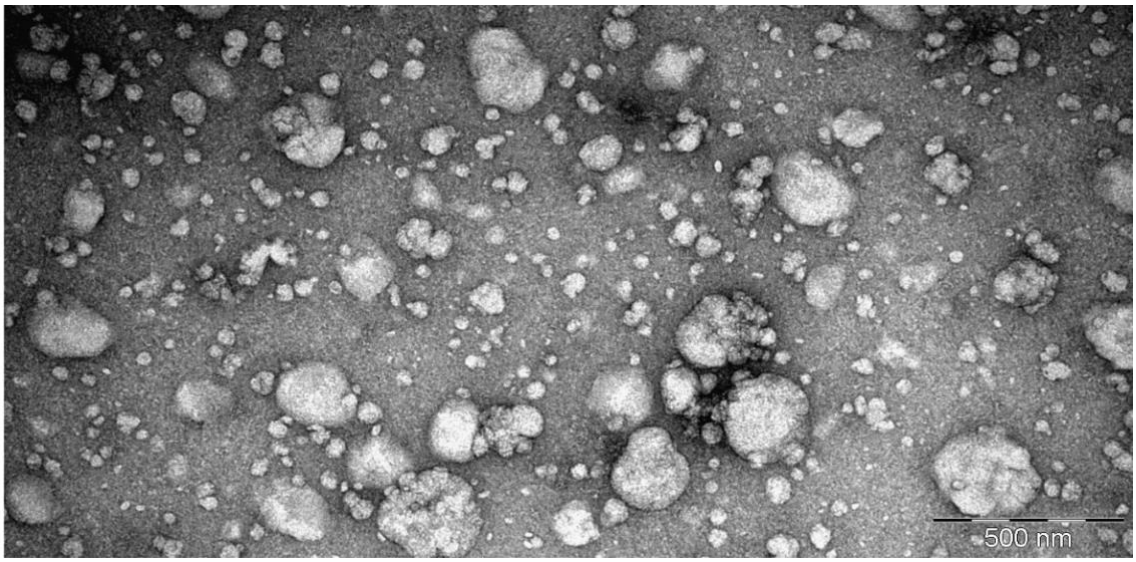

Figure 6. Representative TEM image of plasma EVs. Scale: 500nm

WB was run to investigate the presence of specific EVs protein markers, in order to assess the purity of our EV isolation pipeline. Both, plasma and urinary EVs were positive for ALIX, TSG101, and CD63, distinctive EV markers (Fig. 7) [119]. CD63 expression presented a smear pattern between 30 and 50kDa (Fig. 7). This has been previously reported and it is due to the different glycosylation states of the tetraspanin state, the isolation and the antibody used [232]. The molecular weight of ALIX in plasma EVs is around 75 kDa, which is the same as the product of the C-terminal proteolytic cleavage [233]. Calnexin, an endoplasmic reticulum protein, was not present in EVs (Fig. 7), indicating that there was little to no ER membrane contamination in the EV preparations.

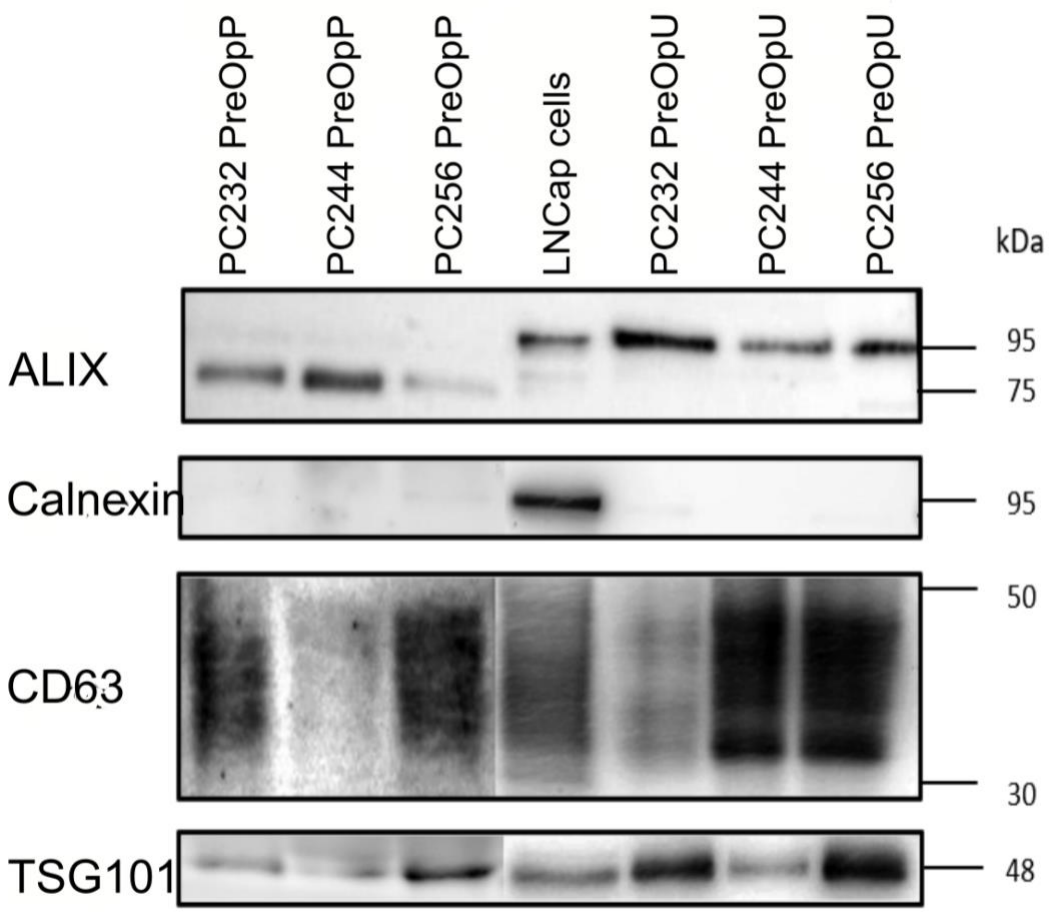

Figure 7. Western blot of CD63, ALIX, TSG101 and calnexin in LNCaP prostate cancer cells and PreOp urinary and plasma EVs from three different patients. kDa: KiloDaltons; PC: Prostate Cancer; PreOp: Pre-operation; PostOp: Post-Operation.

NTA was used to determine the EV concentration in order to compare the yield and EV dynamics before and after the RP from the 30 PC samples in plasma and urine (Figs. 8 & 9). The results revealed that whereas the number of particles per ml in plasma varied from 5.68×10^9 to 7.10×10^{11} particles per ml (Fig. 8), the number per ml in urine ranged from 2.26×10^7 to 1.5×10^{10} particles per ml (Fig. 9). No significant change was observed between the EV numbers before and after RP, as shown in Figures 8 and 9. This observation held true even for patients who experienced recurrence after RP (n = 3). The EV yields were similar with those reported in previous research [148, 234].

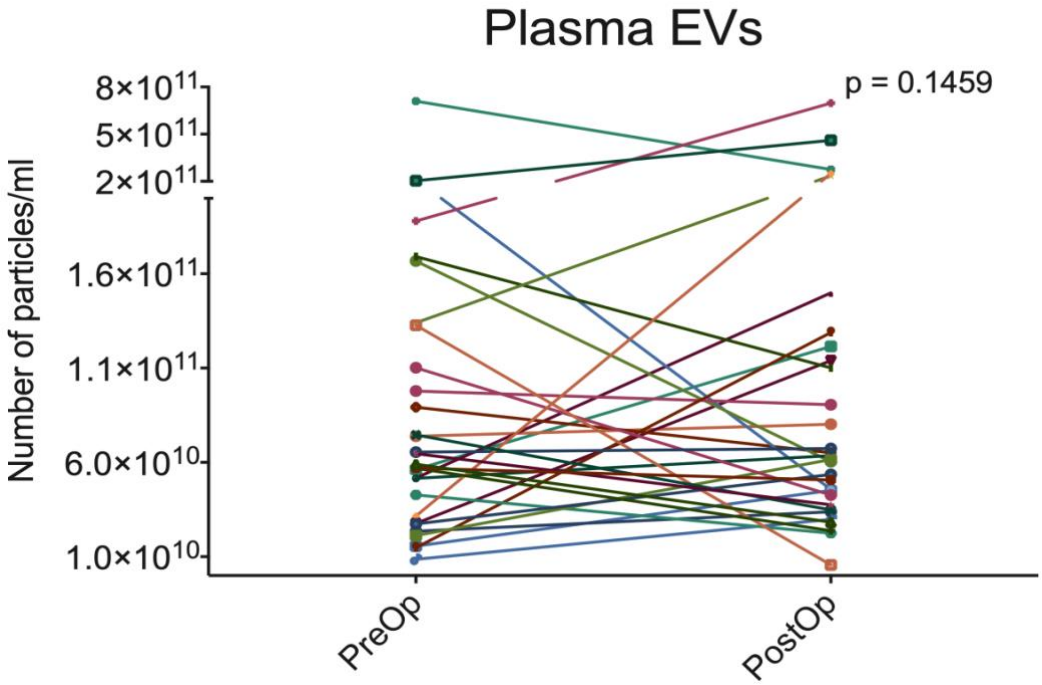

Figure 8. Paired dot plots showing the numbers of EVs per ml of plasma before and after radical prostatectomy. Wilcoxon matched-paired signed rank test was used to assess the statistical significance of the differences between groups. p: p-value

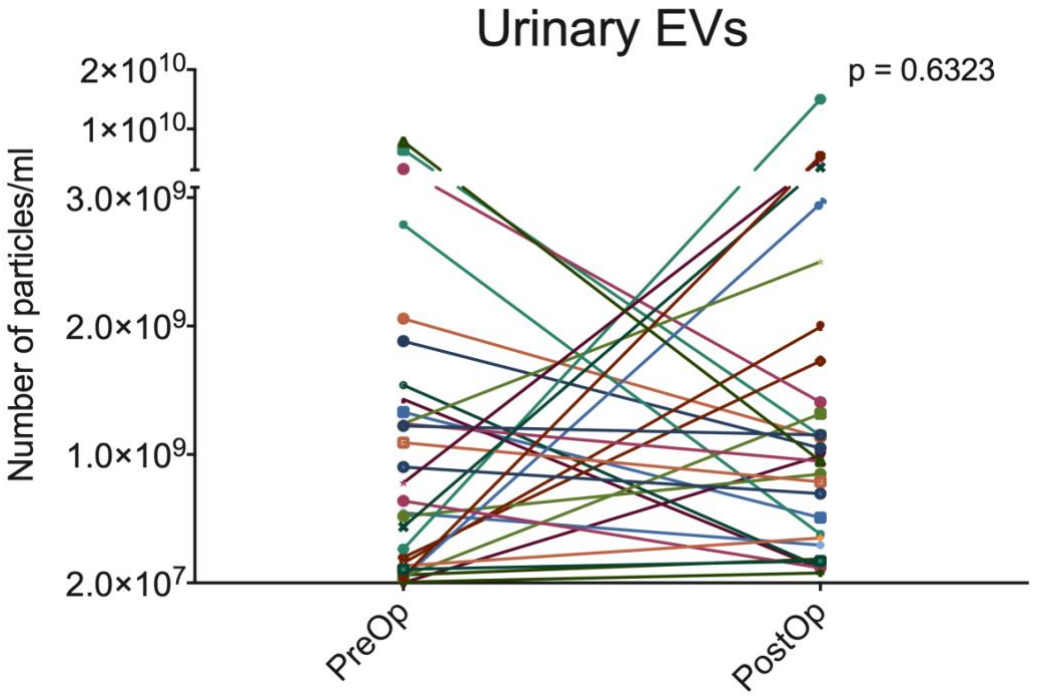

Figure 9. Paired dot plots showing the numbers of EVs per ml of urine before (PreOp) and after radical prostatectomy (PostOp). Wilcoxon matched-paired signed rank test was used to assess the statistical significance of the differences between groups. p: p-value.

We analyzed the EV concentration from BPH and HD samples, and we compared it with PC. BPH plasma EV concentrations ranged from 7.63×10^9 to 2.46×10^{11} particles per ml, with an average value of 9.39×10^{10} (Fig. 10) and HD plasma isolated EV concentrations ranged from 1.46×10^{10} to 1.07×10^{11} with an average of 6.46×10^{10} (Fig. 10). Urine-isolated EV concentrations ranged from 1.94×10^7 to 8.97×10^9 particles per ml with an average value of 1.30×10^9 (Fig. 11). PC PreOp plasma samples displayed a mean value of 1.02 x 10^{11} particles per ml (Fig.10), while their correspondent urinary EVs showed 2.60 x10^9particles per ml (Fig. 11). Both groups, PC and BPH patients revealed similar average mean of particles per ml, showing no statistical significance and similar levels as described before[148, 234].

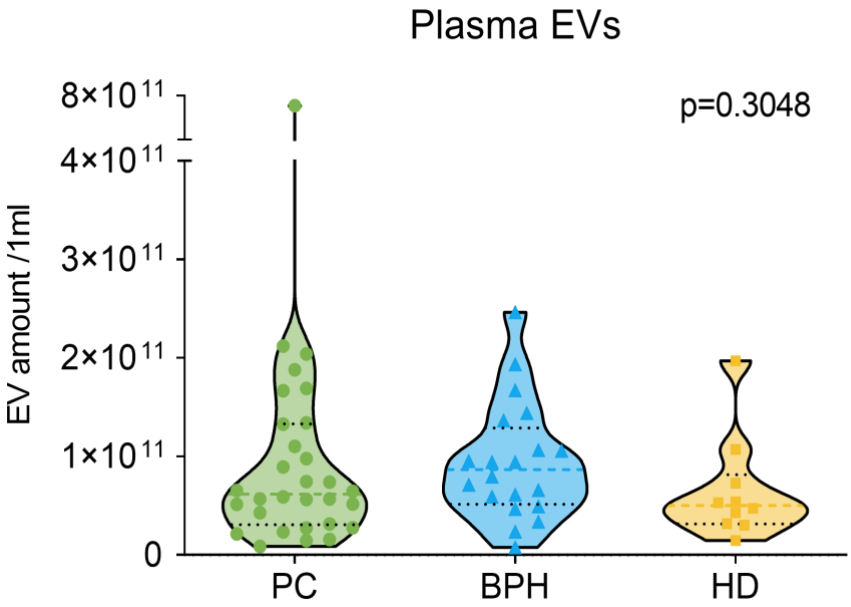

Figure 10. Violin plot showing the number of EVs per ml of plasma in PC, BPH and HD samples. Kruskal-Wallis test was used to assess differences between groups. p: p-value. PC: prostate cancer; BPH: benign prostate hyperplasia; HD: healthy donor

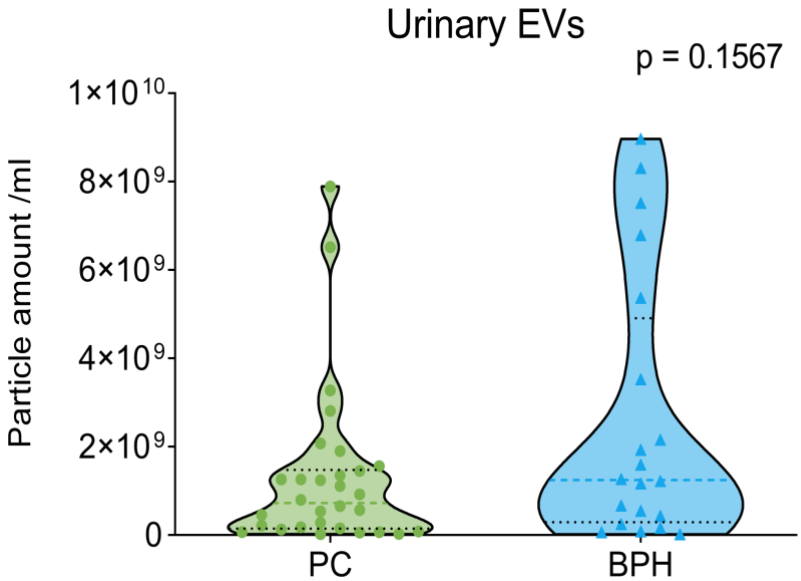

Figure 11. Violin plot showing the number of EVs per ml of urine in prostate cancer and BPH samples. Mann-Whitney test was employed to assess the differences between groups. p: p-value. PC: prostate cancer; BPH: benign prostate hyperplasia

3.3 EVs contain different species of RNA

In order to analyze the RNA content of plasma and urinary EVs, we conducted a comprehensive RNA sequencing analysis (RNAseq) on samples obtained from 10 patients with prostate cancer. The samples included pre-operative plasma (PreOpP), post-operative plasma at 3 months (PostOpP), pre-operative urine (PreOpU), post-operative urine at 3 months (PostOpU), as well as small RNA fractions from histologically confirmed prostate cancer tissue (T_S) and normal prostate tissue (N_S). Furthermore, since the smallRNA fraction present in tissue specimens might contain solely fragments of deteriorated mRNAs and lncRNAs, in order to acquire unbiased long RNA expression profiles, complete transcriptome libraries were constructed from both tumour (T_L) and normal prostate (N_L) tissues. Detailed bioinformatic pipelines for the analysis of RNAseq can be seen in Figure 12.

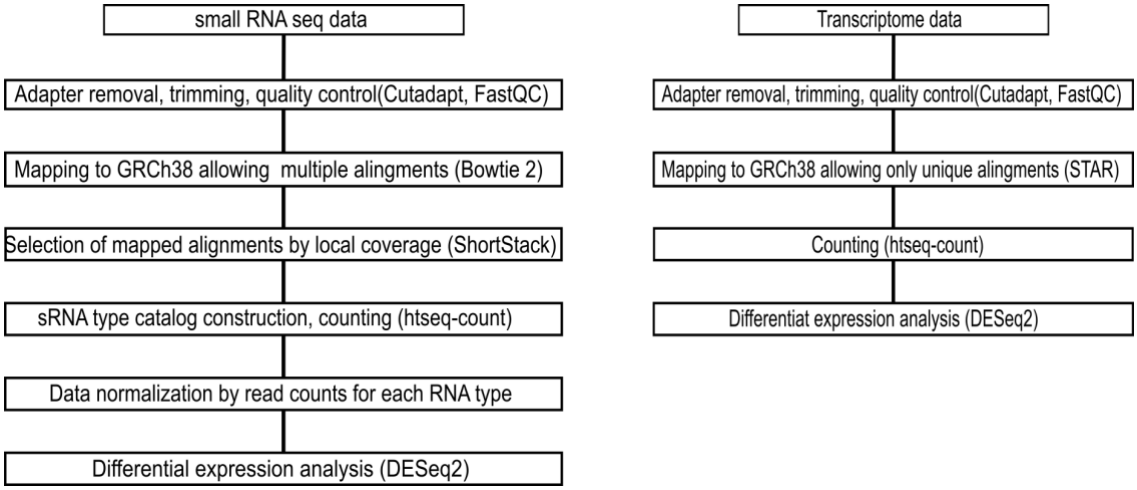

Figure 12. Bioinformatic pipelines followed to analysis small RNA libraries (on the left) and transcriptome libraries (on the right).

The present investigation centered on intraluminal RNAs, thus EVs underwent treatment with proteinase K and RNAse A prior to RNA extraction, in order to eliminate the EV corona and potential associated RNAs to EV surface [138, 140].

The mean number of raw reads acquired per EV library was 4.45 million, with an average of 3.38 million reads remaining after undergoing quality control, adaptor trimming, and removal of fragments smaller than 18 nt. In order to evaluate the presence of different RNA biotypes in plasma and urinary EVs, the sequencing reads that aligned with overlapping features in the human genome were given priority based on the following hierarchy: miRNAs > tRNAs > rRNA > mRNAs > pseudogenes > snRNAs > snoRNAs > piRNAs > lncRNAs > miscellaneous RNAs (miscRNAs). Figure 13 depicts the distribution of RNA biotypes as percentage of reads. The analysis revealed that in urinary EVs, miRNA constituted the highest percentage (32%), followed by piRNAs (26.5%) and tRNAs (15%). Additionally, lincRNA (8%), rRNAs (6%), and fragments of mRNAs (5.5%) were also present. On the other hand, plasma EVs exhibited a higher proportion of piRNAs (32.5%), followed by miRNAs (21%), lincRNAs (13%), tRNAs (9.5%), and fragments of mRNAs (8.5%) (Figure 13). Similarly in tissue small RNA libraries, miRNAs (N = 41.9%; T= 24.75%) and piRNAs (N=20.8%; T=27%), showed the highest proportion, followed by snoRNAs (13.8%) in tumour tissue, mRNAs (N =7.35%, T= 11.7%) and tRNAs (9.45%) in normal prostate tissue (Figure 13).

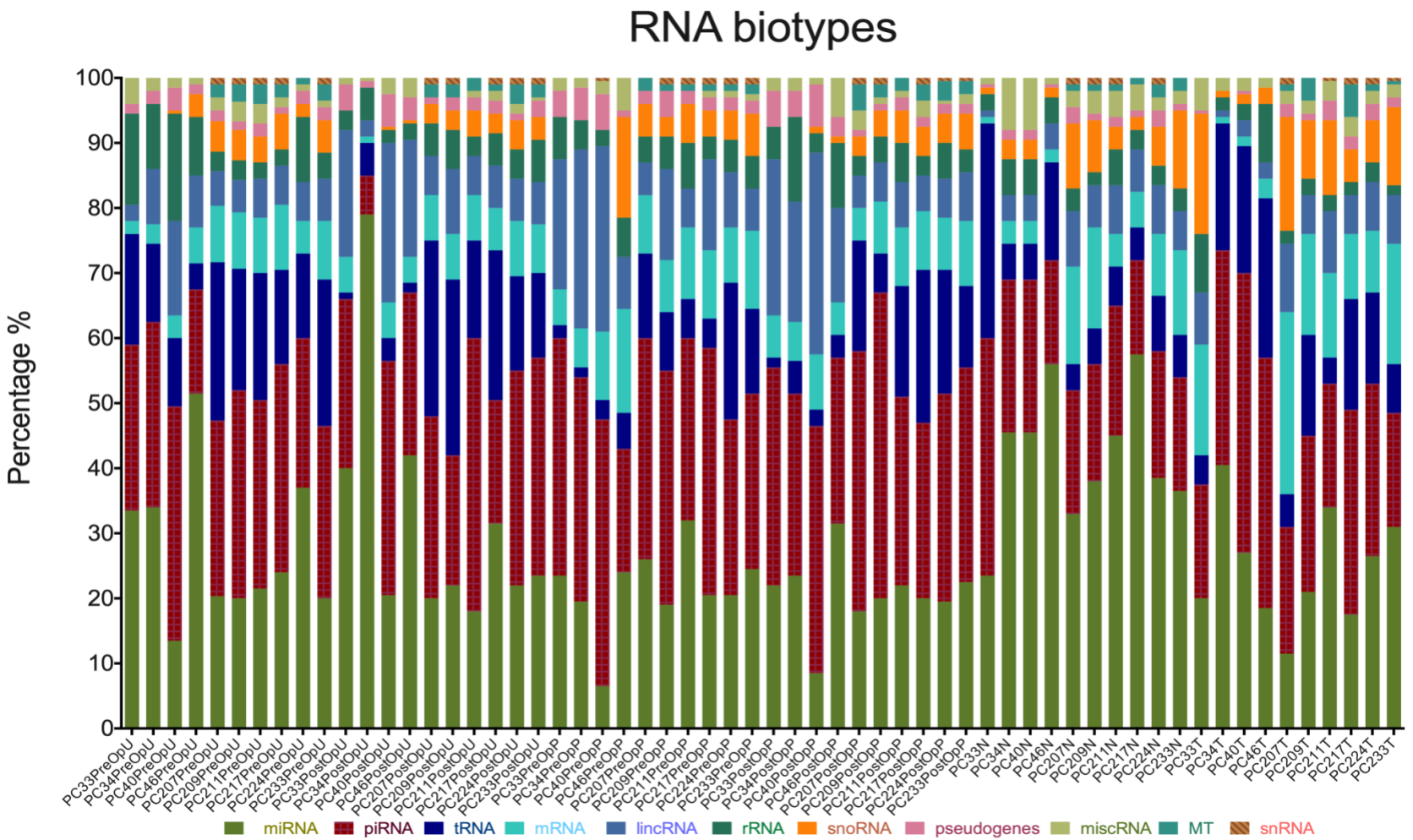

Figure 13. Percentage of reads representing various RNA biotypes in each sample. PC: Prostate Cancer, each number corresponds a patient set. PreOpU: Urine samples before surgery, PostOpU: Uine samples collected 3-months after surgery; PreOpP: Plasma samples collected before surgery; PostOpP: Plasma sampled collected after surgery; T: tumour tissue; N: adjacent prostate tissue.

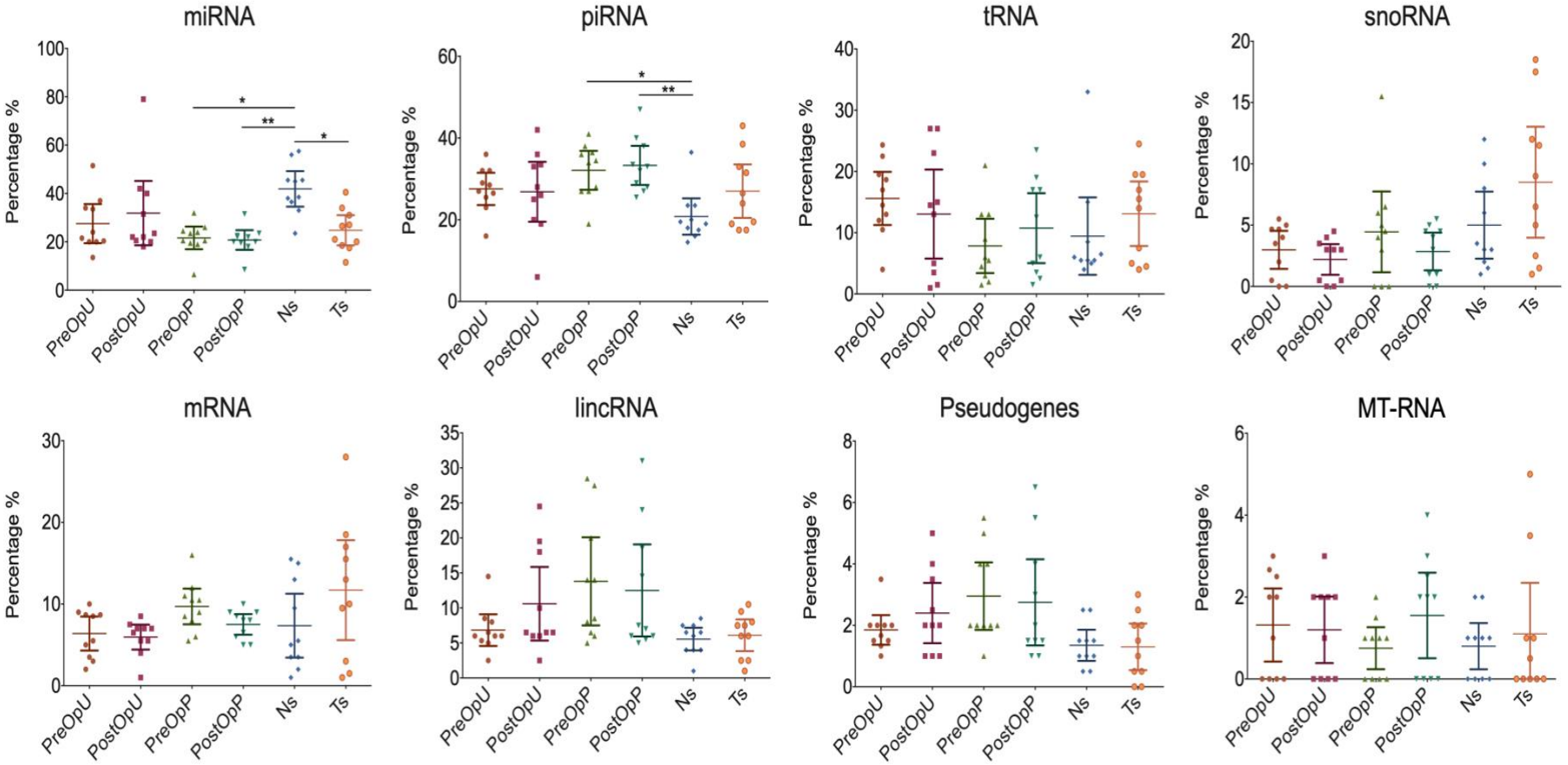

Figure 14. Dot plots showing the comparison of specific RNA biotypes in the sample groups. PreOpU: Urine samples before surgery, PostOpU: Uine samples collected 3-months after surgery; PreOpP: Plasma samples collected before surgery; PostOpP: Plasma sampled collected after surgery; Ts: tumour tissue smallRNA; Ns: adjacent prostate tissue smallRNA. Kruskal – Wallis test with multiple comparison corrected by Dunn's test was used to assess the statistical significance of the differences between groups * p<0.5: ** p<0.01

Compared to prostate tissues, plasma EVs exhibited a higher proportion of piRNA and a lower proportion of miRNA (Fig. 14). Similarly, a significantly higher proportion of miRNAs was identified in prostate compared to tumour tissue (Fig. 14). No statistically significant differences were found in the composition of RNA biotypes between PreOp and PostOp EV samples (Fig. 14).

3.4 Identification of PC – derived RNA biomarkers

In order to identify RNAs that originate from PC tissues and are enclosed in EVs, we conducted a search for RNAs that satisfied specific criteria within each RNA biotype: (1) overexpressed in tumour tissues as compared to normal prostate tissues (log fold change (log2FC)>1, adj. p <0.05); (2) present in the PreOp EVs (at least 10 raw reads in one of the samples) and (3) decrease in the PostOp EVs as compared to PreOp EVs (log2FC>1, adj. P<0.05). RNAs that satisfied these specific criteria were identified across four distinct RNA biotypes, namely miRNA (Fig. 15), piRNA (Fig. 16), lncRNA (Fig. 17), and mRNA (Fig. 18).

The small RNA libraries derived from PC and normal prostate tissues yielded a total of 376 miRNAs, out of which 54 were observed to be overexpressed in tumour tissue (Fig. 15). Among those, miR-182 -5p, miR-183 - 5p, miR-375-3p and 148a - 5p show the highest significant overexpression in tumour tissue (Fig. 15), while miR-490 - 5p, mir-873 - 5p, miR-184 and miR-6507-5p had higher expression level in normal prostate tissue (Fig. 15).

In order to identify miRNAs upregulated in PreOp samples compared to PostOp samples, we analyzed EV data obtained from each biofluid separately. Urinary EVs contained 331 distinct miRNAs, three of which - miRNAs, miR-375 - 3p, miR-378a - 3p and miR-92a-1-5p, were upregulated in PreOp compared to PostOp (Fig. 15); and two miRNAs, miR - 509 - 3p and miR-12113 downregulated in PreOp vs. PostOp (Fig. 15). A total of 288 different miRNAs were identified as plasma EVs cargo, but the analysis did not reveal any potential candidate overexpressed in PreOP vs. PostOP (Fig. 15). Common overexpressed miRNAs present in both tissue samples and PreOp EVs is shown in Figure 15 and Table S2. Analysis revealed that only 2 miRNAs of those found overexpressed in PreOp urinary EVs were common to those overexpressed in tumour tissue. None of the potential miRNAs biomarkers was found commonly overexpressed in tumour tissue and in PreOp EVs isolated from both biofluids (Fig. 15).

piRNA analysis indicates that the tissues, urinary and plasma EVs contained 264, 298, and 221 piRNAs, respectively, as illustrated in Figure 16. The levels of 9 and 1 piRNA were observed to be reduced in the PostOpU and PostOpP EVs, respectively. However, it is noteworthy that only piR-28004 was found to be overexpressed in PC tissues as well (Fig. 16, Appendix Table S3).

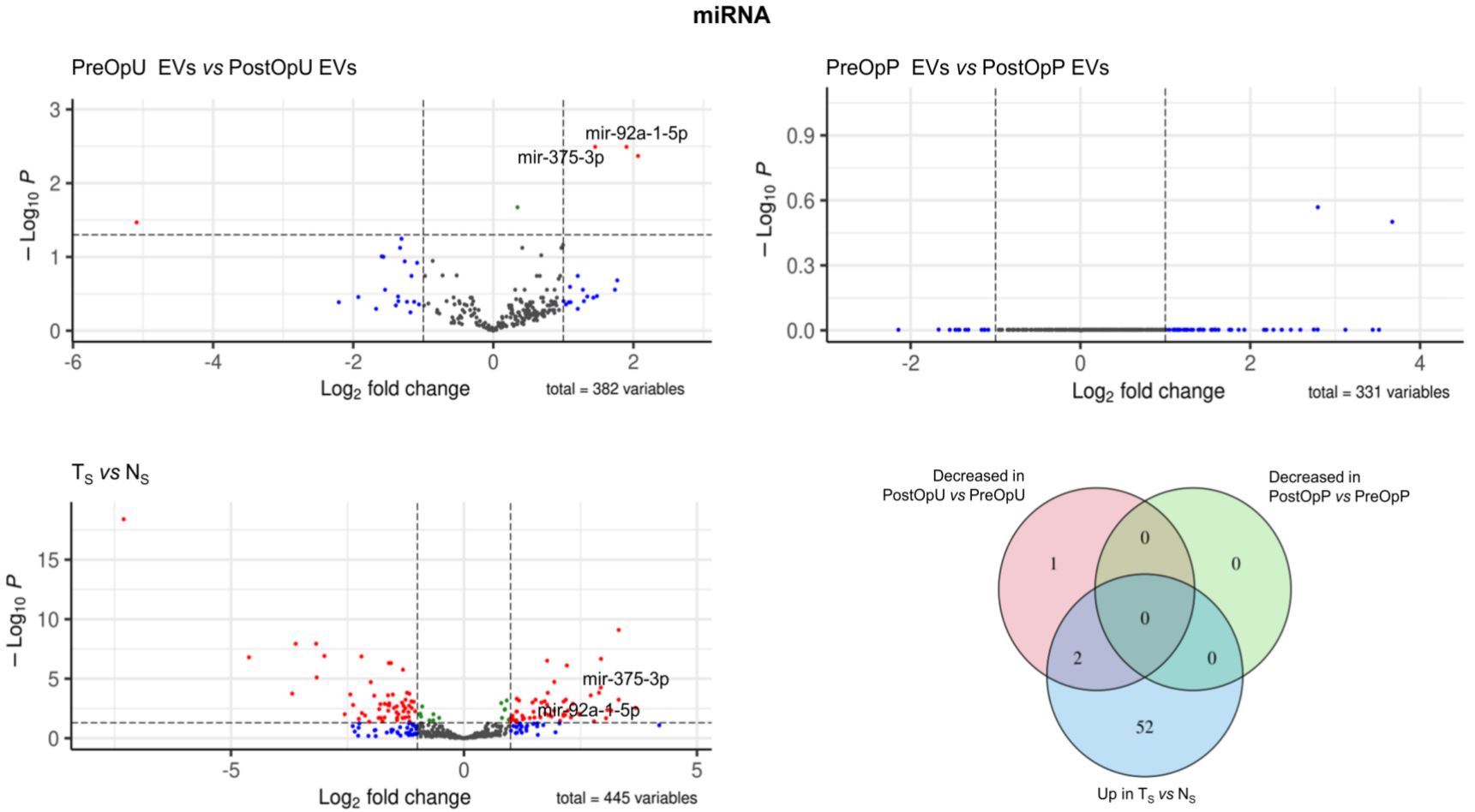

Figure 15. Differential expression analysis of miRNAs. Volcano plots depict significant differences in the urinary or plasma EVs as compared to the post-operation EVs, and in small RNA libraries prepared from tumour (T_S) and normal prostate tissues (N_S). Venn diagram show the numbers of small RNAs overexpressed in tumour tissues vs normal prostate tissues (Up in T_S vs N_S), decreased in the post-operation urinary EVs as compared to pre-operation urinary EVs and decreased in the post-operation plasma EVs as compared to pre-operation plasma EVs (log2FC >1 and adj. P-value ≤ 0.05).

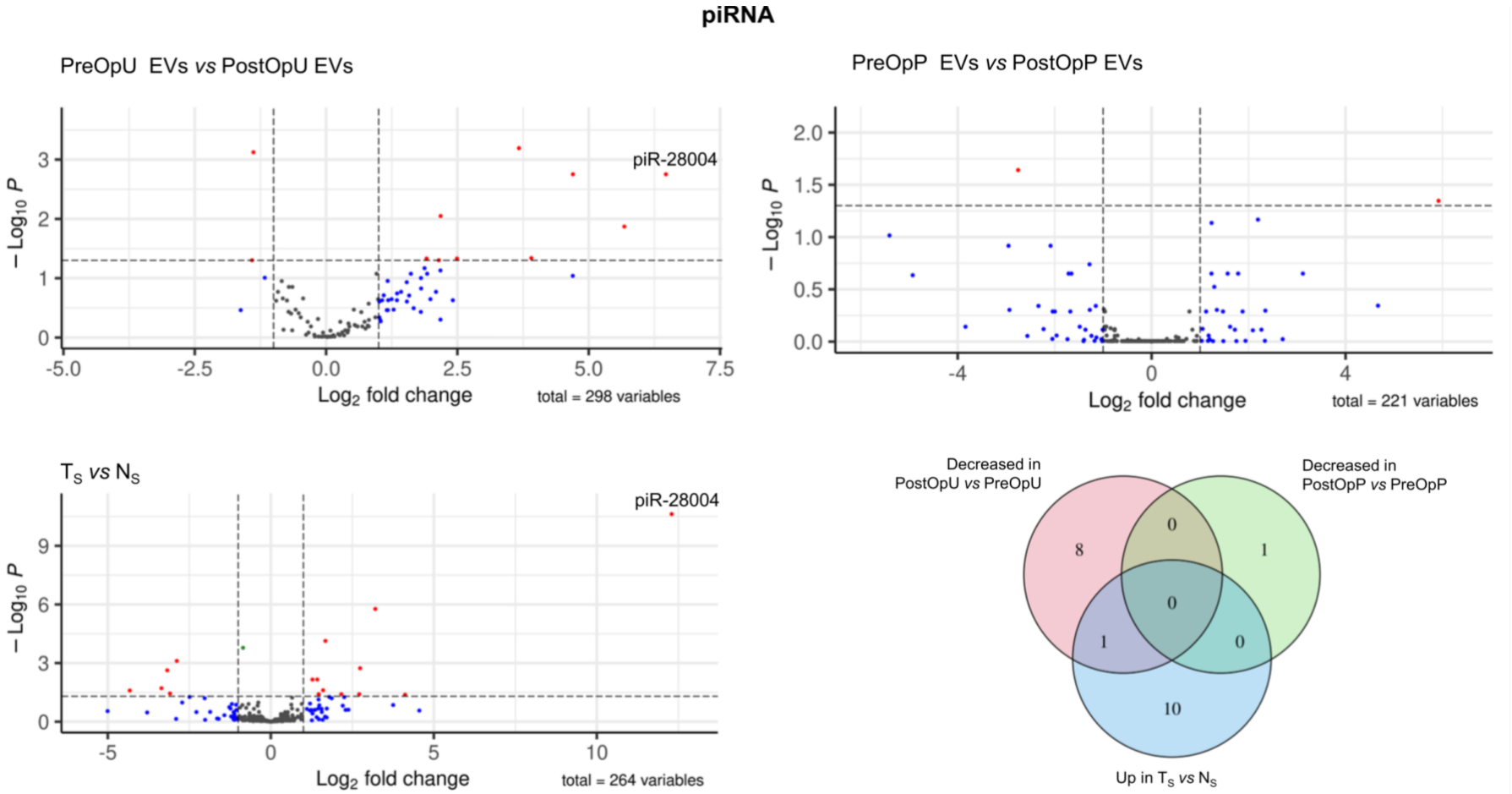

Figure 16. Differential expression analysis of piRNAs. Volcano plots depict significant differences in the pre-operation urinary or plasma EVs as compared to the post-operation EVs, and in small RNA libraries prepared from tumour (T_S) and normal prostate tissues (N_S). Venn diagram show the numbers of small RNAs overexpressed in tumour tissues vs normal prostate tissues (Up in T_S vs N_S), decreased in the post-operation urinary EVs as compared to pre-operation urinary EVs and decreased in the post-operation plasma EVs as compared to pre-operation plasma EVs (log2FC >1 and adj. P-value ≤ 0.05).

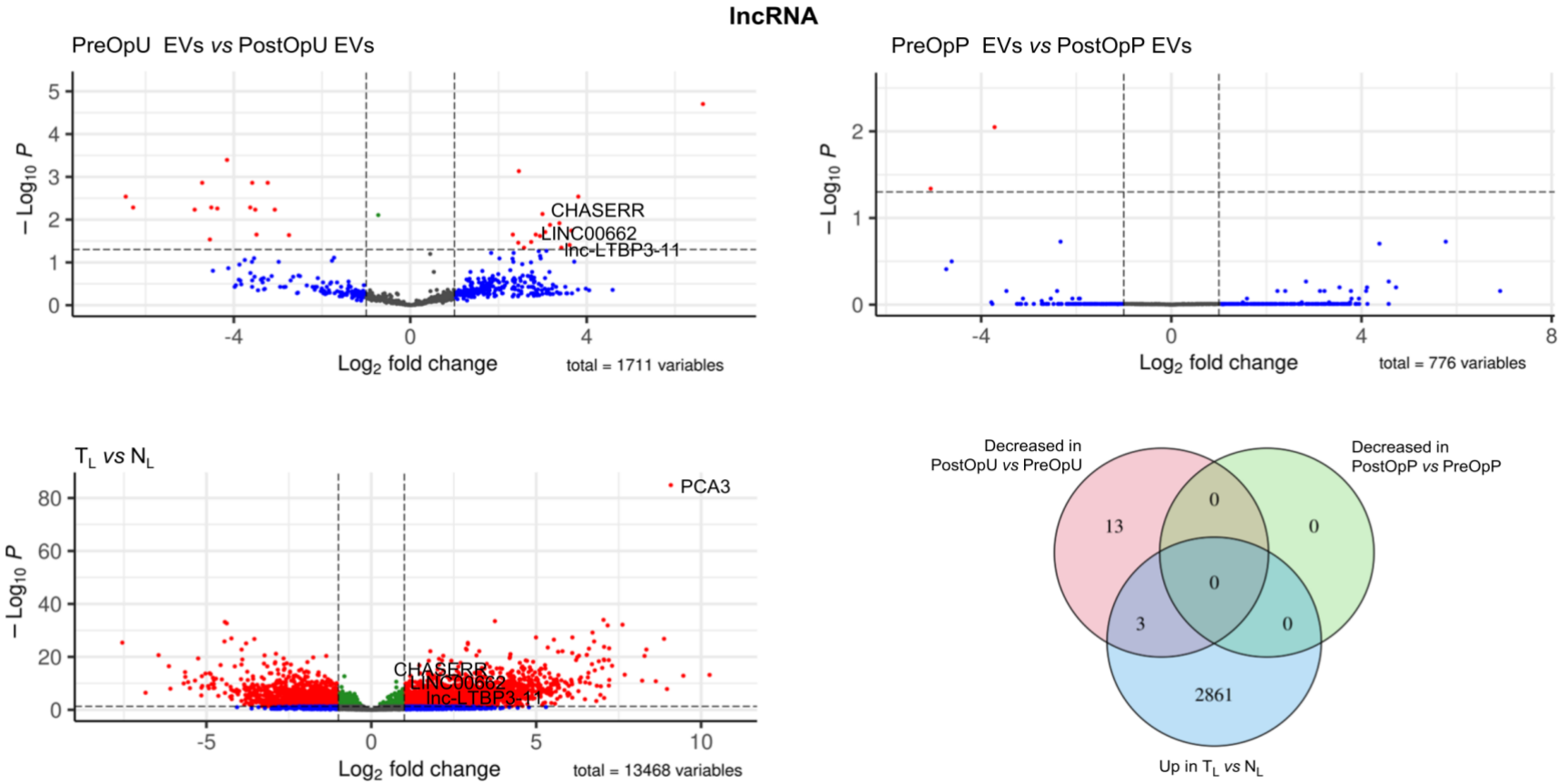

Figure 17. Differential expression analysis of lncRNAs. Volcano plots depict significant differences in the pre-operation urinary or plasma EVs as compared to the post-operation EVs, and in full transcriptome libraries prepared from tumour (T_L) and normal prostate tissues (N_L). Venn diagram show the numbers of lncRNAs overexpressed in tumour tissues vs normal prostate tissues (Up in T_L vs N_L), decreased in the post-operation urinary EVs as compared to pre-operation urinary EVs and decreased in the post-operation plasma EVs as compared to pre-operation plasma EVs (log2FC >1 and adj. P-value ≤ 0.05).

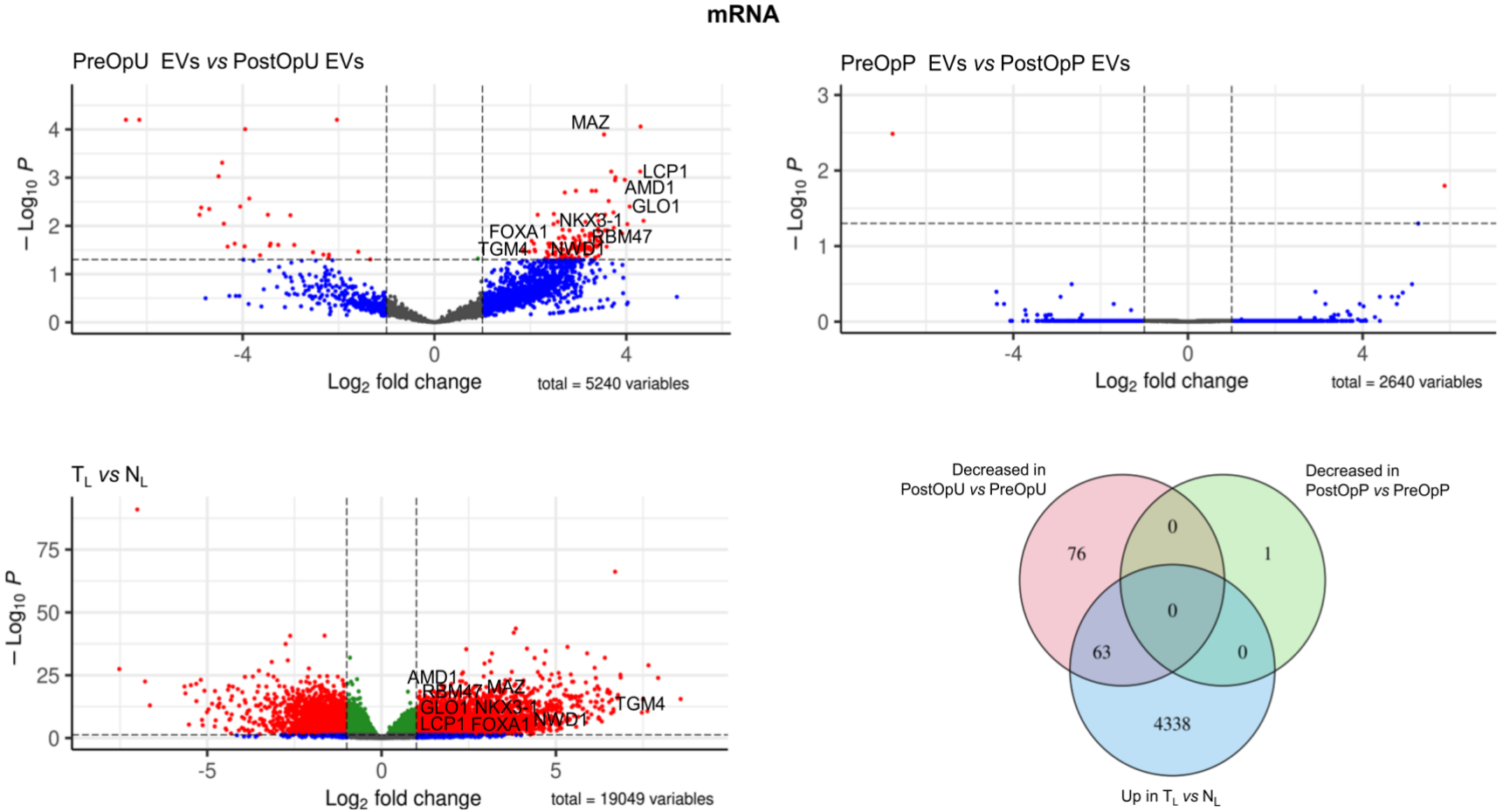

Figure 18. Differential expression analysis of mRNAs. Volcano plots depict significant differences in the pre-operation urinary or plasma EVs as compared to the post-operation EVs, and in full transcriptome libraries prepared from tumour (T_L) and normal prostate tissues (N_L). Venn diagrams show the numbers of mRNAs overexpressed in tumour tissues vs normal prostate tissues (Up in T_L vs N_L), decreased in the post-operation urinary EVs as compared to pre-operation urinary EVs and decreased in the post-operation plasma EVs as compared to pre-operation plasma EVs (log2FC >1 and adj. P-value ≤ 0.05).

The analysis of full transcriptome libraries was conducted to identify overexpressed mRNAs and lncRNAs in PC. The results of the differential expression analysis indicate that there were 2864 lncRNAs and 4401 mRNA that exhibited overexpression in cancer tissues when compared to normal tissues (Figs. 17 & 18). From those lncRNAs, PCA3 with a logfold of 9.08 presented the highest overexpression in PC tissues (Fig. 17). Following surgery, the urinary EVs exhibited a reduction in the levels of 16 long non-coding RNAs. Among these, Linc00662, CHASERR, and lnc-LTBP3-11 were found to be overexpressed in PC tissues, thus indicating their potential as biomarker candidates for prostate cancer (Fig. 17, Appendix Table S3).
The levels of 139 mRNAs were reduced in the urinary EVs after surgery, and 63 of these mRNAs were also found to be overexpressed in PC tissues (Fig. 18). These findings suggest that mRNAs are the predominant type of cancer-derived RNA biomarkers present in urinary EVs. Simultaneously, it was observed that only a single mRNA exhibited a decrease in the PostOpP EVs, and its overexpression in PC was not found to be statistically significant.

In summary, a collective of 63 mRNAs, 3 lncRNAs, 2 microRNAs, and 1 piRNA were identified as potential biomarker candidates originating from PC tissues (Fig. 19; Appendix Table S3).

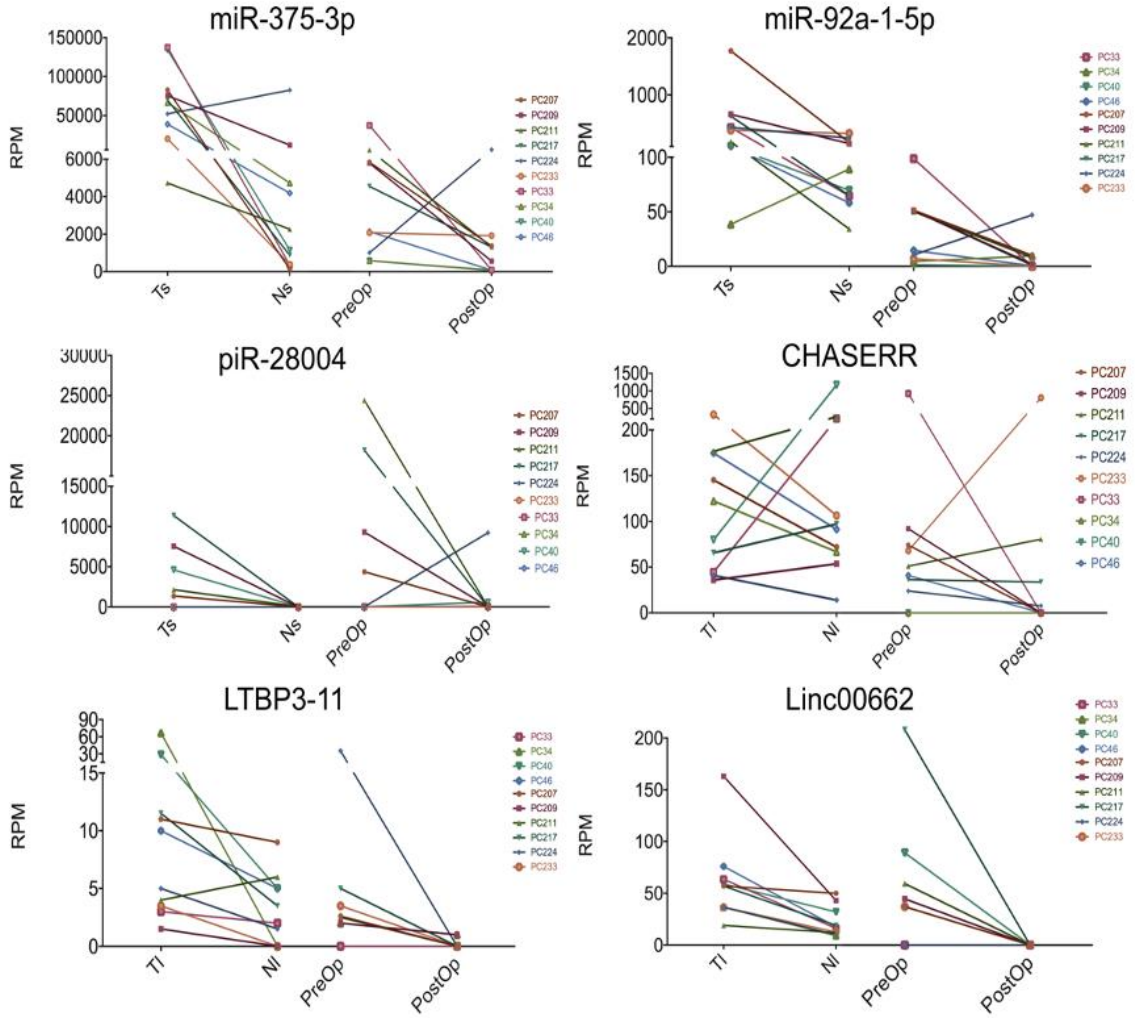

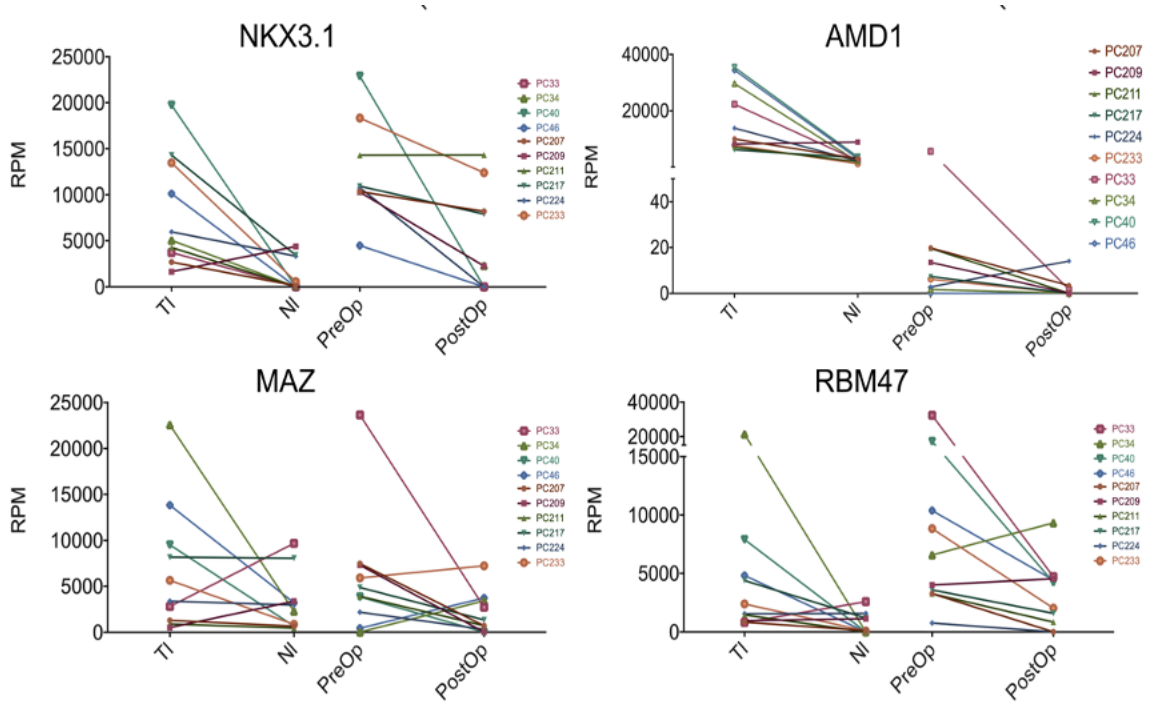

Figure 19. Selected biomarker candidates. The paired dot plots show the normalized read counts (reads per million mapped reads, RPM) for selected RNA biomarkers in tumour and normal prostate tissue small RNA libraries (T_S and N_S, respectively) or full transcriptome libraries (T_L and N_L), and pre-operation and post-operation urinary EVs. Log2 fold changes and multiple testing adjusted *P* values are shown in Table S3.

3.5 Validation of human PC biomarkers by RT- ddPCR

A group of potential biomarkers, encompassing diverse RNA biotypes, was identified based on their functional significance, fold changes, and expression levels (Section 3.4 & Appendix Table S3). Custom assays for PCR amplification were designed for each candidate using either QuantiNova LNA PCR or miRCURY LNA miRNA PCR assays, depending on the target length and RNA biotype (see Methodology Section 2.9). These assays were designed using the GeneGlobe platform provided by Qiagen [235]. Based on the sequencing data, it was determined that the mRNAs and lncRNAs enclosed in EVs were fragmented. To address this issue, we identified target regions that were consistently present in the majority of EV samples. The approach employed was unsuccessful in identifying appropriate target regions for all three long non-coding RNAs and multiple messenger RNAs due to the presence of either excessively short fragments or fragments with an unacceptably high GC content. However, a total of seven RT-ddPCR assays (namely miR-375-3p, hasa-piR-28004, Glyoxalase I (GLO1), NKX3.1, Adenosylmethionine decarboxylase 1 (AMD1), MYC associated zinc finger protein (MAZ), and RNA binding motif protein 47(RBM47) were designed and their efficacy was confirmed by assessing the full sample sets (matched PC and normal prostate specimens, plus the matched urine and plasma samples) utilized for RNA sequencing analysis (data not shown). Appendix Table S2 provides further details on these assays. Subsequently, the assays were employed to examine the concentrations of potential biomarkers in a distinct, extended group of urinary and plasma EV samples collected from 20 patients diagnosed with PC, both prior to and following surgery. Results can be seen in Figures 20 and 21.

Urinary EVs show significant decrease in the levels of miR-375-3p (Log2FC=11.49, p=0.0003), piR-28004 (Log2FC=2.18, p=0.0024), and AMD1 (Log2FC=3.49, p=0.0095) identified in collected PostOp compared to PreOp samples. This is illustrated in Figure 20. The mRNA levels of GLO1, MAZ, and NKX3.1 were observed to have decreased in a subset of patients; however, the decrease did not reach statistical significance (Fig. 20). Similarly, all markers show a tendency of decreasing after the surgery in plasma EVs in a subset of the patients, but none at a statistically significant level (Fig. 21).

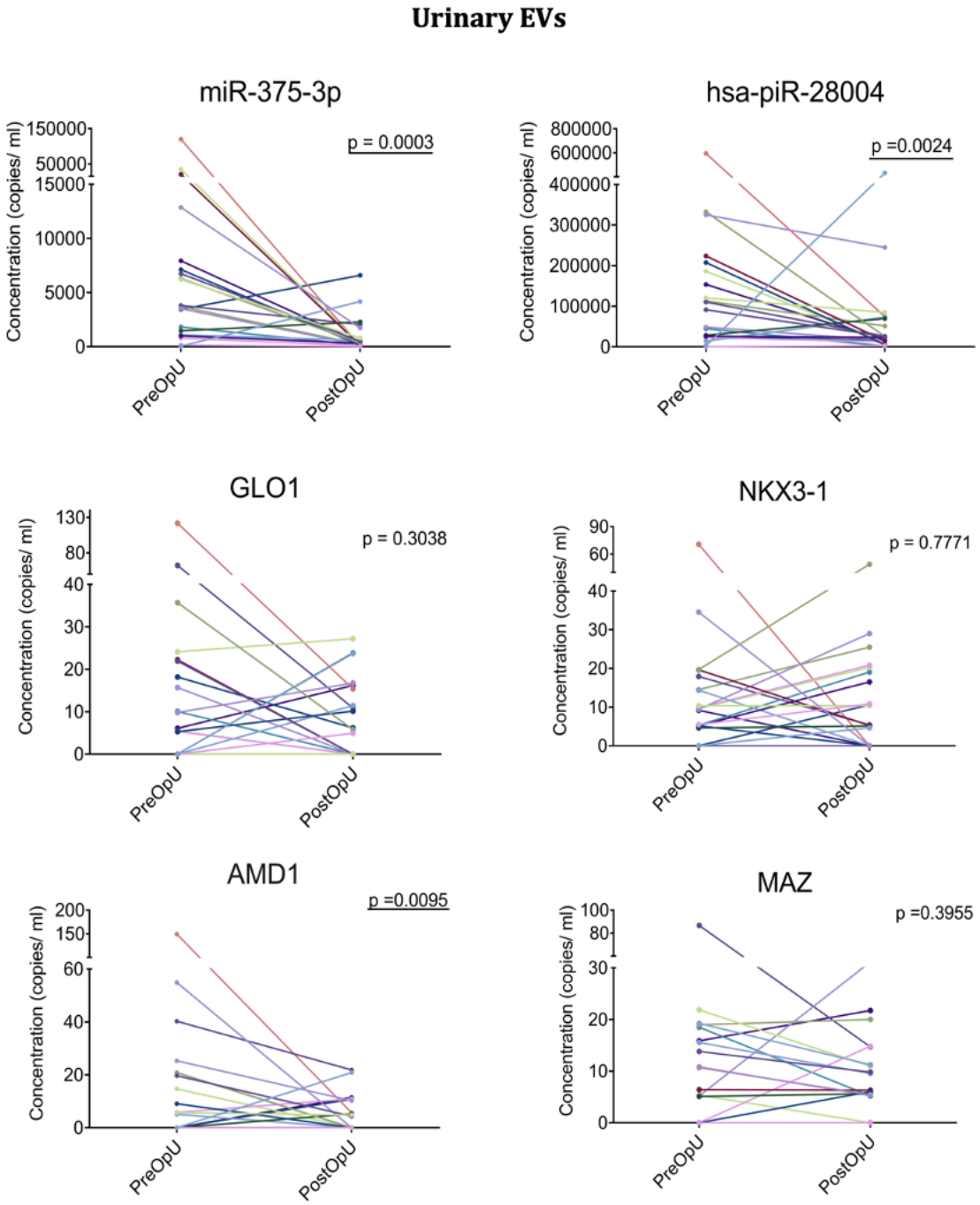

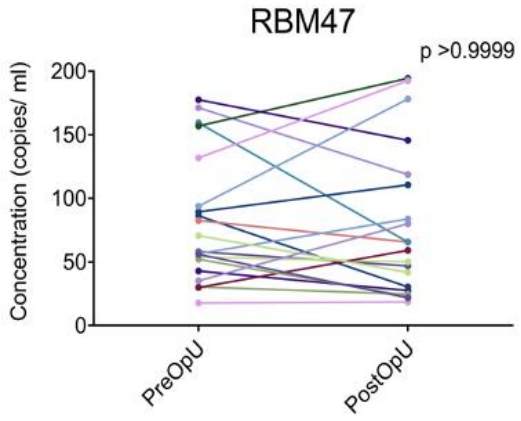

Figure 20. Validation of selected biomarker candidates in urinary EVs from an independent cohort of 20 PC patients by RT-ddPCR. Paired dot plots show the copy number of RNA biomarkers per ml of urine collected before and after radical prostatectomy in 20 PC patients. Wilcoxon matched-paired signed rank test was used to assess the statistical significance of the differences between groups. *P*-value <0.05 was considered significant.

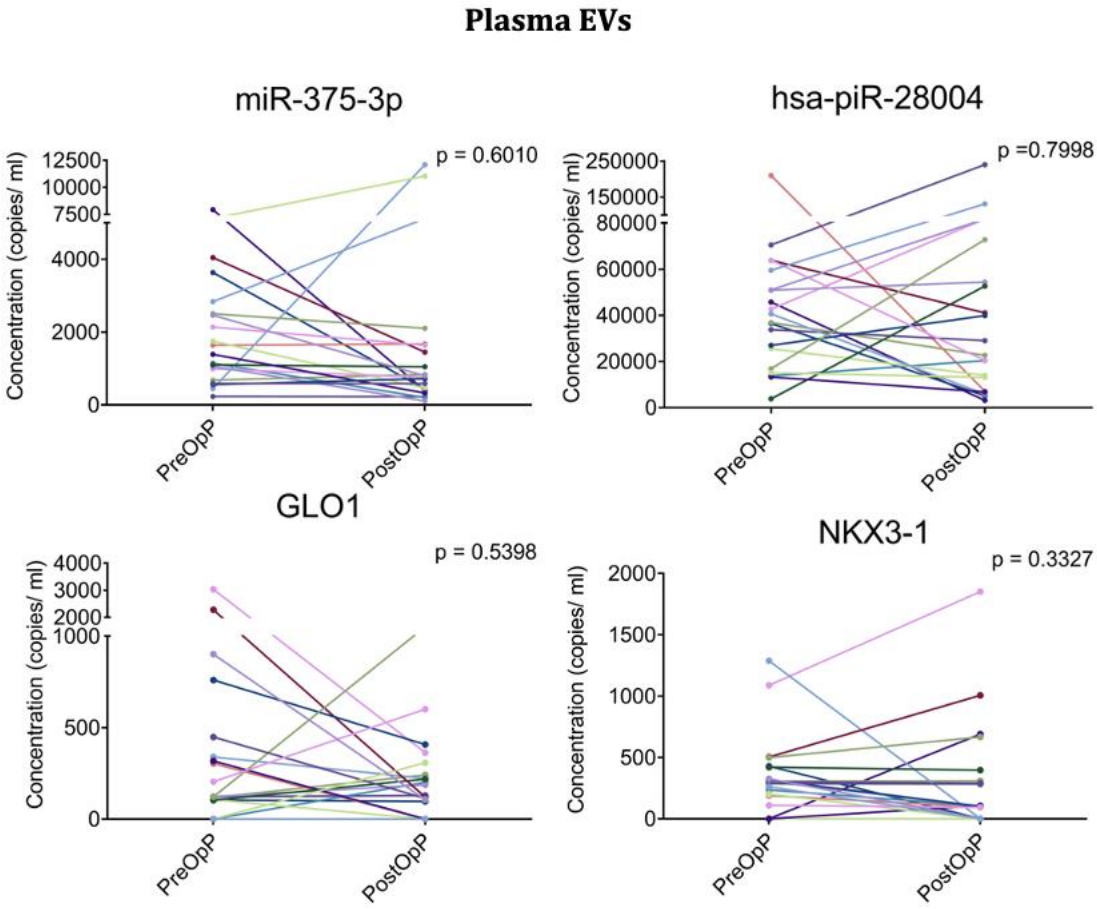

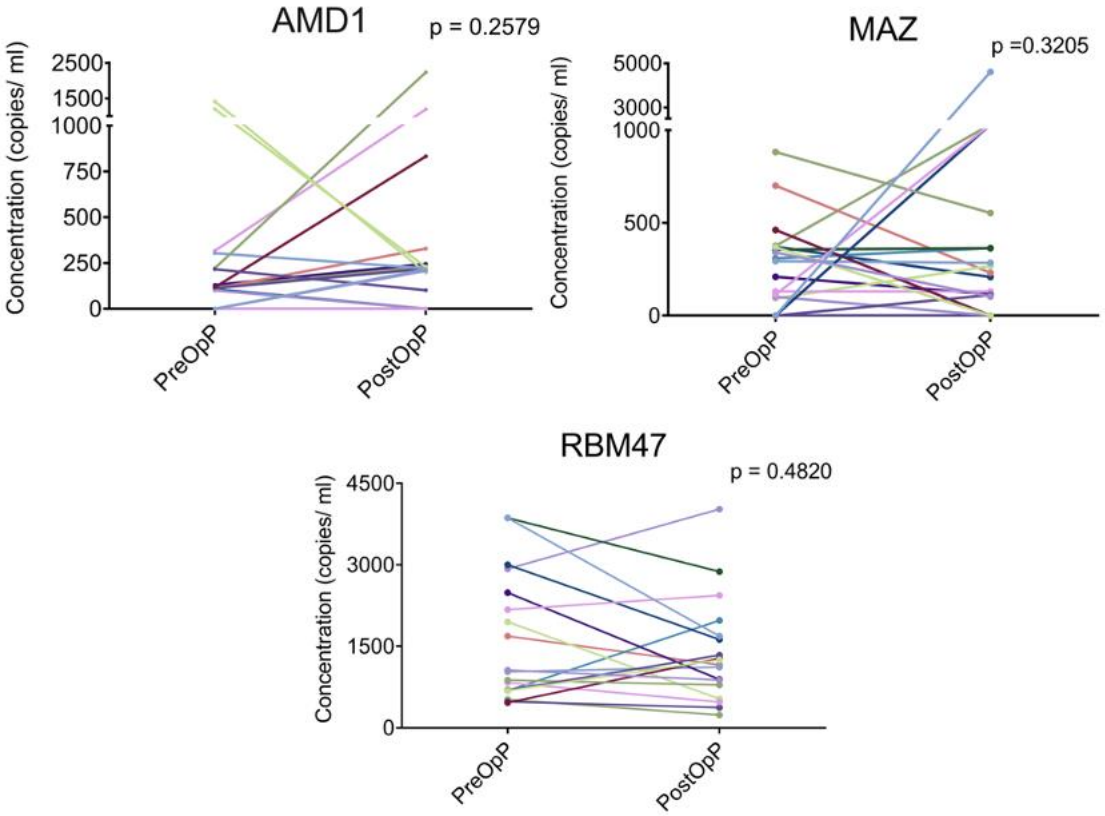

Figure 21. Testing of selected biomarker candidates in plasma EVs from an independent cohort of 20 PC patients by RT-ddPCR. Paired dot plots show the copy number of RNA biomarkers per ml of plasma collected before and after radical prostatectomy in 20 PC patients. Wilcoxon matched-paired signed rank test was used to assess the statistical significance of the differences between groups. *P*-value <0.05 was considered significant.

3.6 Diagnostic potential of selected biomarkers to differentiate PC vs BPH

To assess the diagnostic value of the selected RNA biomarker candidates, their levels in plasma and urinary EVs from BPH vs. PC donors were compared. Plasma EVs revealed a highly significant difference of NKX3-1 level of expression between BPH and PC patient samples (p = 0.003) and significant difference in GLO1 (p = 0.0534) (Fig. 22 A, C), while other markers show a similar expression pattern between both patient groups (Appendix Figs. S1- S2). Receiving Operation Characteristic (ROC) curves for these markers showed that Area under the curve (AUC) for NKX3-1 was 0.82 (95% confidence interval (CI) 0.69 -0.95) while for GLO1 was 0.68 (95% CI 0.51 - 0.85) (Fig. 22B, D). In urinary EVs, some markers, such as miR375-3p (AUC: 0.63; 95%CI 0.49 - 0.85) and NKX3-1 (AUC: 0.65; 95% CI 0.48 - 0.83), demonstrated elevated

expression levels in PC samples compared to BPH. However, these differences did not reach statistical significance (Appendix Figs. S3-S4).

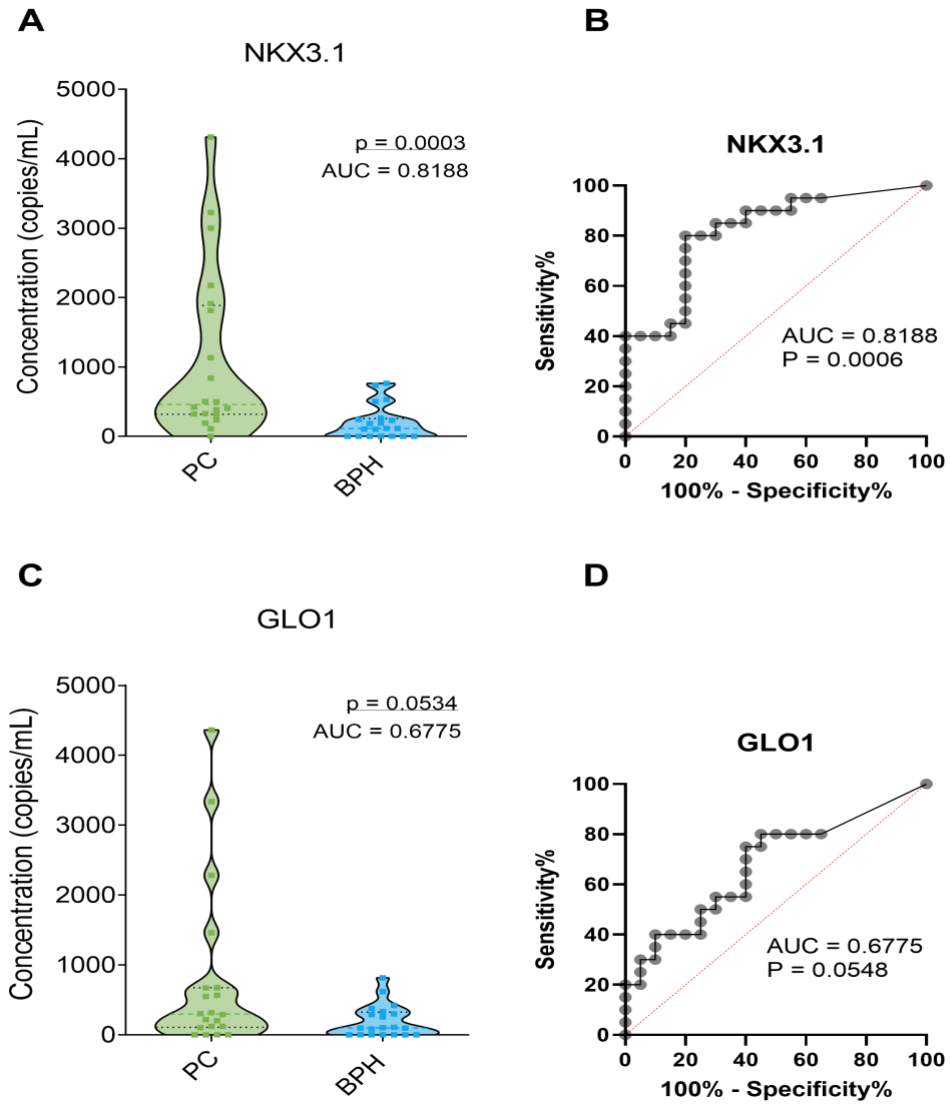

Figure 22. Significant markers that discriminate plasma EVs PC vs BPH. Mann-Whitney test was used to calculate statistical differences. (A). KNX3.1 violin plots. (B). NKX3.1 ROC curve (C). GLO1 Violin plot (D). GLO1 ROC curve. PC: Prostate Cancer, BPH: Benign Prostate hyperplasia. AUC: Area under the curve, p: p-value.

3.7 RNA biomarker model for PC diagnostics

The expression of a single biomarker alone poses challenges, particularly given the diverse content of EVs in terms of the varying amounts present per vesicle [143]. Therefore, an RNA model combining all the seven biomarkers' expressions was made to evaluate their combined diagnostic power. The purpose of this model was to assess the collective ability of all the seven biomarkers to differentiate between PC and BPH, and additionally, to compare the diagnostic potential of these biomarkers to that of PSA.

The visualization of the RNA biomarker model (Fig. 23) provides a comprehensive representation of the collective potential of all seven biomarkers to differentiate between patients with PC and BPH in both plasma (Fig. 23A), and urine (Fig. 23C), along with their respective leave-one-out cross-validations (LOOCV) (Fig. 23B, D). The model exhibited high AUC values, indicating strong diagnostic performance for plasma EVs (AUC = 0.904, sensitivity = 0.7391, specificity = 1) (Fig. 23A) and AUC = 0.8029 with a sensitivity of 0.6957 and specificity of 0.8667 (Fig. 23B) in LOOCV. Urinary EVs also showed promise, with an AUC = 0.817 (sensitivity = 0.7826 and specificity = 0.7333) (Fig. 23C), although their validation values were lower (AUC = 0.5362, sensitivity = 0.1739; specificity = 0.9333 (Fig. 23D). Comparing these results to PSA measurements (Fig. 23E), it becomes evident that PSA fails to distinguish PC from BPH patients, displaying a low AUC of 0.431.

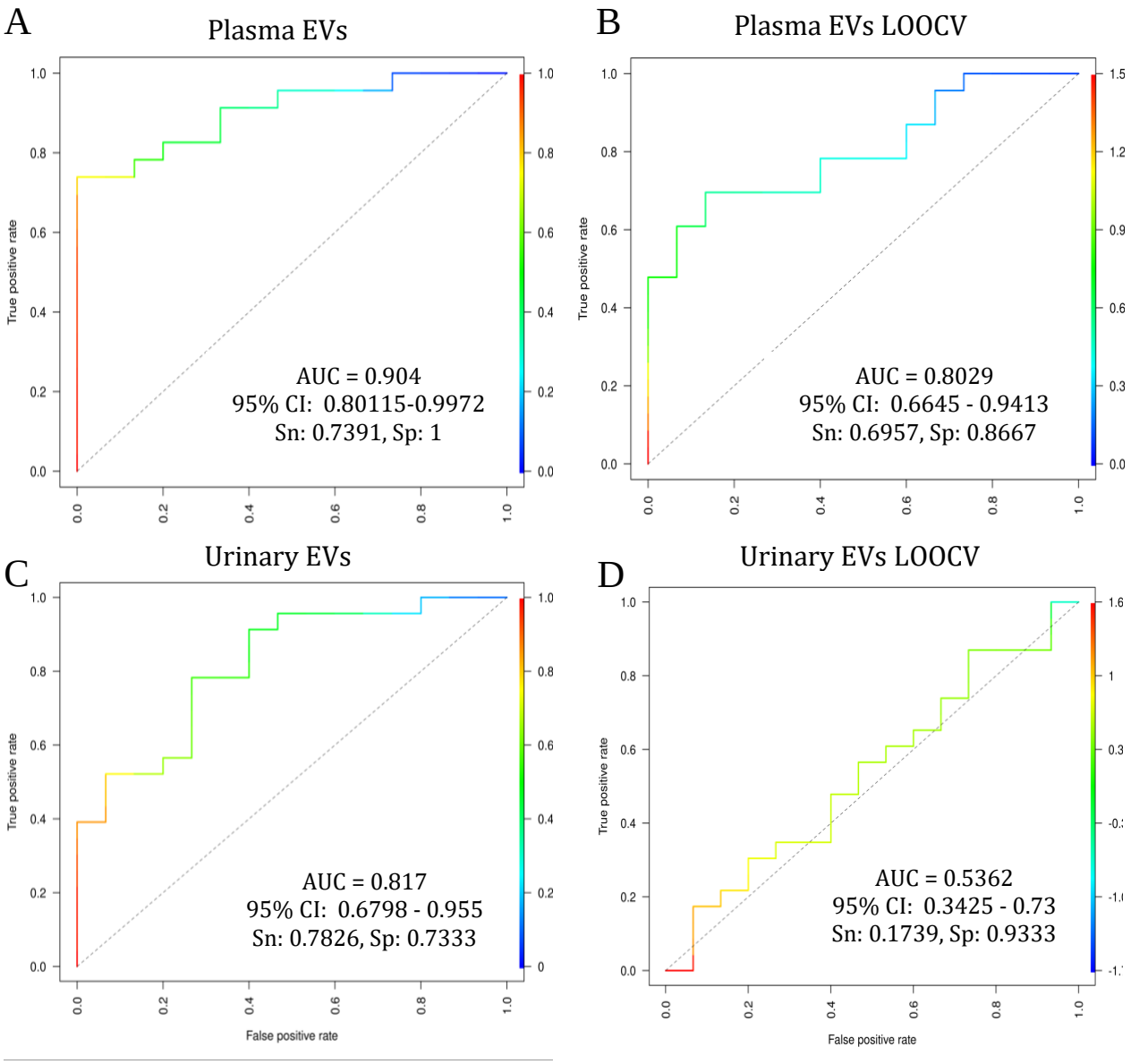

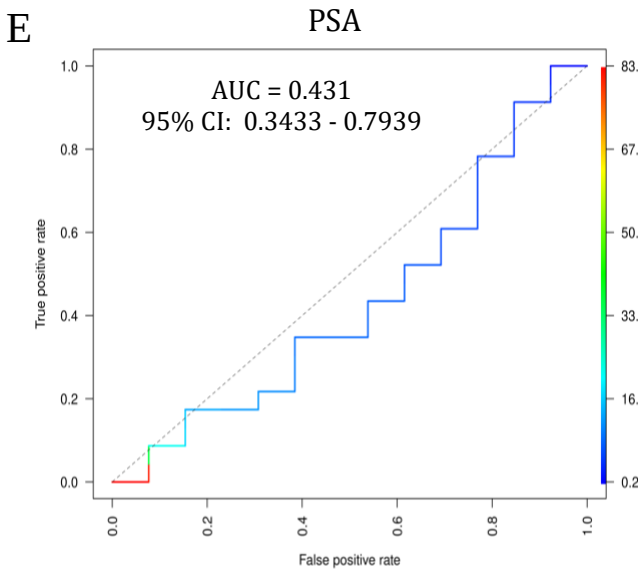

Figure 23. Diagnostic potential of RNA biomarkers model to differentiate between PC and BPH using 7 biomarkers (AMD1, GLO1, NKX3.1, MAZ, RBM47, miR-375-3p and piR-28004) and their LOOCV (A). ROC curve of PC vs BPH in plasma EVs. AUC = 0.904. (B). LOOCV ROC curve of plasma PC vs. BPH AUC = 0.8029 (C). ROC curve of PC vs BPH in urinary EVs. AUC = 0.817. (D). LOOCV ROC curve of urinary PC EVs vs. BPH. AUC = 0.5362. (E). ROC curve of PC vs BPH using PSA levels. AUC = 0.431. AUC = Area under the curve.; CI = Coefficient Interval; Sn = Sensitivity; Sp = Specificity

Table 2 presents the model coefficients associated with each marker in plasma and urine samples. These coefficients provide insight into the relative contributions of the individual biomarkers to the overall diagnostic power of the RNA biomarker model in discriminating between PC and BPH patients.

Table 2. Model coefficients for each marker of the seven biomarkers panel for plasma and urine samples.

Target	**Plasma**	**Urine**
miR375-3p	0.001224445	-4.3250E-05
piR-28004	-1.12543E-06	7.44304E-06
GLO1	0.001948337	0.026789191
NKX3.1	0.003979511	0.012654274
AMD1	-0.0000675664	-0.02026386
MAZ	-0.000568377	0.011160882
RBM47	0.000770798	0.0438523

In plasma samples, the highest model coefficients were observed for NKX3.1 (0.00398), GLO1 (0.00195), and miR-375-3p (0.00122). These coefficients indicate that these biomarkers exhibit the strongest discriminatory ability in distinguishing PC from BPH. In urine samples, the highest model coefficients are RMB47 (0.04385), GLO1 (0.02679), and NKX3-1 (0.01265). These biomarkers demonstrate significant contributions to the overall diagnostic power of the model in urine samples.

It is noteworthy that some biomarkers have negative coefficients, suggesting that their expression levels in PC EV samples are lower compared to the BPH samples. This information provides valuable insights into the differential expression patterns of biomarkers between PC and BPH, aiding in the accurate discriminations of these conditions.

3.8 Prognostic value of the RNA biomarkers.

To assess the prognostic potential of identified biomarkers, we divided the cohort of PC patients (n=30) into two groups: low Gleason score (LG) comprising patients with a GS of 6 or 7a (3+4), and high Gleason (HG) including patients with a GS of 7b (4+3) and higher. This distribution is based on the likelihood of developing biochemical recurrence and has been reported before [47]. Each group consisted of 15 patients. The results are presented in Appendix Figures S5 and S7, and detailed patient information can be found in Appendix Table S1. GS calculations are crucial in clinical decision-making after PC diagnosis. Therefore, we aimed to determine if any of the potential biomarkers could differentiate between the two groups. Data were analyzed using Mann-Whitney statistics, and ROC curves were generated (Appendix Figs. S6 and S8). Overall, mRNA expression levels in the HG cohort were higher than those in the LG group for both biofluids (Fig. 24 and appendix Figs. S5 and S7). Among the tested mRNA markers in urinary EVs, GLO1, NKX3.1, MAZ and RBM47 demonstrated higher than average discriminatory power between the both groups, with AUC values as 0.66 (95%CI 0.46 - 0.86), 0.70 (95%CI 0.5 - 0.9), 0.71 (95%CI 0.52 - 0.9), and 0.66 (95%CI 0.46 - 0.86), respectively. However, none of these markers reached statistical significance (Fig. 24). Similarly, none of the biomarkers examined in plasma EVs exhibited significant differentiation between the two groups. However, consistent with previous findings, mRNA biomarkers displayed a trend towards higher expression in the HG group (Appendix Fig. S5). Notably, NKX3.1 emerged as the most promising marker, with an AUC of 0.70 (95%CI 0.50 - 0.88), although the corresponding p-value of 0.079 did not reach statistical significance (Appendix Fig. S6).

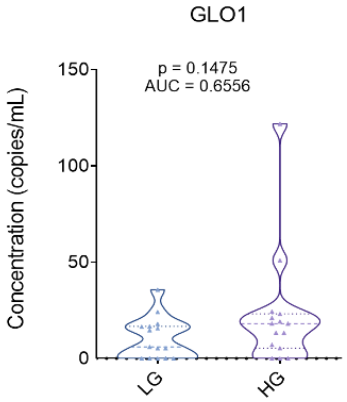

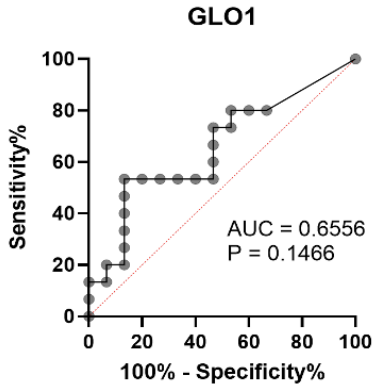

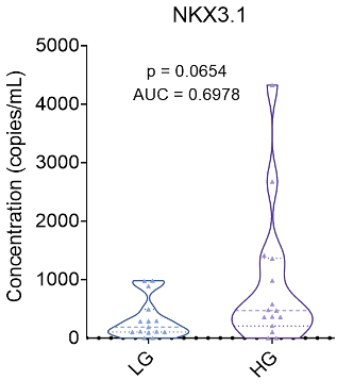

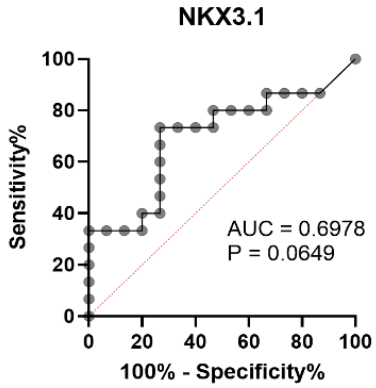

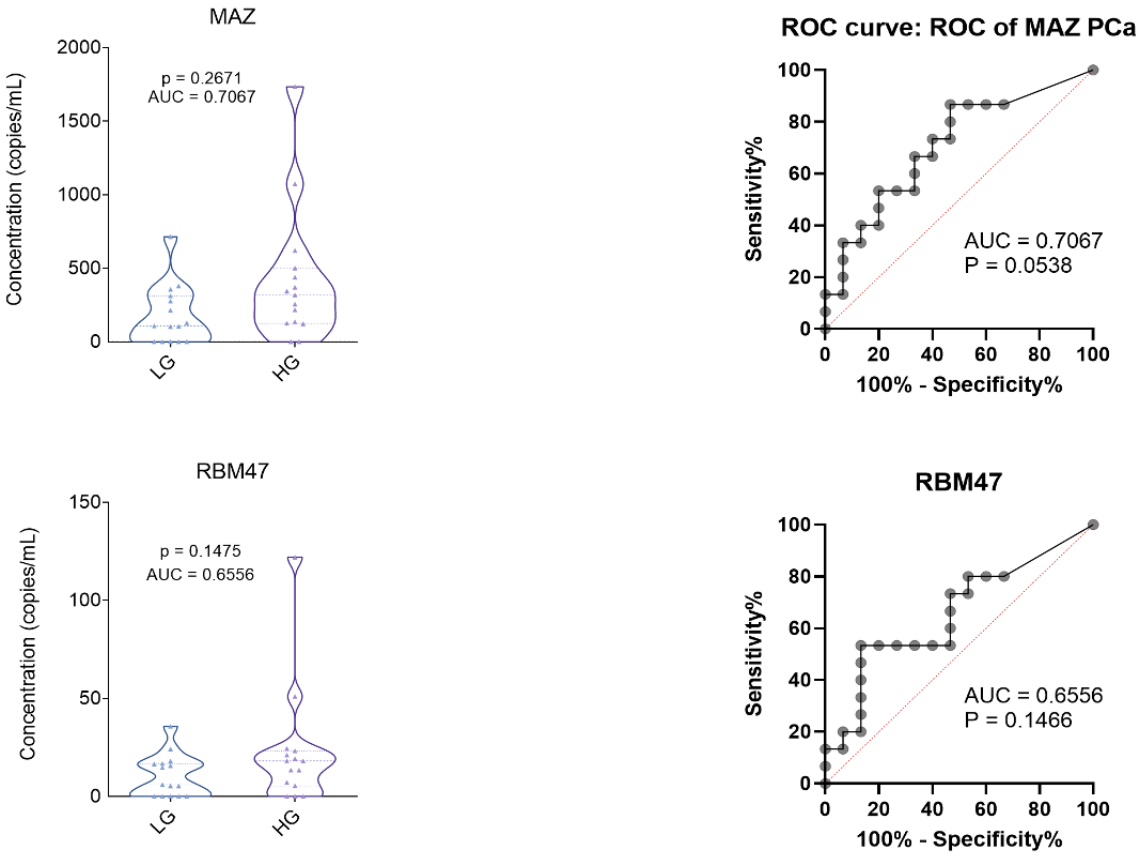

Figure 24. Testing of selected biomarker candidates in urine EVs from PC patients (n=30) divided in two groups based on GS. Low Gleason (LG) = GS 6 or 7a (3+4); and High Gleason (HG) = GS 7b (4+3) or higher by RT-ddPCR. ROC curves and Violin plots showing mean +/- SD show the copy number of RNA biomarkers per ml of urine collected before radical prostatectomy in 30 PC patients, 15 per group. Mann - Whitney test was used to assess the statistical significance of the differences between groups. AUC: Area under the curve *P*-value <0.05 was considered significant. AUC values were calculated and added. The rest of the data can be seen in the Appendix, Figures S5 – S8.

Next, we assessed the association of the RNA biomarkers with the ISUP grade [49] and the CAPRA score [51]. As such, our cohort of 30 PC patients was further categorized based on their ISUP grade (see patients characteristics appendix Table S1), resulting in five distinct groups, as well as their CAPRA score (Appendix Table S1), resulting in three groups: low, intermediate and high risk. The aim was to investigate any potential correlation between the identified biomarkers and these stratifications and to analyze if any of the biomarkers could significantly distinguish between the groups present in each system. To analyze the data, violin plots were generated, Spearman correlation was employed and Kruskal-Wallis test was used to identified differences among groups. Detailed results can be observed in Figures S9 - S12 of the appendix and correlation results can be seen in Tables 4 and 6 (plasma) and Table 5 and 7 (urine).

None of the plasma EV biomarkers tested show any degree of significant correlation with ISUP grade in plasma EVs. Only NKX3.1 with r-factor (r) = 0.28, showed a small positive correlation with ISUP grade, but not enough to be significant (Appendix Fig. S9, Table 4).

On the other hand, three markers from urinary EVs, NKX3.1(r=0.27), AMD1(r = 0.21) show a weak to moderate positive correlation, being MAZ statistically significant with a moderate correlation of r = 0.42 and p -value of 0.0224 (Table 5, Appendix S10).

Table 4. Spearman correlation between ISUP grade and each RNA marker in plasma EV samples.

Plasma	ISUP vs miR375-3P	ISUP vs piR28004	ISUP vs GLO1	ISUP vs NKX3-1	ISUP vs AMD1	ISUP vs MAZ	ISUP vs RBM47
r	-0.1253	-0.004874	-0.1547	0.2806	0.1645	0.08469	-0.05361
95%CI	-0.4733 to 0.2565	-0.3741 to 0.3657	-0.4963 to 0.2283	-0.09968 to 0.5894	-0.2188 to 0.5038	-0.2945 to 0.4408	-0.4153 to 0.3227
p-value	0.5093	0.9796	0.4143	0.1331	0.3851	0.6564	0.7784

Table 5. Spearman correlation of ISUP grade with each RNA biomarker in urinary EVs

Urine	ISUP vs miR375-3P	ISUP vs piR28004	ISUP vs GLO1	ISUP vs NKX3-1	ISUP vs AMD1	ISUP vs MAZ	ISUP vs RBM47
r	0.05221	-0.05083	0.1538	0.2746	0.2133	0.4154	0.09121
95%CI	-0.3240 to 0.4141	-0.4130 to 0.3252	-0.2291 to 0.4956	-0.1061 to 0.5851	-0.1701 to 0.5406	0.05377 to 0.6808	-0.2885 to 0.4461
p-value	0.7841	0.7897	0.4170	0.1420	0.2578	0.0224	0.6317

CAPRA grade system stratifies patients into 3 distinct risk groups: low, intermediate and high, based on various factors such as PSA levels at the time of diagnosis, T-stage, age, GS and the presence of cancer-positive biopsy cores [51]. The corresponding grades and their association with each risk group are presented in Table S1 (Appendix).

In line with previous findings, none of the selected biomarkers displayed significant correlation in plasma EVs (Figure S11 in the appendix). However, MAZ showed a weak positive correlation with CAPRA grade, as indicated in Table 6. Conversely, urinary EVs demonstrated low positive correlations with three of the markers. The weakest correlation (r = 0.25) was observed with GLO1, followed by MAZ (r = 0.30) and NKX3.1 (r = 0.36), as depicted in Table 7. Notably, only the correlation between NKX3.1 and CAPRA reached statistical significance (p = 0.048) (Figure S12 in the appendix).

Table 6. Spearman correlation values of CAPRA grade versus each of the biomarkers in plasma EVs.

Plasma	CAPRA vs miR375-3p	CAPRA vs piR28004	CAPRA vs GLO1	CAPRA vs NKX3-1	CAPRA vs AMD1	CAPRA vs MAZ	CAPRA vs RBM47
r	0.07579	0.007751	-0.06811	0.1361	0.07931	0.2008	-0.1877
95%CI	-0.3026 to 0.4336	-0.3632 to 0.3766	-0.4273 to 0.3096	-0.2463 to 0.4818	-0.2994 to 0.4364	-0.1827 to 0.5313	-0.5214 to 0.1958
p-value	0.6906	0.9676	0.7206	0.4734	0.6770	0.2873	0.3205

Table 7. Spearman correlation values of CAPRA grade versus each of the biomarkers in urinary EVs

Urine	CAPRA vs miR375-3p	CAPRA vs piR28004	CAPRA vs GLO1	CAPRA vs NKX3-1	CAPRA vs AMD1	CAPRA vs MAZ	CAPRA vs RBM47
r	0.07923	-0.1120	0.2462	0.3638	0.1469	0.2964	-0.02584
95%CI	-0.2995 to 0.4364	-0.4627 to 0.2691	-0.1362 to 0.5647	-0.00708 to 0.6467	-0.2358 to 0.4902	-0.08263 to 0.6005	-0.3920 to 0.3474
p-value	0.6773	0.5558	0.1897	0.0481	0.4385	0.1118	0.8922

3.9 The PC tissue microbiome

Approximately 3.6% of the reads from PC tissue transcriptome libraries and 5.78% of the reads from the normal prostate tissue transcriptome libraries were not mapped against the human genome reference GRCh38. To identify microbial species inhabiting PC and normal prostate tissues, the unmapped RNAseq reads were further analyzed using Kraken 2 [217]. A Sankey plot showing the diverse microorganisms identified in PC tissue and their phylogenetic relation can be seen in Figure 25. Results show predominantly members of the Bacteria kingdom, although few Fungi and viruses were present as well (Fig. 25). The main represented phyla corresponded to Firmicutes, followed by Proteobacteria and Actinobacteria. A total of 178 different species were identified being the most prevalent ones *Staphylococcus cohnii* and *Staphylococcus haemolyticus* from Firmicutes; *Ralstonia solenacearum* from Proteobacteria, and *Curtobacterium flaccumfaciens*, from Actinobacteria (Fig. 25).

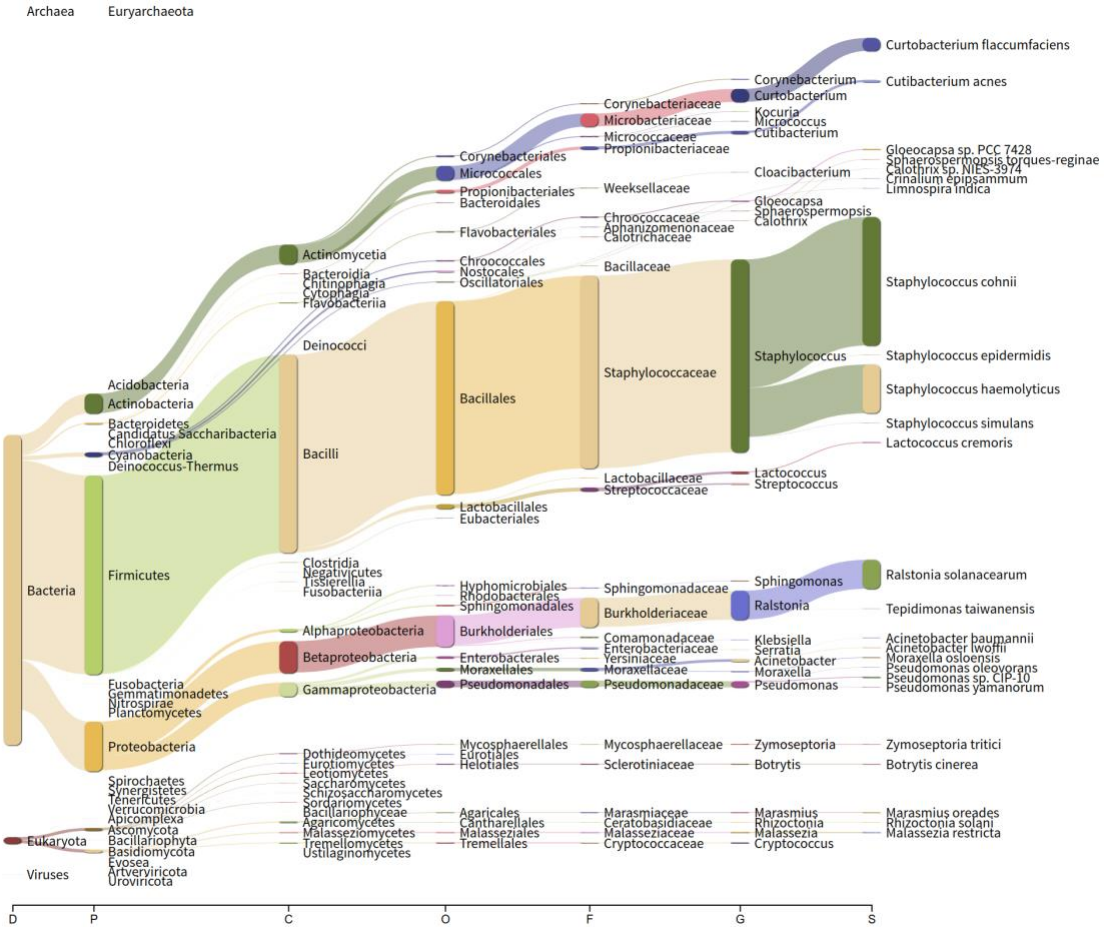

Figure 25. Sankey Plot depicting all the identified microorganisms in our cohort of 10 PC tissues. D: Kingdom, P: Phylum, C: Class, O: Order, F: Family, G: Genus, S: Species.

3.10 Comparison of PC tissue microbiome with normal prostate tissue microbiome

A total of 322 different species were identified as part of the prostate tissue microbiome. Similarly, to PC tissue microbiome, the most representative species were *Staphylococcus cohnii*, *Staphylococcus haemolyticus*, *Ralstonia solenacearum*, *and Curtobacterium flaccumfaciens* (Fig. 26).

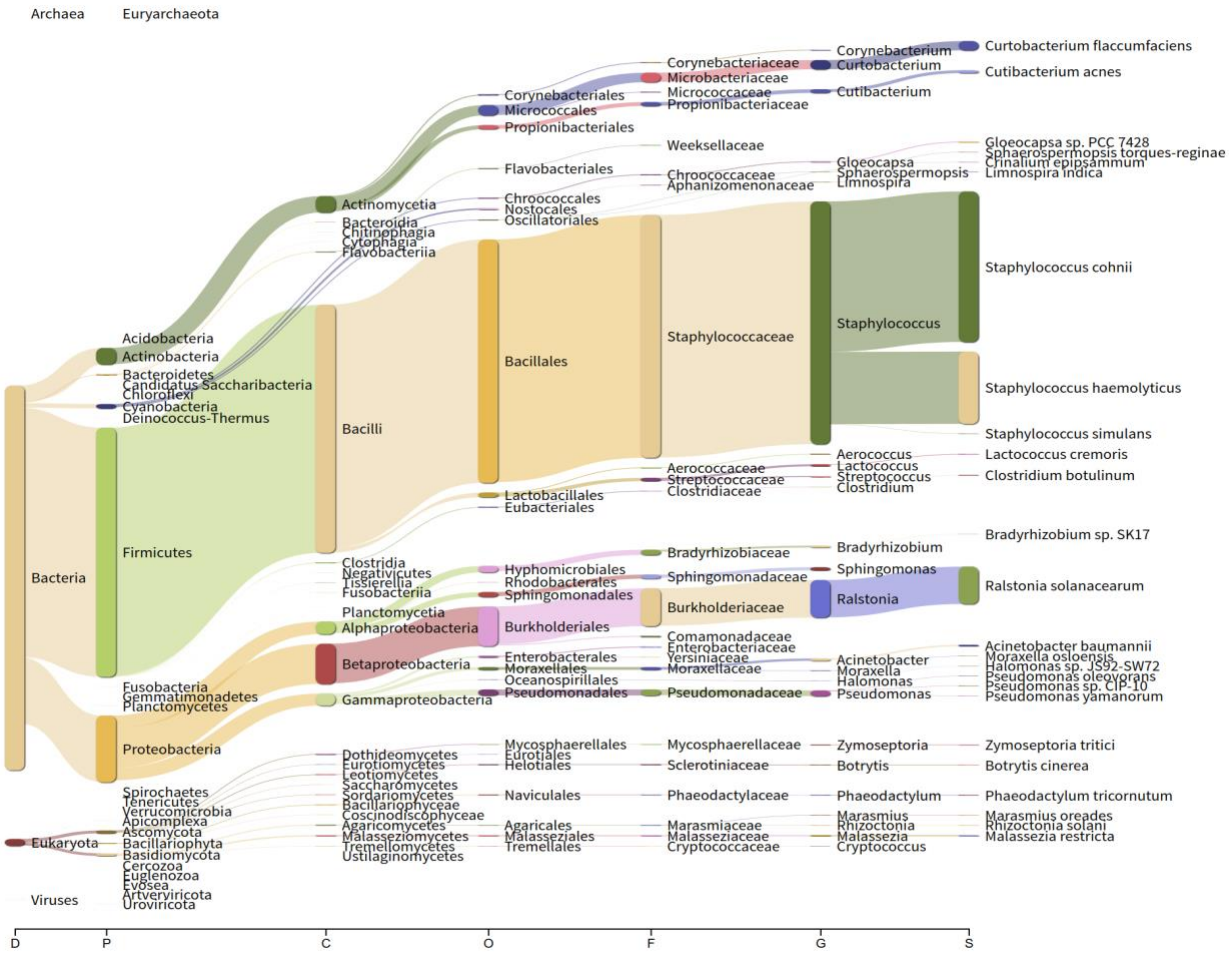

Figure 26. Sankey Plot depicting all the identified microorganisms in our cohort of 10 pro state tissues. D: Kingdom, P: Phylum, C: Class, O: Order, F: Family, G: Genus, S: Species.

Next, a differential expression analysis was performed to identify which species are more abundant in PC tissue compared to prostate tissue. A log2FC greater than 1 and adjusted p-value (adj. p) below 0.05 were set as threshold. Among the total of 367 species analyzed, 28 species were found overrepresented, and 50 species were found underrepresented in PC tissue (Fig. 27, Table S4 in appendix).

The three most abundant species were: *Brasilonema sennae* (log2FC = 8.40, adj. p<0.0001), *Dysgonomonas sp.HDW5B* (log2FC =8.24, adj. p<0.0001) and *Streptococcus sp. NP5* (log2FC = 7.80, adj. p<0.0001). The top three downregulated were: *Pseudomonas sp. KNU1026* (log2FC = -12.11, adj. p<0.0001), *Aerococcus urinaeequi* (log2FC = -12.11, adj. p<0.0001) and *Streptococcus lactarius* (log2FC = -11.43, adj. p<0.0001) (Table S4 in appendix).

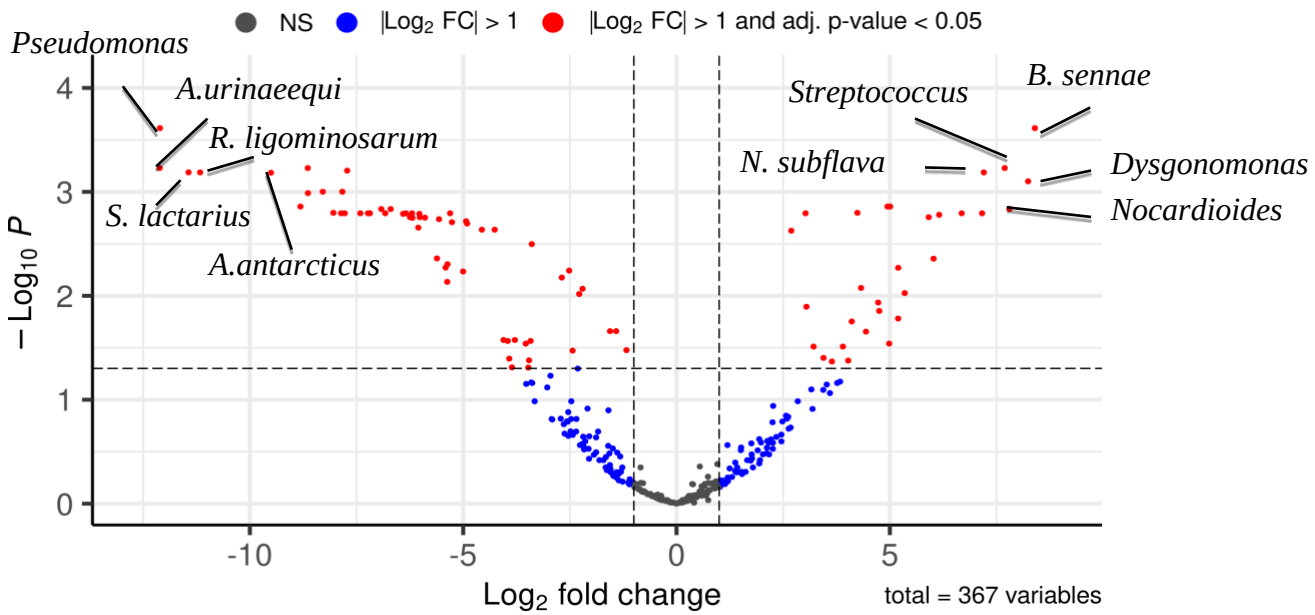

Figure 27. Volcano plot showing abundance of microbiome species identified between tumour and adjacent prostate tissue. Dashed vertical and horizontal lines reflect the filtering criteria. Log2fold >1, adj. p-value<0.05.

3.11 Presence of exogenous RNAs in EVs

EVs are released by various types of cells into the extracellular environment and contain RNA molecules originating from the cell of origin [142]. Therefore, it is possible that urinary and plasma EVs may carry microbial RNA derived from microbial species present in PC tissue, which could potentially serve as biomarkers. In this study, urinary and plasma EV RNAseq data from the previous cohort of 10 PC patients were combined into four groups: PreOpU; PostOpU, PreOpP and PostOpP. In addition, 10 healthy donors (HD) plasma samples were used for comparison. The number of reads mapped or unmapped to the human genome was determined (Fig. 28). The results revealed that, except for PreOpU, with 60% mapped to human reference genome, more than half of the EV content, approximately 60%, could not be mapped to the human genome (Fig. 28).

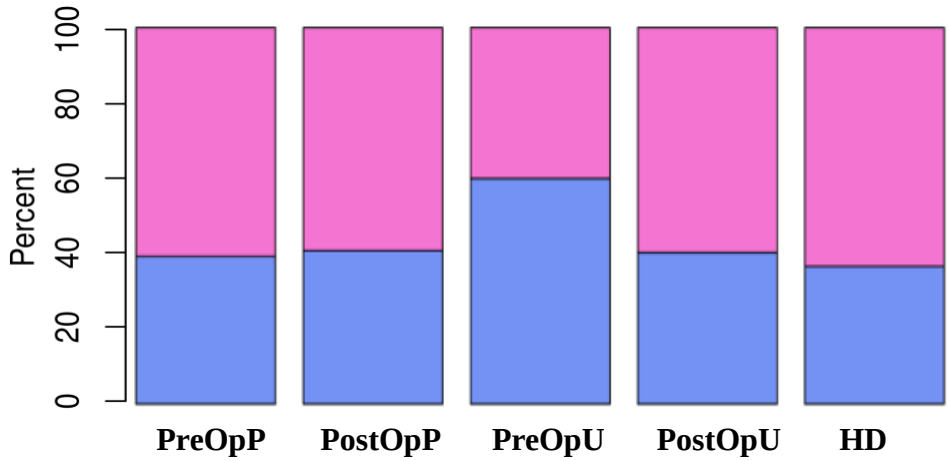

Figure 28. Bar plot showing the percentage of EV reads mapped and unmapped to Gh38 human. Legend: Blue: mapped to Gh38 human genome; Pink: unmapped to Gh38 human genome. PreOpP: Pre-operation plasma; PostOpP: Post-operation plasma; PreOpU: pre-operation urine; PostOpU: post-operation urine; HD: healthy donor plasma.

To address concerns regarding the introduction of microbial RNA signatures from external sources, a set of non -template controls was prepared. The RNA extracted from these controls underwent sequencing. Subsequently, any reads that exhibited exact matches or contained sequences identified in the non-template control libraries were excluded from the EV RNA libraries as described in Methodology 2.8.

Subsequent to this filtering, we conducted an analysis to determine which of the remaining exogenous EV RNAseq reads aligned with the Prostate Metagenome (PM) in order to identify the microbial origin of these reads, as detailed in Methodology section 2.8. The outcomes of this analysis are depicted in Figure 29.

In general, all EV samples displayed a comparable percentage of reads mapped to PM. Specifically, the examination of urinary EV samples revealed that approximately 25% of the RNAseq data originated from the PM, while the majority of the RNAseq data (75%) remained unmapped to any known microbial group, likely originating from various microorganisms not present in our PM (Fig. 29).

Among plasma samples, the highest proportion of mapped reads to the PM was observed in PreOpP, accounting for 28.8%, whereas PostOpP samples exhibited 26.5% mapping to the PM, and a total of 24% of reads mapped to PM was found in HD samples (Fig.29).

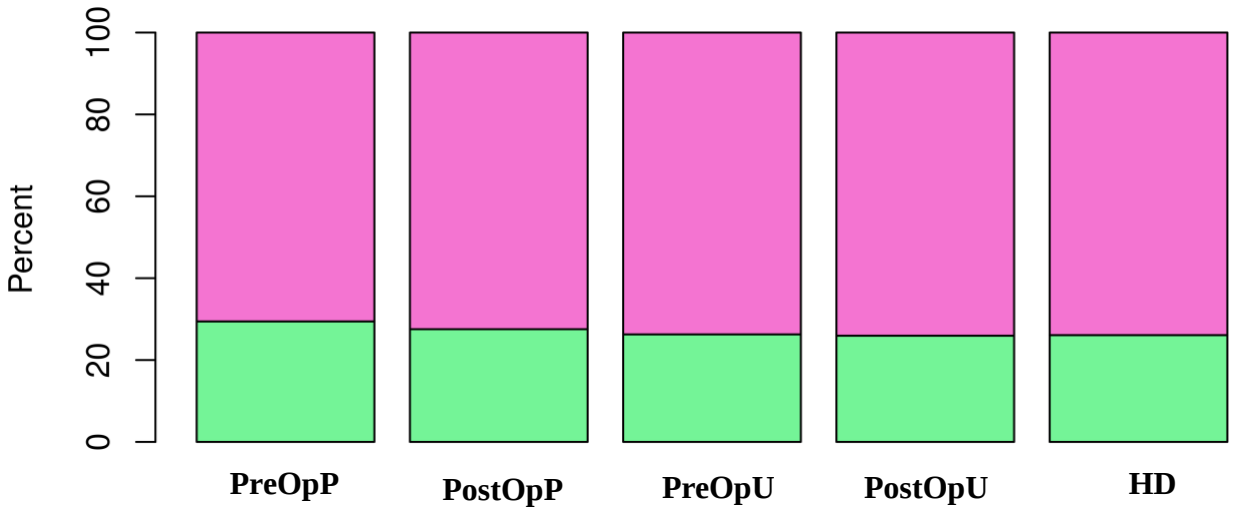

Figure 29. Bar plot showing the previously found unmapped reads to Gh38-human genome mapped to prostate metagenome. Legend: Green: reads mapped to PM; Yellow: reads removed by environmental filter (no – template), and pink: unmapped reads to PM. PreOpP: Pre-operation plasma; PostOpP: Post -operation plasma; PreOpU: Pre-operation urine; PostOpU: Post-operation urine; HD: healthy donor plasma.

3. 12 RNA fragments of PC tissue microbiome are represented in plasma EVs

Subsequently, we focused on the portion of the microbiome that mapped to the PM. The objective was to investigate the differential abundance of species represented in EV RNA and compare their abundance in PreOpP versus HD samples. The threshold for differential expression analysis was set at a LogFold change greater than 1 and adj. p-value below 0.05.

The analysis of plasma samples revealed the presence of 365 different species (Fig. 30). Among these, two species were found to be overrepresented in PreOpP: *Pseudomonas sihuiensis* (log2FC = 3.09, adj. p =0.03) and *Pseudomonas sp.C27* (log2FC = 4.64; adj. p<0.0001). Additionally 30 species were found underrepresented in PreOpP, with: *Pochonia chlamydosporia* (log2FC = -2.8, adj. p-= 0.0013) and *Morococcus cerebrosus* (log2FC = -2.7; adj.p-= -2.7) at the top of the list (Table S5, appendix).

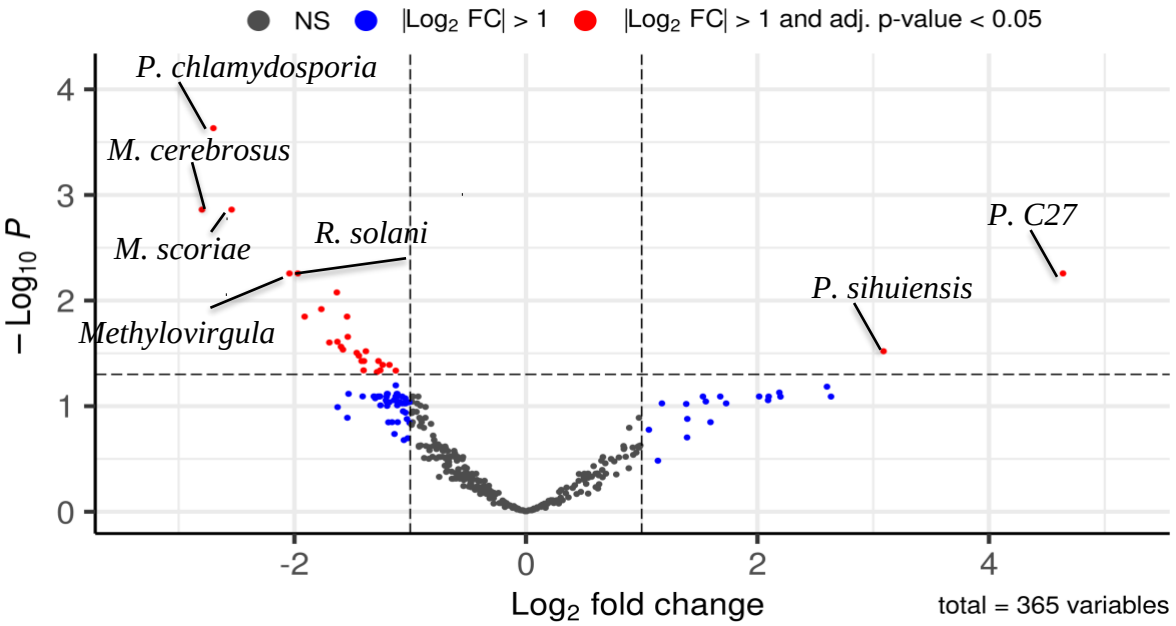

Figure 30. Volcano plot showing differentially expressed species in PreOpP EV versus HD EV samples. Threshold selected log2fold >1 and adj. p-value,0.05.

Then, we investigated the differential abundance of species represented in PreOp EVs vs PostOp EVs in both biofluids. Among them, seven species belonging to the *Pseudomonas* genus, including *Pseudomonas* (*alcaliphila* (log2FC = 2.84, adj. p: 0.011), *phDV1* (log2FC = 2.76, adj. p: 0.011), *pseudoalcaligenes* (log2FC = 2.56, p-value: 0.011), *wenzhouensis* (log2FC = 2.39, p-value: 0.0017), *sediminis* (log2FC = 2.98, adj. p: 0.0017), *mendocina* (log2FC = 2.02, adj. p: 0.0017), *CIP-10* (log2FC = 1.69, adj. p: 0.0032) were found to decrease after surgery (Fig. 31, Table S6 Appendix).

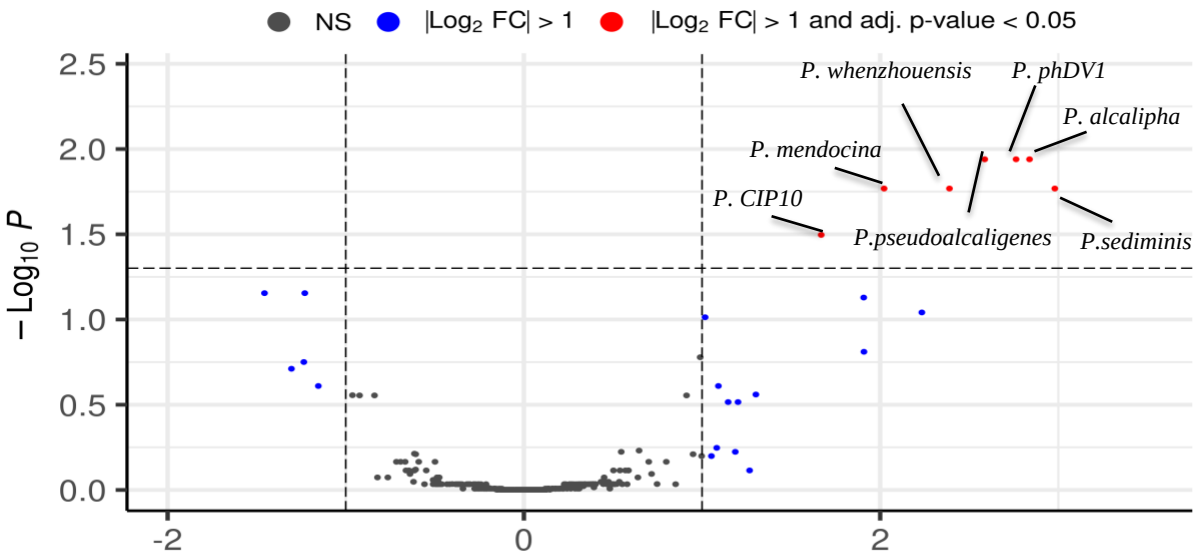

Figure 31. Volcano plot showing differential abundance of species in PreOpP EV vs. PostOpP EV samples. Threshold selected log2fold >1 and adj. p-value < 0.05.

In the analysis of urinary EVs, a total of 366 out of 367 species present in PM were detected (Fig. 32). Among these species, only four showed overrepresentations in PreOpU compared to PostOpU samples. Interestingly, three of these species belonged to the *Pseudomonas* genus, including *Pseudomonas putida* (log2FC = 1.26, adj. p =0.04), *Pseudomonas sp. phDV1* (log2FC = 1.33, adj. p =0.04) and *Pseudomonas pseudoalcaligenes* (log2FC = 1.26, adj. p =0.04). Additionally, *Micrococcus luteus* (log2FC = 1.63, adj. p =0.04) was also found to be overrepresented in PreOpU samples. No species were found to be significantly underrepresented in PreOpU vs. PostOpU (Table S7, appendix).

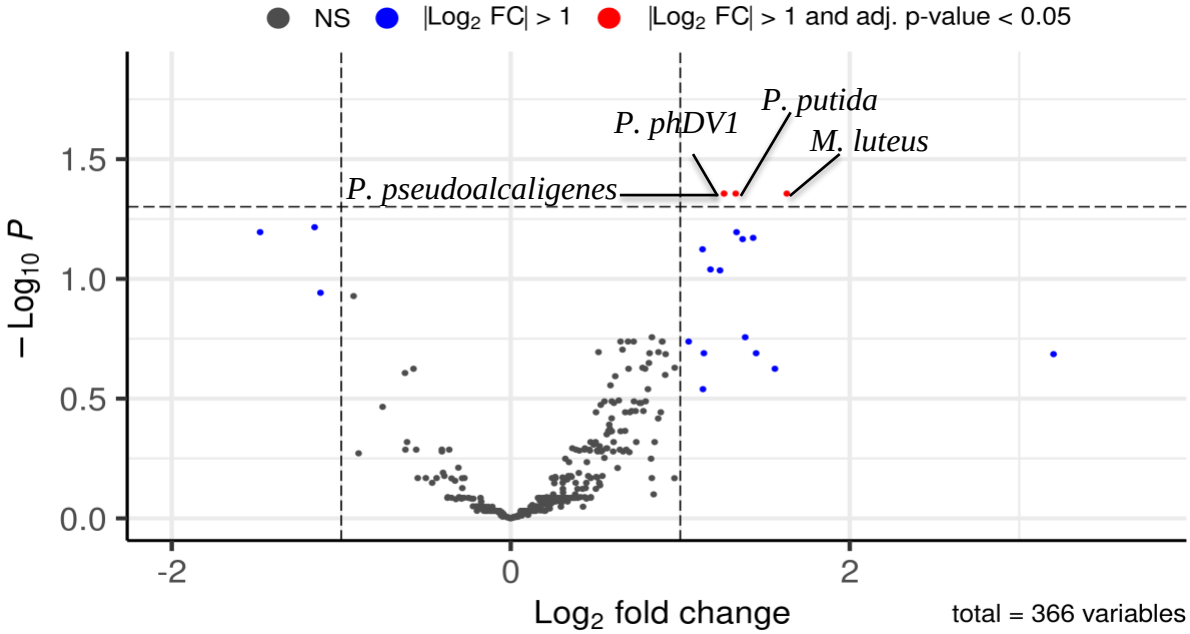

Figure 32. Volcano plot showing differential abundance of species in PreOpU EV vs. PostOpU samples. Threshold selected log2fold >1 and adj. p-value < 0.05.

3.13 Genome-agnostic differential abundance analysis of exogenous RNA reads in EVs.
The majority of the EV RNA-seq reads remained unassigned following their alignment against the PM. To gain insights into the origins of these reads and their relevance to PC, an alternative, genome-independent strategy for differential abundance analysis was devised (Methodology 2.8). In contrast to the aforementioned conventional procedure, this method circumvents the necessity of mapping RNA-seq reads to a reference genome sequence. Instead, it counts identical reads, clusters top differentially abundant reads, generates consensus sequences, and analyzes differential abundance (see Methodology 2.8). Finally, the consensus sequences that were differentially represented in each of the comparisons (PC vs HDs: PreOpP vs PostOpP; PreOpU vs. PostOpU) were identified by BLAST analysis. It is important to note that due to the incomplete nature of some microbial genomes, only the species name could be identified in some cases.

A total of 37 distinct consensus sequences were identified in EV plasma samples, with 14 of them showing significant differences between PreOpP and HD samples (Fig.33).

In PC PreOpP EV samples, the most prevalent overrepresented RNAs were the LysR family transcriptional regulator Acetyl-coA dehydrogenase from *Pseudomonas sp*. (log2FC = 9.82, adj.p= 0.003); a hypothetical protein from *Streptomyces chartreusis* (log2FC = 10.38, adj.p= 0.001), *Mycobacterium gordonae* (log2FC = 8.52, adj.p = 0.01) and two different tRNAs from *Pseudomonas sp*. (log2FC = 3.83, adj.p = 0.01) and (log2FC = 3.01, adj.p = 0.013)) (Fig. 33).

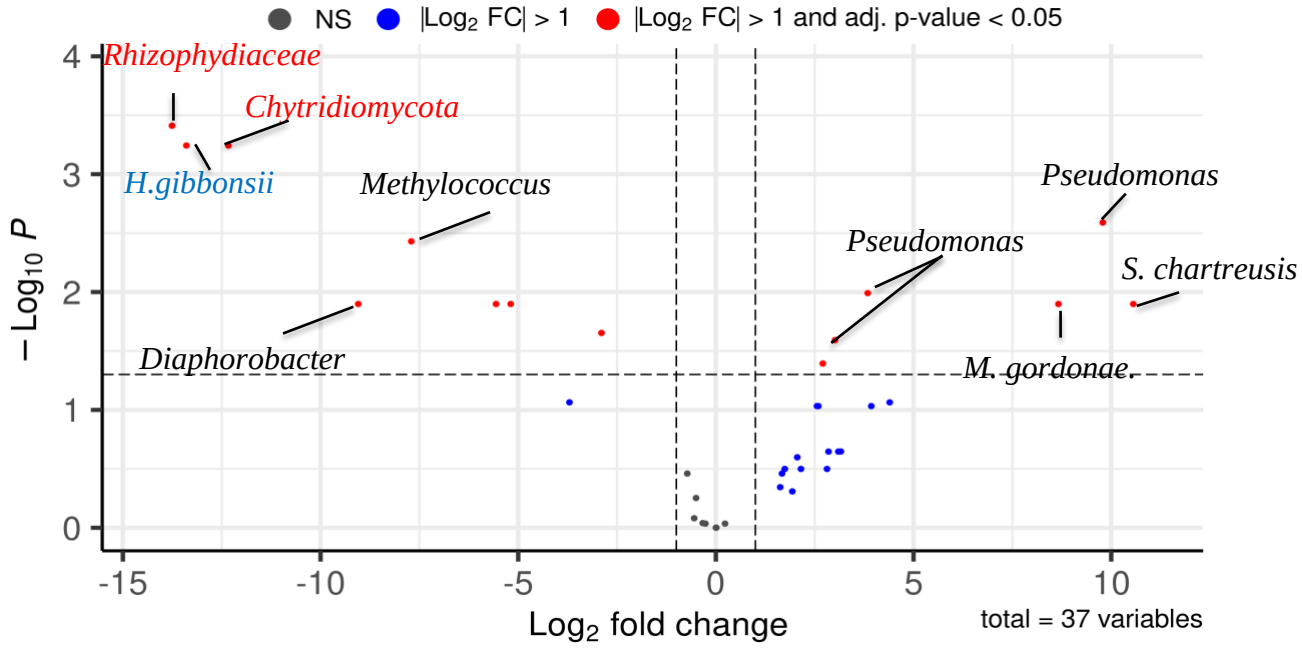

Figure 33. Volcano plot showing differentially expressed microbial sequences in PreOpP EV vs. HD EV samples. Black: Bacteria; Blue: Archaea; Red: Fungi. Threshold selected log2fold >1 and adj. p-value < 0.05.

In HD samples different ribosomal RNAs derived from two different fungi species, *Rhizophydiacea* (log2FC = -13.78; adj. p: 0.0004) and *Chytridiomycota* (log2FC -12.36; adj. p: 0.0006); in addition to *Methylococcus sp*. (log2FC = -0.08, adj. p:0.01) together with *Haloferax gibbonsii* (log2FC = -13.42; adj, p: 0.0006) were found overrepresented compared to PC EV PreOpP samples (Fig. 33).

Comparison of PreOpP and PostOpP EVs yielded 46 differentially expressed microbial sequences (Fig. 34).

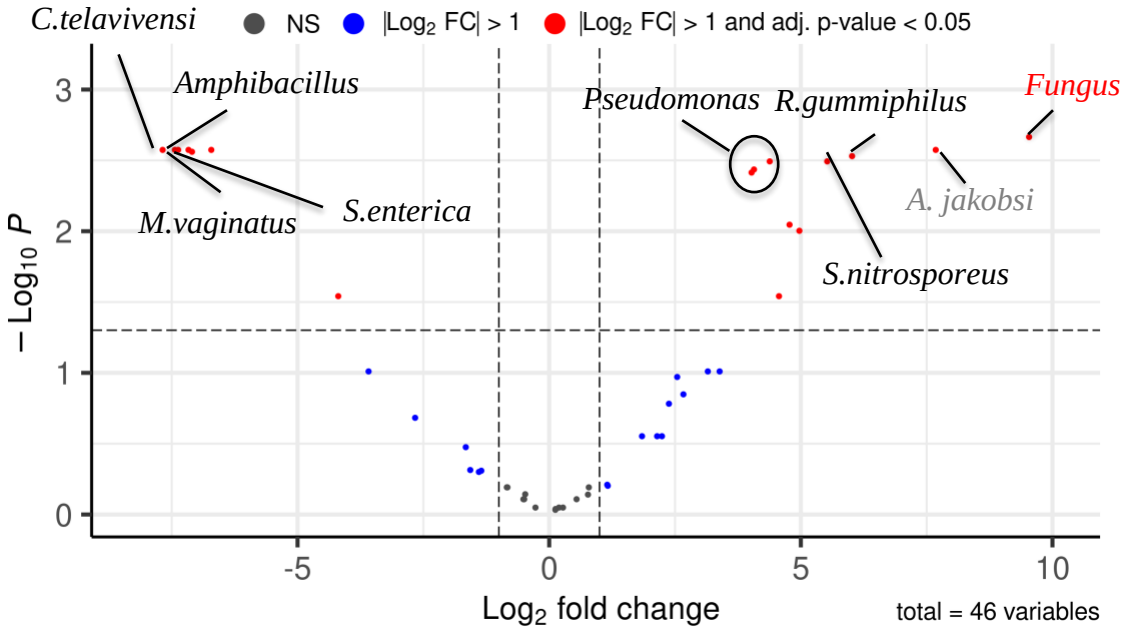

Figure 34. Volcano plot showing differentially expressed sequences in PreOpP vs. PostOpP EV samples. Black: Bacteria; Red: Fungi; Grey: Amoeba. Threshold selected log2fold >1 and adj. p-value<0.05.

Among those, the highest overrepresentation when comparing PreOpP and PostOpP microbial RNA signatures were 18S rRNA from *uncultured fungus* (log2FC = 9.75; adj.p = 0.002); 18S rRNA *Acanthamoeba jacobsi* (log2FC = 7.71; adj. p= 0.003); a tRNA from *Rhizobacter gummiphilus* (log2FC = 6.15; adj. p = 0.003), a fragment coding for a cation transporter from *S. nitrosporeus* (log2FC = 5.73; adj. p = 0.003) as well as a cluster corresponding to *Pseudomonas spp*. (Fig. 34).

Comparison of PreOpU and PostOpU EVs yielded 89 differentially abundant microbial sequences, being 18 of them significantly overrepresented in PreOpU EVs (Fig. 35). These include rRNAs of *Aliterella chasmolithica* (log2FC = 9.95, adj.p = 0.001); different mRNA fragments of *Bipolaris sorokiniana* (log2FC = 8.75, adj.p= 0.0017), an hypothetycal protein of *Schleiferilactobacillus harbinensis* (log2FC = 8.82, adj.p = 0.0009) and tRNA-Arg of *Sulfidibacter corallicola* (log2FC = 7.28, adj.p = 0.0025) (Fig. 35).

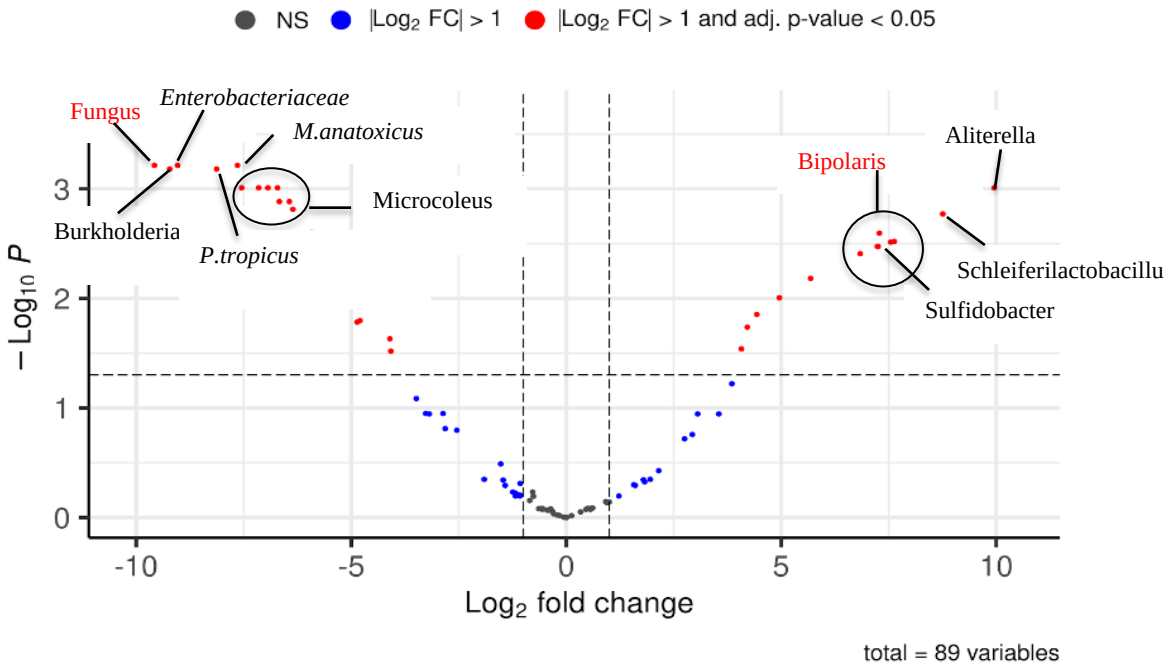

Figure 35. Volcano plot showing differentially expressed microbial sequences in PreOpU EV vs. PostOpU EV samples. Black: Bacteria; Red: Fungi Threshold selected log2fold >1 and adj. p-value<0.05.

4. DISCUSSION

PC represents a significant global burden and has been extensively researched to identify biomarkers for improved diagnostics and management in recent decades [236]. The current limitations of existing diagnostic methods for PC necessitate the exploration and development of novel PC biomarker [25] . The current benchmark, PSA testing, exhibits poor specificity and sensitivity for detecting PC, thereby prompting the quest for alternative approaches [41]. In this context, EVs have emerged as a promising modality for liquid biopsies in PC, providing valuable diagnostic and prognostic information [236]. EVs serve as carriers of biomolecules, rendering them suitable for non-invasive sampling and serial monitoring, which is particularly advantageous for disease surveillance and treatment response assessment [110]. Moreover, the encapsulation of biomarkers within EVs confers protection and ensures the stability and integrity of their contents, allowing for reliable analysis and interpretation [142].

The primary objective of this study was to investigate the RNA cargo of plasma and urinary EVs. To achieve this, the first step involved optimizing the EV isolation pipeline with a focus on maximizing recovery yield while preserving EV integrity and minimizing contaminants co-isolation from the different biofluids. For this purpose, SEC was selected as the preferred method due to its superior recovery and purity rates compared to alternative techniques such as UC or ultrafiltration [132]. SEC offers several advantages, including minimal sample manipulation, and reduced interference from NVEPs. During the fraction selection process, a lower size threshold of approximately 40 nm was implemented to minimize the presence of NVEPs, including supermeres or lipoproteins [112, 128]. This approach aimed to enhance the purity of the isolated EVs.

TEM analysis of the isolated urinary EVs revealed a relatively uniform size distribution, with an average diameter of approximately 80 nm. In contrast, the plasma samples demonstrated a greater diversity in size. WB analysis further supports these findings by confirming the presence of specific EV markers, such as ALIX and CD63, and the absence of cellular contaminants. Furthermore, TEM analysis also revealed the absence of particles larger than 500nm. This observation could potentially be attributed to the precipitation of larger EVs during the pre-processing steps of the biofluids, as the set protocol did not involve specific particle size discrimination in terms of maximum particle size. For plasma sample collection, blood samples were obtained and subjected to a mild centrifugation process to separate plasma from the other components of the blood. On the other hand, urine contains a significant concentration of uromodulin, a protein predominantly synthesized by the kidneys and commonly found in urine [237]. Uromodulin has been extensively documented for its tendency to trap particles during EV isolation process, thereby hindering their recovery [238]. To address this issue and optimize recovery of EVs, a gentle centrifugation step was integrated into our workflow prior SEC as suggested by others [239]. Consequently, during the isolation of EVs from both plasma and urine samples, larger particles may have precipitated and consequently been excluded from further analysis.

Although we cannot definitively conclude that our samples exclusively contain small EVs and other NVEPs of similar size, such as exomeres or vaults [112, 128], the combined analysis of size distribution and identified biomarkers indicates an enrichment of small EVs following the MISEV classification [119], with a reduction of supermeres or lipoproteins.

The quantification of EVs in plasma as potential cancer biomarkers has sparked interest within the scientific community. Previous studies have reported elevated levels of EVs in the bloodstream of individuals affected by different types of cancer, in comparison to cancer-free individuals [240, 241]. These findings have suggested a potential association between elevated EV levels and disease progression, as well as treatment resistance, thereby proposing the potential utility of EV counts as an independent biomarker for cancer [242]. In previous studies focused on PC, the potential of EV levels as promising biomarkers for both diagnosis [243] and prognosis has been highlighted [244-246]. However, contrasting findings have also been reported, with some studies indicating minimal or insignificant changes in EV levels between different groups [234]. In the present study, no significant differences were observed in the levels of EVs in either plasma or urine samples from PC patients compared to samples obtained three months after surgery, as well as to BPH patients or HD.

The enumeration of EVs can be subjected to various technical challenges, leading to contentious outcomes. A major hurdle in utilizing EV quantity as a biomarker lies in the absence of standardized isolation and measurement techniques. The process of isolating EVs from plasma and urine is intricate, and different methodologies can yield disparate results [119, 135]. Factors such as sample collection, processing, and storage can significantly impact EV quantity measurements, resulting in inconsistent findings. Therefore, there is a need for innovative technologies that can effectively isolate EVs in a seamless and continuous workflow [247] or directly measure their quantity in biological fluids.

The heterogeneous composition of EVs presents an additional obstacle in their analysis. EVs encompass a diverse group of particles with varying dimensions, origins, and cargo contents. Differentiating between EVs derived from cancer cells and those from other cellular sources is challenging. The presence of NVEPs further complicates the analysis of EV quantity, potentially leading to false positive or negative results. Furthermore, the levels of EVs can be influenced by various physiological and pathological factors, including inflammation and physical forces. For instance, it has been reported that prostate massage can stimulate the release of prostatic fluid, leading to an increased proportion of prostate - derived EVs in urine [248]. However, the applicability of this approach to routine applications may be limited.

The discovery of cancer- associated RNA molecules within EVs isolated from the biofluids of cancer patients has generated significant interest in EVs as a potential source of RNA biomarkers for cancer liquid biopsies [249]. The specific subset of EVs or their cargo that holds the greatest significance for biomarker purposes is still not fully understood. However, emerging evidence suggests that EV-encapsulated biomolecules may have advantage as liquid biopsies compared to those that are unbound or free in circulation [234]. Furthermore, recent research has uncovered the presence of a biocorona surrounding EVs, which is believed to play a significant role in both healthy and diseased states [139]. Notably, RNAs have been found to specifically associate with the biocorona, indicating their potential involvement in intercellular communication and signaling [138]. In this study, EVs underwent treatment with Proteinase K and RNAse A prior RNA isolation, thereby focusing on the RNA content encapsulated within the EVs. This approach aimed to capture and analyze the RNA molecules contained within the EVs, which could provide valuable insights into their functional roles and potential as biomarkers.

Previous investigations into the RNA cargo encapsulated in EVs among patients with PC have predominantly relied on case-control studies [236, 239, 250]. Although these studies have identified potential PC biomarkers, the cellular source of these EVs has yet to be determined. Moreover, the patient cohorts in these studies have primarily been selected based on PSA and GS levels, which overlooks the heterogenous nature of PC. Additionally, there is a lack of consensus on the criteria for patient selection [236], and the presence or urogenital infections or other oncological diseases may hinder the discovery of PC-related biomarkers. To mitigate these challenges, we implemented stringent exclusion criteria (methodology 2.1). We also ensured that sample collection was performed at consistent time points before and after surgery, considering that the composition of biofluids can vary throughout the day due to factors such as the donor's diet and fitness [236] . By adhering to these criteria and collecting the same volumes of samples at the designated time points, we aimed to minimize preanalytical intervariability.

In this study, a unique and patient-centric approach to elucidate the role of plasma and urinary EVs in transporting RNA molecules derived from PC was employed. A longitudinal cohort was assembled, consisting of patients diagnosed with PC who were scheduled for RP. Samples were obtained from these patients three months after the RP to compare the EV RNA content in biofluids in the presence of PC and prostate tissues and after excision of these tissues. Patients with PSA levels three months after surgery higher than 0.2 ng/ml were excluded. The aim was to identify RNA signatures that are selectively present in EVs from tumour tissue, detectable in PreOp EVs and absent in PosOp EVs. The hypothesis was that by integrating three distinct criteria – elevated expression levels in tumour tissues; significant prevalence in PreOp EVs and a reduction in PostOp EVs – we could identify RNA biomarkers originating from PC tissues. Following this approach, a total of 69 different biomarkers (63 mRNAs, 3 lncRNAs, 2 miRNAs and 1 piRNA) were identified. Subsequently, RT-ddPCR assays were developed to validate the discovered EV biomarkers in an independent cohort of 20 PC patients and 20 BPH samples. While biomarkers were initially identified in urinary EVs, we also assessed their presence in plasma EVs. We adopted this approach because urine predominantly contains EVs released by the urogenital system, whereas plasma contains EVs derived from various tissues and cell types, making it more challenging to specifically identify PC-derived signatures among the diverse EV population in plasma samples.

Moreover, the predominant hypothesis regarding EV RNA cargo selection is based on EV types or biogenesis routes [142]. It is plausible that specific molecular signatures are selectively packaged and transported within EVs based on the intended destination. Previous studies have suggested the existence of various mechanisms involved in the loading of RNA molecules into EVs, indicating the presence of specific cargo selection processes [142]. This combination of specific cargo selection and the capacity of EVs to facilitate the formation of a conducive microenvironment for metastasis [251] supports the notion that EV-mediated communication between cells is intricately regulated and directed towards specific locations. Another potential factor contributing to the selectiveness of different cargo obtained in plasma and urinary EVs, could be the location and opportunity dependence of EV release. Depending on the origin of the EVs and the histological structure at the time of the release, the biofluid in which they are secreted may vary. For example, in the prostate, if EVs originate from luminal cells and are released in the apical zone [10], they are likely to reach the urine. Conversely, if basal cells [10] are responsible for release, the vesicles are more likely to enter the bloodstream. However, during PC progression, epithelial tissue undergoes phenotypic changes [33], potentially altering all communication routes.

Both scenarios could explain why specific signatures have been found in urinary or plasma EVs and not have been found common for both biofluids.

From our identified biomarkers, several protein coding genes have been demonstrated to be upregulated in PC and functionally associated with the advancement or development of PC, thereby validating their potential utility as biomarkers for PC. The modulation of androgen receptor expression by FOXA1, NACHT, WD repeat domain containing 1 (NWD1), and MAZ has been demonstrated to promote tumour progression and is often associated with unfavorable prognosis [66, 252-254]. Furthermore, it has been reported in a study conducted by Yang et al. that MAZ facilitates the promotion of bone metastasis through the transcriptional activation of the RAS signaling pathway in prostate cancer cells [255]. On the other hand, Burdelski et al. found a strong association between GLO1 and early biochemical recurrence [256], and Rounds et al. proposed GLO1 as a potential marker for high-grade PIA [257]. The induction of EMT transition in PC cells has been demonstrated by TGM4 [258], and its association with unfavorable outcomes has been established through its overexpression [259]. TGM4 has been recognized as prostate-restricted marker [260]. Prostate transmembrane protein, androgen induced 1 (PMEPA1) has emerged as a key player in the modulation of signaling pathways in PC. It is involved in a dual role, exhibiting both tumour-suppressive and oncogenic characteristics. On one hand, some PMEPA1 isoforms function to suppress AR signaling pathway, thereby exhibiting inhibitory effects on PC growth and invasion. On the other hand, PMEPA1 also exhibits oncogenic characteristics by interacting with the transforming growth factor-beta pathway [261]. AMD1 is an enzyme intricately involved in the biosynthesis of polyamines [262]. Polyamines play vital roles in cellular processes such as growth, proliferation and differentiation, and their abnormal regulation has been implicated in various cancer types [263, 264]. In the case of PC, there is an observed overexpression of AMD1, and this enzyme is primarily responsible for the conversion of S-adenosylmethionine (SAM), into decarboxylated S-adenosylmethionine (dcSAm), thereby regulating the synthesis of polyamines [265]. Consequently, the heightened levels of polyamines in PC have been associated with enhanced cell proliferation and improved cell survival, thereby contributing to tumour growth [264-266]. To the best of our knowledge, apart from NKX3.1[267], none of the identified mRNA biomarkers have been previously reported in EVs from PC. Despite our diligent efforts, we encountered challenges in developing RT-ddPCR assays for the identified biomarker targets. Ultimately, out of the initial pool of 63 mRNA identified, only five candidates displayed a discernible decrease in PostOp EV compared to PreOp levels. Notably among these candidates, only AMD1 demonstrated statistically significant validation in the independent PC cohort when examining urinary EVs. Interestingly, none of the biomarkers displayed a significant decrease in plasma EVs.

Results yielded three different lncRNAs as potential PC biomarkers. CHD2 adjacent, suppressive regulatory RNA (CHASERR) is an evolutionarily conserved lncRNA that regulates the levels of the chromatin remodeling protein CDH2 [268], but its role in PC has not been understood yet. On the contrary, studies have demonstrated that long intergenic non-protein coding RNA 62 (Linc00662) promotes cancer cell proliferation by facilitating cell cycle progression and inhibiting apoptosis [269]. Additionally, Linc00062 has been suggested to act as a competing endogenous RNA by sponging miRNAs modulating PC progression [270]. However, the precise function of the third lncRNA identified in this study remains unclear. It is worth noting that none of these biomarkers have been previously characterized as specific PC EV- enclosed biomarkers in the

existing literature. Regrettably, we encountered difficulties in designing PCR assays to assess the presence or absence of the identified biomarkers in the validation cohort. Among lncRNA biomarkers, prostate cancer antigen 3 (PCA3), a lncRNA biomarker enclosed within PC EVs, has been extensively studied [271]. Numerous studies have demonstrated its capacity to differentiate between individuals with PC and healthy males, as well as between PC patients with varying GS [236], but so far to the best of our knowledge, none has proved their potential to discriminate between PC and BPH. In our study, PCA3 exhibited significant overexpression in PC tissues (log2FC = 9.08; adj. p = $1.32x\ 10^{-85}$) and could be detected in EVs derived from PreOp urinary EVs. However, although a decrease in PCA3 expression levels was observed, this difference did not reach statistical significance.

Long RNAs, including mRNAs and lncRNAs, hold great potential as biomarkers for their substantial fold changes and established functional significance. While full-length mRNAs smaller than 1kb have been documented in EVs [189], the majority of EV- contained RNA molecules are generally shorter [149]. However, designing PCR assays for long RNA poses challenges due to their fragmented nature within EVs. The fragmentation pattern of RNAs remains unclear, raising questions about whether it is entirely random or if specific fragments have preferential inclusion or exclusion from EVs. One possible explanation for these observations is that EVs are particularly enriched in mRNAs that encode very short proteins [272]. Contrary to the initial assumptions, both full length and truncated mRNAs can be transferred to recipient cells and undergo translation to produce proteins [144, 145]. Multiple mechanisms have been proposed for the incorporation of mRNAs into EVs. One mechanism involves the interaction of mRNAs with RBPs within MVBs, facilitated by unique secondary structures or specific RNA motifs [272]. Alternatively, mRNAs can be passively loaded into EVs based on their high abundance [142]. Furthermore, the variability in the sorting of RNA fragments into EVs among different individuals is not yet fully understood, particularly since EVs derived from the same sample exhibit significant variation in the quantity of their cargo content [143].

On the contrary, developing assays for miRNAs and piRNAs is relatively straightforward due to their fixed structure and specific number of nt. In this study, three distinct small RNAs were identified as potential biomarkers. miR375-3p has previously been reported to be present in serum, plasma and urinary EVs of individuals diagnosed with PC [236]. Notably, the concentration of miR-375-3p has shown promise as a differentiating factor between PC patients and individuals with BPH or HD [236]. Furthermore, its levels have been found to correlate with disease prognosis [273]. On the other hand, miR92a-1-5p levels have been reported to be altered in semen EVs and able to distinguish between PC and HD [273]. In vitro studies have also demonstrated the role of miR92a in promoting cell proliferation through PTEN/AKT signaling pathway in PC cells [274]. Between these two miRNAs, miR375-3p was successfully validated as a significantly differentially expressed miRNA in PreOp versus PostOp urinary EVs. Conversely, the levels of miR-92a did not exhibit any notable significant differences between PreOp and PostOp in either of the examined biofluids (data not shown).

piRNAs were the fourth RNA species where potential biomarkers were successfully identified following our criteria. Dysregulation of piRNA levels has been observed in various cancers, indicating their potential involvement in cancer progression and metastasis. These piRNAs were shown to be implicated in cancer progression and metastasis through transcriptional and post-

transcriptional gene silencing mechanisms [155, 275]. A study carried out by Peng et al. reported the differential expressions of four piRNAs between PC patients and HD in urinary EVs [276]. In this study, one uncharacterized piRNA, piR-28004, was found commonly overexpressed in PreOp urine samples and tumour tissue and was validated in urinary EVs in the independent PC cohort. Despite this finding, the specific role of piR-28004 in PC has not yet been elucidated. Although more than 30000 piRNA genes have been discovered in the genome [157] and their observed deregulation in various cancers suggest that they hold great potential as valuable cancer biomarkers, their analysis is currently impeded by the inadequate annotation in the human genome and the inconsistent data and nomenclature across piRNA sequence databases, including the ones used in this study: piRBase [212], piRNABank [213] and piRNAdb [214]. These limitations hinder the comprehensive understanding and reliable interpretation of piRNA data in the context of cancer research.

PC molecular diagnostics approaches are essential due to limitations in traditional methods like DRE and PSA tests, including overdiagnosis and overtreatment [41, 42]. Molecular profiling can enable early detection and monitoring in a non-invasive manner. In this study, the significance of AMD1, miR-375-3p and piR28004 levels were observed to exhibit a significant decrease in urinary EVs following RP. However, these biomarkers did not demonstrate the capability to distinguish between BPH and PC. This suggests that these biomarkers might represent prostate-dependent signatures, which could be employed for active surveillance before prostatectomy, but might not serve as discriminators among various prostatic diseases.

In contrast, GLO1 and NKX3.1 demonstrated the ability to discriminate between BPH and PC when examined plasma EV samples from the independent cohort. However, this discrimination was not observed when analyzing urine samples, despite the initial discovery of these biomarkers in urinary EVs through RNAseq. Several factors may contribute to this observed discrepancy. One potential explanation is the utilization of different normalization techniques employed between the two methodologies. RNAseq data was normalized based on sequencing depth and RNA composition, whereas RT-ddPCR data were normalized to the volume of the biofluids. While this normalization approach is commonly employed in the analysis of plasma EVs [234, 277], it may not be optimal for normalizing urinary EVs due to the inherent fluctuations in volume and concentration. A more desirable approach to normalize RT-ddPCR data would involve the use of a set of stable reference genes. While some potential genes have been identified for plasma EVs [278-280], no such candidates have been identified for urinary EVs. Additionally, it is worth noting that the majority of the proposed candidates' genes are miRNAs, which may not be suitable for normalizing other RNA biotypes. Furthermore, none of these proposed reference genes have been validated in independent cohorts.

Alternative methodologies have been proposed and reviewed, such as utilizing creatinine levels or EV number [281]. Creatinine, a byproduct of muscle catabolism, has been shown to vary among individuals due to factors such as age, physical activity, muscle mass, diet, etc. [282]. Moreover, the levels of prostate - derived EVs are unlikely to be directly proportional to creatinine excretion rates. On the other hand, EV number is highly dependent on the method used for EV isolation and quantification, which can introduce significant biases [119, 135]. Additionally, this approach might pose challenges if increased EV production is a part of the disease pathophysiology. More recently, urinary PSA levels have been suggested as a potential

normalization method specifically for studying prostate - derived EVs [248]. However, further validation is required to establish its effectiveness in normalizing urinary EVs. Consequently, the question of suitable normalization methods for urinary EV research remains a topic of debate, and a consensus has not yet been reached within the EV research community [283]. Considering our objective of comparing the potential of different biofluids to serve as PC biomarkers source, we minimized disparities in isolation procedures and analytical techniques employed. Therefore, the same normalization strategy, to the volume of the biofluids, was employed for the analysis of both.

The identification of reliable prognostic biomarkers is equally crucial as it can significantly impact patient stratification, disease monitoring and treatment evaluation. Currently, the most widely utilized prognostic assessment tools for patient risk stratification in PC are the CAPRA score [51, 53] and ISUP grade [37]. Nevertheless, these tools predominantly rely on the recognition of GS patterns [51, 53]. Although GS is a robust tool in the management of PC [65], GS determination based on biopsy samples is constrained due to the inherent heterogeneity of PC. In certain cases, obtaining additional biopsies may be neccessary to attain a more precise diagnosis, and repetitive biopsies might be required for patients undergoing active surveillance. Consequently, it is imperative to discover biomarkers that can accurately predict risk stratification or correlate with existing tests while being obtained through non-invasive means.

In this study, a significant moderate positive correlation ($r = 0.36$, $p = 0.04$) was detected between the CAPRA score and the levels of NKX3.1 in urinary EVs. In the prostate, NKX3.1 has been elucidated as a tumour suppressor with the capacity to modulate AR transcription [284] and protects mitochondria from oxidative stress [284]. Concurrently, it demonstrates upregulation in response to androgen stimulation [285, 286], thereby highlighting the existence of a reciprocal relationship wherein NKX3.1 and AR mutually influence each other within a fee-forward regulatory loop [287]. Interestingly, NKX3.1 has also been reported in castration resistant NKX3.1-expressing cells (CARNs), which are luminal epithelial cells with stem cell properties involved in prostate regeneration [288]. Polymorphisms in NKX3.1 and translocations/ deletions affecting this gene have been previously reported in advanced PC cases [68], and NKX3.1 has been found to be overexpressed in urinary EVs released by androgen-independent cells [267]. Furthermore, two independent studies demonstrated a reduction in NKX3.1 protein expression in the prostate of mice following inoculation with *E. coli* [289, 290]. Notably, the combination of NKX3.1 loss and inflammation exhibited a synergistic effect in promoting the development of a more aggressive basal phenotype [289, 290]. Mechanistically, exposure to inflammatory cytokines was found to rapidly diminish the levels of NKX3.1 protein. This reduction was mediated by phosphorylation of the C-terminal domain of NKX3.1, leading to its subsequent labeling for proteasomal degradation through ubiquitination [291]. Ubiquitination has been previously recognized as one of the modifications for inclusion of cargo within EVs at mRNA and protein levels [142, 292]. Considering these findings, along with the observed overexpression of NKX3.1 in both EVs and tumour tissue as demonstrated in our study, it is plausible to suggest that NKX3.1 might undergo selective packaging within EVs. This phenomenon could potentially serve as a mechanism employed by cancer cells to either enhance their survival or in response of stress-induced and inflammation-associated processes inherent to cancer progression. While initially these dual findings might appear paradoxical, they could potentially be elucidated by the intrinsic heterogeneity of PC. For instance, existing evidence indicates that NKX3.1 is involved in

stabilizing p53, and PTEN, in turn, safeguards NKX3.1 protein from ubiquitination [293, 294]. However, in cases of PTEN loss, the degradation of NKX3.1 protein occurs, accompanied by AR activation and p53 inhibition, ultimately facilitating cell proliferation and advancing cancer progression [293, 294]. Considering the transition of cells from relatively indolent behavior to more aggressive phenotypes in PC, it is plausible that these expression levels might experience alterations along this trajectory, varying among difference calls and at different points in time.

On the other hand, GLO1, an enzyme dependent on glutathione, plays a dual role in the progression of cancer. Firstly, GLO1 has been reported as a detoxifier methylglyoxal (MG), a byproduct of glycolysis and an oncometabolite involved in the reprogramming of cellular metabolism [295]. Moreover, GLO1 has been implicated in the maintenance of an immunosuppressive microenvironment by facilitating the up-regulation of programmed death-ligand 1 (PD-L1) through MG mediated pathways, thereby promoting cancer progression [296]. Experimental studies involving GLO1 knockout mice and GLO1 inhibition have revealed an augmentation of cancer invasion and progression, particularly in melanoma [295]. Conversely, elevated expression of GLO1 has been associated with a poor prognosis and increased tumour invasiveness, attributed to its ability to activate genes associated with epithelial – to – mesenchymal transition (EMT) and its correlation with the presence of TMPRSS2: ERG fusion [256, 257].

In addition, the RT-ddPCR data revealed a moderate correlation between MAZ expression and ISUP grade ($r = 0.42$, $p = 0.02$). MAZ is involved in the regulation of multiple molecular pathways that play crucial roles in PC progression. Notably, MAZ has been demonstrated to enhance AR transcriptional activity [297], activate the transcription of the RAS signaling pathway [255] and suppress TGF-beta transcription factor [298]. These molecular events contribute to increased proliferation, invasiveness, and metastasis in PC [255, 297, 298].

A panel of biomarkers offers superior power and information compared to a single biomarker test, as it can capture disease heterogeneity, enhance diagnostic accuracy, and provides multidimensional insights. By minimizing individual variations and confounding factors, a biomarker panel increasing its overall reliability and robustness. While numerous studies have proposed various miRNAs and mRNAs as single biomarkers to improve PC diagnosis and prognosis [236], and several biomarker models combining protein levels or derivatives of PSA with or without clinical data have been proposed for PC diagnosis [299, 300], only few models have involved different RNA signatures.

In urine, one initial RNA model involved detecting the TMPRSS2: ERG transcript within urinary exosomes. This model exhibited a significant predictive value for PC detection (AUC = 0.79), particularly when combined with the European Randomized Study of Screening for PC (ERSPC) risk calculator [301]. Subsequent studies highlighted the importance of combining urinary TMPRSS2: ERG transcript with other markers, such as PCA3 (AUC = 0.83) and PSA (AUC = 0.84) [301, 302]. Although this combination may hold prognostic value, its effectiveness for detection purposes remains uncertain, since the expression of the TMPRSS2: ERG mutation varies considerably, ranging from 23 to 50% among confirmed PC cases across different cohorts [303]. A couple of miRNA biomarker panels have been proposed to discriminate between PC and BPH. One panel, consisting of three different miRNAs (miR-142-3p; miR-142-5p and miR-223) combined with PSA, demonstrated the ability to discriminate between PC and BPH with an AUC

= 0.82 [304]. Meanwhile, the second panel, derived from semen samples, showed the collaborative effect of miR-375 and miR-451a in discriminating between BPH and PC (AUC= 0.72) [305]. Although these two studies show promise, they lack validation, and the initial sample set of either BPH or PC patients consisted of fewer than 10 individuals.

In clinical settings, the SelectMDx nucleic acid biomarker diagnostic model is commonly utilized in urine. This test combines the expression of Homeobox C6 (HOXC6) and distal-less homeobox 1 (DLX1), along with clinical factors to evaluate the risk of high-grade PC [306]. Originally designed to aid in risk stratification for biopsy decision-making in patients with elevated PSA levels, recent studies have demonstrated its potential for PC diagnostics, surpassing other markers such as PCA3, PSA, multiparametric MRI [307, 308]. However, it should be noted that prior to urine collection for the SelectMDx test, DRE is required, which may potentially impact the secretion of marker levels. Another test called ExoDx PC test, assesses the expression of PCA3, ERG, and SAM pointed domain containing ETS transcription factor (SPDEF) in exosomes present in urine samples to determine the probability of high-grade PC. This test has received U.S Food and Drug Administration (FDA) approval and helps determine the need for prostate biopsy in men with PSA levels ranging from 2 to 10ng/ml [309].

In this study we assessed the diagnostic potential of an RNA biomarker panel consisting of seven different biomarkers identified in our cohort (miR375-3p, piRNA-28004, AMD1, MAZ, NKX3.1, GLO1 and RBM47) using both plasma and urinary EVs samples from 20 PC and 20 BPH samples. In both plasma and urinary EVs, our panel outperformed PSA in differentiating between PC and BPH. The LOOCV demonstrated the potential of the plasma model. Compared to the previously aforementioned models [299, 300], that aimed to discriminate between BPH and PC, and to the individual markers identified in the discovery cohort, our plasma model exhibited superior specificity and sensitivity. Additionally, the plasma model achieved comparable AUC values in the LOOCV assessment. Our urinary model did not perform as well in validation, potentially due to the normalization challenges mentioned earlier. It is noteworthy that all the previously proposed models primarily rely on urinary samples [301, 302, 307-309], and therefore face similar normalization issues since they are PCR-based. Additionally, to the best of my knowledge, this is the first time a model combining different RNA types has been proposed for PC diagnostics.

Despite the traditional belief of the prostate as a sterile organ, emerging evidence suggests the presence of a diverse microbial community [77, 78]. The prostate gland harbors a heterogeneous microbial community, known as the prostate microbiome, which has been implicated in the development of PC [77-79]. Investigating the composition and dynamics of the PC microbiome can provide valuable insights into its potential role in disease initiation, progression, and treatment response [79]. Moreover, the study of the PC microbiome offers insights into microbial biomarkers that could be used for diagnosis and prognosis. As such, PC tissue and adjacent normal prostate tissue transcriptome RNAseq data obtained from the previous 10 PC patients' cohort, was merged in two groups: PC tissue and adjacent normal prostate tissue. Then both groups were reassessed in search of reads unmapped to the human genome. Only a small fraction, specifically 3.6% of the entire transcriptome RNAseq data derived from tumour tissue, and 5.78% from adjacent normal prostate tissue, exhibited variations from the human origin. To determine the source of these reads, they were subjected to mapping using Kraken 2 [217].

Using this approach, three different phyla, namely Firmicutes, Proteobacteria and Actinobacteria, were found to be the most representative in prostate tissues. This finding is consistent with previous studies that have investigated the microbiota of PC tissues [87, 89]. Among the identified species, the most abundant ones in tissues were *Staphylococcus cohnii, Staphylococcus haemolyticus, Ralstonia solenacea and Curtobacterium flaccumfaciens*, all opportunistic pathogens. *Staphylococci* are spherical Gram-positive bacteria with a diameter ranging from 0.5 to 1.0 μm, typically forming clusters, pairs, or short chains [310]. *Staphylococcus cohnii* and *Staphylococcus haemolyticus*, belong to the coagulase-negative staphylococci group and were previously considered uncommon pathogens [311]. These species are primarily known to inhabit the human skin. Empirical evidence has shown that clinical isolates of these species exhibit a notable degree of antibiotic resistance [312-314]. Although *Staphylococcus cohnii* is infrequently associated with human infections, when it does occur, it usually affects the skin and bile duct and has been reported as a cause of septicemia in a patient with colon cancer [315]. Interestingly, in the prostate, *Staphylococcus cohnii* has been reported to be overexpressed in BPH tissue samples compared to PC [316]. Additionally, *Staphylococcus haemolyticus* has recently been classified as an emerging microbe causing different types of infections [314], including prostatitis [317]. Cavarretta et al. also reported an abundance of *Staphylococci* in PC tissues[87]. Unlike their findings, we did not observe a significant difference in abundance between tumour and normal adjacent prostate tissue. Therefore, they could be considered part of the prostate *in situ* microbiome. Furthermore, analysis of alpha diversity revealed a nearly twofold reduction in species diversity within tumour tissue compared to prostate tissue (data not shown), although the difference was not statistically significant. This lack of significance may be attributed to the similarity in abundance of the most prevalent species, with the less common species potentially lacking sufficient representation to significantly alter the overall gene pool. In terms of beta diversity, there was a similarity in species diversity among the majority of the samples independently of their source, with a few outliers (data not shown). Interestingly, these outliers corresponded to different patient duplicates. The heterogeneity of biological replicates may explain these variations. While efforts were made to uniformly mince the tissue, it is possible that in one of the replicates, a particular cell or tissue type was more predominant than the other.

The presence of *Ralstonia solanacearum* and *Curtobacterium flaccumfaciens* in prostate tissue, both known to be bacterial plant pathogens [318, 319] likely acquired through the ingestion of contaminated food, provides evidence supporting the proposed gut-prostate-axis [101]. According to this hypothesis, during pathological conditions, inflammatory processes in the gut can lead to gut dysbiosis, facilitating the entry of gut microbial metabolites and microbiota into the bloodstream and subsequent dissemination to other organs, including the prostate [97]. It is worth noting that specific species within the *Curtobacterium* genus have previously been linked to PC [87]. While the data from this study aligns with this assumption, further investigations, including the analysis of fecal samples from the same patient cohort would be required to confirm the presence of these microbiome species in the gut of the population set.

Differential expression analysis between prostate tissue and tumour tissue revealed over representation of several species from the normal human flora, including different *Streptococcus* species [320, 321] and *Dysgonomas* [322]. Additionally, opportunistic pathogenic species such as *Aerococcus Urinase* [323] and *Pseudomonas* [324] were found dysregulated. Surprisingly, species from the *Cyanobacteria* family were identified as well. Thus, in addition to the presence of

different species typically associated with human skin indicates the potential inclusion of environmental microbiota within our samples. The tissue samples were directly obtained during prostatectomy, and although efforts were made to maintain the sample in sterile conditions, contamination from the surgical environment is still a possibility. Such contamination can introduce transient environmental microbes that may not accurately represent the actual microbiome. It is worth noting that *Streptococcus spp*. are commonly encountered as contaminants in laboratory analyses [105, 106]. Therefore, while this data provides valuable insights, further studies and the inclusion of appropriate no-template controls would be necessary to accurately identify and exclude potential contaminants from the tissue analysis.

During the analysis of EV RNAseq data, it became evident that over fifty percent of the reads could not be aligned to the human genome. To ascertain their source, the unmapped reads were mapped to our reference PM, following the removal of potential environmental signals derived from the non-template control samples. About a quarter of the EV reads were successfully mapped to the PM, indicating a potential microbial origin. The remaining reads likely stem from various microbial species not present in our reference PM. It is noteworthy that all the 365 species identified in the PM were also detected in EVs from both biofluids. When studying differential species abundance between samples, different *Pseudomonas* species were overrepresented in PreOpP samples compared to HD and PostOpP samples. In urinary EV samples, the predominant species identified were *Micrococcus luteus* and *Pseudomonas* species. *Pseudomonas* is a genus of gram negative, rod-shaped bacteria with a single polar flagellum , known for its opportunistic pathogenic nature [325]. *Pseudomonas* species (*spp*.) are commonly found in various environments such as terrestrial, aquatic, and flora habitats. They can be part of microbiota in asymptomatic individuals and are known to colonize hospital facilities. The transmission of *Pseudomonas* occurs through patient-to-patient contact via fomites or through ingestion of contaminated food and water [325]. Considering these factors, one might argue whether the presence of *Pseudomonas* species in the samples from the cohort could be attributed to environmental contamination during sample collection at the hospital. However, while it cannot be completely ruled out, multiple studies consistently identify *Pseudomonas spp*. as part of the prostate microbiome, being associated with prostatitis [326] and the development of PC [88, 327, 328]. Moreover, their abundance in urine microbial communities has been shown to differentiate between BPH and PC [328]. Additionally, in a Chinese patient cohort, transcriptome analysis of metagenome isolated form PC tissues revealed a significant correlation in the expression profiles between *Pseudomonas spp.* and human small RNAs. The researchers hypothesized that *Pseudomonas* may have an inhibitory effect on metastasis [88]. While the release of EVs by *Pseudomonas spp.* have been extensively studied [329], to the best of our knowledge, this is the first time that *Pseudomonas spp.* content have been identified in EVs isolated from human biofluids, rather than in bacterial control studies or total urine pellets.

We also identified overrepresented *Micrococcus luteus* in our PreOpU EVs. *Micrococcus luteus* is a Gram-positive cocci bacterium that possesses catalase and oxidase enzymes [318]. It is commonly found in various natural environments such as soil and water resources. Additionally, it is considered a normal resident of human skin and the mucosa of the oropharynx [330]. Interestingly, *Micrococcus luteus* has been observed in abundance within PC [331]. While the association between *Micrococcus luteus* EVs and PC has not been previously established, studies

have shown that *Micrococcus luteus* EVs possess immunomodulatory potential by inhibiting neutrophilic inflammation in a mouse asthma model [332].

Afterwards, a novel genome-agnostic approach was employed to analyze all exogenous reads from the RNAseq data. For this, fold changes and p-values were calculated for each read individually. Then the top 1000 reads based on adj. p-values were selected and cluster analysis was performed. Selected clusters were assigned a consensus sequence, which was then subjected to BLAST analysis to identify their origin. In comparing plasma EVs from PreOp PC sample to HD samples, a significant overrepresentation of the LysR family transcriptional regulator from *Pseudomonas* was observed (log2FC = 9.82; adj. p = 0.003). The LysR family transcriptional regulator in *Pseudomonas* plays a crucial role in various cellular processes, including metabolic pathways, stress responses, virulence mechanisms, and antibiotic resistance multifaceted roles that aid in several cellular processes such as antibiotic resistance. This multifaceted roles enable *Pseudomonas* to effectively adapt and respond to diverse environmental stimuli [333].

Furthermore, overrepresented fragments of tRNA-Val and tRNA-Lys were observed from *Pseudomonas spp.* as well. Although the functionality of these fragments may be questioned since no full tRNA molecule were discovered, other studies have highlighted the potential significance of human tRNA fragments as PC biomarkers [165, 334]. Additionally, it is important to note that due to the incomplete nature of some microbial genomes, only the species names could be identified in some cases. This is evident in a sequence *Streptomyces chartreusis* (log2FC = 10.38, adj. p = 0.01), encoding a hypothetical unidentified protein, and another sequence from *Mycobacterium gordonae* (log2FC = 8.52, adj. p = 0.01), respectively. These sequences were found overrepresented in PreOpP samples compared to HD samples, but their functional relevance has not yet been assessed.

In the comparison of PreOpP vs PostOpP, thioredoxin and porin sequences from *Pseudomonas spp.* were overrepresented. Thioredoxins are widely distributed proteins that exhibit redox activity, facilitating reactions involving thiol-disulfide bonds exchange [335]. Deletions in porins by *Pseudomonas* have been associated with antimicrobial resistance [336]. In the comparison of PreOpU versus PostOpU, different rRNAs, tRNA-Arg and notably, a fragment of the rRNA maturation enzyme RNase YbeY from *Micrococcus luteus* were identified. YbeY is hypothesized to play a critical role in in the maturation of 16S rRNA and its potential association with other ribosomal components, which may contribute to the development of the small ribosomal subunit.[337] YbeY is also known to be critical for fitness and host-microbe interaction [338].Nevertheless, further investigation is needed to elucidate the exact roles and mechanisms of these molecules in PC and their potential as diagnostic or therapeutic targets.

The relationship between the microbiome and cancer is intricate and not yet fully elucidated [97]. While the microbiome is believed to play a role in cancer development and progression, there is no concrete evidence that it does directly originate cancer. Dysbiosis, characterized by microbial imbalances in the microbiome, has been implicated in cancer development [98]. Conversely, the microbiome can access tumour areas and influence cancer progression [99], indicating a synergistic relationship. It is important to note, that PC is a multifactorial disease influenced by various factors [26]. For instance, HF diets have been associated with the progression and increased risk of PC [339]. Specifically, saturated fats have been linked to metastatic processes

[339, 340]. A previous study investigating the prostate microbiome reported an abundance of SCFA producing bacteria in severe PC cases [101]. In mouse models, PC progression was induced by HF diets in mice, but it was hindered with the administration of antibiotics [101]. Furthermore, there could be a collaborative effect among different bacteria. Microbes have rapid reproduction rates, and their growth may largely dependent on available resources, particularly within an immunosuppressed environment. Consequently, the availability of nutrients in a specific area can lead to a shift in microbiota species composition. This phenomenon is exemplified by mucin-degrading microbes (MDM) that produce SCFAs, which serve as an abundant valuable carbon source for non-fermenting microbes such as *Pseudomonas* [341]. This explanation aligns with our data and could account for the overrepresentation of *Pseudomonas* in EVs from PreOp biofluids. Moreover, it has been observed that treatment with antibiotics can impede PC progression [101]. While this finding requires further validation, it presents an intriguing clinical application. If we are able to identify the microbial species that preferentially colonize or contribute to cancer processes, targeted interventions such as specific antibiotics or medications against these microbial species or their molecular targets could potentially halt or even prevent cancer progression. This highlights the importance of understanding the interplay between the microbiome and cancer in order to explore novel therapeutic strategies that might exploit these interactions for improved patient outcomes.

This study has some limitations that need to be considered. Firstly, the relatively small sample size of 30PC and 20 BPH patients highlights the need for a larger and more diverse cohort to ensure robustness and generalizability of the proposed biomarkers. The limited sample size was a result of strict patient selection criteria and challenges in obtaining follow-up material after the surgery, which hindered the recruitment of a larger cohort. However, it is worth noting that similar or even smaller sample sizes have been currently used in PC biomarker studies [236]. Nonetheless, future studies should aim to include larger cohorts to strengthen the validity of the findings. Furthermore, the scarcity of nucleic acid template obtained from EV samples presents additional challenges. The limited amount of template material restricts the number of tests that can be performed, potentially impacting the reproducibility of the results, especially considering the high heterogeneity of PC. Additionally, the fragmented nature of certain long RNA targets posed challenges in developing assays specifically targeting them. Furthermore, there is currently no consensus on normalization strategies for biofluids, despite attempts to establish them [281, 283]. Optimization of amplification methods is essential to maximize template availability, improve assay specificity, and ensure accurate analysis in future validation studies.

Moreover, it is important to consider the heterogeneity of the EV source in this study. While the focus was on signatures overexpressed in tumour tissue, the EVs obtained from biofluids also include those derived from normal cells of different tissues alongside cancer - derived EVs. Future studies could benefit from isolating specific subsets of EVs based on surface markers that are indicative of PC, such as PSMA-positive EVs [342, 343], to gain deeper insights into their unique characteristics and potential diagnostic value. Furthermore, it is worth noting that no-template controls were used for EV microbiological studies, but no controls were employed for analyzing the microbiome present in tissue samples. Therefore, the possibility of environmental contamination in theses samples cannot be ruled out. In future studies, proper controls should be included to accurately assess tissue sampling for microbiological analysis [344]. Lastly, PC is highly heterogeneous disease, and while the findings of this study provide valuable insights, they

only represent a specific subset of Caucasian males. The lack of information on other important factors such as dietary habits or family predisposition, known to contribute to the heterogeneity of PC [26, 31], further adds to the limitation of the study.

In future studies, it is imperative to validate the microbiome sequencing results obtained in this study in an independent cohort of PC EV samples to verify the accuracy and reliability of our novel genome-agnostic pipeline and to assess the clinical value of the identified microbial markers. Furthermore, the exploration of a prognostic RNA model using the biomarkers identified in this study, can provide valuable insights to improve PC patient classification. Additionally, given the heterogeneity of cell populations within the prostate tissue at different stages of PC development, the integration of single-cell sequencing approaches can aid in identifying the main cellular sources contributing to the EV content. This comprehensive understanding of the cellular origins of EVs can provide valuable insights into the underlying mechanisms of PC progression and facilitate the development of targeted therapeutic strategies. Moreover, it would be advantageous to perform sequencing analysis of single EVs. However, the current technological limitations in isolating single EVs and detecting and analyzing the low amounts of nucleic acids present within EVs pose challenges in achieving this goal. The approach used in this study holds also potential for personalized medicine. Building upon previous examples [345], sequencing the molecular profile of a patient's biopsy can enable the identification of specific markers that can be monitored and tracked over time. This personalized approach would allow for a more tailored and targeted treatment strategy based on the individual characteristic and progression of the disease.

In conclusion, the utilization of EV-enclosed biomarkers holds significant potential to revolutionize the management of PC, offering early detection, improved risk stratification, and personalized treatment strategies. This study has introduced a diverse range of novel small RNA biomarkers for PC diagnosis and prognosis, originating from both human sources and the PC-associated microbiome. Alternatively, combining both sample types or integrating human and microbial signatures could provide a more comprehensive assessment of the disease. Notably, the inclusion of repeated measures from the same individuals at different time points strengthens the statistical power of the study, minimizing the influence of confounding variables, while enabling the detection of subject-specific effects. Furthermore, we have proposed a novel biomarker model for PC diagnosis based on different RNA types that outperformed PSA test in discriminating between BPH and PC. Our proposed model, derived from plasma samples obtained without previous treatment, offers improved accuracy, particularly in the context of PC heterogeneity. This plasma-based assay enhances the non-invasive nature of the diagnostic procedure, minimizing patient discomfort and providing more convenient testing option. Additionally, we present here a novel genome-agnostic approach to identify overrepresented sequences, which has the potential to guide future studies in identifying specific targets for disease intervention and the development of target-based strategies.

However, it is important to note that further investigations involving larger patient cohorts are necessary to validate and confirm the robustness of these findings. Continued research in this field will help refine and optimize the diagnostic and prognostic potential of EV-enclosed biomarkers for PC, ultimately benefiting patient care and outcomes.

5. CONCLUSIONS

1. The EV population isolated from biofluids is enriched in small EVs as demonstrated by NTA, TEM and WB techniques.

2. Plasma and urinary EVs contained various RNA species, including miRNAs, piRNAs, lncRNAs and mRNAs.

3. mRNA fragments were the most abundant type of RNA biomarkers identified in EVs; however their fragmentation hampers the design of PCR assays.

4. EV RNA sequencing analysis showed that urine is enriched with PC/prostate-derived EVs as compared to plasma and therefore is a superior source of biomarkers for the diagnosis, prognosis and active surveillance, however, the development of PCR-based assays for quantification of RNA biomarkers in urinary EVs is challenging due to lack of reliable normalization methods.

5. NKX3.1 identified in plasma EVs, exhibited the highest diagnostic potential as a marker for distinguishing PC vs. BPH (AUC:0.82, $P<0.001$).

6. The plasma seven-biomarker model demonstrated superior performance in discriminating between BPH vs. PC, achieving a sensitivity of 0.74 and a specificity of 1 with an AUC value of 0.91.

7. Levels of NKX3.1 and MAZ expression in urinary EVs demonstrate correlation with CAPRA and ISUP scores, respectively.

8. A significant fraction of plasma and urinary EV RNA is derived from human microbiota.

9. A total of 365 microbial species were found in the prostate/PC tissues and all of them were represented in the plasma and urinary EV RNA.

10. Microbial RNA composition in plasma EVs of cancer patients is altered compared to healthy controls and is associated with the clinical events in cancer patients.

6. THESIS

1. Urine appears to be a superior source of EV RNAs for the diagnosis and active surveillance of PC, however, it is unlikely to be suitable for post-operative monitoring of PC progression.

2. Although PC-derived EV fraction in blood plasma is low, detection of PC-derived RNA biomarkers by RT-ddPCR is feasible and the seven-biomarker model generated in this study outperforms PSA test in distinguishing between PC and BPH.

3. Microbial RNA composition in plasma EVs may reflect the composition of human microbiome and therefore monitoring the changes in microbial RNA cargo in plasma EVs may have a clinical utility in detection, prognosis, and monitoring of various diseases, including cancer.

7. PUBLICATIONS

1. **Bajo-Santos C.,** Brokāne A., Zayakin P., Endzeliņš E., Soboļevska K., Belovs A., Jansons J., Sperga M., Llorente A., Radoviča/Spalviņa I., Lietuvietis V., Linē A. Plasma and urinary extracellular vesicles as a source of RNA biomarkers for prostate cancer in liquid biopsies. *Front. Mol. Biosci*. (2023) doi: 10.3389/fmolb.2023.980433.

2. §Ramirez-Garracho M., **§Bajo-Santos C**., Line A., Martens-Uzunova E.S., Martínez de la Fuente J., Moros M., Soekmadji C., Austlid Tasken K., Llorente A. Extracellular vesicles as a source of prostate cancer biomarkers in liquid biopsies: a decade of research. *Br J Cancer* (2021) doi: 10.1038/s41416-021-01610-8 (§ contributed equally to this work)

3. Brokāne A., **Bajo-Santos C.,** Zayakin P., Belovs A., Jansons J., Lietuvietis V., Martens-Uzunova E., Jenster G. Linē A. Validation of potential RNA biomarkers for prostate cancer diagnosis and monitoring in plasma and urinary extracellular vesicles. Front. Mol. Biosci. *Under Revision*

8. APPROBATION OF RESEARCH

1. **Bajo-Santos C.,** Brokane A., Zayakin P., Enzelins E., Beloc A., Jansons J., Sperga M., Llorente A., Lietuvietis V., Line A. Plasma and Urinary EVs as a source of RNA biomarkers for Prostate Cancer in liquid biopsies. BSEV 2022. September 30th - 2nd October 2022. **Invited Speaker**

2. **Bajo-Santos C**., Brokane A., Zayakin P., Enzelins E., Belocs A., Jansons J., Sperga M., Llorente A., Lietuvietis V., Line A. EV content as `potential biomarkers for Prostate Cancer Surveillance. Molecular Biology section of 80th conference of University of Latvia. 18 February, 2022. **Oral Presentation**

3. **Bajo-Santos C**., Brokāne A., Zayakin P., Belovs A., Jansons J., Sperga M., Lietuvietis V., Linē A. Comparison of plasma and urinary EVs as a source of RNA biomarkers in liquid biopsies of prostate cancer. uEV2022 Inaugural virtual symposium on Urinary extracellular vesicles. Feb 15-16, 2022, online.

4. **Bajo-Santos C**., Zayakin P., Jansons J., Belovs A., Melderis M., Lietuvietis V., Linē A. Comparative analysis of plasma and urinary EV RNA content in prostate cancer patients. ISEV 2021. E-conference. May 18-21, 2021

5. **Bajo-Santos C**., Soboļevska K., Zayakin P., Laiviņa E., Melderis M., Melne V., Lietuvietis V., Llorente A., Linē A. Profiling of Prostate Cancer-derived Extracellular Vesicles: New insights. Molecular Biology section of 78th conference of University of Latvia. 31 January, 2020. **Oral presentation**

6. **Bajo-Santos C.,** Melne V., Soboļevska K., Zayakin P., Lietuvietis V., Llorente A., Linē A. Profiling of smallRNA cargo from blood and urinary Prostate Cancer derived EVs, correlates with Prostate Cancer matching tumour. EARC 25 Amsterdam, The Netherlands, 30 June - 3 July 2018.

7. **Bajo Santos C.**, Melne V., Soboļevska K., Zajakins P., Endzeliņš E., Šantare D.; Rodríguez M., Sperga M., Lietuvietis V., Llorente A., Linē A. Characterization of smallRNA cargo of plasma and urinary EVs in Prostate Cancer patients. 3rd. conference of Latvian Biochemical Society and Molecular Biology section of 76th conference of University of Latvia. 02 February, 2018. **Oral presentation**

8. **Bajo-Santos C.**, Sobolevska K., Zayakin P., Linē A. EVs microRNA cargo sequencing analysis, a step forward understanding Prostate Cancer. 2nd.conference of Latvian Biochemical Society and Molecular Biology section of 75th conference of University of Latvia. 30 January, 2017. **Oral presentation**

9. **Bajo-Santos C**., Melne V., Sobolevska K., Zayakin P., Lietuvietis V., Llorente A., Linē A. Characterization of small RNA content in urinary and plasma EVs and matching prostate cancer tissues. ISEV 2017 annual meeting, Toronto, Canada 17-21 May, 2017. Abstract Book: ISEV2017, Journal of Extracellular Vesicles, 6:sup1, 1310414, pp112

9. ACKNOWLEDGEMENTS

I would like to extend my sincere gratitude to Prof. Aija Linē, for granting me the opportunity to work in her lab and pursue my Ph.D. under her guidance. Her unwavering support, mentorship, and invaluable insights have played a pivotal role in shaping my research journey into the EV field and personal development as a scientist.

I would also like to express my profound thanks to my dedicated colleagues and peers who have been or were part of Linē's lab or the BMC during these years. Their consistent assistance, collaboration and encouragement have been instrumental in navigating the challenges encountered during this doctoral pursuit. I extend my special thanks to Dr. Pawel Zayakin for his invaluable contributions in conducting sequencing data analysis for this research project and to the patients who generously donated the materials essential for this research.

Furthermore, I would like to express my sincere gratitude and appreciation to our collaborator, Dr. Alicia Llorente from Oslo University Hospital in Norway, for hosting me during the PhD exchange and providing guidance in the adoption of new methodologies. Her support and knowledge sharing have been instrumental in expanding my skillset and broadening the scope of my research.

Additionally, I would like to extend special thanks to Kristīne Soboļevska for embracing the challenge and joining me in the complex world of EV RNA content. Your willingness to embark on this journey together has made the experience more manageable and rewarding.

I would like to acknowledge the financial support provided by the State Education Development Agency of the Republic of Latvia, the Norway grants, the European Social Fund and L'Oréal UNESCO "For Women in Science" Young Talents Program-Baltic with the support of the Latvian National Commission for UNESCO and the Latvian Academy of Sciences. Their investment in this research has enabled the successful completion of this project.

Lastly, I would like to express my sincere appreciation to my family and friends, whose unwavering support, patience, and encouragement have been crucial throughout my Ph.D. journey. Their belief in my abilities and constant motivation have been instrumental in my academic progress and overall well-being.

Thank you! Paldies! Gracias!

THE END

REFERENCES

1. Sung, H., et al., *Global Cancer Statistics 2020: GLOBOCAN Estimates of Incidence and Mortality Worldwide for 36 Cancers in 185 Countries.* CA: A Cancer Journal for Clinicians, 2021. **71**(3): p. 209-249.
2. Organization, W.H. *Cancer*. 2021 [cited 2023 June]; Available from: https://www.who.int/news-room/fact-sheets/detail/cancer.
3. M, H., *Introduction to Cancer Biology*. 2 ed. 2013: Ventus Publishing.
4. Hanahan D., W.R.A., *The Hallmarks of Cancer.* Cell, 2000. **100**(1): p. 57-70.
5. Hanahan D., W.R.A., *Hallmarks of cancer: the next generation.* Cell, 2011. **144**(5): p. 646-674.
6. Hanahan, D., *Hallmarks of Cancer: New Dimensions.* Cancer Discovery, 2022. **12**(1): p. 31-46.
7. Toivanen, R. and M.M. Shen, *Prostate organogenesis: tissue induction, hormonal regulation and cell type specification.* Development, 2017. **144**(8): p. 1382-1398.
8. G., P., *Prostate gland and seminal vesicle*, in *Diagnostic Pathology:Genitourinary E-book*, AminMB, T. SK, and e. al., Editors. 2022, Elsevier. p. 4-156.
9. Verze, P., T. Cai, and S. Lorenzetti, *The role of the prostate in male fertility, health and disease.* Nat Rev Urol, 2016. **13**(7): p. 379-86.
10. Ittmann, M., *Anatomy and Histology of the Human and Murine Prostate.* Cold Spring Harb Perspect Med, 2018. **8**(5).
11. Rebello, R.J., et al., *Prostate cancer.* Nature Reviews Disease Primers, 2021. **7**(1): p. 9.
12. Shannon, B.A., J.E. McNeal, and R.J. Cohen, *Transition zone carcinoma of the prostate gland: a common indolent tumour type that occasionally manifests aggressive behaviour.* Pathology, 2003. **35**(6): p. 467-71.
13. Greene, D.R., et al., *A comparison of the morphological features of cancer arising in the transition zone and in the peripheral zone of the prostate.* J Urol, 1991. **146**(4): p. 1069-76.
14. Noguchi, M., et al., *An analysis of 148 consecutive transition zone cancers: clinical and histological characteristics.* J Urol, 2000. **163**(6): p. 1751-5.
15. Guo, C.C., et al., *Prostate cancer of transition zone origin lacks TMPRSS2–ERG gene fusion.* Modern Pathology, 2009. **22**(7): p. 866-871.
16. Mirosevich, J., et al., *Androgen receptor expression of proliferating basal and luminal cells in adult murine ventral prostate.* Journal of Endocrinology, 1999. **162**(3): p. 341-350.
17. Wang, Y., et al., *Cell differentiation lineage in the prostate.* Differentiation, 2001. **68**(4-5): p. 270-9.
18. Hayward, S.W., et al., *Stromal development in the ventral prostate, anterior prostate and seminal vesicle of the rat.* Acta Anat (Basel), 1996. **155**(2): p. 94-103.
19. Tuxhorn, J.A., G.E. Ayala, and D.R. Rowley, *Reactive stroma in prostate cancer progression.* J Urol, 2001. **166**(6): p. 2472-83.
20. Abrahamsson, P.A., *Neuroendocrine cells in tumour growth of the prostate.* Endocr Relat Cancer, 1999. **6**(4): p. 503-19.
21. Ferlay J, E.M., Lam F, Colombet M, Mery L, Piñeros M, et al. *Global Cancer Observatory: Cancer Today.* 2020 [cited 2023 June]; Available from: https://gco.iarc.fr/today.

22. Wang, L., et al., *Prostate Cancer Incidence and Mortality: Global Status and Temporal Trends in 89 Countries From 2000 to 2019.* Frontiers in Public Health, 2022. **10**.
23. Hugosson, J., et al., *A 16-yr Follow-up of the European Randomized study of Screening for Prostate Cancer.* Eur Urol, 2019. **76**(1): p. 43-51.
24. Schröder, F.H., et al., *Screening and prostate-cancer mortality in a randomized European study.* N Engl J Med, 2009. **360**(13): p. 1320-8.
25. Loeb, S., et al., *Overdiagnosis and overtreatment of prostate cancer.* Eur Urol, 2014. **65**(6): p. 1046-55.
26. KL, N., *The Etiology of Prostate Cancer.*, in *Prostate Cancer [Internet].* N.K. Bott SRJ, Editor. 2021, Exon Publications: Brisbane (AU).
27. Johns, L.E. and R.S. Houlston, *A systematic review and meta-analysis of familial prostate cancer risk.* BJU Int, 2003. **91**(9): p. 789-94.
28. Nyberg, T., M. Tischkowitz, and A.C. Antoniou, *BRCA1 and BRCA2 pathogenic variants and prostate cancer risk: systematic review and meta-analysis.* British Journal of Cancer, 2022. **126**(7): p. 1067-1081.
29. Nyberg, T., et al., *Homeobox B13 G84E Mutation and Prostate Cancer Risk.* European Urology, 2019. **75**(5): p. 834-845.
30. Rebbeck, T.R., et al., *Global patterns of prostate cancer incidence, aggressiveness, and mortality in men of african descent.* Prostate Cancer, 2013. **2013**: p. 560857.
31. Clinton, S.K., E.L. Giovannucci, and S.D. Hursting, *The World Cancer Research Fund/American Institute for Cancer Research Third Expert Report on Diet, Nutrition, Physical Activity, and Cancer: Impact and Future Directions.* The Journal of Nutrition, 2019. **150**(4): p. 663-671.
32. Bostwick, D.G. and J. Qian, *High-grade prostatic intraepithelial neoplasia.* Mod Pathol, 2004. **17**(3): p. 360-79.
33. Testa, U., G. Castelli, and E. Pelosi, *Cellular and Molecular Mechanisms Underlying Prostate Cancer Development: Therapeutic Implications.* Medicines (Basel), 2019. **6**(3).
34. Siegel, R.L., et al., *Cancer statistics, 2023.* CA: A Cancer Journal for Clinicians, 2023. **73**(1): p. 17-48.
35. Mottet, N., et al., *EAU-EANM-ESTRO-ESUR-SIOG Guidelines on Prostate Cancer-2020 Update. Part 1: Screening, Diagnosis, and Local Treatment with Curative Intent.* Eur Urol, 2021. **79**(2): p. 243-262.
36. Brierley JD, G.M., Wittekind C., *TNM classification of malignant tumors.* Ed.8 ed, ed. U.I.U.A. Cancer. 2017: Wiley-Blackwell.
37. Epstein, J.I., et al., *The 2014 International Society of Urological Pathology (ISUP) Consensus Conference on Gleason Grading of Prostatic Carcinoma: Definition of Grading Patterns and Proposal for a New Grading System.* The American Journal of Surgical Pathology, 2016. **40**(2): p. 244-252.
38. Balk, S.P., Y.J. Ko, and G.J. Bubley, *Biology of prostate-specific antigen.* J Clin Oncol, 2003. **21**(2): p. 383-91.
39. Ilic, D., et al., *Prostate cancer screening with prostate-specific antigen (PSA) test: a systematic review and meta-analysis.* BMJ, 2018. **362**: p. k3519.
40. Merriel, S.W.D., et al., *Systematic review and meta-analysis of the diagnostic accuracy of prostate-specific antigen (PSA) for the detection of prostate cancer in symptomatic patients.* BMC Medicine, 2022. **20**(1): p. 54.

41. Yamamoto, M., K. Hibi H Fau - Miyake, and K. Miyake, *Role of prostate-specific antigen and digital rectal examination in the detection of prostate cancer.* Int, J. Urol, 2020. **69(2)**(0919-8172 (Print)): p. 99-107.
42. Macefield, R.C., et al., *Impact of prostate cancer testing: an evaluation of the emotional consequences of a negative biopsy result.* Br J Cancer, 2010. **102**(9): p. 1335-40.
43. Søndergaard, M.E.J., et al., *Men's perception of information and psychological distress in the diagnostic phase of prostate cancer: a comparative mixed methods study.* BMC Nursing, 2022. **21**(1): p. 266.
44. Mainwaring, J.M., et al., *The Psychosocial Consequences of Prostate Cancer Treatments on Body Image, Sexuality, and Relationships.* Front Psychol, 2021. **12**: p. 765315.
45. Rosen RD, S.A., *TNM Classification.*, ed. S. Publishing. 2023, Treasure Island Treasure Island
46. Gleason, D.F., *Classification of prostatic carcinomas.* Cancer Chemother Rep, 1966. **50**(3): p. 125-8.
47. Epstein, J.I., *An update of the Gleason grading system.* J Urol, 2010. **183**(2): p. 433-40.
48. Harnden, P., et al., *Should the Gleason grading system for prostate cancer be modified to account for high-grade tertiary components? A systematic review and meta-analysis.* The Lancet Oncology, 2007. **8**(5): p. 411-419.
49. van Leenders, G.J.L.H., et al., *The 2019 International Society of Urological Pathology (ISUP) Consensus Conference on Grading of Prostatic Carcinoma.* Am J Surg Pathol, 2020. **44**(8): p. e87-e99.
50. D'Amico, A.V., et al., *Biochemical outcome after radical prostatectomy or external beam radiation therapy for patients with clinically localized prostate carcinoma in the prostate specific antigen era.* Cancer,, 2002. **95(2)**(0008-543X (Print)): p. 281-6.
51. Cooperberg, M.R., et al., *The University of California, San Francisco Cancer of the Prostate Risk Assessment score: a straightforward and reliable preoperative predictor of disease recurrence after radical prostatectomy.* J Urol, 2005. **173**(6): p. 1938-42.
52. Ondracek, R.P., et al., *Validation of the Kattan Nomogram for Prostate Cancer Recurrence After Radical Prostatectomy.* J Natl Compr Canc Netw, 2016. **14**(11): p. 1395-1401.
53. Cooperberg, M.R., J.F. Hilton, and P.R. Carroll, *The CAPRA-S score: A straightforward tool for improved prediction of outcomes after radical prostatectomy.* Cancer, 2011. **117**(22): p. 5039-46.
54. Cooperberg, M.R., J.M. Broering, and P.R. Carroll, *Risk assessment for prostate cancer metastasis and mortality at the time of diagnosis.* J Natl Cancer Inst, 2009. **101**(12): p. 878-87.
55. Peng, Z., et al., *Improving the Prediction of Prostate Cancer Overall Survival by Supplementing Readily Available Clinical Data with Gene Expression Levels of IGFBP3 and F3 in Formalin-Fixed Paraffin Embedded Core Needle Biopsy Material.* PLoS One, 2016. **11**(1): p. e0145545.
56. Saemundsson, A., et al., *Validation of the prognostic value of a three-gene signature and clinical parameters-based risk score in prostate cancer patients.* Prostate, 2023.
57. Röbeck, P., et al., *P-score in preoperative biopsies accurately predicts P-score in final pathology at radical prostatectomy in patients with localized prostate cancer.* Prostate, 2023. **83**(9): p. 831-839.

58. Cornford, P., et al., *EAU-EANM-ESTRO-ESUR-SIOG Guidelines on Prostate Cancer. Part II-2020 Update: Treatment of Relapsing and Metastatic Prostate Cancer.* Eur Urol, 2021. **79**(2): p. 263-282.
59. Network, C.G.A.R., *The Molecular Taxonomy of Primary Prostate Cancer.* Cell, 2015. **163**(4): p. 1011-25.
60. Hieronymus, H., et al., *Copy number alteration burden predicts prostate cancer relapse.* Proc Natl Acad Sci U S A, 2014. **111**(30): p. 11139-44.
61. Ciriello, G., et al., *Emerging landscape of oncogenic signatures across human cancers.* Nature Genetics, 2013. **45**(10): p. 1127-1133.
62. Carver, B.S., et al., *ETS rearrangements and prostate cancer initiation.* Nature, 2009. **457**(7231): p. E1; discussion E2-3.
63. Tomlins, S.A., et al., *Recurrent fusion of TMPRSS2 and ETS transcription factor genes in prostate cancer.* Science, 2005. **310**(5748): p. 644-8.
64. Magi-Galluzzi, C., et al., *TMPRSS2-ERG gene fusion prevalence and class are significantly different in prostate cancer of Caucasian, African-American and Japanese patients.* Prostate, 2011. **71**(5): p. 489-97.
65. Dai, X., et al., *Prostate cancer-associated SPOP mutations confer resistance to BET inhibitors through stabilization of BRD4.* Nat Med, 2017. **23**(9): p. 1063-1071.
66. Barbieri, C.E., et al., *Exome sequencing identifies recurrent SPOP, FOXA1 and MED12 mutations in prostate cancer.* Nat Genet, 2012. **44**(6): p. 685-9.
67. Fraser, M., et al., *Genomic hallmarks of localized, non-indolent prostate cancer.* Nature, 2017. **541**(7637): p. 359-364.
68. Robinson, D., et al., *Integrative clinical genomics of advanced prostate cancer.* Cell, 2015. **161**(5): p. 1215-1228.
69. Fujita, K. and N. Nonomura, *Role of Androgen Receptor in Prostate Cancer: A Review.* World J Mens Health, 2019. **37**(3): p. 288-295.
70. Hubbard, G.K., et al., *Combined MYC Activation and Pten Loss Are Sufficient to Create Genomic Instability and Lethal Metastatic Prostate Cancer.* Cancer Res, 2016. **76**(2): p. 283-92.
71. Baena-Del Valle, J.A., et al., *MYC drives overexpression of telomerase RNA (hTR/TERC) in prostate cancer.* J Pathol, 2018. **244**(1): p. 11-24.
72. Mateo, J., et al., *Genomics of lethal prostate cancer at diagnosis and castration resistance.* J Clin Invest, 2020. **130**(4): p. 1743-1751.
73. Abida, W., et al., *Genomic correlates of clinical outcome in advanced prostate cancer.* Proc Natl Acad Sci U S A, 2019. **116**(23): p. 11428-11436.
74. de Bono, J., et al., *Olaparib for Metastatic Castration-Resistant Prostate Cancer.* N Engl J Med, 2020. **382**(22): p. 2091-2102.
75. Sender, R., S. Fuchs, and R. Milo, *Revised Estimates for the Number of Human and Bacteria Cells in the Body.* PLoS Biol, 2016. **14**(8): p. e1002533.
76. Malard, F., et al., *Introduction to host microbiome symbiosis in health and disease.* Mucosal Immunol, 2021. **14**(3): p. 547-554.
77. Wheeler, K.M. and M.A. Liss, *The Microbiome and Prostate Cancer Risk.* Curr Urol Rep, 2019. **20**(10): p. 66.
78. Porter, C.M., et al., *The microbiome in prostate inflammation and prostate cancer.* Prostate Cancer Prostatic Dis, 2018. **21**(3): p. 345-354.

79. Bhatt, A.P., M.R. Redinbo, and S.J. Bultman, *The role of the microbiome in cancer development and therapy.* CA Cancer J Clin, 2017. **67**(4): p. 326-344.
80. De Marzo, A.M., et al., *Inflammation in prostate carcinogenesis.* Nat Rev Cancer, 2007. **7**(4): p. 256-69.
81. Sfanos, K.S., et al., *The inflammatory microenvironment and microbiome in prostate cancer development.* Nat Rev Urol, 2018. **15**(1): p. 11-24.
82. Cai, T., et al., *versus common uropathogens as a cause of chronic bacterial prostatitis: Is there any difference? Results of a prospective parallel-cohort study.* Investig Clin Urol, 2017. **58**(6): p. 460-467.
83. Paulis, G., *Inflammatory mechanisms and oxidative stress in prostatitis: the possible role of antioxidant therapy.* Res Rep Urol, 2018. **10**: p. 75-87.
84. Hochreiter, W.W., J.L. Duncan, and A.J. Schaeffer, *Evaluation of the bacterial flora of the prostate using a 16S rRNA gene based polymerase chain reaction.* J Urol, 2000. **163**(1): p. 127-30.
85. Sfanos, K.S., et al., *A molecular analysis of prokaryotic and viral DNA sequences in prostate tissue from patients with prostate cancer indicates the presence of multiple and diverse microorganisms.* Prostate, 2008. **68**(3): p. 306-20.
86. Yow, M.A., et al., *Characterisation of microbial communities within aggressive prostate cancer tissues.* Infect Agent Cancer, 2017. **12**: p. 4.
87. Cavarretta, I., et al., *The Microbiome of the Prostate Tumor Microenvironment.* Eur Urol, 2017. **72**(4): p. 625-631.
88. Feng, Y., et al., *Metagenomic and metatranscriptomic analysis of human prostate microbiota from patients with prostate cancer.* BMC Genomics, 2019. **20**(1): p. 146.
89. Banerjee, S., et al., *Microbiome signatures in prostate cancer.* Carcinogenesis, 2019. **40**(6): p. 749-764.
90. André, A.R., et al., *Gastric adenocarcinoma and Helicobacter pylori: correlation with p53 mutation and p27 immunoexpression.* Cancer Epidemiol, 2010. **34**(5): p. 618-25.
91. Miyake, M., et al., *Infection and Chronic Inflammation in Human Prostate Cancer: Detection Using Prostatectomy and Needle Biopsy Specimens.* Cells, 2019. **8**(3).
92. Ma, J., et al., *Influence of Intratumor Microbiome on Clinical Outcome and Immune Processes in Prostate Cancer.* Cancers (Basel), 2020. **12**(9).
93. Aragón, I.M., et al., *The Urinary Tract Microbiome in Health and Disease.* Eur Urol Focus, 2018. **4**(1): p. 128-138.
94. Bao, Y., et al., *Questions and challenges associated with studying the microbiome of the urinary tract.* Ann Transl Med, 2017. **5**(2): p. 33.
95. Shrestha, E., et al., *Profiling the Urinary Microbiome in Men with Positive versus Negative Biopsies for Prostate Cancer.* J Urol, 2018. **199**(1): p. 161-171.
96. Alanee, S., et al., *A prospective study to examine the association of the urinary and fecal microbiota with prostate cancer diagnosis after transrectal biopsy of the prostate using 16sRNA gene analysis.* Prostate, 2019. **79**(1): p. 81-87.
97. Fujita, K., et al., *The Gut-Prostate Axis: A New Perspective of Prostate Cancer Biology through the Gut Microbiome.* Cancers (Basel), 2023. **15**(5).
98. Fan, X., et al., *Gut Microbiota Dysbiosis Drives the Development of Colorectal Cancer.* Digestion, 2021. **102**(4): p. 508-515.
99. Golombos, D.M., et al., *The Role of Gut Microbiome in the Pathogenesis of Prostate Cancer: A Prospective, Pilot Study.* Urology, 2018. **111**: p. 122-128.

100. Liss, M.A., et al., *Metabolic Biosynthesis Pathways Identified from Fecal Microbiome Associated with Prostate Cancer.* Eur Urol, 2018. **74**(5): p. 575-582.
101. Matsushita, M., et al., *Gut Microbiota-Derived Short-Chain Fatty Acids Promote Prostate Cancer Growth via IGF1 Signaling.* Cancer Res, 2021. **81**(15): p. 4014-4026.
102. Pernigoni, N., et al., *Commensal bacteria promote endocrine resistance in prostate cancer through androgen biosynthesis.* Science, 2021. **374**(6564): p. 216-224.
103. Terrisse, S., et al., *Immune system and intestinal microbiota determine efficacy of androgen deprivation therapy against prostate cancer.* J Immunother Cancer, 2022. **10**(3).
104. Liu, Y., et al., *Gut Microbiota Dysbiosis Accelerates Prostate Cancer Progression Through Increased LPCAT1 Expression and Enhanced DNA Repair Pathways.* Front Oncol, 2021. **11**: p. 679712.
105. Eisenhofer, R., et al., *Contamination in Low Microbial Biomass Microbiome Studies: Issues and Recommendations.* Trends Microbiol, 2019. **27**(2): p. 105-117.
106. Glassing, A., et al., *Inherent bacterial DNA contamination of extraction and sequencing reagents may affect interpretation of microbiota in low bacterial biomass samples.* Gut Pathog, 2016. **8**: p. 24.
107. Fair, W.R. and R.F. Parrish, *Antibacterial substances in prostatic fluid.* Prog Clin Biol Res, 1981. **75A**: p. 247-64.
108. Hall, S.H., K.G. Hamil, and F.S. French, *Host defense proteins of the male reproductive tract.* J Androl, 2002. **23**(5): p. 585-97.
109. Hu, T., J. Wolfram, and S. Srivastava, *Extracellular Vesicles in Cancer Detection: Hopes and Hypes.* Trends Cancer, 2021. **7**(2): p. 122-133.
110. Xie, J., et al., *The tremendous biomedical potential of bacterial extracellular vesicles.* Trends Biotechnol, 2022. **40**(10): p. 1173-1194.
111. Yáñez-Mó, M., et al., *Biological properties of extracellular vesicles and their physiological functions.* Journal of Extracellular Vesicles, 2015. **4**(1): p. 27066.
112. Jeppesen, D.K., et al., *Extracellular vesicles and nanoparticles: emerging complexities.* Trends Cell Biol, 2023.
113. van Niel, G., G. D'Angelo, and G. Raposo, *Shedding light on the cell biology of extracellular vesicles.* Nat Rev Mol Cell Biol, 2018. **19**(4): p. 213-228.
114. Atkin-Smith, G.K. and I.K.H. Poon, *Disassembly of the Dying: Mechanisms and Functions.* Trends Cell Biol, 2017. **27**(2): p. 151-162.
115. Dieudé, M., et al., *The 20S proteasome core, active within apoptotic exosome-like vesicles, induces autoantibody production and accelerates rejection.* Sci Transl Med, 2015. **7**(318): p. 318ra200.
116. Buzas, E.I., et al., *Emerging role of extracellular vesicles in inflammatory diseases.* Nat Rev Rheumatol, 2014. **10**(6): p. 356-64.
117. Di Vizio, D., et al., *Large oncosomes in human prostate cancer tissues and in the circulation of mice with metastatic disease.* Am, J. Pathol, 2012. **181(5)**(1525-2191 (Electronic)): p. 1573-84.
118. Di Vizio, D., et al., *Oncosome formation in prostate cancer: association with a region of frequent chromosomal deletion in metastatic disease.* Cancer Res, 2009. **69**(13): p. 5601-9.
119. Théry, C.A.-O., et al., *Minimal information for studies of extracellular vesicles 2018 (MISEV2018): a position statement of the International Society for Extracellular*

Vesicles and update of the MISEV2014 guidelines. J. Extracell Vesicles, 2018. **7(1)**(2001-3078 (Print)): p. 1535750.
120. Huang, Y., et al., *Migrasome formation is mediated by assembly of micron-scale tetraspanin macrodomains.* Nat Cell Biol, 2019. **21**(8): p. 991-1002.
121. Yu, S. and L. Yu, *Migrasome biogenesis and functions.* FEBS J, 2022. **289**(22): p. 7246-7254.
122. Jiao, H., et al., *Mitocytosis, a migrasome-mediated mitochondrial quality-control process.* Cell, 2021. **184**(11): p. 2896-2910.e13.
123. Melentijevic, I., et al., *C. elegans neurons jettison protein aggregates and mitochondria under neurotoxic stress.* Nature, 2017. **542**(7641): p. 367-371.
124. Nicolás-Ávila, J.A., et al., *A Network of Macrophages Supports Mitochondrial Homeostasis in the Heart.* Cell, 2020. **183**(1): p. 94-109.e23.
125. Zhang, Q., et al., *Transfer of Functional Cargo in Exomeres.* Cell Rep, 2019. **27**(3): p. 940-954.e6.
126. Zhang, H., et al., *Identification of distinct nanoparticles and subsets of extracellular vesicles by asymmetric flow field-flow fractionation.* Nat Cell Biol, 2018. **20**(3): p. 332-343.
127. Zhang, Q., et al., *Supermeres are functional extracellular nanoparticles replete with disease biomarkers and therapeutic targets.* Nature Cell Biology, 2021. **23**(12): p. 1240-1254.
128. Jeppesen, D.K., et al., *Are Supermeres a Distinct Nanoparticle?* J Extracell Biol, 2022. **1**(6).
129. Rome, L.H. and V.A. Kickhoefer, *Development of the vault particle as a platform technology.* ACS Nano, 2013. **7**(2): p. 889-902.
130. Frascotti, G., et al., *The Vault Nanoparticle: A Gigantic Ribonucleoprotein Assembly Involved in Diverse Physiological and Pathological Phenomena and an Ideal Nanovector for Drug Delivery and Therapy.* Cancers (Basel), 2021. **13**(4).
131. Carter, S.D., et al., *Correlated cryogenic fluorescence microscopy and electron cryo-tomography shows that exogenous TRIM5α can form hexagonal lattices or autophagy aggregates in vivo.* Proc Natl Acad Sci U S A, 2020. **117**(47): p. 29702-29711.
132. Konoshenko, M.Y., et al., *Isolation of Extracellular Vesicles: General Methodologies and Latest Trends.* Biomed Res Int, 2018. **2018**: p. 8545347.
133. Théry, C., et al., *Isolation and characterization of exosomes from cell culture supernatants and biological fluids.* Curr Protoc Cell Biol, 2006. **Chapter 3**: p. Unit 3.22.
134. Lane, R.E., et al., *Purification Protocols for Extracellular Vesicles.* Methods Mol Biol, 2017. **1660**: p. 111-130.
135. Monguió-Tortajada, M., et al., *Extracellular vesicle isolation methods: rising impact of size-exclusion chromatography.* Cell Mol Life Sci, 2019. **76**(12): p. 2369-2382.
136. Böing, A.N., et al., *Single-step isolation of extracellular vesicles by size-exclusion chromatography.* J Extracell Vesicles, 2014. **3**.
137. Bajo-Santos, C., et al., *Plasma and urinary extracellular vesicles as a source of RNA biomarkers for prostate cancer in liquid biopsies.* Frontiers in Molecular Biosciences, 2023. **10**.
138. Tóth, E., et al., *Formation of a protein corona on the surface of extracellular vesicles in blood plasma.* J Extracell Vesicles, 2021. **10**(11): p. e12140.

139. Yerneni, S.S., et al., *Radioiodination of extravesicular surface constituents to study the biocorona, cell trafficking and storage stability of extracellular vesicles.* Biochimica et Biophysica Acta (BBA) - General Subjects, 2022. **1866**(2): p. 130069.
140. Buzas, E.I., *Opportunities and challenges in studying the extracellular vesicle corona.* Nat Cell Biol, 2022. **24**(9): p. 1322-1325.
141. Michell, D.L. and K.C. Vickers, *Lipoprotein carriers of microRNAs.* Biochim Biophys Acta, 2016. **1861**(12 Pt B): p. 2069-2074.
142. O'Brien, K., et al., *RNA delivery by extracellular vesicles in mammalian cells and its applications.* Nat Rev Mol Cell Biol, 2020. **21**(10): p. 585-606.
143. Chevillet, J.R., et al., *Quantitative and stoichiometric analysis of the microRNA content of exosomes.* Proc Natl Acad Sci U S A, 2014. **111**(41): p. 14888-93.
144. Skog, J., et al., *Glioblastoma microvesicles transport RNA and proteins that promote tumour growth and provide diagnostic biomarkers.* Nat Cell Biol, 2008. **10**(12): p. 1470-6.
145. Valadi, H., et al., *Exosome-mediated transfer of mRNAs and microRNAs is a novel mechanism of genetic exchange between cells.* Nat Cell Biol, 2007. **9**(6): p. 654-9.
146. Huang, X., et al., *Characterization of human plasma-derived exosomal RNAs by deep sequencing.* BMC Genomics, 2013. **14**: p. 319.
147. van Balkom, B.W., et al., *Quantitative and qualitative analysis of small RNAs in human endothelial cells and exosomes provides insights into localized RNA processing, degradation and sorting.* J Extracell Vesicles, 2015. **4**: p. 26760.
148. Li, M., et al., *Analysis of the RNA content of the exosomes derived from blood serum and urine and its potential as biomarkers.* Philosophical transactions of the Royal Society of London. Series B, Biological sciences, 2014. **369**(1652): p. 20130502.
149. Nolte-'t Hoen, E.N., et al., *Deep sequencing of RNA from immune cell-derived vesicles uncovers the selective incorporation of small non-coding RNA biotypes with potential regulatory functions.* Nucleic Acids Res, 2012. **40**(18): p. 9272-85.
150. Ha, M. and V.N. Kim, *Regulation of microRNA biogenesis.* Nat Rev Mol Cell Biol, 2014. **15**(8): p. 509-24.
151. Huntzinger, E. and E. Izaurralde, *Gene silencing by microRNAs: contributions of translational repression and mRNA decay.* Nat Rev Genet, 2011. **12**(2): p. 99-110.
152. Dharap, A., et al., *MicroRNA miR-324-3p induces promoter-mediated expression of RelA gene.* PLoS One, 2013. **8**(11): p. e79467.
153. Peng, Y. and C.M. Croce, *The role of MicroRNAs in human cancer.* Signal Transduct Target Ther, 2016. **1**: p. 15004.
154. Ali Syeda, Z., et al., *Regulatory Mechanism of MicroRNA Expression in Cancer.* Int J Mol Sci, 2020. **21**(5).
155. Wu, X., et al., *The Biogenesis and Functions of piRNAs in Human Diseases.* Mol Ther Nucleic Acids, 2020. **21**: p. 108-120.
156. Martinez, V.D., et al., *Unique somatic and malignant expression patterns implicate PIWI-interacting RNAs in cancer-type specific biology.* Sci Rep, 2015. **5**: p. 10423.
157. Han, Y.N., et al., *PIWI Proteins and PIWI-Interacting RNA: Emerging Roles in Cancer.* Cell Physiol Biochem, 2017. **44**(1): p. 1-20.
158. Hanusek, K., et al., *piRNAs and PIWI Proteins as Diagnostic and Prognostic Markers of Genitourinary Cancers.* Biomolecules, 2022. **12**(2).

159. Kirchner, S. and Z. Ignatova, *Emerging roles of tRNA in adaptive translation, signalling dynamics and disease.* Nat Rev Genet, 2015. **16**(2): p. 98-112.
160. Rodnina, M.V. and W. Wintermeyer, *The ribosome as a molecular machine: the mechanism of tRNA-mRNA movement in translocation.* Biochem Soc Trans, 2011. **39**(2): p. 658-62.
161. Keam, S.P. and G. Hutvagner, *tRNA-Derived Fragments (tRFs): Emerging New Roles for an Ancient RNA in the Regulation of Gene Expression.* Life (Basel), 2015. **5**(4): p. 1638-51.
162. Kumar, P., C. Kuscu, and A. Dutta, *Biogenesis and Function of Transfer RNA-Related Fragments (tRFs).* Trends Biochem Sci, 2016. **41**(8): p. 679-689.
163. Huang, S.Q., et al., *The dysregulation of tRNAs and tRNA derivatives in cancer.* J Exp Clin Cancer Res, 2018. **37**(1): p. 101.
164. Speer, J., et al., *tRNA breakdown products as markers for cancer.* Cancer, 1979. **44**(6): p. 2120-3.
165. Olvedy, M., et al., *A comprehensive repertoire of tRNA-derived fragments in prostate cancer.* Oncotarget, 2016. **7**(17): p. 24766-77.
166. Fischer, U., C. Englbrecht, and A. Chari, *Biogenesis of spliceosomal small nuclear ribonucleoproteins.* Wiley Interdiscip Rev RNA, 2011. **2**(5): p. 718-31.
167. Cao, H., et al., *Down regulation of U2AF1 promotes ARV7 splicing and prostate cancer progression.* Biochem Biophys Res Commun, 2021. **541**: p. 56-62.
168. Scott, M.S. and M. Ono, *From snoRNA to miRNA: Dual function regulatory non-coding RNAs.* Biochimie, 2011. **93**(11): p. 1987-92.
169. Williams, G.T. and F. Farzaneh, *Are snoRNAs and snoRNA host genes new players in cancer?* Nat Rev Cancer, 2012. **12**(2): p. 84-8.
170. Dong, X.Y., et al., *Implication of snoRNA U50 in human breast cancer.* J Genet Genomics, 2009. **36**(8): p. 447-54.
171. Valkov, N. and S. Das, *Y RNAs: Biogenesis, Function and Implications for the Cardiovascular System.* Adv Exp Med Biol, 2020. **1229**: p. 327-342.
172. Gulìa, C., et al., *Y RNA: An Overview of Their Role as Potential Biomarkers and Molecular Targets in Human Cancers.* Cancers (Basel), 2020. **12**(5).
173. Christov, C.P., E. Trivier, and T. Krude, *Noncoding human Y RNAs are overexpressed in tumours and required for cell proliferation.* Br J Cancer, 2008. **98**(5): p. 981-8.
174. Meiri, E., et al., *Discovery of microRNAs and other small RNAs in solid tumors.* Nucleic Acids Res, 2010. **38**(18): p. 6234-46.
175. Hahne, J.C., A. Lampis, and N. Valeri, *Vault RNAs: hidden gems in RNA and protein regulation.* Cell Mol Life Sci, 2021. **78**(4): p. 1487-1499.
176. Berger, W., et al., *Vaults and the major vault protein: novel roles in signal pathway regulation and immunity.* Cell Mol Life Sci, 2009. **66**(1): p. 43-61.
177. Kickhoefer, V.A., et al., *Vaults are up-regulated in multidrug-resistant cancer cell lines.* J Biol Chem, 1998. **273**(15): p. 8971-4.
178. Jedynak-Slyvka, M., A. Jabczynska, and R.J. Szczesny, *Human Mitochondrial RNA Processing and Modifications: Overview.* Int J Mol Sci, 2021. **22**(15).
179. Kalsbeek, A.M.F., et al., *Mitochondrial genome variation and prostate cancer: a review of the mutational landscape and application to clinical management.* Oncotarget, 2017. **8**(41): p. 71342-71357.

180. Delaunay, S., et al., *Mitochondrial RNA modifications shape metabolic plasticity in metastasis.* Nature, 2022. **607**(7919): p. 593-603.
181. Parker, M.S., et al., *The Expansion Segments of 28S Ribosomal RNA Extensively Match Human Messenger RNAs.* Front Genet, 2018. **9**: p. 66.
182. Gaviraghi, M., C. Vivori, and G. Tonon, *How Cancer Exploits Ribosomal RNA Biogenesis: A Journey beyond the Boundaries of rRNA Transcription.* Cells, 2019. **8**(9).
183. Penzo, M., et al., *The Ribosome Biogenesis-Cancer Connection.* Cells, 2019. **8**(1).
184. Quinn, J.J. and H.Y. Chang, *Unique features of long non-coding RNA biogenesis and function.* Nat Rev Genet, 2016. **17**(1): p. 47-62.
185. Li, W., et al., *Functional roles of enhancer RNAs for oestrogen-dependent transcriptional activation.* Nature, 2013. **498**(7455): p. 516-20.
186. Khalil, A.M., et al., *Many human large intergenic noncoding RNAs associate with chromatin-modifying complexes and affect gene expression.* Proc Natl Acad Sci U S A, 2009. **106**(28): p. 11667-72.
187. Jarroux, J., A. Morillon, and M. Pinskaya, *History, Discovery, and Classification of lncRNAs.* Adv Exp Med Biol, 2017. **1008**: p. 1-46.
188. Choi, J., et al., *How Messenger RNA and Nascent Chain Sequences Regulate Translation Elongation.* Annu Rev Biochem, 2018. **87**: p. 421-449.
189. Wei, Z., et al., *Coding and noncoding landscape of extracellular RNA released by human glioma stem cells.* Nat Commun, 2017. **8**(1): p. 1145.
190. Fong, Z. and W.-L. Lee, *An emerging role of KRAS in biogenesis, cargo sorting and uptake of cancer-derived extracellular vesicles.* Future Medicinal Chemistry, 2022. **14**(11): p. 827-845.
191. Vishweshwaraiah, Y.L. and N.V. Dokholyan, *mRNA vaccines for cancer immunotherapy.* Front Immunol, 2022. **13**: p. 1029069.
192. Das, S., et al., *The Extracellular RNA Communication Consortium: Establishing Foundational Knowledge and Technologies for Extracellular RNA Research.* Cell, 2019. **177**(2): p. 231-242.
193. Eliscovich, C., et al., *mRNA on the move: the road to its biological destiny.* J Biol Chem, 2013. **288**(28): p. 20361-8.
194. Ragusa, M., et al., *Asymmetric RNA Distribution among Cells and Their Secreted Exosomes: Biomedical Meaning and Considerations on Diagnostic Applications.* Front Mol Biosci, 2017. **4**: p. 66.
195. Arroyo, J.D., et al., *Argonaute2 complexes carry a population of circulating microRNAs independent of vesicles in human plasma.* Proc Natl Acad Sci U S A, 2011. **108**(12): p. 5003-8.
196. Iavello, A., et al., *Role of Alix in miRNA packaging during extracellular vesicle biogenesis.* Int J Mol Med, 2016. **37**(4): p. 958-66.
197. Villarroya-Beltri, C., et al., *Sumoylated hnRNPA2B1 controls the sorting of miRNAs into exosomes through binding to specific motifs.* Nat Commun, 2013. **4**: p. 2980.
198. Santangelo, L., et al., *The RNA-Binding Protein SYNCRIP Is a Component of the Hepatocyte Exosomal Machinery Controlling MicroRNA Sorting.* Cell Rep, 2016. **17**(3): p. 799-808.
199. Ahadi, A., et al., *Long non-coding RNAs harboring miRNA seed regions are enriched in prostate cancer exosomes.* Sci Rep, 2016. **6**: p. 24922.

200. Koppers-Lalic, D., et al., *Nontemplated nucleotide additions distinguish the small RNA composition in cells from exosomes.* Cell Rep, 2014. **8**(6): p. 1649-1658.
201. Liu, X., et al., *A MicroRNA precursor surveillance system in quality control of MicroRNA synthesis.* Mol Cell, 2014. **55**(6): p. 868-879.
202. Yáñez-Mó, M., et al., *Biological properties of extracellular vesicles and their physiological functions.* Journal of Extracellular Vesicles, 2015. **4**(1): p. 27066.
203. Team, R.C., *R: A language and environment for statistical computing*. 2021, R Foundation for Statistical Computing: Vienna, Austria.
204. Martin, M., *Cutadapt removes adapter sequences from high-throughput sequencing reads.* 2011, 2011. **17**(1): p. 3.
205. Langmead, B. and S.L. Salzberg, *Fast gapped-read alignment with Bowtie 2.* Nature Methods, 2012. **9**(4): p. 357-359.
206. Axtell, M.J., *ShortStack: comprehensive annotation and quantification of small RNA genes.* RNA (New York, N.Y.), 2013. **19**(6): p. 740-751.
207. Putri, G.H., et al., *Analysing high-throughput sequencing data in Python with HTSeq 2.0.* Bioinformatics, 2022. **38**(10): p. 2943-2945.
208. Kozomara, A., M. Birgaoanu, and S. Griffiths-Jones, *miRBase: from microRNA sequences to function.* Nucleic acids research, 2019. **47**(D1): p. D155-D162.
209. Chan, P.P. and T.M. Lowe, *GtRNAdb 2.0: an expanded database of transfer RNA genes identified in complete and draft genomes.* Nucleic Acids Research, 2016. **44**(D1): p. D184-D189.
210. Volders, P.-J., et al., *LNCipedia 5: towards a reference set of human long non-coding RNAs.* Nucleic Acids Research, 2018. **47**(D1): p. D135-D139.
211. Quek, X.C., et al., *lncRNAdb v2.0: expanding the reference database for functional long noncoding RNAs.* Nucleic acids research, 2015. **43**(Database issue): p. D168-D173.
212. Wang, J., et al., *piRBase: a comprehensive database of piRNA sequences.* Nucleic Acids Research, 2018. **47**(D1): p. D175-D180.
213. Sai Lakshmi, S. and S. Agrawal, *piRNABank: a web resource on classified and clustered Piwi-interacting RNAs.* Nucleic acids research, 2008. **36**(Database issue): p. D173-D177.
214. Piuco, R. and P.A.F. Galante, *piRNAdb: A piwi-interacting RNA database.* bioRxiv, 2021: p. 2021.09.21.461238.
215. Dobin, A., et al., *STAR: ultrafast universal RNA-seq aligner.* Bioinformatics, 2012. **29**(1): p. 15-21.
216. Love, M.I., W. Huber, and S. Anders, *Moderated estimation of fold change and dispersion for RNA-seq data with DESeq2.* Genome Biology, 2014. **15**(12): p. 550.
217. Wood, D.E., J. Lu, and B. Langmead, *Improved metagenomic analysis with Kraken 2.* Genome Biol, 2019. **20**(1): p. 257.
218. Soverini, M., et al., *HumanMycobiomeScan: a new bioinformatics tool for the characterization of the fungal fraction in metagenomic samples.* BMC Genomics, 2019. **20**(1): p. 496.
219. O'Leary, N.A., et al., *Reference sequence (RefSeq) database at NCBI: current status, taxonomic expansion, and functional annotation.* Nucleic Acids Res, 2016. **44**(D1): p. D733-45.
220. Cunningham, F., et al., *Ensembl 2022.* Nucleic Acids Research, 2021. **50**(D1): p. D988-D995.

221. Clark, K., et al., *GenBank.* Nucleic Acids Res, 2016. **44**(D1): p. D67-72.
222. Sonet, G., et al., *Adhoc: an R package to calculate ad hoc distance thresholds for DNA barcoding identification.* Zookeys, 2013(365): p. 329-36.
223. Chen, Y., A.T. Lun, and G.K. Smyth, *From reads to genes to pathways: differential expression analysis of RNA-Seq experiments using Rsubread and the edgeR quasi-likelihood pipeline.* F1000Res, 2016. **5**: p. 1438.
224. Bodenhofer, U., et al., *msa: an R package for multiple sequence alignment.* Bioinformatics, 2015. **31**(24): p. 3997-9.
225. Thompson, J.D., D.G. Higgins, and T.J. Gibson, *CLUSTAL W: improving the sensitivity of progressive multiple sequence alignment through sequence weighting, position-specific gap penalties and weight matrix choice.* Nucleic Acids Res, 1994. **22**(22): p. 4673-80.
226. Blighe, R., and Lewis, *EnhancedVolcano: Publication-ready volcano plots with enhanced colouring and labeling*. 2018.
227. Johnson, M., et al., *NCBI BLAST: a better web interface.* Nucleic Acids Res, 2008. **36**(Web Server issue): p. W5-9.
228. Tay, J.K., B. Narasimhan, and T. Hastie, *Elastic Net Regularization Paths for All Generalized Linear Models.* Journal of Statistical Software, 2023. **106**(1): p. 1 - 31.
229. Venables, W.N.a.R., B.D, *Modern Applied Statistics with S.Springer*. 2002, New York: Springer. 271-300.
230. Sing, T., et al., *ROCR: visualizing classifier performance in R.* Bioinformatics, 2005. **21**(20): p. 3940-1.
231. Yuan, J., et al. *Leave-One-Out Cross-Validation Based Model Selection for Manifold Regularization*. in *Advances in Neural Networks - ISNN 2010*. 2010. Berlin, Heidelberg: Springer Berlin Heidelberg.
232. Freitas, D., et al., *Different isolation approaches lead to diverse glycosylated extracellular vesicle populations.* J Extracell Vesicles, 2019. **8**(1): p. 1621131.
233. Vanessa, L.-R., et al., *ALIX protein analysis: storage temperature may impair results.* JMCM, 2019. **2**(2): p. 29-34.
234. Endzeliņš, E., et al., *Detection of circulating miRNAs: comparative analysis of extracellular vesicle-incorporated miRNAs and cell-free miRNAs in whole plasma of prostate cancer patients.* BMC Cancer, 2017. **17**(1): p. 730.
235. Qiagen. *QIAGEN GeneGlobe Data Analysis Center (RRID:SCR_021211)*. Available from: https://geneglobe.qiagen.com/us/analyze.
236. Ramirez-Garrastacho, M., et al., *Extracellular vesicles as a source of prostate cancer biomarkers in liquid biopsies: a decade of research.* British Journal of Cancer, 2022. **126**(3): p. 331-350.
237. Serafini-Cessi, F., N. Malagolini, and D. Cavallone, *Tamm-Horsfall glycoprotein: biology and clinical relevance.* Am J Kidney Dis, 2003. **42**(4): p. 658-76.
238. Wachalska, M., et al., *Protein Complexes in Urine Interfere with Extracellular Vesicle Biomarker Studies.* J Circ Biomark, 2016. **5**: p. 4.
239. Rodríguez, M., et al., *Identification of non-invasive miRNAs biomarkers for prostate cancer by deep sequencing analysis of urinary exosomes.* Molecular Cancer, 2017. **16**(1): p. 156.
240. Matsumoto, Y., et al., *Quantification of plasma exosome is a potential prognostic marker for esophageal squamous cell carcinoma.* Oncol Rep, 2016. **36**(5): p. 2535-2543.

241. Rodríguez Zorrilla, S., et al., *A Pilot Clinical Study on the Prognostic Relevance of Plasmatic Exosomes Levels in Oral Squamous Cell Carcinoma Patients.* Cancers (Basel), 2019. **11**(3).
242. König, L., et al., *Elevated levels of extracellular vesicles are associated with therapy failure and disease progression in breast cancer patients undergoing neoadjuvant chemotherapy.* Oncoimmunology, 2017. **7**(1): p. e1376153.
243. Wang, Y., et al., *Microfluidic Raman biochip detection of exosomes: a promising tool for prostate cancer diagnosis.* Lab Chip, 2020. **20**(24): p. 4632-4637.
244. Biggs, C.N., et al., *Prostate extracellular vesicles in patient plasma as a liquid biopsy platform for prostate cancer using nanoscale flow cytometry.* Oncotarget, 2016. **7**(8).
245. Nanou, A., et al., *Circulating tumor cells, tumor-derived extracellular vesicles and plasma cytokeratins in castration-resistant prostate cancer patients.* Oncotarget, 2018. **9**(27): p. 19283-19293.
246. Malla, B., D.M. Aebersold, and A. Dal Pra, *Protocol for serum exosomal miRNAs analysis in prostate cancer patients treated with radiotherapy.* Journal of Translational Medicine, 2018. **16**(1): p. 223.
247. Bajo-Santos, C., et al., *Extracellular Vesicles Isolation from Large Volume Samples Using a Polydimethylsiloxane-Free Microfluidic Device.* Int J Mol Sci, 2023. **24**(9).
248. Duijvesz, D., et al., *Immuno-based detection of extracellular vesicles in urine as diagnostic marker for prostate cancer.* Int J Cancer, 2015. **137**(12): p. 2869-78.
249. Vasconcelos, M.H., et al., *Extracellular vesicles as a novel source of biomarkers in liquid biopsies for monitoring cancer progression and drug resistance.* Drug Resist, Updat, 2019. **47**(1532-2084 (Electronic)): p. 10047.
250. Ramirez-Garrastacho, M., et al., *Potential of miRNAs in urinary extracellular vesicles for management of active surveillance in prostate cancer patients.* Br J Cancer, 2022. **126**(3): p. 492-501.
251. Peinado, H., et al., *Pre-metastatic niches: organ-specific homes for metastases.* Nat Rev Cancer, 2017. **17**(5): p. 302-317.
252. Parolia, A., et al., *Distinct structural classes of activating FOXA1 alterations in advanced prostate cancer.* Nature, 2019. **571**(7765): p. 413-418.
253. Correa, R.G., et al., *The NLR-related protein NWD1 is associated with prostate cancer and modulates androgen receptor signaling.* Oncotarget, 2014. **5**(6): p. 1666-82.
254. Zheng, C., et al., *Roles of Myc-associated zinc finger protein in malignant tumors.* Asia Pac J Clin Oncol, 2022. **18**(6): p. 506-514.
255. Yang, Q., et al., *MAZ promotes prostate cancer bone metastasis through transcriptionally activating the KRas-dependent RalGEFs pathway.* J Exp Clin Cancer Res, 2019. **38**(1): p. 391.
256. Burdelski, C., et al., *High-Level Glyoxalase 1 (GLO1) expression is linked to poor prognosis in prostate cancer.* Prostate, 2017. **77**(15): p. 1528-1538.
257. Rounds, L., et al., *Glyoxalase 1 Expression as a Novel Diagnostic Marker of High-Grade Prostatic Intraepithelial Neoplasia in Prostate Cancer.* Cancers (Basel), 2021. **13**(14).
258. Jiang, W.G. and R.J. Ablin, *Prostate transglutaminase: a unique transglutaminase and its role in prostate cancer.* Biomark Med, 2011. **5**(3): p. 285-91.
259. Cao, Z., et al., *Overexpression of transglutaminase 4 and prostate cancer progression: a potential predictor of less favourable outcomes.* Asian J Androl, 2013. **15**(6): p. 742-6.

260. Lopez-Bujanda, Z.A., et al., *TGM4: an immunogenic prostate-restricted antigen.* J Immunother Cancer, 2021. **9**(6).
261. Sharad, S., et al., *Gene Isoforms: A Potential Biomarker and Therapeutic Target in Prostate Cancer.* Biomolecules, 2020. **10**(9).
262. Pegg, A.E., *S-Adenosylmethionine decarboxylase.* Essays Biochem, 2009. **46**: p. 25-45.
263. Pegg, A.E., *Mammalian polyamine metabolism and function.* IUBMB Life, 2009. **61**(9): p. 880-94.
264. Holbert, C.E., et al., *Polyamines in cancer: integrating organismal metabolism and antitumour immunity.* Nat Rev Cancer, 2022. **22**(8): p. 467-480.
265. Zabala-Letona, A., et al., *mTORC1-dependent AMD1 regulation sustains polyamine metabolism in prostate cancer.* Nature, 2017. **547**(7661): p. 109-113.
266. Ali, H.E.A., et al., *Dysregulated gene expression predicts tumor aggressiveness in African-American prostate cancer patients.* Sci Rep, 2018. **8**(1): p. 16335.
267. Lázaro-Ibáñez, E., et al., *Distinct prostate cancer-related mRNA cargo in extracellular vesicle subsets from prostate cell lines.* BMC Cancer, 2017. **17**(1): p. 92.
268. Antonov, I. and Y. Medvedeva, *Direct Interactions with Nascent Transcripts Is Potentially a Common Targeting Mechanism of Long Non-Coding RNAs.* Genes (Basel), 2020. **11**(12).
269. Yao, Z.F., et al., *[Long noncoding RNA Linc00662 promotes the tumorigenesis of prostate cancer cells].* Zhonghua Nan Ke Xue, 2020. **26**(7): p. 588-594.
270. Li, N., et al., *Long noncoding RNA LINC00662 functions as miRNA sponge to promote the prostate cancer tumorigenesis through targeting miR-34a.* Eur Rev Med Pharmacol Sci, 2019. **23**(9): p. 3688-3698.
271. Bussemakers, M.J., et al., *DD3: a new prostate-specific gene, highly overexpressed in prostate cancer.* Cancer Res, 1999. **59**(23): p. 5975-9.
272. Batagov, A.O. and I.V. Kurochkin, *Exosomes secreted by human cells transport largely mRNA fragments that are enriched in the 3'-untranslated regions.* Biol Direct, 2013. **8**: p. 12.
273. Mercadal, M., et al., *Impact of Extracellular Vesicle Isolation Methods on Downstream Mirna Analysis in Semen: A Comparative Study.* Int J Mol Sci, 2020. **21**(17).
274. Yanshen, Z., et al., *miR-92a promotes proliferation and inhibits apoptosis of prostate cancer cells through the PTEN/Akt signaling pathway.* Libyan J Med, 2021. **16**(1): p. 1971837.
275. Zhang, J., et al., *Emerging roles and potential application of PIWI-interacting RNA in urological tumors.* Front Endocrinol (Lausanne), 2022. **13**: p. 1054216.
276. Peng, Q., et al., *Identification of piRNA Targets in Urinary Extracellular Vesicles for the Diagnosis of Prostate Cancer.* Diagnostics (Basel), 2021. **11**(10).
277. van Eijndhoven, M.A., et al., *Plasma vesicle miRNAs for therapy response monitoring in Hodgkin lymphoma patients.* JCI Insight, 2016. **1**(19): p. e89631.
278. Gouin, K., et al., *A comprehensive method for identification of suitable reference genes in extracellular vesicles.* J Extracell Vesicles, 2017. **6**(1): p. 1347019.
279. Dai, Y., et al., *Unbiased RNA-Seq-driven identification and validation of reference genes for quantitative RT-PCR analyses of pooled cancer exosomes.* BMC Genomics, 2021. **22**(1): p. 27.
280. Damanti, C.C., et al., *MiR-26a-5p as a Reference to Normalize MicroRNA qRT-PCR Levels in Plasma Exosomes of Pediatric Hematological Malignancies.* Cells, 2021. **10**(1).

281. Vago, R., et al., *Urine stabilization and normalization strategies favor unbiased analysis of urinary EV content.* Sci Rep, 2022. **12**(1): p. 17663.
282. Tang, K.W., Q.C. Toh, and B.W. Teo, *Normalisation of urinary biomarkers to creatinine for clinical practice and research--when and why.* Singapore Med J, 2015. **56**(1): p. 7-10.
283. Erdbrügger, U., et al., *Urinary extracellular vesicles: A position paper by the Urine Task Force of the International Society for Extracellular Vesicles.* J Extracell Vesicles, 2021. **10**(7): p. e12093.
284. Papachristodoulou, A., et al., *NKX3.1 Localization to Mitochondria Suppresses Prostate Cancer Initiation.* Cancer Discov, 2021. **11**(9): p. 2316-2333.
285. He, W.W., et al., *A novel human prostate-specific, androgen-regulated homeobox gene (NKX3.1) that maps to 8p21, a region frequently deleted in prostate cancer.* Genomics, 1997. **43**(1): p. 69-77.
286. Bieberich, C.J., et al., *Prostate-specific and androgen-dependent expression of a novel homeobox gene.* J Biol Chem, 1996. **271**(50): p. 31779-82.
287. Tan, P.Y., et al., *Integration of regulatory networks by NKX3-1 promotes androgen-dependent prostate cancer survival.* Mol Cell Biol, 2012. **32**(2): p. 399-414.
288. Kim, K.P., et al., *Reprogramming competence of OCT factors is determined by transactivation domains.* Sci Adv, 2020. **6**(36).
289. Le Magnen, C., et al., *Cooperation of loss of.* Dis Model Mech, 2018. **11**(11).
290. Khalili, M., et al., *Loss of Nkx3.1 expression in bacterial prostatitis: a potential link between inflammation and neoplasia.* Am J Pathol, 2010. **176**(5): p. 2259-68.
291. Markowski, M.C., C. Bowen, and E.P. Gelmann, *Inflammatory cytokines induce phosphorylation and ubiquitination of prostate suppressor protein NKX3.1.* Cancer Res, 2008. **68**(17): p. 6896-901.
292. Chen, Y., et al., *Mechanism of cargo sorting into small extracellular vesicles.* Bioengineered, 2021. **12**(1): p. 8186-8201.
293. Lei, Q., et al., *NKX3.1 stabilizes p53, inhibits AKT activation, and blocks prostate cancer initiation caused by PTEN loss.* Cancer Cell, 2006. **9**(5): p. 367-78.
294. Bowen, C., et al., *Loss of PTEN Accelerates NKX3.1 Degradation to Promote Prostate Cancer Progression.* Cancer Res, 2019. **79**(16): p. 4124-4134.
295. Jandova, J. and G.T. Wondrak, *Genomic GLO1 deletion modulates TXNIP expression, glucose metabolism, and redox homeostasis while accelerating human A375 malignant melanoma tumor growth.* Redox Biol, 2021. **39**: p. 101838.
296. Antognelli, C., et al., *Glyoxalase-1-Dependent Methylglyoxal Depletion Sustains PD-L1 Expression in Metastatic Prostate Cancer Cells: A Novel Mechanism in Cancer Immunosurveillance Escape and a Potential Novel Target to Overcome PD-L1 Blockade Resistance.* Cancers (Basel), 2021. **13**(12).
297. Jiao, L., et al., *The prostate cancer-up-regulated Myc-associated zinc-finger protein (MAZ) modulates proliferation and metastasis through reciprocal regulation of androgen receptor.* Med Oncol, 2013. **30**(2): p. 570.
298. Yang, R., et al., *Downregulation of.* Genes Dis, 2022. **9**(4): p. 1086-1098.
299. J, V.A., *Prostate Cancer Screening: Time to Question How to Optimize the Ratio of Benefits and Harms.* Annals of Internal Medicine, 2017. **167**(7): p. 509-510.

300. Jansen, F.H., et al., *Prostate-Specific Antigen (PSA) Isoform p2PSA in Combination with Total PSA and Free PSA Improves Diagnostic Accuracy in Prostate Cancer Detection.* European Urology, 2010. **57**(6): p. 921-927.
301. Leyten, G.H.J.M., et al., *Prospective Multicentre Evaluation of PCA3 and TMPRSS2-ERG Gene Fusions as Diagnostic and Prognostic Urinary Biomarkers for Prostate Cancer.* European Urology, 2014. **65**(3): p. 534-542.
302. Tomlins, S.A., *Urine PCA3 and TMPRSS2:ERG using cancer-specific markers to detect cancer.* Eur Urol, 2014. **65**(3): p. 543-5.
303. Pettersson, A., et al., *The TMPRSS2:ERG rearrangement, ERG expression, and prostate cancer outcomes: a cohort study and meta-analysis.* Cancer Epidemiol Biomarkers Prev, 2012. **21**(9): p. 1497-509.
304. Guo, S.C., S.C. Tao, and H. Dawn, *Microfluidics-based on-a-chip systems for isolating and analysing extracellular vesicles.* J Extracell Vesicles, 2018. **7**(1): p. 1508271.
305. Barceló, M., et al., *Semen miRNAs Contained in Exosomes as Non-Invasive Biomarkers for Prostate Cancer Diagnosis.* Sci Rep, 2019. **9**(1): p. 13772.
306. Leyten, G.H., et al., *Identification of a Candidate Gene Panel for the Early Diagnosis of Prostate Cancer.* Clin Cancer Res, 2015. **21**(13): p. 3061-70.
307. Busetto, G.M., et al., *Prospective assessment of two-gene urinary test with multiparametric magnetic resonance imaging of the prostate for men undergoing primary prostate biopsy.* World Journal of Urology, 2021. **39**(6): p. 1869-1877.
308. Maggi, M., et al., *SelectMDx and Multiparametric Magnetic Resonance Imaging of the Prostate for Men Undergoing Primary Prostate Biopsy: A Prospective Assessment in a Multi-Institutional Study.* Cancers (Basel), 2021. **13**(9).
309. Tutrone, R., et al., *Clinical utility of the exosome based ExoDx Prostate(IntelliScore) EPI test in men presenting for initial Biopsy with a PSA 2-10 ng/mL.* Prostate Cancer Prostatic Dis, 2020. **23**(4): p. 607-614.
310. T., F., *Staphylococcus*, in *Medical Microbiology*, B. S., Editor. 1996: Galveston (TX) : University of Texas Medical Branch at Galveston.
311. Pfaller, M.A. and L.A. Herwaldt, *Laboratory, clinical, and epidemiological aspects of coagulase-negative staphylococci.* Clin Microbiol Rev, 1988. **1**(3): p. 281-99.
312. Garza-González, E., et al., *Microbiological and molecular characterization of human clinical isolates of Staphylococcus cohnii, Staphylococcus hominis, and Staphylococcus sciuri.* Scand J Infect Dis, 2011. **43**(11-12): p. 930-6.
313. Zong, Z. and X. Lü, *Characterization of a new SCCmec element in Staphylococcus cohnii.* PLoS One, 2010. **5**(11): p. e14016.
314. Eltwisy, H.O., et al., *Clinical Infections, Antibiotic Resistance, and Pathogenesis of.* Microorganisms, 2022. **10**(6).
315. Basaglia, G., et al., *Staphylococcus cohnii septicaemia in a patient with colon cancer.* J Med Microbiol, 2003. **52**(Pt 1): p. 101-102.
316. Sarkar, P., et al., *Differential Microbial Signature Associated With Benign Prostatic Hyperplasia and Prostate Cancer.* Front Cell Infect Microbiol, 2022. **12**: p. 894777.
317. Wan, C.D., et al., *[Pathogens of prostatitis and their drug resistance: an epidemiological survey].* Zhonghua Nan Ke Xue, 2013. **19**(10): p. 912-7.
318. Peeters, N., et al., *Ralstonia solanacearum, a widespread bacterial plant pathogen in the post-genomic era.* Mol Plant Pathol, 2013. **14**(7): p. 651-62.

319. Evseev, P., et al., *Curtobacterium spp. and Curtobacterium flaccumfaciens: Phylogeny, Genomics-Based Taxonomy, Pathogenicity, and Diagnostics.* Curr Issues Mol Biol, 2022. **44**(2): p. 889-927.
320. Huang, M.-S., et al., *Most commensally bacterial strains in human milk of healthy mothers display multiple antibiotic resistance.* MicrobiologyOpen, 2019. **8**(1): p. e00618.
321. Gomaa, E.Z., *Human gut microbiota/microbiome in health and diseases: a review.* Antonie Van Leeuwenhoek, 2020. **113**(12): p. 2019-2040.
322. Bilen, M., et al., *Dysgonomonas massiliensis sp. nov., a new species isolated from the human gut and its taxonogenomic description.* Antonie Van Leeuwenhoek, 2019. **112**(6): p. 935-945.
323. Zhang, Q., et al., *Aerococcus urinae in urinary tract infections.* J Clin Microbiol, 2000. **38**(4): p. 1703-5.
324. Dulabon, L.M., et al., *Pseudomonas aeruginosa Acute Prostatitis and Urosepsis after Sexual Relations in a Hot Tub.* Journal of Clinical Microbiology, 2009. **47**(5): p. 1607-1608.
325. Baron, S., *Medical Microbiology*. 1996.
326. Meares, E.M., *Prostatitis.* Med Clin North Am, 1991. **75**(2): p. 405-24.
327. Karami, A.A., et al., *Detection of bacterial agents causing prostate infection by culture and molecular methods from biopsy specimens.* Iran J Microbiol, 2022. **14**(2): p. 161-167.
328. Tsai, K.Y., et al., *Exploring the Association between Gut and Urine Microbiota and Prostatic Disease including Benign Prostatic Hyperplasia and Prostate Cancer Using 16S rRNA Sequencing.* Biomedicines, 2022. **10**(11).
329. Henriquez, T. and C. Falciani, *Extracellular Vesicles of.* Antibiotics (Basel), 2023. **12**(4).
330. Zhu, M., et al., *Clinical Characteristics of Patients with.* Pol J Microbiol, 2021. **70**(3): p. 321-326.
331. Ashida, S., et al., *Abstract A38: RNA-seq analysis identified candidate pathogens for prostate cancer.* Cancer Research, 2020. **80**(8_Supplement): p. A38-A38.
332. Sim, S., et al., *Micrococcus luteus-derived extracellular vesicles attenuate neutrophilic asthma by regulating miRNAs in airway epithelial cells.* Experimental & Molecular Medicine, 2023. **55**(1): p. 196-204.
333. Modrzejewska, M., A. Kawalek, and A.A. Bartosik, *The LysR-Type Transcriptional Regulator BsrA (PA2121) Controls Vital Metabolic Pathways in.* mSystems, 2021. **6**(4): p. e0001521.
334. Martens-Uzunova, E.S., M. Olvedy, and G. Jenster, *Beyond microRNA--novel RNAs derived from small non-coding RNA and their implication in cancer.* Cancer Lett, 2013. **340**(2): p. 201-11.
335. Lillig, C.H. and A. Holmgren, *Thioredoxin and related molecules--from biology to health and disease.* Antioxid Redox Signal, 2007. **9**(1): p. 25-47.
336. González-Vázquez, M.C., et al., *Location of OprD porin in Pseudomonas aeruginosa clinical isolates.* APMIS, 2021. **129**(4): p. 213-224.
337. Andrews, E.S.V. and W.M. Patrick, *The hypothesized role of YbeZ in 16S rRNA maturation.* Arch Microbiol, 2022. **204**(1): p. 114.
338. Möller, P., et al., *The RNase YbeY Is Vital for Ribosome Maturation, Stress Resistance, and Virulence of the Natural Genetic Engineer.* J Bacteriol, 2019. **201**(11).

339. Di Sebastiano, K.M. and M. Mourtzakis, *The role of dietary fat throughout the prostate cancer trajectory.* Nutrients, 2014. **6**(12): p. 6095-109.
340. Pascual, G., et al., *Targeting metastasis-initiating cells through the fatty acid receptor CD36.* Nature, 2017. **541**(7635): p. 41-45.
341. Cho, D.Y., et al., *Contribution of Short Chain Fatty Acids to the Growth of.* Front Cell Infect Microbiol, 2020. **10**: p. 412.
342. Allelein, S., et al., *Prostate-Specific Membrane Antigen (PSMA)-Positive Extracellular Vesicles in Urine-A Potential Liquid Biopsy Strategy for Prostate Cancer Diagnosis?* Cancers (Basel), 2022. **14**(12).
343. Kawakami, K., et al., *Diagnostic potential of serum extracellular vesicles expressing prostate-specific membrane antigen in urologic malignancies.* Scientific Reports, 2021. **11**(1): p. 15000.
344. Hornung, B.V.H., R.D. Zwittink, and E.J. Kuijper, *Issues and current standards of controls in microbiome research.* FEMS Microbiology Ecology, 2019. **95**(5).
345. Sivapatham, S. and L. Selvaraj, *Currently available molecular analyses for personalized tumor therapy (Review).* Biomed Rep, 2022. **17**(6): p. 95.

Appendix

Table S1. Patient's characteristics. nd:non-determines

	Discovery Cohort (RNA-seq)		Validation Cohort (RT-ddPCR)			
	PC		PC		BPH	
Number	10		20		20	
Age (Median, ages)	66.4		65.2		66.8	
Age (range)	[60-73]		[49-74]		[53-84]	
Diagnostic PSA (ng/ml)	Number	%	Number	%	Number	%
< 4			2	10	2	10
> 4 -10	7	70	8	40	9	45
>10	3	30	10	50	9	45
PostOp PSA (ng/ml)					nd	
<1	9	90	18	90		
>1-4			2	10		
> 10	1	10				
Gleason Score					nd	
6 (3+3)	1	10	7	35		
7(3+4)	7	70	3	15		
7 (4+3)	1	10	4	20		
8 (4+4)	1	10	3	15		
9 (4+5)			3	15		
Clinical Staging					nd	
T2a	3	30	5	25		
T2c	2	20	6	30		
T3a	3	30	5	25		
T3b	2	20	4	20		
CAPRA score					nd	
Low	4	40	5	25		
Intermediate	2	20	3	15		
High	4	40	12	60		
ISUP grade					nd	
GG1	5	50	7	35		
GG2	0	0	3	15		
GG3	3	30	3	15		
GG4	2	20	4	20		
GG5	0	0	3	15		

Table S2. RT-ddPCR primer specifications. Accession numbers corresponding to GeneGlobe platform (Qiagen).

Target name	Assay Type	Accession number	Annealing temperature	Description
miR-375-3p	miRCURY LNA	YCP1552280	55ºC	microRNA 375
hsa-piR-28004	miRCURY LNA	YCP1551995	54ºC	Piwi-interacting RNA 28004
GLO1	QuantiNova LNA	SCB0419367	54ºC	Glyoxalase I
NKX3-1	QuantiNova LNA	SCB0419359	56ºC	NK3 homeobox 1
AMD1	QuantiNova LNA	SCB0419381	55ºC	Adenosylmethionine decarboxylase 1
MAZ	QuantiNova LNA	SCB0420996	54ºC	MYC associated zinc finger protein
RBM47	QuantiNova LNA	SCB0412069	56ºC	RNA binding motif protein 47

Table S3. RNAs that are overexpressed in PC tissues, present in PreOp urinary EVs and decreased after the surgery.

Gene name	T vs N log2FC	T vs N adj. P	BH corrected P	PreOpU vs PostOpU log2FC	PreOpU vs PostOp U adj. P	BH corrected P
IGF1R	1.02635395	1.64591E-06	1.64591E-06	1.843948337	0.033660637	0.052153086
ODC1	2.16772269	1.23453E-12	1.23453E-12	1.865650176	0.031149008	0.048261621
MLEC	1.285031148	1.04592E-13	1.04592E-13	1.976028772	0.034412026	0.053317273
FOXA1	3.080836931	0.000195807	0.000195807	2.086999489	0.031183697	0.048315367
ANKRD9	3.835459068	0.005127541	0.005127541	2.174471433	0.005467282	0.066348716
MXD4	3.857548358	4.22011E-17	4.22011E-17	2.343577394	0.034412026	0.053317273
TGM4	6.78318959	7.05933E-18	7.05933E-18	2.358246902	0.04762515	0.07378941
TRIM28	1.492998709	0.000158692	0.000158692	2.360580597	0.037086994	0.057461812
NFIX	1.901085869	4.7351E-07	4.7351E-07	2.372974735	0.02335868	0.036191449
RBM47	2.738347117	1.35645E-08	1.35645E-08	2.48321985	0.009173951	0.014213927
DISP2	1.127470612	0.009972153	0.009972153	2.563626521	0.049351669	0.076464443
NWD1	3.259178077	1.20427E-07	1.20427E-07	2.592955629	0.017896441	0.027728371
NCDN	2.105570891	2.22645E-08	2.22645E-08	2.638858254	0.042230483	0.065431026
YJEFN3	2.216694641	0.004537612	0.004537612	2.639113936	0.029560237	0.045800013
ABHD2	1.824082538	7.5723E-11	7.5723E-11	2.640016842	0.045972033	0.071228105
TTLL12	3.300997577	1.47427E-16	1.47427E-16	2.64696008	0.039465723	0.061147365
NKX3-1	2.762436186	4.66525E-05	4.66525E-05	2.670707347	0.01199036	0.018577612
LSS	1.461808904	3.67746E-06	3.67746E-06	2.677444267	0.049551562	0.076774152
PCDH1	3.245748012	2.65341E-14	2.65341E-14	2.687419254	0.031183697	0.048315367
UPF1	2.016472594	1.07942E-06	1.07942E-06	2.689652192	0.031149008	0.048261621
PMEPA1	2.852499812	5.35448E-16	5.35448E-16	2.717613518	0.002034951	0.00315291
LTBP3	1.786429219	0.002879463	0.002879463	2.780122805	0.034412026	0.053317273
TOM1L2	1.510023331	7.488E-06	7.488E-06	2.79087929	0.045992157	0.071259286
TMEM87A	1.046990087	7.48716E-11	7.48716E-11	2.800723803	0.032759048	0.050756183

HLCS	1.428321379	3.09525E-16	3.09525E-16	2.851912244	0.047805378	0.074068651
CORO1B	4.02058694	4.39204E-08	4.39204E-08	2.858754626	0.041127242	0.063721688
PIEZO1	2.204014479	3.51768E-06	3.51768E-06	2.875858886	0.02335868	0.036191449
CLCN3	1.104867594	6.75783E-09	6.75783E-09	2.897636211	0.017896441	0.027728371
PKP1	3.134839135	0.001148626	0.001148626	2.925804808	0.02335868	0.036191449
GCNT2	1.114243093	0.01529478	0.01529478	3.015382341	0.016855224	0.026115132
MAGT1	1.02021323	9.13719E-09	9.13719E-09	3.021242159	0.04776633	0.074008152
TAPBP	1.315899654	3.96498E-05	3.96498E-05	3.025930174	0.026564612	0.041158654
DBI	1.718903029	1.7171E-12	1.7171E-12	3.033340569	0.019945804	0.030903611
SIN3B	1.561586151	4.5303E-05	4.5303E-05	3.09172842	0.025806577	0.039984171
XBP1	2.667262899	3.43754E-21	3.43754E-21	3.135148832	0.01565568	0.024256583
TFF3	3.614755798	2.39463E-14	2.39463E-14	3.164470765	0.039041437	0.060489986
SCAMP2	1.284838515	4.88704E-06	4.88704E-06	3.193850638	0.028601598	0.044314717
PPM1H	2.899416354	2.24679E-10	2.24679E-10	3.228506509	0.030661719	0.047506625
ELAPOR1	3.034995993	3.58251E-05	3.58251E-05	3.230971668	0.01660099	0.025721226
CDYL2	1.017743825	4.89633E-06	4.89633E-06	3.243339553	0.019945804	0.030903611
SOAT1	1.568081773	2.98073E-10	2.98073E-10	3.270687165	0.014382417	0.022283815
MSMB	2.765272715	0.009191762	0.009191762	3.278706657	0.001876341	0.002907164
PTPRN2	2.20842705	2.73681E-14	2.73681E-14	3.282307902	0.030661719	0.047506625
CHPF	2.414972055	1.96342E-08	1.15583E-06	3.284974797	0.033210237	0.051455245
SLC30A4	2.160232903	1.54693E-06	1.54693E-06	3.302469453	0.015563298	0.024113448
PCED1A	1.57951808	3.1393E-06	3.1393E-06	3.353487222	0.045111851	0.069895357
LAMA5	3.491044109	6.3204E-05	6.3204E-05	3.379052867	0.005885635	0.00911908
PLPP5	1.94105954	2.10392E-09	2.10392E-09	3.381245726	0.027297997	0.042294946
HYOU1	2.270169489	3.81487E-12	3.81487E-12	3.421870183	0.012989129	0.020125085
EGR3	1.355768846	0.001075647	0.001075647	3.464588434	0.016855224	0.026115132
MAZ	3.367926089	1.63089E-20	1.63089E-20	3.535853895	0.000127305	0.000197244
VPS26B	3.056344798	2.08079E-05	2.08079E-05	3.59017068	0.026956369	0.041765633

GPAA1	2.555441864	3.28598E-07	3.28598E-07	3.592760411	0.012424147	0.019249713
BEND4	4.617837304	1.94549E-24	1.94549E-24	3.63339089	0.003054176	0.004732076
MEX3D	1.691451385	4.48123E-07	4.48123E-07	3.732610579	0.005268842	0.008163434
ABCA2	3.540987877	2.19274E-09	2.19274E-09	3.765376306	0.001133266	0.001755859
H2AJ	1.770908051	1.14606E-13	1.14606E-13	3.776235044	0.000989398	0.001532952
ADAMTSL1	2.746053048	4.24402E-09	4.24402E-09	3.912787294	0.014382417	0.022283815
AMD1	2.002351415	2.77734E-22	2.77734E-22	3.96850544	0.001108259	0.001717114
SEC14L2	3.727341734	1.83107E-12	1.83107E-12	4.022212141	0.009206074	0.014263698
GLO1	1.471804443	3.16128E-13	3.16128E-13	4.071356408	0.00398259	0.006170541
LCP1	1.420885449	0.000342187	0.000342187	4.289868145	0.000749018	0.001160512
COQ6	3.687414449	5.50093E-24	4.23047E-05	4.298355257	8.72294E-05	0.000135151
miRNAs	T vs N log2FC	T vs N adj. P	BH corrected P	PreOpU vs PostOpU log2FC	PreOpU vs PostOp U adj. P	BH corrected P
miR-375-3p	2,897,121,967	0.0001509618859	0.0001509618859	1,454,122,511	0.003219721528	0.005301438033
miR-92a-1-5p	1,732,624,104	0.0007949241867	0.0007949241867	2,897,121,967	0.0001509618859	0.0001509618859
piRNAs	T vs N log2FC	T vs N adj. P	BH corrected P	PreOpU vs PostOpU log2FC	PreOpU vs PostOp U adj. P	BH corrected P
piR28004	1,229,581,814	0	0	6,468,977,662	0.001770594476	0.004977708997
lincRNAs	T vs N log2FC	T vs N adj. P	BH corrected P	PreOpU vs PostOpU log2FC	PreOpU vs PostOp U adj. P	BH corrected P
CHASERR	1.030763145	7.69097E-08	7.69497E-08	3.380412156	0.012115576	0.026956764
LINC00662	1.652267756	7.94816E-07	2.23902E-11	3.059548754	0.019465425	0.043309937
lnc-LTBP3-11	1.989295644	0.001482074	0.001482845	3.611107836	0.039134482	0.08707295

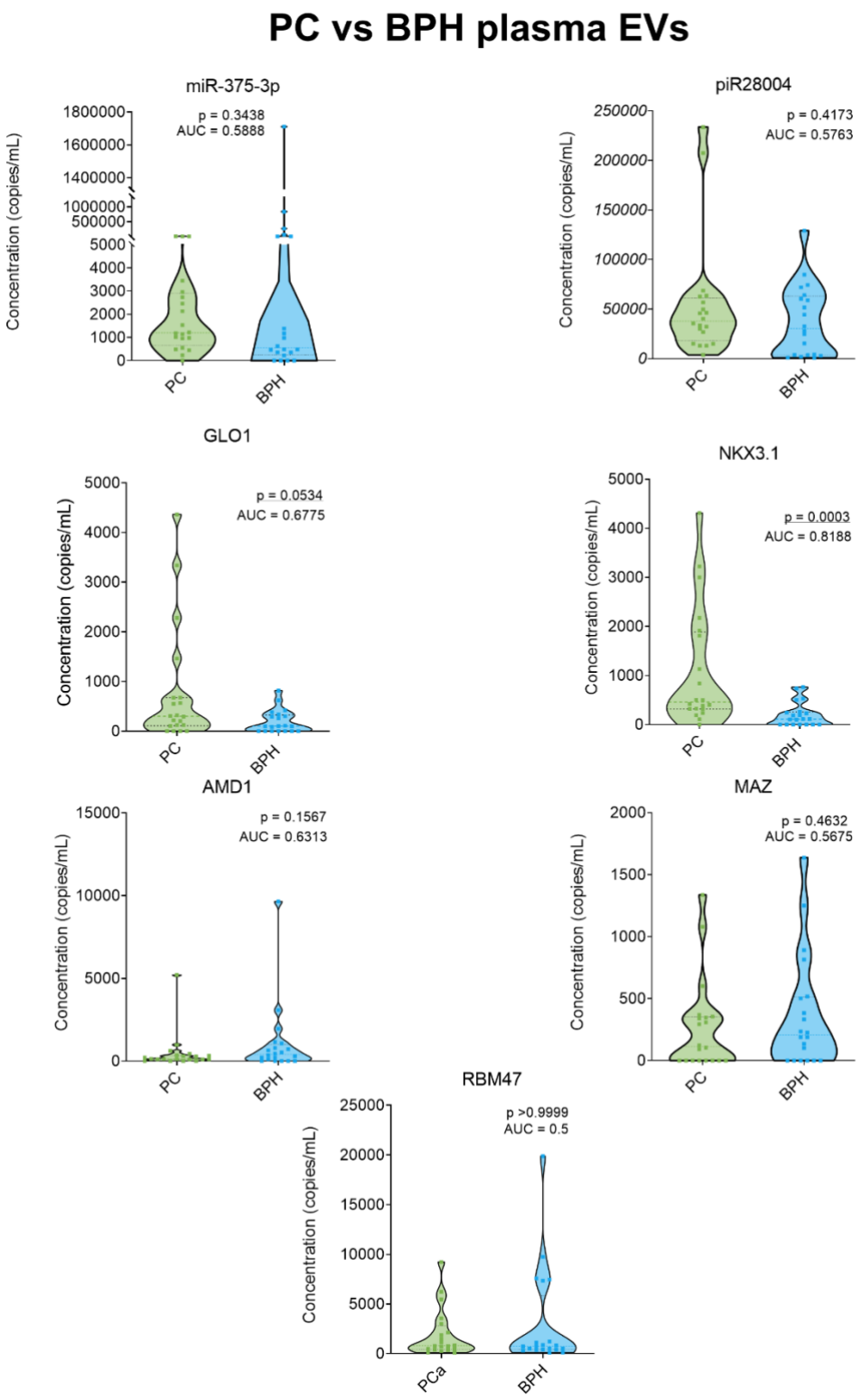

Figure S1. Testing of selected biomarker candidates in plasma EVs from an independent cohort of 20 PC patients and 20 BPH patient by RT-ddPCR. Violin plots show the copy number of RNA biomarkers per ml of plasma. Mann-Whitney test was performed to assess differences between groups. p-value<0.05 was considered significant.

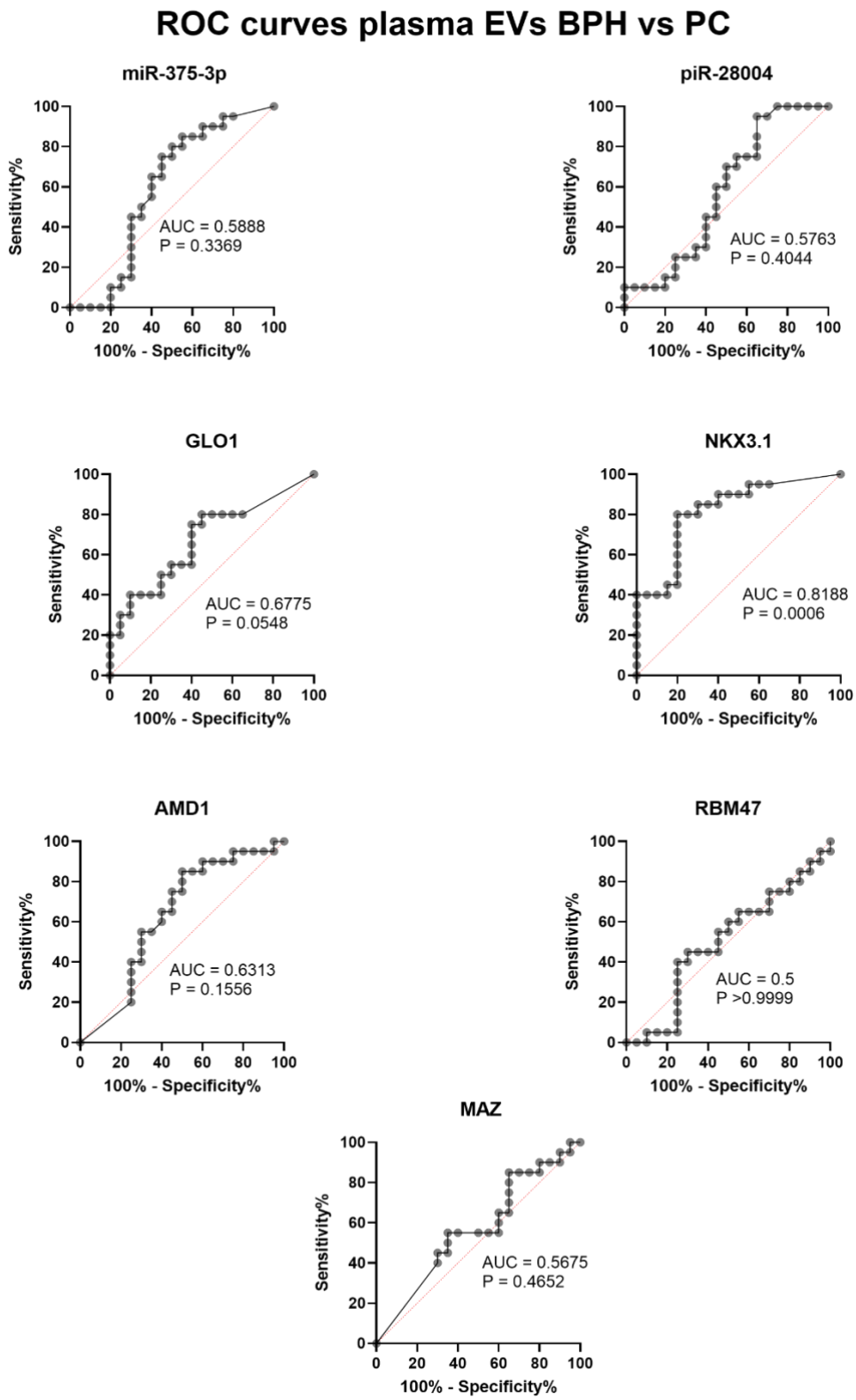

Figure S2. ROC curves of selected biomarker candidates' discrimination between BPH vs PC EV plasma samples. AUC: Area under the curve. P: p-value

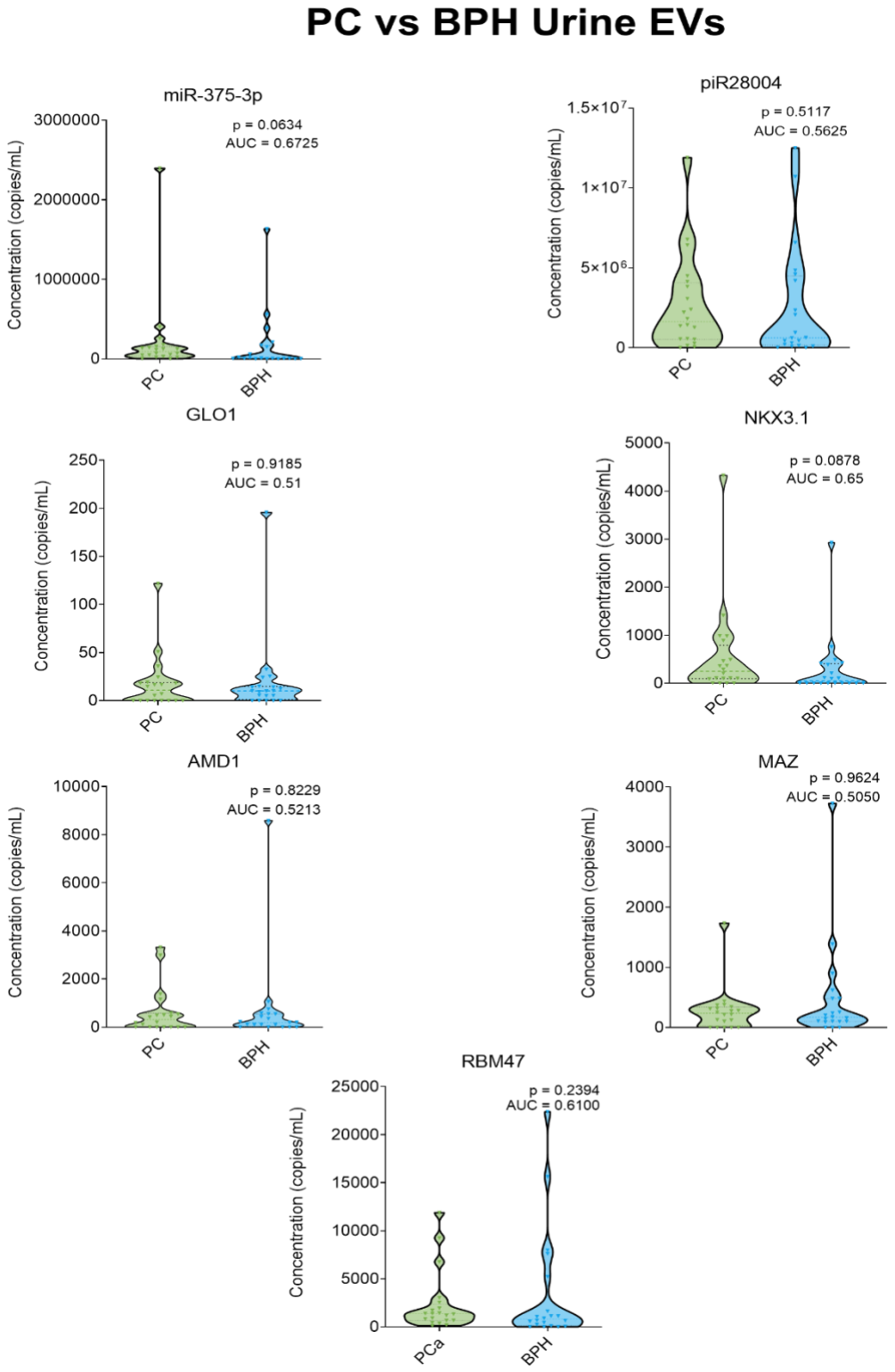

Figure S3. Testing of selected biomarker candidates in urinary EVs from an independent cohort of 20 PC patients and 20 BPH patient by RT-ddPCR. Violin plots show the copy number of RNA biomarkers per ml of urine. Mann-Whitney test was performed to assess differences between groups. p-value<0.05 was considered significant.

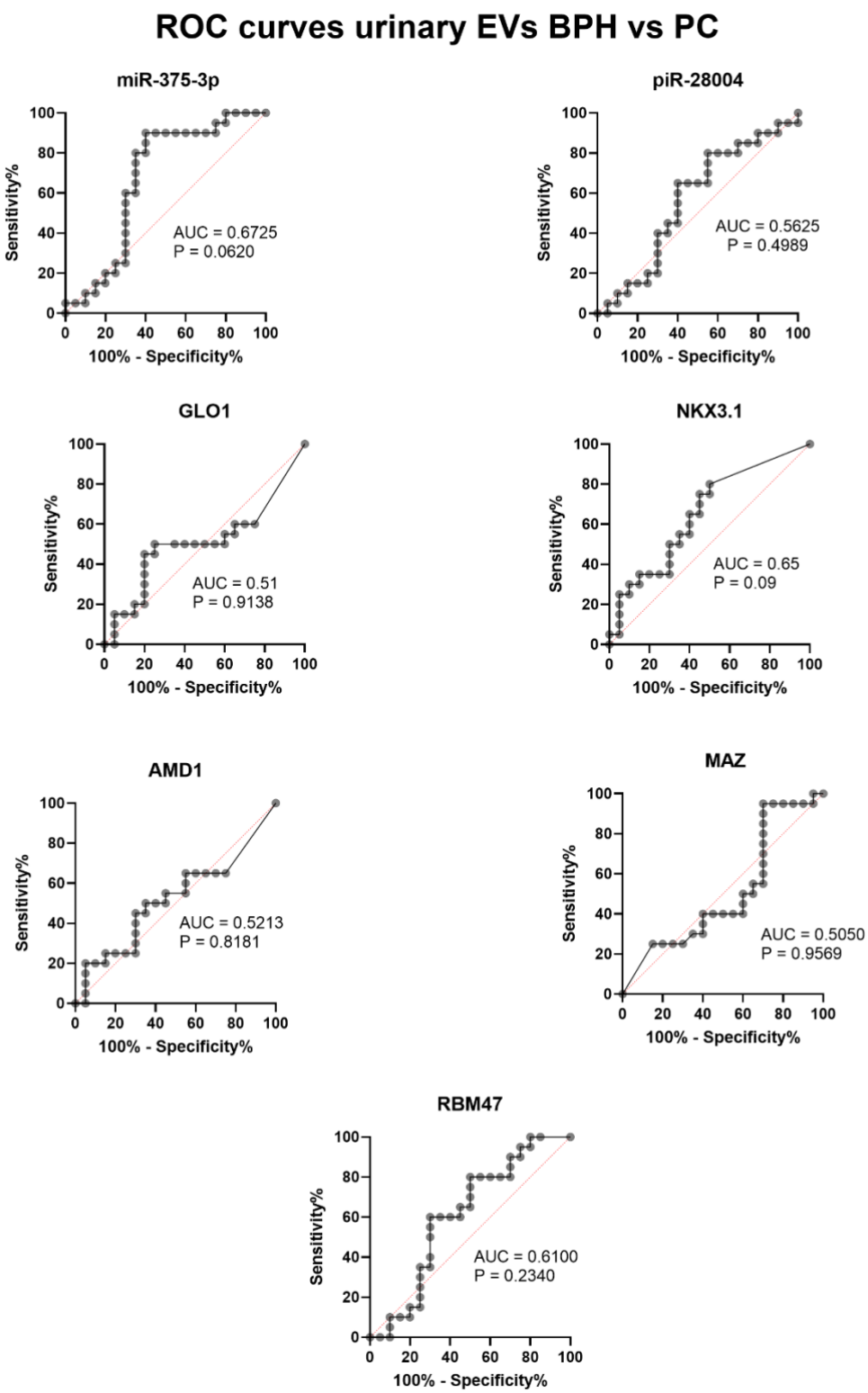

Figure S4. ROC curves of selected biomarker candidates' discrimination between BPH vs PC EV urinary samples. AUC: Area under the curve. P: p-value

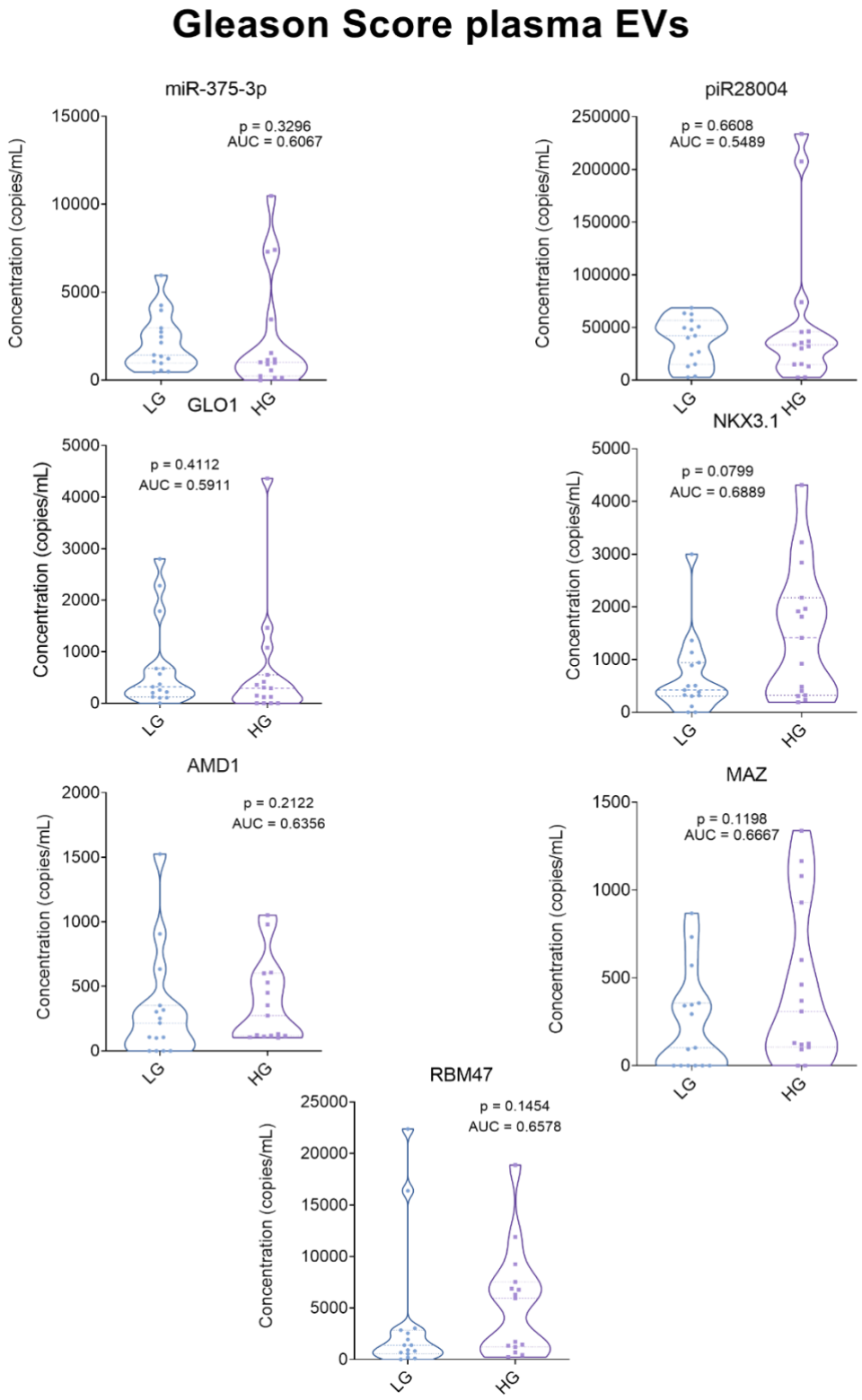

Figure S5. Testing of selected biomarker candidates in plasma EVs from PC patients (n=30) divided in two groups (n=15) based on GS. Low Gleason (LG) = GS 6 or 7a (3+4); and High Gleason (HG) = GS 7b (4+3) or higher by RT-ddPCR. Violin plots show the copy number of RNA biomarkers per ml of plasma. Mann - Whitney test was used to assess the statistical significance of the differences between groups. *P*-value <0.05 was considered significant. AUC values were calculated and added. Corresponding ROC curves can be seen ir Figure S6, in this appendix.

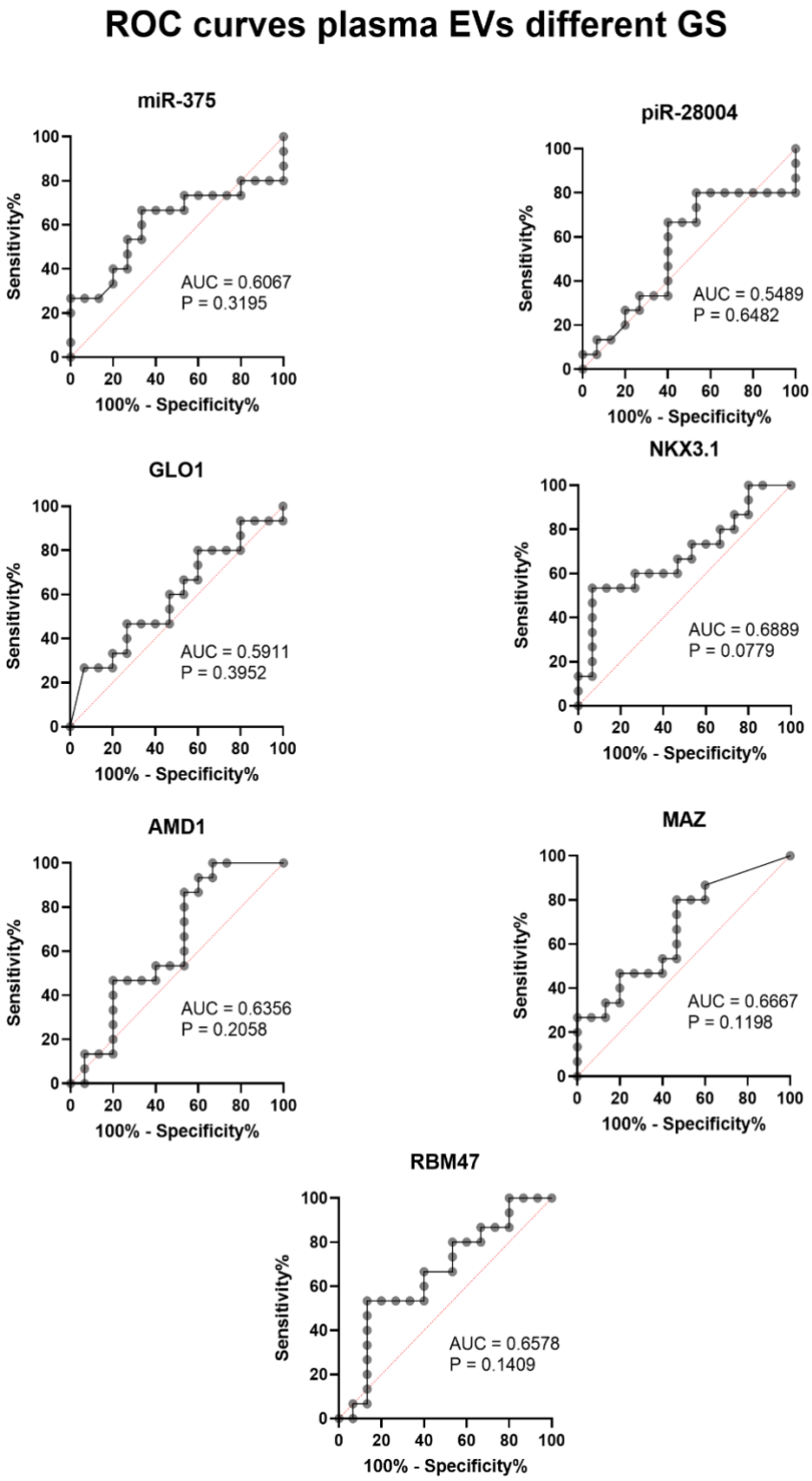

Figure S6. ROC curves of selected biomarker candidates of plasma EVs from PC patients (n=30) divided in two groups (n=15) based on GS. Low Gleason (LG) = GS 6 or 7a (3+4); and High Gleason (HG) = GS 7b (4+3) or higher by RT-ddPCR. AUC: Area under the curve. p: p-value

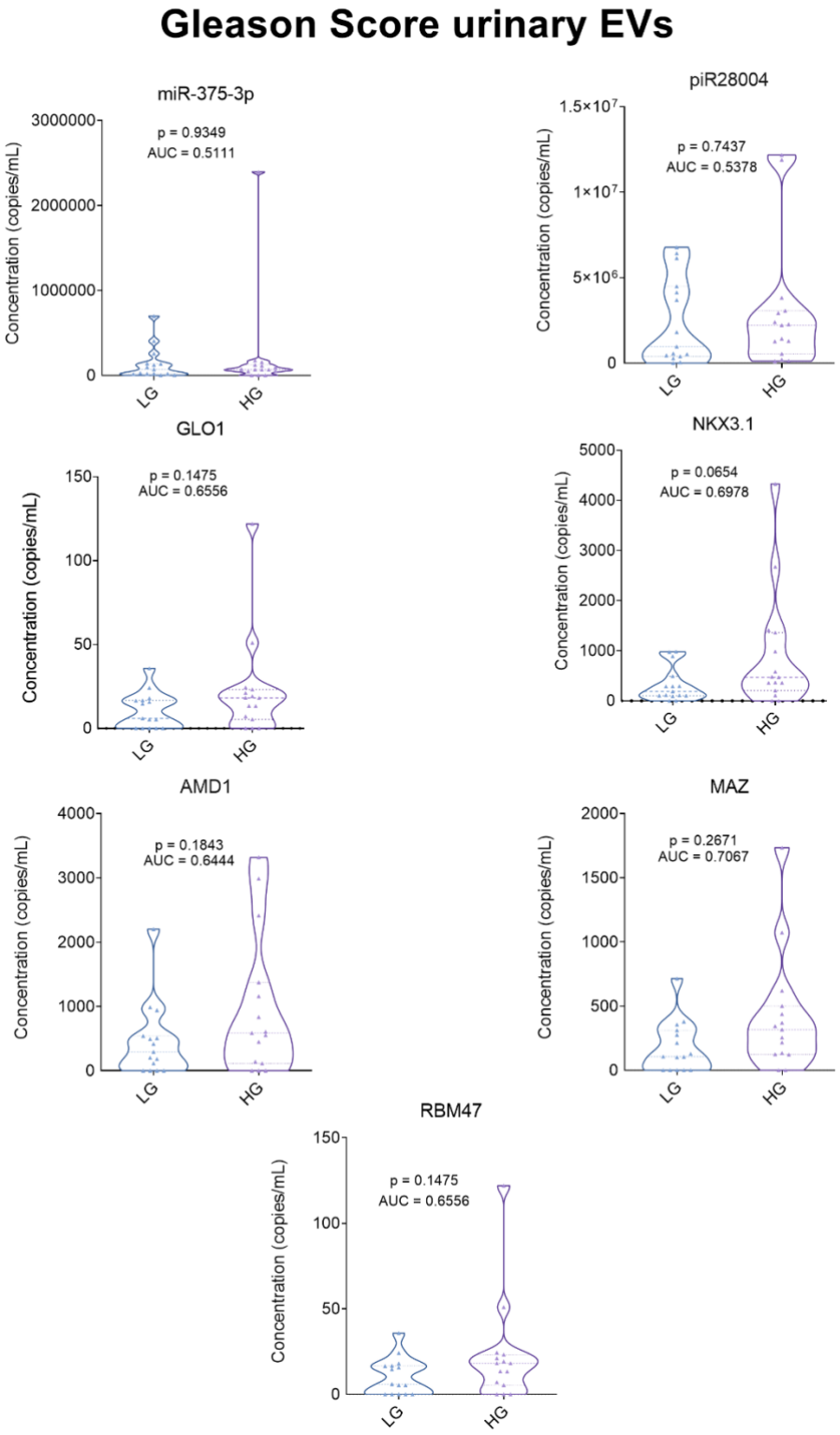

Figure S7. Testing of selected biomarker candidates in urinary EVs from PC patients (n=30) divided in two groups (n=15) based on GS. Low Gleason (LG) = GS 6 or 7a (3+4); and High Gleason (HG) = GS 7b (4+3) or higher by RT-ddPCR. Violin plots show the copy number of RNA biomarkers per ml of urine. Mann - Whitney test was used to assess the statistical significance of the differences between groups. *P*-value <0.05 was considered significant. AUC values were calculated and added. Corresponding ROC curves can be seen ı Figure S8, in this appendix.

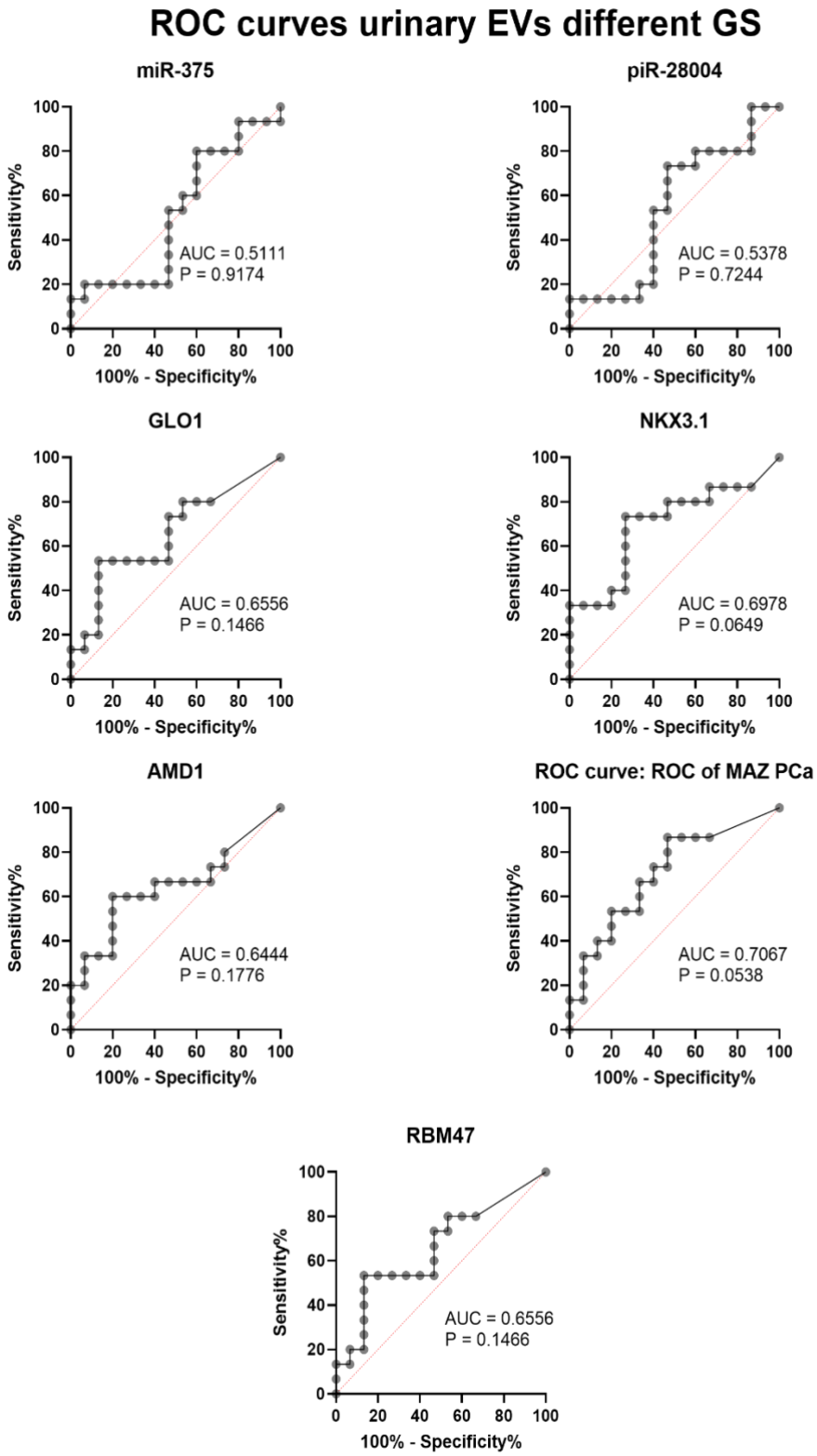

Figure S8. ROC curves of selected biomarker candidates of urinary EVs from PC patients (n=30) divided in two groups (n=15) based on GS. Low Gleason (LG) = GS 6 or 7a (3+4); and High Gleason (HG) = GS 7b (4+3) or higher by RT-ddPCR. AUC: Area under the curve. p: p-value

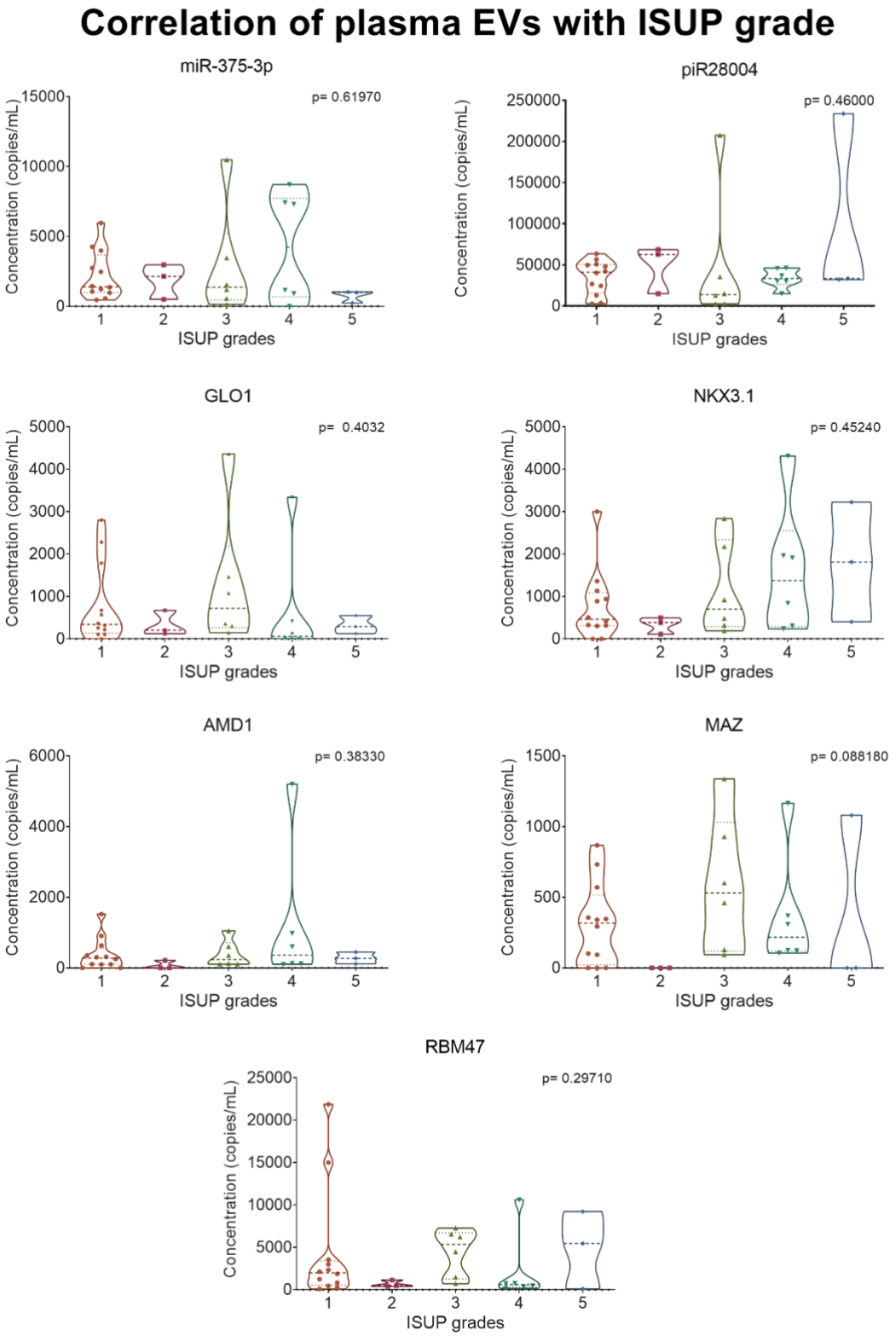

Figure S9. Testing of selected biomarker candidates in plasma EVs from PC patients (n=30) by RT-ddPCR assessing ISUP grade correlation. Violin plots show the copy number of RNA biomarkers per ml of plasma. Kruskal - Wallis test was used to assess the statistical significance among the differences groups. *P*-value <0.05 was considered significant.

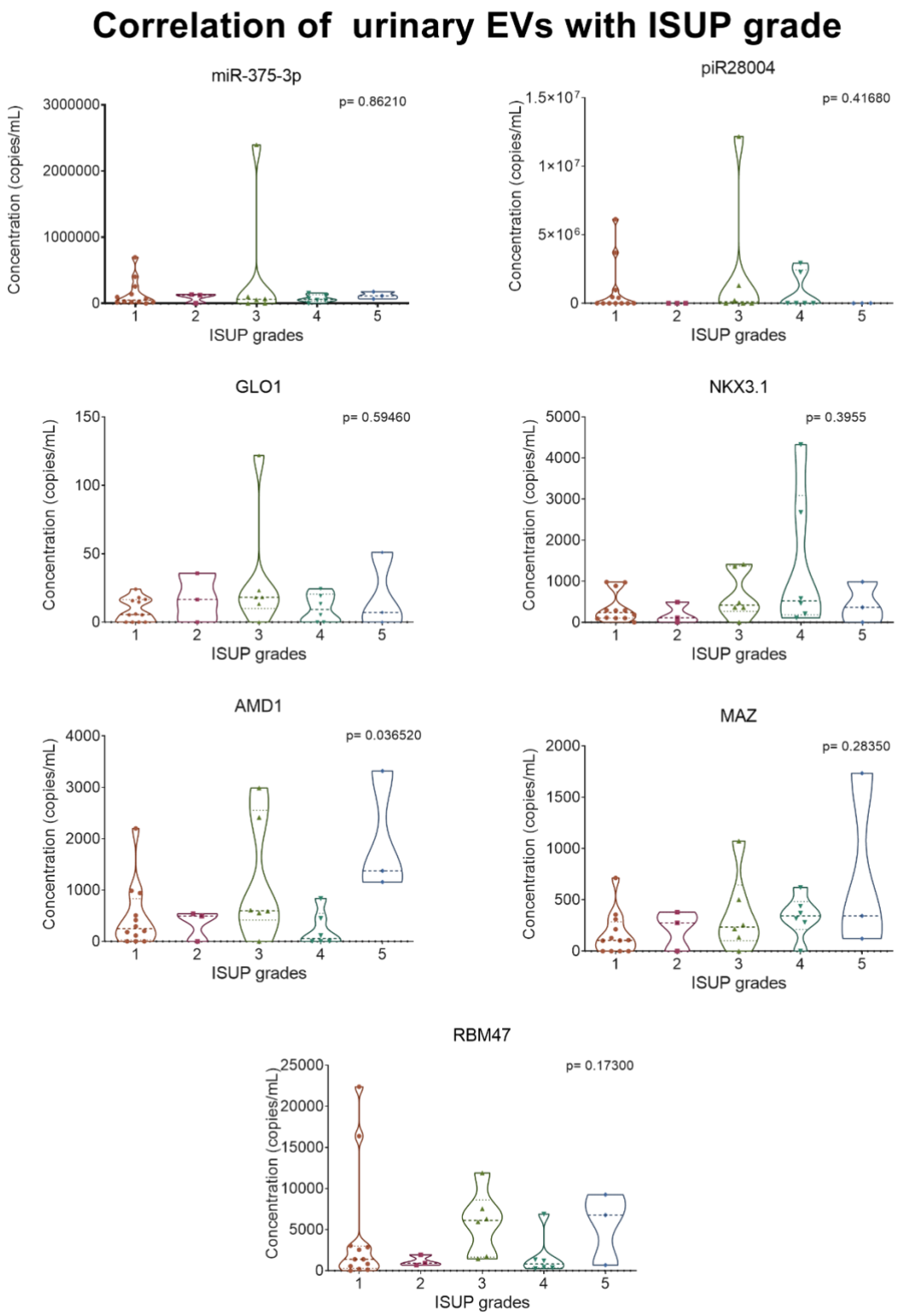

Figure S10. Testing of selected biomarker candidates in urinary EVs from PC patients (n=30) by RT-ddPCR assessing ISUP grade correlation. Violin plots show the copy number of RNA biomarkers per ml of urine. Kruskal - Wallis test was used to assess the statistical significance among the differences groups. *P*-value <0.05 was considered significant.

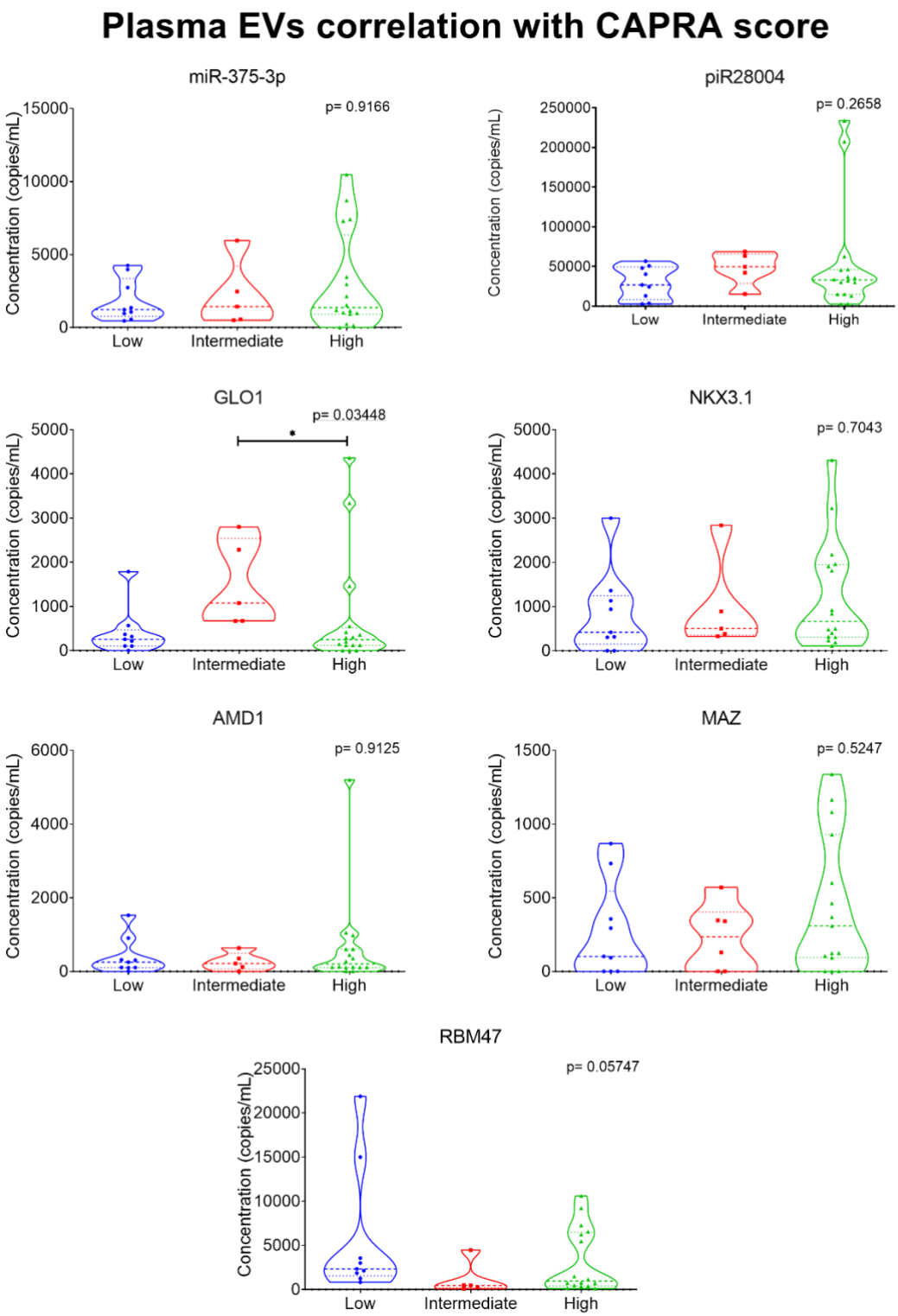

Figure S11. Testing of selected biomarker candidates in plasma EVs from PC patients (n=30) by RT-ddPCR assessing CAPRA score correlation. Violin plots show the copy number of RNA biomarkers per ml of plasma. Kruskal - Wallis test was used to assess the statistical significance among the differences groups. *P*-value <0.05 was considered significant. * p-value <0.05.

Urinary EVs correlation with CAPRA score

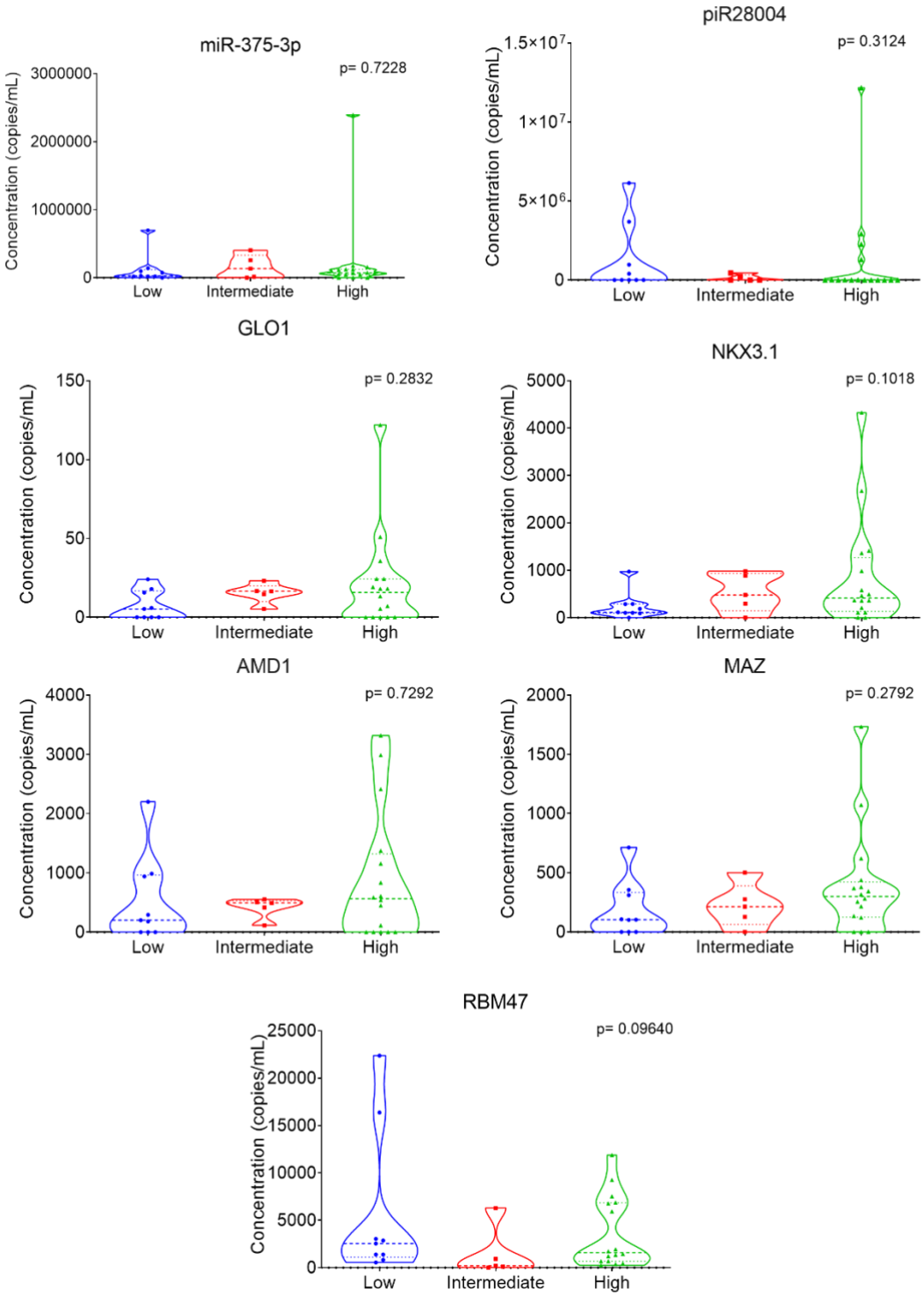

Figure S12. Testing of selected biomarker candidates in urinary EVs from PC patients (n=30) by RT-ddPCR assessing CAPRA score correlation. Violin plots show the copy number of RNA biomarkers per ml of urine. Kruskal - Wallis test was used to assess the statistical significance among the differences groups. *P*-value <0.05 was considered significant.

Table S4. Differential abundant species between tumour and normal prostate.

Species	log2FoldChange	Adj. p-value	BH corrected p-value
Pseudomonas sp.KNUC1026	-12.1133	0.00059	0.000589962
Aerococcus urinaeequi	-12.1085	0.000244	0.000243703
Streptococcus lactarius	-11.4373	0.00065	0.000649558
Rhizobium leguminosarum	-11.1661	0.00065	0.000649558
Acidovorax antarcticus	-9.50615	0.000655	0.0006548
Variovorax sp.PAMC	-8.81493	0.001384	0.001383835
Aerococcus viridans	-8.64282	0.00059	0.000589962
Sutterella wadsworthensis	-8.639	0.001028	0.001027949
Simonsiella muelleri	-8.29149	0.000997	0.00099716
Cupriavidus sp.EM10	-8.04298	0.00159	0.001590373
Frigoriglobus tundricola	-7.86251	0.001607	0.001607139
Brevundimonas sp.Bb-A	-7.83279	0.000997	0.00099716
Neorhizobium sp.NCHU2750	-7.77668	0.001607	0.001607139
Novosphingobium aromaticivorans	-7.71994	0.000625	0.000624817
Qipengyuania sediminis	-7.41088	0.001607	0.001607139
Rhizobium sp.Y9	-7.23241	0.001607	0.001607139
Neisseria weixii	-7.18738	0.001607	0.001607139
Sphingomonas sp.MM-1	-6.92067	0.001463	0.001463107
Synechococcus sp.JA-2-3B'a(2-13)	-6.82641	0.001607	0.001607139
Microbacterium sediminis	-6.70016	0.001463	0.001463107
Aureimonas sp.SA4125	-6.40798	0.001627	0.00162673
Sphingomonas lacunae	-6.3467	0.001607	0.001607139
Fusobacterium pseudoperiodonticum	-6.2467	0.001753	0.001753143
Sulfuricurvum kujiense	-6.201	0.001607	0.001607139
Streptomyces mobaraensis	-6.19989	0.001753	0.001753143
Neisseria meningitidis	-6.19194	0.00178	0.001779701
Citrobacter sp.CF971	-6.0523	0.002208	0.002207897
Staphylococcus arlettae	-6.02737	0.001627	0.00162673
Planctopirus ephydatiae	-6.0182	0.001753	0.001753143
Methylobacterium currus	-5.89635	0.00177	0.001770029
Nakamurella sp.PAMC28650	-5.61549	0.004368	0.004368373

Massilia sp.PAMC28688	-5.56669	0.001832	0.001831994
Vitreoscilla sp.C1	-5.41281	0.005354	0.005354196
Corynebacterium imitans	-5.37459	0.007344	0.007344129
Phycicoccus endophyticus	-5.36851	0.004967	0.004966717
Delftia tsuruhatensis	-5.30703	0.001607	0.001607139
Klebsiella huaxiensis	-5.26335	0.001959	0.001958636
Corynebacterium lizhenjunii	-5.00202	0.005837	0.005836987
Koribacter versatilis	-4.93324	0.001916	0.001915619
Bradyrhizobium sp.41S5	-4.90917	0.002018	0.002017599
Psychrobacter sp.PraFG1	-4.56255	0.002312	0.002311769
Bradyrhizobium sp.CCBAU	-4.26289	0.002312	0.002311769
Bigelowiella natans	-4.05434	0.026624	0.026624398
Achromobacter xylosoxidans	-3.95672	0.027198	0.027198206
Fusobacterium gonidiaformans	-3.92013	0.040238	0.040237925
Cryptomonas paramecium	-3.85877	0.04883	0.048829832
Corynebacterium vitaeruminis	-3.79023	0.026624	0.026624398
Bradyrhizobium quebecense	-3.5347	0.028838	0.028837685
Neisseria gonorrhoeae	-3.47491	0.049041	0.049040929
Pseudomonas sp.Tri1	-3.45714	0.041746	0.041746466
Corynebacterium kefirresidentii	-3.42101	0.027198	0.027198206
Paracoccus suum	-3.39242	0.003185	0.003184542
Aureimonas altamirensis	-2.68944	0.006676	0.006676263
Cupriavidus malaysiensis	-2.51702	0.005722	0.005721528
Cupriavidus metallidurans	-2.4362	0.0337	0.033700235
Aureimonas populi	-2.28039	0.00962	0.009619833
Actinomyces sp.432	-2.20248	0.008556	0.008556263
Methanocorpusculum labreanum	-1.55854	0.021886	0.021886498
Streptomyces nodosus	-1.41426	0.021886	0.021886498
Shewanella bicestrii	-1.17352	0.033357	0.033357184
Rhodococcus sp.008	2.689964	0.002364	0.0023642
Burkholderia pseudomallei	3.02263	0.001607	0.001607139

Microbacterium sp.cx-55	3.045065	0.012741	0.012740559
Actinomyces sp.oral	3.211713	0.030824	0.030823904
Streptococcus sanguinis	3.444899	0.039578	0.039577991
Sphingomonas aliaeris	3.64236	0.042874	0.042873551
Clostridium tetani	3.899854	0.030824	0.030823904
Sphingomonas sp.AAP5	4.023658	0.042003	0.042003134
Kluyveromyces marxianus	4.10686	0.017665	0.017664649
Dietzia psychralcaliphila	4.238893	0.00159	0.001590373
Ruminococcus torques	4.324795	0.008401	0.008401181
Sphingomonas alpina	4.440098	0.022134	0.022134264
Acinetobacter sp.MYb10	4.726461	0.011603	0.011603417
Caldicellulosiruptor acetigenus	4.751129	0.013985	0.013985219
Streptomyces platensis	4.944089	0.001384	0.001383835
Sphingomonas hengshuiensis	4.983582	0.028838	0.028837685
Methylobacterium indicum	5.00627	0.001384	0.001383835
Bradyrhizobium sp.SK17	5.193968	0.016551	0.016551055
Methylocystis parvus	5.195905	0.005375	0.005375071
Rhodoferax sp.PAMC	5.347185	0.009417	0.009417407
Elizabethkingia bruuniana	5.91084	0.001753	0.001753143
Pseudoxanthomonas mexicana	6.023667	0.004392	0.00439226
Paracoccus kondratievae	6.156005	0.001662	0.001662024
Luteitalea pratensis	6.682711	0.001607	0.001607139
Ramlibacter tataouinensis	7.161079	0.001607	0.001607139
Neisseria subflava	7.201775	0.00065	0.000649558
Nocardioides sp.JS614	7.691173	0.00059	0.000589962
Streptococcus sp.NPS	7.801461	0.001463	0.001463107
Dysgonomonas sp.HDW5B	8.240212	0.000792	0.000791814
Brasilonema sennae	8.397407	0.000244	0.000243703

Table S5. Differential abundant species between PreOpP and HD EVs.

Species	log2FoldChange	Adj. p-value	BH corrected p-value
Pochonia chlamydosporia	-2.79883	0.001377	0.001377
Morococcus cerebrosus	-2.70011	0.000233	0.000233
Marmoricola scoriae	-2.54258	0.001377	0.001377

Methylovirgula sp.HY1	-2.04319	0.005536	0.005536
Rhizoctonia solani	-1.97093	0.005536	0.005536
Brettanomyces nanus	-1.91188	0.014193	0.014193
Thermothielavioides terrestris	-1.76776	0.012062	0.012062
Pichia kudriavzevii	-1.69846	0.024966	0.024966
Luteitalea pratensis	-1.63381	0.008375	0.008375
Variibacter gotjawalensis	-1.62924	0.024558	0.024558
Streptomyces platensis	-1.59787	0.027381	0.027381
Frigoriglobus tundricola	-1.5813	0.029137	0.029137
Sphingomonas paucimobilis	-1.54552	0.014193	0.014193
Planctopirus ephydatiae	-1.53963	0.022055	0.022055
Capnocytophaga sputigena	-1.46234	0.031264	0.031264
Mycobacteroides chelonae	-1.44381	0.033294	0.033294
Meiothermus silvanus	-1.42008	0.037388	0.037388
Haemophilus parainfluenzae	-1.40275	0.045798	0.045798
Methylobacterium indicum	-1.39966	0.037388	0.037388
Bradyrhizobium quebecense	-1.38317	0.030197	0.030197
Bradyrhizobium guangzhouense	-1.28689	0.047534	0.047534
Bradyrhizobium sp.41S5	-1.27435	0.037388	0.037388
Aspergillus puulaauensis	-1.25903	0.045798	0.045798
Leptolyngbya sp.7M	-1.23813	0.040661	0.040661
Ramlibacter tataouinensis	-1.17963	0.040661	0.040661
Rhodovulum sp.P5	-1.12479	0.046074	0.046074
Pseudomonas sihuiensis	3.089277	0.030197	0.030197
Pseudomonas sp.C27(2019)	4.639183	0.005536	0.005536

Table S6. Differential abundant species between PreOpP and PostOpP EVs.

Gene	log2FoldChange	Adj. p-value	BH corrected p-value
Pseudomonas alcaliphila	2.838451	0.011483	0.011483
Pseudomonas sp.phDV1	2.762837	0.011483	0.011483
Pseudomonas pseudoalcaligenes	2.586857	0.011483	0.011483
Pseudomonas wenzhouensis	2.388905	0.017047	0.017047
Pseudomonas sediminis	2.980364	0.017047	0.017047
Pseudomonas mendocina	2.0219	0.017047	0.017047
Pseudomonas sp.CIP-10	1.668879	0.031878	0.031878

Table S7. Differential abundant species between PreOpU and PostOpU EVs.

Gene	log2FoldChange	Adj. p-value	BH corrected p-value
Pseudomonas putida	1.258226	0.044041	0.044041
Pseudomonas sp.phDV1	1.32713	0.044041	0.044041
Micrococcus luteus	1.628718	0.044041	0.044041
Pseudomonas pseudoalcaligenes	1.25855	0.044041	0.044041